UNIVERSITÉ PIERRE & MARIE CURIE — PARIS VI
LABORATOIRE OCÉANOGRAPHIQUE DE VILLEFRANCHE-SUR-MER
LOV UMR7093

THÈSE

présentée en vu d'obtenir le grade de Docteur, spécialité Science de l'environnement — Océanographie

par

Pieter Vandromme

ÉVOLUTION DÉCENNALE DU ZOOPLANCTON DE LA MER LIGURE EN RELATION AVEC LES FLUCTUATIONS ENVIRONNEMENTALES. DE L'IMAGERIE À LA MODÉLISATION BASÉE EN TAILLE.

—

DECADAL EVOLUTION OF LIGURIAN SEA ZOOPLANKTON LINKED TO ENVIRONMENTAL FLUCTUATIONS. FROM IMAGING SYSTEMS TO SIZE-BASED MODELS.

Thèse soutenue le 26 Novembre 2010 devant le jury composé de :

Pr.	LOUIS LEGENDRE	(Président)
Dr.	JEAN-HENRI HECQ	(Rapporteur)
Dr.	MARIA-GRAZIA MAZZOCCHI	(Rapportrice)
Pr.	VICTOR SMETACEK	(Examinateur)
Dr.	LARS STEMMANN	(Directeur)
Pr.	GABY GORSKY	(Directeur)
Pr.	JEAN-MARC GUARINI	(Directeur)

UNIVERSITÉ PIERRE & MARIE CURIE — PARIS VI
LABORATOIRE OCÉANOGRAPHIQUE DE VILLEFRANCHE-SUR-MER
LOV UMR7093

THÈSE

présentée en vu d'obtenir le grade de Docteur, spécialité Science de l'environnement — Océanographie

par

Pieter Vandromme

ÉVOLUTION DÉCENNALE DU ZOOPLANCTON DE LA MER LIGURE EN RELATION AVEC LES FLUCTUATIONS ENVIRONNEMENTALES. DE L'IMAGERIE À LA MODÉLISATION BASÉE EN TAILLE.

—

DECADAL EVOLUTION OF LIGURIAN SEA ZOOPLANKTON LINKED TO ENVIRONMENTAL FLUCTUATIONS. FROM IMAGING SYSTEMS TO SIZE-BASED MODELS.

Thèse soutenue le 26 Novembre 2010 devant le jury composé de :

Pr.	LOUIS LEGENDRE	(Président)
Dr.	JEAN-HENRI HECQ	(Rapporteur)
Dr.	MARIA-GRAZIA MAZZOCCHI	(Rapportrice)
Pr.	VICTOR SMETACEK	(Examinateur)
Dr.	LARS STEMMANN	(Directeur)
Pr.	GABY GORSKY	(Directeur)
Pr.	JEAN-MARC GUARINI	(Directeur)

Remerciements

Je tiens tout d'abord à remercier mes superviseurs qui ont rendu ce travail possible. Ces 3 ans passés à travailler à vos côtés furent extrêmement enrichissants, aussi bien au niveau scientifique qu'humain, merci d'avoir partagé votre savoir et de m'avoir permis de vivre une thèse aussi remplie. Je remercie tout particulièrement *Lars Stemmann* pour sa sympathie, ses idées, pour le temps passé à m'encadrer au jour le jour et pour l'avoir si bien fait. *Gaby Gorsky* pour sa vision de la science et pour les nombreux sobriquets dont il m'a affublé. Et aussi *Jean-Marc Guarini*, mon troisième directeur, pour ses idées toujours très enrichissantes.

Merci aussi à *Victor Smetacek*, *Louis Legendre*, *Maria-Grazia Mazzocchi* et *Jean-Henri Hecq* pour avoir accepté d'être membres de mon jury et particulièrement à Maria-Grazia et Jean-Henri pour avoir évalué ce travail dans le détail et donc lu ces presque 200 pages. Merci !

Ce travail n'aurait pas été possible sans l'aide des nombreux membres de l'équipe, présent ou passé, avec qui j'ai eu la chance de travailler, principalement *Marc Picheral*, *Léo Berline*, *Carmen Garcia-Comas Rubio*, *Corinne Desnos*, *Franck Prejger*, *Steven Colbert*, *Ornella Passafiume*, *Lionel Guidi*, *Stéphane Gasparini*, *Laure Mousseau*, les nombreux stagiaires à avoir travaillé sur le ZooScan et le PVM, et beaucoup d'autres que je remercie énormément !

Je n'aurais pas pu non plus réaliser une partie de ce travail, et pas la moindre, sans avoir eu la chance de collaborer avec l'équipe Comore de l'INRIA de Sophia-Antipolis: *Éric Benoît*, *Jonathan Rault* et *Jean-Luc Gouzé* ! Je vous remercie pour ces très bons moments passés à Sophia et pour ce savoir acquis en mathématique et modélisation ! J'espère que cette collaboration ne s'arrêtera pas là et Jonathan, bon courage pour ta dernière année de thèse !

Au cours de ces 3 ans j'ai aussi eu l'immense opportunité de partir 2 mois et demi sur le *FS Polarstern* pour fertiliser l'Océan Atlantique Sud à coup de sacs de poudre de fer ! Vivre 70 jours au milieu des icebergs et des albatrosses à apprendre et partager tant de choses fut une des meilleures expériences de ma vie. Alors merci à *Wajih Naqvi* et *Victor Smetacek* pour m'avoir accueilli dans ce projet et à *Maria-Grazia Mazzocchi* pour m'avoir accueilli dans l'équipe zooplancton. Être remercié deux fois n'est pas de trop ! La place manque ici pour remercier les 47 autres scientifiques présents (plus ceux rencontrés au séminaire à Goa qui ont aussi participés à ce projet) et les presque 50 membres d'équipage, cependant il ne serait pas correct d'oublier le Capitaine *Schwarz*.

Mais au boulot, il n'y a pas que le boulot, et je remercie donc toutes les personnes passées par le laboratoire de Villefranche-sur-Mer, particulièrement ceux dont j'ai partagé le bureau (la crique et l'open space), et qui en ont rendus la vie drôle, festive et amicale ! Coco charnel, Marc, Léo, Francky, Ornella, Martina Tartina, Christophe, Mika, Martinouschka, Carmen, Jean-Baptiste, Steevie et sa baronne, Sasha, François le Beatnik, Noémie, Rizou, Samir Alliouâne, La mère maquerelle, les nombreux scientifiques, techniciens, stagiaires, doctorant, CDD à être passé par là, Les Master des différentes promo, tout ceux qui râleront de ne pas avoir été mentionnés et encore beaucoup d'autres qui de toute façon ne liront jamais ces lignes donc c'est pas trop grave si ils n'y sont pas !

Ce travail, ainsi que le bon fonctionnement du laboratoire, ne serait pas possible sans l'aide et la patience de tout les membres de l'administration et des services du Laboratoire : Isabelle, Corinne, Manuelle, Susy, Martine, Thierry, Didier, Danièle, Cécile, Alejandra, Laurent, Olivier, Stéphane, Jean-Yves, Jean-Luc, Fabrice, Alain…

Et, bien évidemment, *Louis Legendre* et *Antoine Sciandra*, directeur du LOV et *Fauzi Mantoura*

(bientôt Gaby) directeur de l'OOV, dont je suis très reconnaissant de m'avoir accueilli dans leurs locaux.

Finalement, je gardais le meilleur, je remercie mes amis et ma famille (avec une mention spéciale pour ma mère) pour m'avoir toujours soutenus, aidés et d'être là ! Merci !

à Villefranche-sur-Mer, le 26 Novembre 2010.

Pieter Vandromme

RÉSUMÉ

Le suivi à long terme de la baie de Villefranche-sur-Mer et le développement de méthodes d'imagerie pour l'analyse du zooplancton ont apporté une grande quantité d'informations permettant de mieux comprendre les écosystèmes marins, et ceux de la mer Ligure en particulier. La présente thèse représente une partie de ce suivi. L'objectif principal était de mieux comprendre — grâce à une analyse conjointe de divers ensembles de données, une évaluation des méthodes de mesure et la modélisation — la dynamique à long terme du zooplancton et ses liens directs avec l'environnement biologique et physique ainsi qu'avec les indicateurs du climat mondial.

Dans la première partie, « Identification de nouveaux biais dans les spectres de taille dérivés de l'image », chapitre II, nous avons évalué la validité des systèmes d'imagerie comme outils pour mesurer la taille de la structuration des communautés de zooplancton. Plus de 20 échantillons (plus 13 sur le filet Régent) ont été analysés au maximum d'efforts possible, c'est à dire avec une séparation manuelle des objets en contact sur la vitre du scanner, puis avec une séparation numérique de ces objets restants, suivi d'une classification visuelle complète. Les effets de différents biais sur les spectres de taille du zooplancton ont été ensuite examinés. Ces biais ont été produits par le contact des objets les uns avec les autres lors de l'acquisition des images, l'efficacité de la classification automatique et le fait d'utiliser un modèle unique au lieu d'un modèle basé sur la taxonomie pour calculer les biovolumes et les biomasses. Il a été constaté qu'il est nécessaire de séparer manuellement les échantillons avant l'acquisition des images sur le plateau du scanner, que la classification automatique n'est efficace que pour les classes de taille les plus abondantes du groupe le plus abondant et, par conséquent, qu'une correction visuelle est nécessaire au moins pour les plus grands organismes. Enfin, les disparités taxonomiques et/ou de forme en fonction de la taille des échantillons analysés étaient trop petites pour détecter une différence dans l'utilisation d'un modèle unique ou d'un modèle

basées sur la taxonomie pour convertir la taille individuelle en biovolume ou en biomasse. Il est apparu que l'utilisation de systèmes d'imagerie, tel que le ZooScan, sans séparation manuelle d'objets ni, entre autres, de correction de la séparation manuelle, peuvent donner un spectre de taille incorrect. Il est par conséquent nécessaire d'y passer du temps. Toutefois, les systèmes d'imagerie permettent un traitement rapide des échantillons et fournissent une quantité importante de données, à la fois sur la distribution des tailles et sur la taxonomie.

Dans la deuxième partie, « La variabilité inter-annuelle des écosystèmes de la mer Ligure », chapitre III, nous avons exploré la période 1995-2005 de la baie de Villefranche-sur-Mer. Cette période était la plus riche en données disponibles. Nous avons ensuite analysé conjointement le zooplancton, l'hydrologie à partir des données de sonde CTD (température, salinité, densité), les éléments nutritifs et le phytoplancton à partir des échantillons des bouteilles Niskin (nitrates, phosphates, silicates, chlorophylle-*a*), les particules en suspension à partir des mêmes bouteilles analysées avec un Coulter Coulter (distribution de taille de 3 à 90 μm), les conditions météorologiques mesurées au Sémaphore, situé à 1,2 km du site de surveillance (température, précipitations, irradiation) et le climat mondial (NHT, NAO, ENSO, AO, AMO). Le zooplancton a été échantillonné chaque semaine avec un filet WP2 allant de 60 m à la surface et les échantillons ont été analysés avec le ZooScan. Une classification visuelle en 9 groupes zooplanctoniques des grands organismes a été faite ($>$ 0,724 mm^3) et les petits copépodes issus de la classification automatique ont été utilisés (10 groupes au total). Nous avons observé un changement de régime de faible à forte abondance de presque tous ces groupes aux environs de l'an 2000, avec un décalage d'environ 2 ans entre les petits copépodes et les plus grands. Ce changement semble infirmer les tendances prévues vers une oligotrophie ainsi que les antagonismes entre certains groupes comme les copépodes, les chaetognathes et les méduses. On est frappé par la tendance clairement opposée entre les nitrates et le zooplancton par rapport à la chlorophylle-*a*. Un fort broutage semble contrôler le phytoplancton. Cela a des implications dans

l'utilisation de la chlorophylle-*a* comme indicateur de l'état trophique de la baie de Villefranche-sur-Mer et de ses fluctuations à long terme. Les principaux forçages de la variabilité inter-annuelle observée sont la force de la convection hivernale et le rayonnement solaire printanier et estival. La force de la convection hivernale est déterminée par la température et les précipitations d'hiver. La convection hivernale détermine le mélange et donc la remise en suspension des éléments nutritifs qui affecte le réseau trophique par un contrôle « bottom-up ». L'irradiation solaire printanière et estivale semble également jouer un rôle déterminant dans la dynamique inter-annuelle. Elle est fortement corrélée au zooplancton et a la possibilité d'inverser l'effet de la convection hivernale dans les deux sens (observé en 1995, 1999 et 2001). Nous supposons que cela joue sur la disponibilité de la lumière pour la croissance du phytoplancton. Enfin, des corrélations avec les indicateurs du climat apparaissent seulement sur une période plus longue, à savoir de 1960 à 2008. Quelques liens ont été constatés entre la température de l'hémisphère Nord (NHT) et l'oscillation Nord Atlantique (NAO) avec les précipitations et salinité en hiver, et entre l'oscillation multidécennale de l'Atlantique (AMO) et l'irradiation printanière et estivale.

Puis dans la dernière partie, « Modélisation continue du zooplancton basée sur la taille », chapitre IV, nous avons développé un modèle continu basé sur la taille de la dynamique du zooplancton. Les principaux objectifs du développement de ce modèle sont d'étudier les moyens possibles d'améliorer la représentation du zooplancton dans les modèles et de faire fonctionner le modèle avec les données mesurées localement. Il a été choisi de développer un modèle basé sur la taille car de nombreux processus physiologiques et inter-individuels sont proportionés à la taille. Par conséquent, le fait de ne considérer qu'une structuration de taille permet de réduire le nombre de paramètres. Ces modèles permettent également d'étudier une dynamique complexe. Le modèle actuel est un modèle continu basé sur la taille de la dynamique du zooplancton, c'est-à-dire que la formulation ne tient pas compte des classes de taille, et intègre une formulation du broutage, de la prédation, de la croissance, de la

mortalité extérieure et de la reproduction. L'entrée du modèle est l'énergie créée par le phytoplancton (le taux de croissance) et la sortie est le spectre de taille du zooplancton sur lequel nous avons mesuré le biovolume total et la pente log-linéaire. Un point clé du modèle est d'utiliser un cas mathématique particulier pour assurer certaines propriétés mathématiques et réduire le nombre de paramètres qui doivent être définis. Le cas particulier est appelé « cas infini » sur lequel le spectre est infini dans les deux sens. Dans ce cas il n'y a pas de phytoplancton et aucune mortalité exterieur : nous étendons la formulation de prédation à l'infini ; dans ce cas, la prédation sur l'extension du côté gauche est utilisée pour calculer l'affinité de broutage, de même, la prédation sur l'extension du côté droit est utilisée pour calculer les taux de mortalité exterieur. En étudiant les solutions pour atteindre un équilibre allométrique, nous avons réduit le nombre de paramètres de 13 à 7. La comparaison avec les données a été faite sur les deux scénarii principaux identifiés dans le chapitre précédent. Pour calculer l'entrée du modèle, à savoir le taux de croissance du phytoplancton, nous avons utilisé un modèle déjà mis au point pour le même endroit. Pour l'instant seule une optimisation de base a été réalisée. Il semble qu'en changeant seulement deux paramètres de leurs valeurs types obtenues dans la littérature, nous sommes en mesure de représenter assez bien la dynamique observée du zooplancton, notamment une forme saisonnière particulière de la dynamique des pentes des spectres de taille ainsi que la saisonnalité du biovolume de zooplancton. Cela tend à confirmer que les modèles basés sur la taille du zooplancton sont efficaces pour représenter des dynamiques réalistes et complexes en utilisant un nombre limité de paramètres.

Beaucoup de débouchés se dégagent de ce manuscrit, dont certains sont présentés dans les discussions générales (chapitre V). Notamment, la série temporelle de zooplancton a été étendue avec des échantillons récemment traités afin de couvrir la période 1966-2010, soit 45 années de données avec une haute résolution temporelle. Cette série temporelle apparaît comme l'une des plus longues dans le monde. En utilisant les résultats obtenus, en particulier ceux du chapitre III, nous avons

commencé l'analyse de cette série temporelle dans un contexte de changements à long terme dans l'environnement physique de la baie de Villefranche-sur-Mer. Quelques premières observations et hypothèses sont présentées à la fin du manuscrit.

ABSTRACT

Long-term monitoring of the bay of Villefranche-sur-Mer and development of new imaging methodologies to analyze zooplankton have brought about large amount of knowledge in the comprehension of marine ecosystems and of the Ligurian Sea. This thesis is a part of it. The main objective was — through joint analysis of various datasets, methodology assessment and modeling — to better understand the long-term dynamics of the zooplankton and its links with the direct biological and physical environment as well as with global climate indicators.

In the first part ("Identifying new biases from image-derived size spectra", chapter II) we have assessed the validity of imaging systems as tools to measure the size structuration of zooplankton communities. More than 20 samples (plus 13 from the Régent net) were analyzed with maximum effort, i.e., with manual separation of touching objects on the scanning tray, with numerical separation of remaining touching objects and with complete visual classification. The effect of different biases on the zooplankton size spectra were then investigated. These biases were the effects of objects in contact with each other during the image acquisition, the efficiency of the automatic classification and the effect of using a single model instead of a taxon-based one to calculate biovolumes and biomasses. It was found that it is needed to separate manually samples before the image acquisition on the scanning tray. Then that the automatic classification is efficient only for the most abundant size classes of the most abundant group, hence a visual correction is needed for at least the largest organisms. Finally, size dependent taxonomic and/or shapes differences were too small within the samples analyzed to detect some variations in using a single model or a taxon-based model of converting individual size to biovolume/biomass. It appeared that using imaging systems such as the ZooScan without manual separation of objects and correction of the manual separation, among others, can lead to incorrect size

spectrum. Hence it is needed to spend time on it. However, imaging systems allow a fast processing of samples and provide a rich amount of data, both on size distribution and on taxonomy.

In the second part ("Inter-annual variability of the Ligurian Sea pelagic ecosystem", chapter III) we have explored the time period 1995-2005 of the bay of Villefranche-sur-Mer. This period was the richest according to available datasets. We have then jointly analyzed the zooplankton, the hydrology from CTD casts (temperature, salinity, density), the nutrients and phytoplankton from Niskin bottles (nitrates, phosphates, silicates, chlorophyll-*a*), the suspended particles from Niskin bottles and analyzed with the Coulter Counter (size distribution from 3 to 90 μm), the weather from the Sémaphore station 1.2 km away from the monitoring site (temperature, precipitations, irradiation) and the global climate (NHT, NAO, ENSO, AO, AMO). The zooplankton was sampled weekly with a WP2 net from 60 m to surface, and samples were analyzed with the ZooScan. A visual classification in 9 zooplanktonic groups of larger organisms was made ($>$0.724 mm^3) and smaller copepods from automatic classification were used (total of 10 groups). We found a shift from low to high abundances of nearly all groups ca. 2000, with a time-lag of about 2 years between small copepods and larger groups. This shift seems to invalidate predicted trends toward oligotrophy as well as antagonisms between some groups like copepods, chaetognaths and jellyfish. A striking result was the clear opposite trend on inter-annual time scale of nitrates and zooplankton vs. chlorophyll-*a*. A strong grazing seems to control the phytoplankton. This has some implications in using chlorophyll-*a* as an indicator of the trophic state of the bay of Villefranche-sur-Mer and its long-term fluctuations. The main forcings of the observed inter-annual variability were the strength of the winter convection and the solar irradiation in spring / summer. The strength of the winter convection is determined by winter temperature and precipitations. The winter convection will determine the mixing and hence the nutrients replenishment that will ultimately affect larger organisms through a "bottom-up" control. Yet, the spring / summer solar irradiation also seems to play a determining role in the inter-annual dynamics. It is

strongly correlated to zooplankton and has the possibility to reverse the effect of the winter convection in both directions (observed in 1995, 1999 and 2001). We hypothesized that it plays on the light availability for the phytoplankton growth. Finally, correlations with climate indicators were only found on a longer time scale, i.e. from 1960 to 2008. Some links were pointed out between the North Hemisphere Temperature (NHT), the North Atlantic Oscillation (NAO) and precipitations and salinities in winter, and between the Atlantic Multidecadal Oscillation (AMO) and the spring / summer solar irradiation.

Then in the last part ("Continuous size-based modeling of zooplankton", chapter IV) a continuous size-based model of zooplankton dynamics is developed. The major aims of developing a model were to explore possible ways of improving the representation of zooplankton in models and to run the model with locally-measured data. It was chosen to develop a model based on size because many physiological and inter-individuals processes scale with size, hence considering only a size structuration will reduce the numbers of parameters. Such models also allow a complex dynamics. The present model is a continuous size-based model of zooplankton dynamics, i.e., the formulation does not consider size classes, and includes grazing, predation, growth, external mortality and reproduction. The entry of the model is the energy created by the phytoplankton (the growth rate) and the output is the size spectrum of the zooplankton on which we measured the total biovolume and the log-linear slope. A key point of the model is the use of a particular mathematical case to ensure some mathematical properties and reduce the number of parameters that need to be set. The particular case is called the "infinite case" on which the spectrum is infinite in both directions. In this case there is no phytoplankton and no external mortality: we extended the predation formulation to infinity and then predation upon the extended left side was used to calculate the grazing affinity; it is similar to the right side on which the predation by the right extension was used to compute the external mortality rates. By looking at solutions for an allometric equilibrium we reduced the number of parameters from 13 to 7. The

comparison with available data was made on the two main scenarii identified in the previous chapter. To compute the entry of the model, i.e., the growth rate of phytoplankton, we used a model previously worked out for the same location. Up to know only a basic optimization has been performed. It appears that by changing only two parameters from their typical values obtained from literature we are able to represent fairly well the observed dynamics of the zooplankton in the two main scenarii, notably a particular seasonal shape of the dynamics of the slopes as well as the seasonality of total biovolume of zooplankton. This tends to confirm that size-based models of zooplankton are efficient to represent realistic and complex dynamics with a limited number of parameters.

Many prospects emerge from this manuscript, some of them are presented in the general discussions (chapter V). In particular, the time series of zooplankton was extended with recently processed samples to cover the period 1966-2010, i.e., 45 years of data with a high temporal resolution. This time series appears as one of the longest in the world. Using findings from mainly chapter III we started analyzing this time series in a context of long-term changes in the physical environment of the bay of Villefranche-sur-Mer. Some first observations and hypotheses are presented at the end of the manuscript.

CONTENTS

List of Figures

List of Tables

GENERAL INTRODUCTION I

THE marine realm and its inhabitants are a fantastic area of discovery and, besides their beauty, play a major role in the global earth system. The living part of the water column is composed — apart from marine mammals and adult fishes — of plankton (from the greek *planktos*, i.e. drifter, wanderer). Then, plankton represent the most part of the sea life. A distinction is made between its different components, the viroplankton, the bacterioplankton, the nano-, micro- and macro-phytoplankton, the micro-, meso- and macro-zooplankton. This thesis is focused on mesozooplankton and their links with other plankton components as well as with the chemical and physical environment. The mesozooplankton comprises all animals living in the water column from about 200 μm length to few mm and belonging to various taxonomic groups such as crustaceans, cnidarians, ctenophors, gastropods, chaetognaths, annelids, tunicates and fish larvæ. The most important group, in terms of abundance, being the crustaceans and especially copepods, (see Mauchline 1998, for a review of marine calanoid copepods) which play major roles in marine food webs and biogeochemical cycles (e.g., Smetacek 1985, Banse 1995, Verity & Smetacek 1996, Mackas & Beaugrand 2010). Copepods transfer energy from phytoplankton to higher trophic levels such as fish and large gelatinous predators. More than 80 years ago, Charles Elton said, “It will be shown that the periodic fluctuations in the number of animals must be due to climatic variation” (Elton 1924). With the growing concern on climate change, tracing and understanding the impact of climate onto the dynamics of marine animals and ecosystems has become a major issue in biological oceanography (e.g., Aebischer et al. 1990, Fromentin & Planque 1996, Beaugrand & Ibañez 2002, Drinkwater et al. 2003, Mysterud et al. 2003, Stenseth & Mysterud 2003, Richardson 2008, Kirby & Beaugrand 2009, Berline et al. accepted, Mackas & Beaugrand 2010, Goberville et al. 2010). Because of their rapid

response to ecosystem variability, their non-exploitation for commercial purposes and their amplification of subtle changes through non-linear processes, zooplankton have been pointed out as good sentinels of climate changes (Taylor et al. 2002, Perry et al. 2004, Hays et al. 2005).

I.1 Zooplankton changes in the Mediterranean Sea

The Mediterranean Sea is the largest quasi-enclosed sea on the Earth connected to the Atlantic Ocean through the Gibraltar strait that is only 14 km width. The Mediterranean has a total area of nearly 2.5×10^6 km^2 (52000 km^2 for the Ligurian Sea) and 46000 km of coasts which makes the coast / surface ratio particularly high (Meybeck et al. 2007) and highlights the importance of the land-sea interface and of the impact of human activities. The Mediterranean geology and particular climatic features allow for a rich and complex physical dynamics with unique thermohaline features, distinct multilayer circulation, topographic gyres, meso- and submeso-scale activity (Zavatarelli & Mellor 1995, Millot 1999, Pinardi & Masetti 2000). A nice review of the Mediterranean Sea, focused on plankton and factors affecting it had been recently published by Siokou-Frangou et al. (2010).

The trophic state of the Mediterranean Sea ranks from oligotrophic to ultra-oligotrophic, with a clear decrease from the western to the eastern basin and from the north to the south (D'Ortenzio & d'Alcala 2009). According to phytoplankton biomass, estimated as chlorophyll-*a* from remote sensing, different oceanic provinces were defined (D'Ortenzio & d'Alcala 2009). The North Western (NW) region shows patterns similar to temperate areas, unique in the Mediterranean Sea, consisting in a late winter / spring phytoplankton bloom lasting as long as three months with a biomass increase up to 6 times the background value (Levy et al. 1998) and a frequent autumn bloom. The coastal and central parts of the NW Mediterranean belong to another province characterized by an intermittency of temperate and subtropical modes, i.e. more oligotrophic and less marked spring bloom (D'Ortenzio & d'Alcala 2009). The rest of the Mediterranean is less productive, except for regions affected by

river runoff, atmospheric fertilization, or continental shelf dynamic: mainly Alboran Sea, Adriatic Sea, south of Tunisia, Catalan front, Gulf of Lion. This applies however only to autotrophs. The low standing stocks of them are generally justified by "bottom-up" constraints. It was however shown that purely heterotrophic processes may produce a rapid transfer to higher levels, even in less productive area, suggesting possible strong "top-down" effects (Thingstad et al. 2005, for ciliates and bacteria). Therefore, two possible views emerged, the low abundance of autotrophs being the result of low nutrients availability or being the result of an effective control by grazers, with a trophic cascade propagating up to top predators (Siokou-Frangou et al. 2010). The latter view is supported by the observation that standing stocks of top predators (fishes) are higher than would have been expected on the basis of chlorophyll-*a* and nutrient stocks (Fiorentini et al. 1997). "Bottom-up" and "top-down" controls can both affect the structure of food webs. This is at the origin of the "Mediterranean paradox" (Sournia 1973, Estrada 1996, Siokou-Frangou et al. 2010), which moderates the view of the Mediterranean Sea as an oligo- to ultra- oligotrophic Sea.

Some trends toward oligotrophy have recently been observed in marine basins (Molinero et al. 2005; 2008, Barale et al. 2008, Mozetic et al. 2010, Steinacher et al. 2010) suggesting climate driven changes in the trophic states of ecosystems. Regime shifts, i.e., abrupt changes in the state of a system, were reported with effects on zooplankton communities. For example, in the Atlantic ocean, a regime shift from cold to warm biotopes, with a turning point in 1987, has been described and related to the North Atlantic Oscillation (NAO, Hurrell & Deser 2010) and surface temperature anomalies in the Northern Hemisphere (NHT, Reid et al. 2001; 2003, Beaugrand 2004, Beaugrand et al. 2008). Regarding Mediterranean plankton, very few studies on long-term variations have been conducted, due to the paucity of long-term time series (Mazzocchi et al. 2007). Recently, it has been highlighted the appearance of regime shifts — toward more oligotrophic states — with their turning points in 1987 in two northern Mediterranean coastal ecosystems (Adriatic and Ligurian Seas) and their synchrony

with changes in the Atlantic Ocean and the Baltic and Black seas (Conversi et al. 2010). The authors pointed out the positive trend of surface temperature in the northern hemisphere as the main forcing for the concomitant changes in such far and different regions. In the Balearic Sea (Fernàndes de Puelles et al. 2007, studied period: 1994-2003), a decrease of zooplankton abundance was observed from 1995 to 1998 with a recovery of all groups from 2000. Such an inter-annual variability was linked to the NAO forcing. In its positive phase, the NAO drives colder temperature during winter months enhancing the southward spread of rich northern Mediterranean waters in the Balearic Sea (Fernàndes de Puelles et al. 2007, Fernàndes de Puelles & Molinero 2008). From a comparative study of six zooplankton time series in the Mediterranean Sea, synchronous cooling and warming phases was observed in Trieste, Naples and Villefranche-sur-Mer, with, again, a main turning point in 1987 associated to a decrease of zooplankton abundances (Berline et al. accepted) — yet, no significant links with large scale climate indicators such as the NAO were found. Other studies in the Ligurian Sea, based on a long time series (1963-1993) in the bay of Villefranche-sur-mer, have also suggested that the pelagic ecosystem was heading toward a more regenerated system dominated by jellyfish in the early ’90s (Molinero et al. 2008). A more recent study from the same time series extended until 2003 revealed that the zooplankton and mainly copepods recovered their initial concentrations after 2000 suggesting a quasi decadal cycle (Garcia-Comas et al. Submitted). Such a recovery from ca. 2000 was also observed by Berline et al. (accepted) in Villefranche-sur-Mer, by Fernàndes de Puelles et al. (2007) in the Balearic Sea. In Naples the recovery occured in 2004 (Berline et al. accepted). The higher abundance of zooplankton were correlated to dry and cold winter resulting in high winter mixing. Dry and cold winters lead to a rise in surface density increasing the winter convection and, as suggested by the authors, enhancing nutrients replenishment and strengthening the spring bloom. The positive effect of dry winters was observed on the entire zooplankton community suggesting that it was controlled by it’s resource. This hypothesis of a strong “bottom-up” control

initiated by the intensity of the winter convection is also supported by observations in the southern and central Ligurian Sea (Goffart et al. 2002, Nezlin et al. 2004, Marty & Chiavérini 2010), yet with no consideration of zooplankton.

The Mediterranean appears then as a complex system with a strong heterogeneity at the basin scale, but also at the mesoscale. To understand the zooplankton dynamics and how it is affected by environmental and climatic factors different approaches can be followed. A very promising approach is based on the size distribution of zooplankton communities and will be presented hereafter.

I.2 Size-based analysis and modeling of the zooplankton

Common models utilized for investigating marine ecosystems are partitioned in different boxes (nutrients, phytoplankton, zooplankton, detritus) each of them being defined by an input and an output of matter. To make this kind of models more realistic, authors generally try to add more and more boxes — the zooplankton box becoming for example: copepods and appendicularians. Each box is defined by a gain and a loss of matter at each time step — generally computed by one equation (Fasham et al. 1990). But these models drive to a multiplication of links and parameters (Moloney & Field 1991) that are not available and consequently are generally arbitrary in such models. An observation allows to avoid this problem: organisms belonging to different taxonomic categories can be grouped according to their size. This means that, for example, a fish larvæ is closer to an adult copepod than to an adult fish of the same species (Bertalanffy 1957, Peters & Wassenberg 1983). Hence, it becomes possible to simplify zooplankton by a measurement of their biomass by size, the so-called biomass-size spectra (N-BSS, Sheldon et al. 1972, Platt & Denman 1977). This is “A simple, understandable, first-order approximation to the dynamics of the system as a whole” (Heath 1995). A mathematical framework has emerged from this measurement, used to calculate some parameters of the ecosystem like the standing stock of a trophic level (e.g., monsters in loch Ness) knowing another one (Sheldon

& Kerr 1972) and several other parameters (Edvardsen et al. 2002, Zhou 2006). This measurement starts to be commonly used in ecosystem models (Moloney & Field 1991, Moloney et al. 1991, Gin et al. 1998, Armstrong 1999, Benoît & Rochet 2004, Baird & Suthers 2007, De Eyto & Irvine 2007, Maury et al. 2007a;b, Stock et al. 2008, Zhou et al. 2010). A review of models for zooplankton studies can be found in Carlotti & Poggiale (2010). The following sections will present the importance of size for the physiology and the interactions within zooplankton. Theoretical and modeling studies based on the size spectrum will also be shown.

I.2.1 Meaning of size for zooplankton

It is now well known that physiological rates scale with size more than with taxonomy (Bertalanffy 1957, Fenchel 1974, Peters & Wassenberg 1983, West et al. 2003, Glazier 2005, Hendriks 2007). It is also commonly accepted that the scaling has the form (Brown et al. 2004)

$$Y = \alpha x^{\beta} \tag{I.1}$$

where Y is the response (for example metabolic rate), x the size, α a normalization constant and β the scaling exponent. If β equals 1, the relation is isometric, otherwise it is allometric. This relation is linear but this is not always the case as it can also be non-linear. There are different kinds of possible scaling in nature. Glazier (2005), in the continuum of Bertalanffy (1957), separated four kinds of relations. But for the sake of simplicity most of the works used the linear one (type I). This kind of scaling (power-law) is considered to be universal (Stanley 1995). Marquet et al. (2005) reviewed these power-laws in ecological systems.

Yet, this is not always the case in biology (e.g., Chaui-Berlinck 2006, O'Connor et al. 2007), but a large part of the scientific community went further by arguing that the exponent α of the relation is always $3/4$ (West et al. 2003, Brown et al. 2004). This $3/4$ scaling is usually observed in allometric regression but, as shown by Glazier (2005), in a comprehensive review, it is more like an average in

nature as it can sometimes be very far from this value. Copepods, for example, show a mean scaling exponent of 0.84 and, if we include all other pelagic species, this exponent rise to 0.94 (Glazier 2005). This scaling is explained by the fractal geometry of organisms, while an euclidean geometry would lead to a $2/3$ scaling (Peters & Wassenberg 1983), also observed in nature (Glazier 2005). Yet, Brown et al. (2004) proposed the "metabolic theory of ecology", a size-based allometry with an exponent of $3/4$ and a temperature normalization (i.e., $e^{-E/kT}$). This is a simplification of the complex ensemble of physiological processes but it may suffice to study high levels of organization like ecosystems. Starting from the same type of relation, other authors gave more complex definitions of allometric scaling that allowed for different values of the exponent (Demetrius 2006, Hendriks 2007, da Silva et al. 2007).

Another way of explaining the relation between size and physiology emerged from the so-called "Dynamic Energy Budget" theory (DEB, Kooijman 1986; 2001, Nisbet et al. 2000, van der Meer 2006, Sousa et al. 2006; 2008). In this theory, the $3/4$ scaling was not assumed but found back very easily. This global model of the physiology of organisms can have different parameters and variables but the main mechanisms are the same for all living organisms (Kooijman 1986; 2001). A fraction of the energy ingested is assimilated while the other part is directly rejected (feces). The assimilation is then separated in two fractions: one for the soma and the other one for the gonads and reproduction (plus maintenance costs). Between organisms of different species, parameters can change, but between organisms of the same species the only differences occur in the state variables, i.e., reserve and structural mass. Using DEB theory, a small organism invests relatively less energy in somatic maintenance than a larger one, so a small organism has a metabolic rate lower than that of a large organism of the same species. Metabolic rates are linear combinations of actual body length and volume. Using realistic parameters the scaling exponent of these relations is often close to $3/4$

(Nisbet et al. 2000). This theory seems to be a good approach to the physiology of individuals and has been used by Maury et al. (2007a) to model the physiology of the consumers in an ecosystem model.

Size is also of great importance in the way organisms get in contact for processes such as predation, grazing, mating, swarming or aggregation (e.g., Jackson 1990, Jackson & Burd 1998, Kiorboe 2001, Kriest & Evans 2000, Jackson & Kiorboe 2004, Stemmann et al. 2004a;b, Visser & Kiorboe 2006, Visser 2007). Encounter rates in marine environment were first studied on inert particles by Jackson (1990) who proposed a model to calculate the probability of encounter of two particles defined by their size based on different processes: the Brownian diffusion, the differential sedimentation and the shear or turbulence. The Brownian diffusion is the intrinsic behavior of particles. The model of Jackson et al. (1995) was used by Baird & Suthers (2007) to model encounter rates between living organisms in a size-resolved pelagic ecosystem. In the perspective to resolve a global model by size, models of encounter rates are useful because all kernels (processes by which encounters occur) are related to the size of particles (living or not). Yet, for zooplankton, the behavior is far more complex than a Brownian motion and is affected by many external factors (e.g., Schmitt & Seuront 2001, Schmitt et al. 2006, Vandromme et al. 2010) — this is why some studies have been undertaken to describe other processes. For example, Jackson & Kiorboe (2004) give a kernel formulation for finding particles by zooplankton using a chemodetection of the chemical plume following particles in marine environment — such formulation being also related to the size of both zooplankters and particles. This can be added to other grazing behaviors defined by Visser (2001) like ambush, cruising or flux feeding (also related to size). The last step is to define the encounter mechanisms and rates between living zooplankton. An attempt was made by Visser & Kiorboe (2006) to define the encounter kernel for two kinds of movement: ballistic and diffusive. The shift between these two motion behaviors depends on the interaction scale compared to the movement scale. The variety of swimming behaviors in zooplankton is very large but some simplifications can work: e.g., Baird & Suthers (2007) used the

simple curvilinear model of Jackson et al. (1995) to represent all the interactions between particles in a pelagic ecosystem.

I.2.2 Measuring the size

In this study we focus on the measurement of biomass or abundance size spectrum of mesozooplankton. The traditional method to obtain data on zooplankton size is the use of plankton tows for collecting samples, and then microscopes for manual classification, counting and measurement of size. These steps are labor-intensive and limit the number of samples and/or organisms that can be processed. Hence, automated techniques were developed since the '60s to obtain rapidly data on size directly *in situ* or in laboratory from net sampling (Wiebe & Benfield 2003, Benfield et al. 2007, and references therein). Some of these new techniques measure only the size, through optical or electronic methods. Among them the most used were the Coulter Counter (Parsons 1969), the Optical Plankton Counter (OPC Herman 1992) and the Laser-OPC (L-OPC Herman et al. 2004). These instruments can be used *in situ* or in laboratory and measure the shadow of all particles crossing a light beam (OPC), a laser (L-OPC), or the electronic signal disturbance (Coulter Counter). A major problem is that these techniques do not distinguish the kind of particles, i.e., detritus or living organism and do not provide the orientation of the particle when crossing the detector — this is a problem because all particles are not spherical. Nevertheless these tools have been used in numerous studies (more than 100 for the OPC from ISI web of knowledge) and had brought about a large quantity of new data and knowledge.

Improvement of size measurements came from imaging systems which offer the possibility to record an image of each object. Then, images obtained in the laboratory or in situ can be processed automatically by software which performs classification, counting, and size measurements (Jeffries et al. 1984, Rolke & Lenz 1984, Gorsky et al. 1989, Grosjean et al. 2003, Benfield et al. 2007, Bell

& Hopcroft 2008, Gorsky et al. 2010). It became possible to sort the images in different categories. First plankton images were measured by silhouette photography (Ortner et al. 1979). Then, in the late 80s, *in situ* imaging systems such as the Underwater Video Profiler (UVP) (Gorsky et al. 1992) were created, among others, to characterize plankton community structure and to estimate the fluxes to the deep ocean (Benfield et al. 2007). Preserved samples of micro- and meso-plankton can also be treated by automated systems such as the FlowCAM (a flow cytometer adapted to microplankton) and the ZooScan (a scanning system adapted to water samples of mesozooplankton) (Sieracki et al. 1998, Grosjean et al. 2003, Gorsky et al. 2010). Imaging systems allow the user to identify what is measured and how it is done, since different size categories can be measured through image analysis. Imaging systems and their future prospect were reviewed by Benfield et al. (2007) while all kinds of instruments used to measure plankton were reviewed by Wiebe & Benfield (2003). A sketch of these different instruments is presented in fig. I.1. All the aforementioned instruments ultimately allow the measurement of the size distribution of organisms, i.e., size spectra — according to user-made classification for imaging systems (see section I.3.2).

I.2.3 Size-based theory and models

The model of Platt & Denman (1977) was one of the first to explain the distribution of biomass by size in aquatic ecosystems, and probably the most used. It is more complex than previous models such as the one of Sheldon et al. (1977) which represents a simple food chain, whereas Platt & Denman (1977) presented ecosystems as food webs (Borgmann 1987) where predators are able to feed in more than one lower trophic levels. Their model has been widely used and most of the successive models were improvement of it (e.g., Silvert & Platt 1978, Borgmann 1982, Heath 1995, Zhou & Huntley 1997, Zhou 2006, Zhou et al. 2010). The model of Platt & Denman (1977) is based on a normalized continuous size spectra expressed in logarithmic scales. Logarithmic scales represent the scaling in

nature: we need thinner size classes for zooplankton than for whales. They have also introduced the concept of normalization, which is made by dividing the value of the spectrum for a particular size by the size of the bin:

$$\beta(w) \cong \frac{b(w)}{w} \tag{I.2}$$

where w is the size (or weight) of organisms, b the biomass-size spectrum and β the normalized biomass-size spectrum (N-BSS). This step of normalization is necessary because biomass must always be expressed relating to some size range. If the spectrum is not normalized, the ordinate is not the number of individuals (or biomass) of size w, but of a size class whose lower limit is w and upper limit cw, where c is the log base used to built the classes. It is much more useful to normalize the raw data by the class width, to get a function that does not depend on the partition size (Blanco et al.

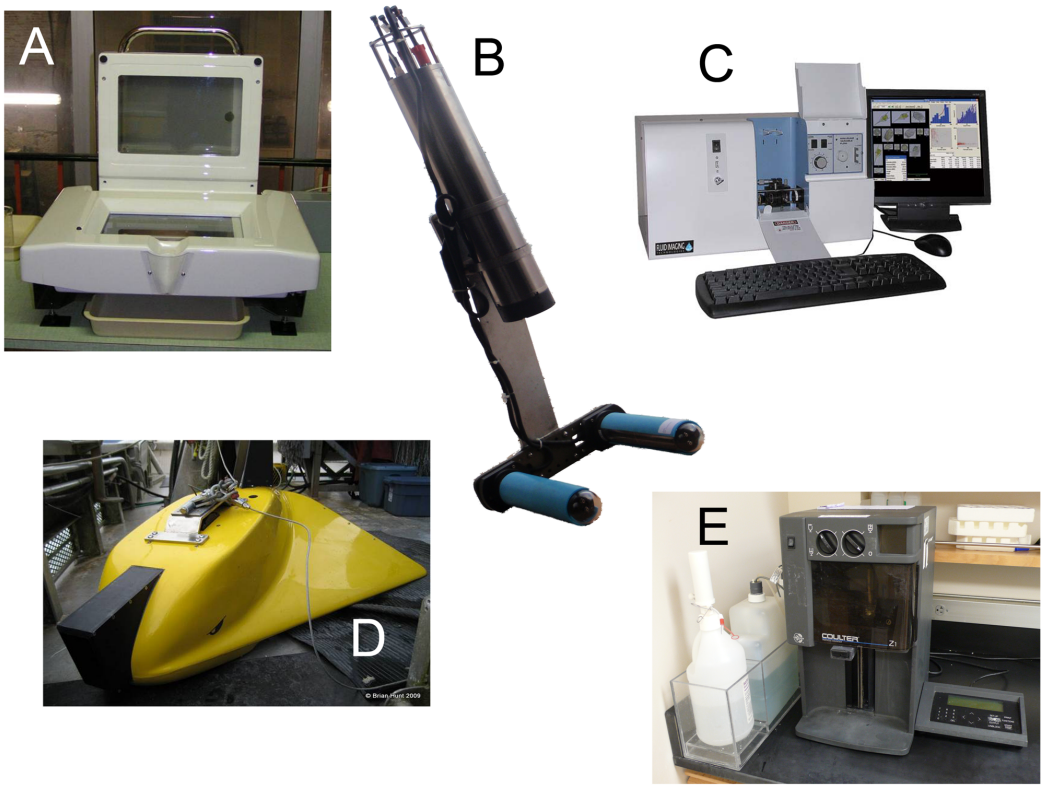

Figure I.1 – *Sketch of the different instruments mentioned in the text that are commonly used to measure the size distribution of a community. Some only measure the size of particles without any discrimination — OPC (D), Coulter Counter (E) — whereas other are also used to perform an identification — FlowCAM (C), ZooScan (A) and UVP (B). Copyright Marc Picheral (A, B), Brian Hunt (D), fluidimaging (C) and Tim Vickers (E).*

1994). Then, departing from this N-BSS, Platt & Denman (1977) proposed a solution for a steady-state pelagic ecosystem. To solve the N-BSS they first considered the flux of biomass, of which the simplest estimate is the total biomass in the band divided by its turnover time. Then they used an empirical estimate of the turnover time, a power-law given by Fenchel (1974). In a thermodynamical sense the flux cannot be conservative so we have to consider the different losses of the system. Platt & Denman (1977) included here the respiration and losses to the detritus food chain. Losses due to respiration are given using the relation for the weight dependence of metabolism found in Fenchel (1974). Assimilation of these process drive to the main equation proposed by Platt & Denman (1977) to describe the N-BSS:

$$\frac{\beta(w)}{\beta_0} \sim \left(\frac{w}{w_0}\right)^{-(1-x+\alpha A+q)} \tag{I.3}$$

where x is the turnover time of body weight, αA the time scale of system energy loss and q an exponent for feeding efficiency. According to Borgmann (1987), the model of Platt & Denman (1977) is not directly comparable to others (Sheldon et al. 1977, Borgmann 1982) and gives a steeper slope because there is no mechanism to decrease the biomass in one trophic level and to increase it in another one such as it occurs during predation. But by assuming that biomass flux due to predation is proportional to turnover rates we can introduce a predation in this model. Doing this, results are analogous to Platt & Denman (1977) but with an additional proportionality constant which gives a solution of the slope equivalent to the models of Sheldon et al. (1977) and Borgmann (1982) (Borgmann 1987).

A generalization of the model of Platt & Denman (1977) is given in Silvert & Platt (1978). They generalized this model in time and for non-steady-state. Moreover, they included a predation term in their equations. The general equation is then

$$\frac{\partial \beta}{\partial t} + \frac{\partial (\beta\, g)}{\partial w} + \mu\, \beta = 0 \tag{I.4}$$

where g is a general growth term depending on both growth of particles and predation by larger

particles and μ the energy lost by the system, in a steady state $\partial\beta/\partial t = 0$. This gives a slope of the N-BSS equals to $x-1-\alpha A$ when assuming that respiration dominates the loss term and individual growth dominates the growth term (Platt & Denman 1977). If we add the predation we can no longer make simplifications and the slope becomes

$$x - 1 - \left(\frac{\alpha A}{\gamma + x} \left(w + g(w)\mathrm{d}t \right)^{\gamma+x-1} \right) \tag{I.5}$$

without predation $\gamma+x=1$. Then, in a non-steady state — and assuming that $\beta_0(w)$ is the steady-state solution — we have the N-BSS at time t equals to

$$\beta(w,t) = \beta(w_0,0) \cdot \frac{\beta_0(w)}{\beta_0(w_0)} \tag{I.6}$$

with w_0 the initial weight range of the biomass carried to w during the time t. According to Silvert & Platt (1978) this model is more rigorous than the one of Platt & Denman (1977), i.e., it does not require to measure the weight on a logarithmic scale and the transition from finite-difference to continuous mathematics is more secure. The interpretation they gave for the general solution (eq. I.6) is that a peak in the biomass spectrum will propagate intact through the spectrum, without any spreading, which is due to the simplicity of this model (Silvert & Platt 1978).

Such models developed in the '70s and early '80s were used as a framework for many other studies which have improved them. After Platt & Denman (1977), Thiebaux & Dickie (1993) and Heath (1995) for example, proposed different solutions for the modeling of the N-BSS. In Heath (1995) the energy balance was between growth and mortality while it was between growth and respiration in Platt & Denman (1977). Yet, the solution of the N-BSS should be unique and objective. Zhou & Huntley (1997) proposed to unify the models of Platt & Denman (1977) and Heath (1995) and provided a new model "without any" approximations on processes. They gave the following equation of the biomass spectrum

$$\frac{\partial b(w,t)}{\partial t} + \frac{\partial [wgb(w,t)]}{\partial w} = gb(w,t) + \mu b(w,t) \tag{I.7}$$

where g is the specific growth rate of a given class of weight and μ the intrinsic rate of abundance increase (change in population number by birth, death and predation). On the left side of this equation, the first term represents the rate of change in biomass within unit weight intervals and the second term represents the net flux of biomass through a weight intervals due to individual growth. On the right side, the first term represents the change in biomass due to individual growth, and the second term the change in biomass due to a change in population number. For a steady-state, the slope (s_b), computed on the basis of the above equation is

$$s_b = \mu / g \tag{I.8}$$

where μ is negative. This gives the slope of the N-BSS. But for a steady state, a balance is needed so μ must be positive under a critical weight. This corresponds to the birth: eggs or larvæ have lower weight than their parents. So in steady-state, the slope of N-BSS is governed by birth, death, predation and the specific growth rate of individuals. Zhou & Huntley (1997) gave also solutions for non-steady state. By making simplifications based on the magnitude of the terms previously used. The general equation becomes then

$$\frac{\partial b}{\partial t} = b\overline{g}\left[\overline{\frac{\partial \ln b}{\partial \ln w}} - \frac{\partial \ln b}{\partial \ln w}\right] \tag{I.9}$$

where $\bar{\cdot}$ is a time average. We can easily use this equation to estimate the rate of change in biomass or production for plankton (only between 10^0 and 10^4 μg C, a range used to make the approximations). Zhou & Huntley (1997) then used these equations to predict population dynamics with observed biomass spectra. Later, Edvardsen et al. (2002) used Zhou & Huntley (1997) theory to deduce μ and g from biomass-size spectrum. By merging and simplifying these methods, Zhou (2006) proposed a more general description of processes determining a size spectrum. Considering a size spectrum, from time t to t_{+1}, changes in a specific size class are due to the biomass import from the left border

(growth of smaller individuals), the biomass removal due to reproduction, death and predation, the recycle of biomass between different trophic levels and the growth of all individuals.

Other conceptual frameworks exists in literature with, for example, some attempt to reducing size spectra dynamics to a single process, e.g., predation (Camacho & Solé 2001) or asymptotic growth (Andersen & Beyer 2006). The size spectrum can also be viewed through the metabolic theory (Brown et al. 2004). The metabolic theory gives a theoretical background for the physiology based on the empirical observation of a constant $3/4$ scaling in nature — but see Glazier (2005) or Demetrius (2006) for a critic of this universal value. By increasing the scale, we reach the ecosystem level. Brown et al. (2004) proposed equations for the standing stock of biomass, the energy flux and biomass production, the biomass turnover and energy flux, and the abundance-size spectrum. They considered two parameters to describe the abundance-size spectrum. The first one is the Lindeman efficiency (α), which characterizes the loss of energy between two adjacent trophic levels 0 and 1 and is always <1 (due to inefficiency in transferring the biomass). The second parameter β is related to prey/predator size ratio and is only added for pelagic ecosystems, because in such ecosystems there are powerful body size constraints on the flow of energy, the size increasing from primary producers to top predators, which is not the case in terrestrial ecosystems. This leads to an estimation of the total number of organisms for a given size as being:

$$N = N_0 \left(\frac{M}{M_0}\right)^{[\log\alpha/\log\beta]-\frac{3}{4}} \tag{I.10}$$

Since Brown et al. (2004) considered Lindeman efficiency to around 10% and the predator/prey body size ratio to about four orders of magnitude, we have $\log\alpha/\log\beta = -1/4$. Consequently, abundance declines with body size as $-1/4-3/4=-1$, which is consistent with common thinking and observation (Sheldon et al. 1972). This solution is mostly theoretical, based on empirical observations and assumptions of individual level processes.

The size spectrum has also been viewed in a completely thermodynamical point of view (Schnei-

der & Kay 1994, Choi et al. 1999) where the life and its increasing complexity is not only driven by evolution but also by the need of dissipating energy (Schneider & Kay 1994). If we view the earth as an open thermodynamic system with a large gradient impressed by the sun, the thermodynamic imperative is that the system will strive to reduce this gradient by using all physical and chemical processes available to it. The solar energy is here the negentropy input (i.e., it creates order). So, Schneider & Kay (1994) suggested that life exists on earth as a mean to dissipate the solar induced gradient (with the exception of some deep sea areas, anyway this is the same process). This is similar to ecosystems which can be thermodynamically analyzed. In this sense, ecosystems are viewed as the result of the biotic, physical and chemical components acting together as a dissipative process. The maturation of ecosystems will make them being more and more effective dissipative structures, and the processes involved are: more energy capture, more energy flow activity, more cycling, higher average trophic structure, higher respiration and transpiration, larger ecosystem biomass and more types of organisms. All these processes are used to compute some goal-functions to measure perturbation in ecosystems (e.g., the determination coefficient r^2 between the observed spectrum and a power law as in Choi et al. 1999).

I.2.4 Incorporating size in models

The theoretical framework presented above was used for biogeochemical models. A biogeochemical model simplifie the reality to reproduce the pathway of matter, i.e., generally carbon, nitrogen or energy, through the different physical and biological boxes of an ecosystem — zooplankton being one of them. Two major possibilities to model the zooplankton have emerged. The first one is based on the multiplication of sub-boxes inside a major zooplankton box, each of them defined by a single differential equation (e.g., Le Quere et al. 2005, Vichi et al. 2007). The second one is base on zooplankton size structure and such models seem adapted to regional and to seasonal towards pluri-annual scales

(Carlotti & Poggiale 2010). The structuration by size in models was first made by Moloney & Field (1991) but was mainly used for fish (Jennings et al. 2002, Benoît & Rochet 2004, Andersen & Beyer 2006). In the model of Maury et al. (2007a) the size structuration appears for the consumer (of phytoplankton) but most parameters were taken from fishery literature. Few size-based models specifically dedicated to zooplankton exist (e.g., Baird & Suthers 2007, Zhou et al. 2010). Recently, Carlotti & Poggiale (2010) presented a review of existing zooplankton models and their spatio-temporal scale and utilities. In the followings paragraphs, the focus will be put on three models: (1) Baird & Suthers (2007), which uses allometric relationships and an aggregation model for encounter rates (Jackson et al. 1995); (2) Maury et al. (2007a), in which the physiological formulation is based on the DEB theory (Kooijman 2001); and (3) Zhou et al. (2010) which is based on the framework developed by Zhou & Huntley (1997) and incorporates a direct comparison to observations. They will be the subjects of the following paragraphs. These models are the most recent that use size to model the zooplankton dynamics.

The biological part of the model of Baird & Suthers (2007) consists in allometric relationships which determine physiological rates. This part is separated in three functional groups (phytoplankton, protozoans and metazoans) spreading over 62 size-classes. Size of metazoans and allometric relationships used for them correspond to zooplankton (mainly copepods). These relationships are empirical — mainly from Hansen et al. (1997) — and do not come from the "Metabolic Theory". Metazoans are defined by predation, growth and reproduction. They obtain their biomass from phytoplankton, protozoans and metazoans. The predation is defined by an encounter rate of prey that is related to size using the curvilinear formulation of aggregation of Jackson et al. (1995) followed by selectivity and affinity formulations. The metazoans life cycle involves growing over many orders of magnitude from an egg to an adult capable of reproduction. Biomass comes from smaller prey through the process of predation and goes back to smaller sizes by spawning and mortality (biomass goes back to nitrogen

pool and is assimilated by organisms). Another limiting factor is added to the metazoans cycle to represent the predation of larger organisms unsettled in this model. All these processes are resolved by size, in a discrete way. To summarize the results of the model, the N-BSS theoretical framework of Platt & Denman (1977) is used. This model is purely theoretical and has not been validated by field measurements. Conclusions on this model are satisfactory, the size based approach avoids the proliferation of model parameters when increasing the number of compartments and the need to change the model formulation for every change in model structure (the addition of a new compartment).

The model of Maury et al. (2007a;b) is close to the one of Baird & Suthers (2007) in the sense that it is based on physiological relationships scaled with size — this is a mechanistic and deterministic model. Yet, their model is based on the DEB theory (Kooijman 1986; 2001, Nisbet et al. 2000). This model considers two functional groups: the producers and the consumers — decomposers are ignored for simplicity. Consumers (zooplankton and fishes) is the only group resolved by size. Processes used to model consumers are predation, mortality, assimilation and the use of energy for maintenance, growth and reproduction. All the physiological processes used here are size and temperature dependent. The basic equation of consumers dynamics is based on the McKendrick-Von Foerster equation (steady-state equation for conservation of mass):

$$\begin{cases} \frac{\partial \xi^c_{t,w}}{\partial t} = -\frac{\partial(\gamma_{t,w}\xi^c_{t,w})}{\partial w} - (\lambda_{t,w} + Z_w + M^{starv}_{t,w})\,\xi^c_{t,w}\dots \\ \dots \forall w \subset [w_{eggs}; w_{max}] \\ \xi^c_{0,w} = \xi^0_w \end{cases} \tag{I.11}$$

with $\xi^c_{t,w}$ the energy-size spectrum of consumers, γ the growth rate, λ the mortality rate due to predation, Z the loss of energy due to non-predatory mortality and M^{starv} the mortality due to starvation. t and w refer to time and weight. Maintenance, growth and reproduction are modeled using the DEB theory. In the DEB theory, the ingested energy is assimilated by organisms and stocked into reserves. A fixed fraction κ of the energy is then allocated to growth and somatic maintenance. The other fraction $1-\kappa$ is devoted to gonad development, maturity maintenance and egg formation. Every

consumer organism is described by the same set of physiological relationships using a total of 18 parameters for the whole model. The DEB theory drives the conceptualization of each process. According to this theory, the maximum amount of preyed energy that can be ingested by a predator for example, is a function of body surface. The growth depends also on body volume. It corresponds to the use of a fraction κ of the assimilated energy diminished by a maintenance cost proportional to the organism body volume and finally converted into structural material at an energy cost proportional to growth (according to Kooijman 2001). Reproduction is the use of the fraction $1-\kappa$ of the assimilated energy diminished by a maintenance cost proportional to $(1-\kappa)/\kappa$ times the body weight. Starvation mortality corresponds to the end of growth and reproduction, and to the use of stored energy for maintaining the basic metabolism. At ecosystem level, this is a net dissipation of energy. To conserve the mass it is considered that the quantity of energy that is needed for maintenance but cannot be provided by food intake, is removed from the ecosystem. Starvation acts as a mortality term at the level of the ecosystem. And the non-predatory mortality is simply considered as a decreasing allometric function. All parameters are linked to temperature. This enables the authors to perform simulations in a companion paper (Maury et al. 2007b), with the main conclusion that an increase of temperature of 2-4°C would lead to a 20-43% decrease of biomass in oligotrophic regions and 15-32% in eutrophic regions. DEB theory appears here to be more realistic and avoids the problems that occur when dealing only with allometric relationships. For example, if the biomass of prey tends to infinity, the growth rate of predators will also tend to infinity when using allometry. This generates instability in the model (Benoît & Rochet 2004). When using a DEB approach, any organism targets a maximal amount of energy to meet its needs and cannot eat more than its demand, consequently growth rate is limited. The same kind of auto-limitation appears in the other processes. DEB theory allows taking into account more biological and ecological processes in a rigorous mass-balanced physiologically-based formulation.

The last model dealing with zooplankton in a size-based context is the one of Zhou et al. (2010), a size spectrum zooplankton closure model. To the best of my knowledge, this is also the first model of this kind that integrates observations by taking the time series of temperature and chlorophyll-*a* as inputs and by comparing outputs of the model to observations — here the abundance of mesozooplankton. The model is based on the size spectra theory previously developed, mainly works of Zhou & Huntley (1997) and Zhou (2006), and a more complex formulation of the growth of zooplankton based on works of Huntley & Boyd (1984) and Hirst & Bunker (2003). The core equation of the model of Zhou et al. (2010) represents the biomass flux conservation:

$$\frac{\partial \ln b}{\partial t} + g\frac{\partial \ln b}{\partial \ln w} = \mu - \frac{\partial g}{\partial \ln w} \tag{I.12}$$

where b is the normalized biomass spectrum (m^{-3}), w is the individual body weight (mgC), g the specific individual growth rate (d^{-1}) and μ the specific rate of net abundance change (d^{-1}). The notation is the same as in previous models. Then the zooplankton closure term for the growth rate is

$$g(w,T,C_a) = 0.033\left(\frac{C_a}{C_a + 205\,e^{-0.125T}}\right)e^{0.09T}\,w^{-0.06} \tag{I.13}$$

where T is the measured temperature and C_a is the measured quantity of phytoplankton in mg Chla m^{-3}. Parameters and formulation comes from Huntley & Boyd (1984) and Hirst & Bunker (2003). Finally, the closure term for the net abundance change, the mortality rate, is

$$\mu(w,t) = gS \tag{I.14}$$

where S is the mean slope of biomass spectra within the period of τ given by

$$S = \frac{1}{\tau}\int_t^{t+\tau}\frac{\partial \ln b}{\partial \ln t}\,dt \tag{I.15}$$

The main difference between this model and the previously mentioned ones is the use of the slope of the biomass spectra to account for the mortality and so the predation without any formulation of prey

/ predators interactions and size relationships of affinities. In this approach the slope is considered to be the ratio of the mortality and the growth — as in Zhou & Huntley (1997), see eq. I.8. Hence, the product of the slope and the growth rate may be a valid approach to account for the predation mortality due to growth need and removal. In this approach, the slope is then considered as an input of the model and not an output — which is an important assumption, the objective of the model appears then different from the ones of Baird & Suthers (2007) and Maury et al. (2007a). The assumption made is that the observed size spectra are linear and their slope is known as it is an entry of the model; this implies that instruments used to measured this slope and their efficiency are the sensible and critical aspects. A discussion about the efficiency of some of these methods is performed in chapter II. The model of Zhou et al. (2010) was used to model the carbon fluxes within the ecosystem at a monitoring station near Marseille (South of France). Even if the model overestimates the observed zooplankton abundance (which is not the real abundance), the seasonality seems to be well represented, leading to promising and enthusiastic results for this first direct comparison of a zooplankton size-based model and *in situ* observations.

I.3 METHODS

I.3.1 Localization of the sampling site

The present thesis is mainly based on the analysis of datasets from a monitoring study of a coastal station (Point B) in the Bay of Villefranche-sur-Mer, between the cities of Nice and Monaco (Northern Ligurian Sea, see fig. I.2 and www.obs-vlfr.fr/Rade). The Ligurian Sea is delimited by the French and Italian coast on the north, and by the Corsica on the south. Hydrology of this area is characterized by a cyclonic circulation of waters along the coast and forming the Liguro-Provençal Current — a component of the Northern Mediterranean Current flowing less saline Atlantic Water from Italy towards Spain (Prieur et al. 1983, Millot 1999). The central part of the Ligurian Basin is separated

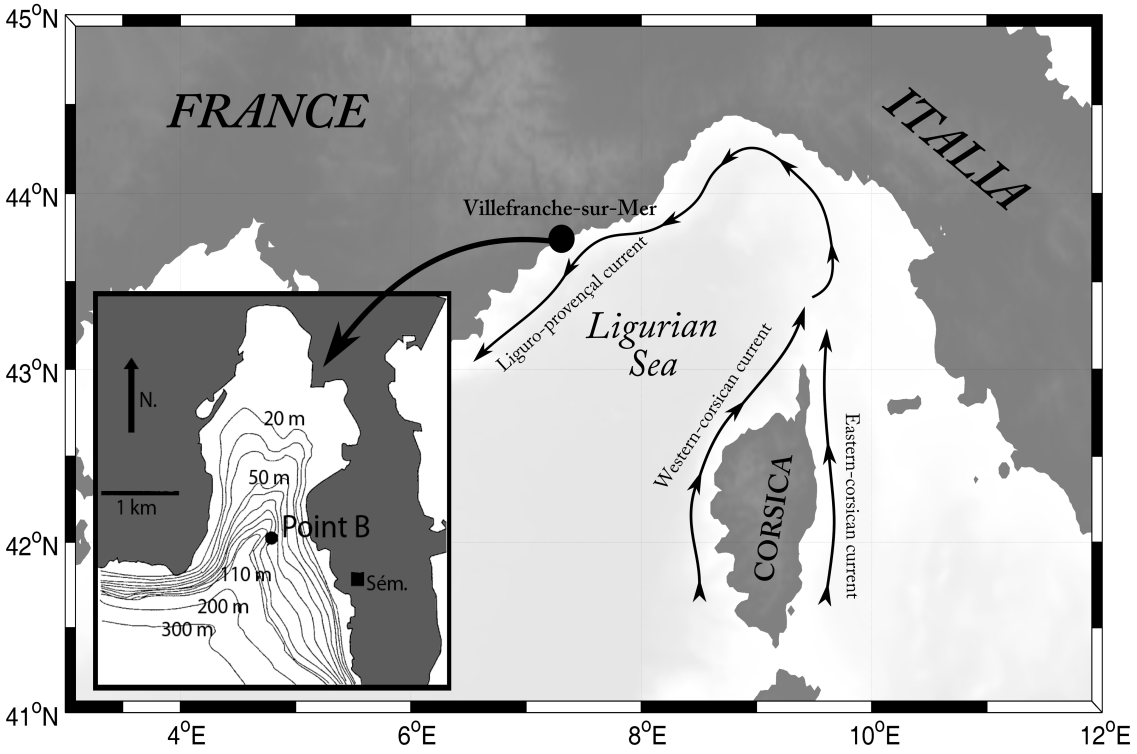

Figure I.2 – *Location of the sampling site (Pt. B) in the Ligurian Sea and the meteorological station Sémaphore (Sé.) situated in Cap Ferrat 1.2 km from Point B. The other meteorological station, Nice Airport, is situated 8 km west. The cyclonic circulation of the Ligurian Sea with the Liguro-Provençal Current, the Western Corsican Current and the Eastern Corsican Current are also shown on this map. The central zone of the Ligurian Sea is separated from more coastal areas by the frontal zone*

from the coastal zone by a permanent thermohaline front. This central part is monthly monitored since 1991 at a station called DYFAMED (Marty 2002, Marty & Chiavérini 2010).

The Point B station (fig. I.2) is located at the entrance of the Bay of Villefranche-sur-Mer (43°41.10'N, 7°18.94'E; 85 m depth). The site is affected by hydro-climatic variability such as the Ligurian Current flow, wind patterns and by open sea conditions due to a narrow continental shelf and the presence of the Nice submarine canyon (2000 m depth) in front of the bay. This station has been monitored since 1957 with the measurement of hydrological variables at different depths (salinity, temperature and density). Since 1966, a regular sampling (often on a weekly basis) of zooplankton communities using a Régent net (680 μm mesh, 0.5 m^2 mouth opening) and a Juday-Bogorov net (330 μm mesh, 0.25 m^2 mouth opening) is maintained. Yet, the Juday-Bogorov sampling stopped in 2003 to restart in 2010. Since 1966, regular measurements of chlorophyll-*a* with Niskin bottles are

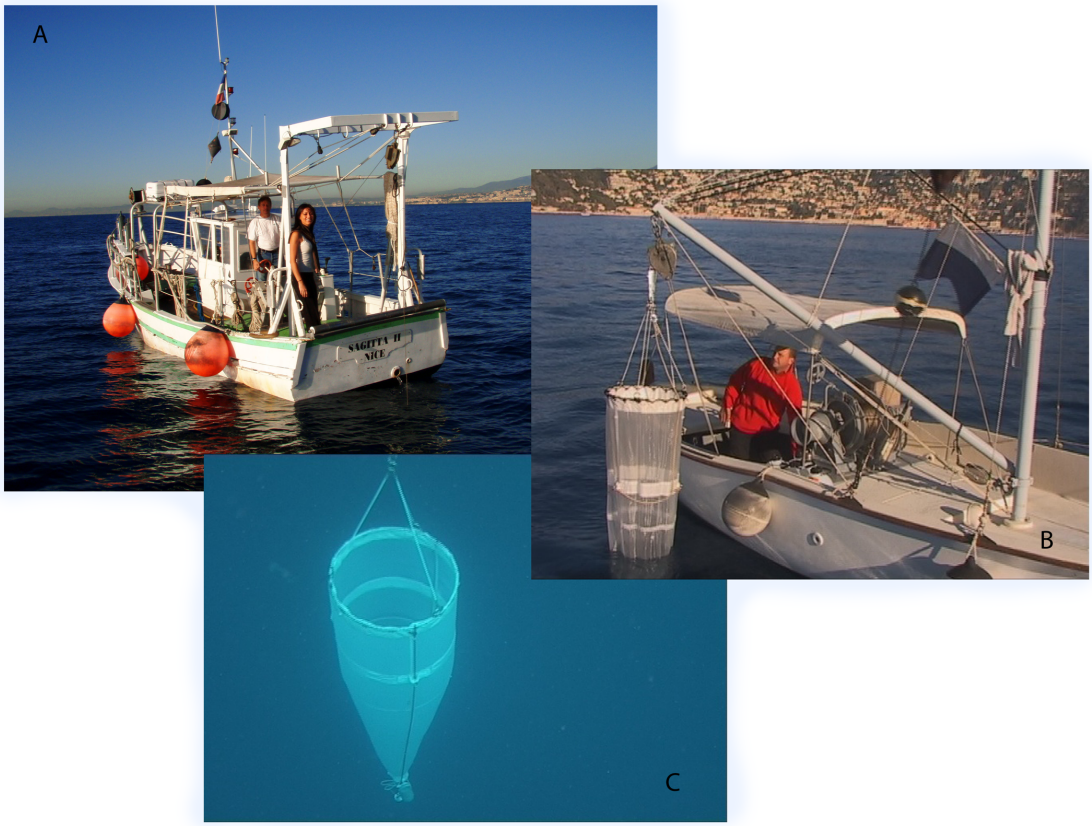

Figure I.3 – *(A) Picture of the NO Sagitta II in station with Ornella Passafiume and Jean-Yves Carval. (B) picture of the NO Vellele and the WP2 net being operated by Mickaël Cayol and (C) the WP2 net underwater. Copyright Christophe Mocquet for A and B, and David Luquet for C.*

performed. An increase sampling effort has been done since 1995 together with the integration of the Point B in the French national program SOMLIT (www.domino.u-bordeaux.fr/somlit_national). Since 1995, nutrients, chlorophyll-*a*, suspended particles with the Coulter Counter, zooplankton with the internationally used WP2 net (mesh size of 200 μm, mouth aperture of 0.25 m^2), Seabird SBE25 CTD casts, fluorescence have been weekly measured at Point B. Yet, gaps and change of techniques occurred during from 2006 and are currently being filled. In the present work, the period from 1995 to 2005/2006, the longest and most complete one according to the available parameters, was considered. Meteorological parameters used were measured daily by Météo France at the Cap-Ferrat Sémaphore station, located 1.2 km away from Point B (fig. I.2).

I.3.2 Imaging procedure

I.3.2.1 Samples used

Zooplankton samples were collected weekly using the WP2 net (mesh size of 200 μm, mouth aperture of 0.25 m^2) by vertical tows (60 m depth to surface) weekly from 1995 to 2006 (a total of 509 samples are present in the time series, $\approx$ 43 per year). Then, each sample was separated in two subsamples of different size fractions with a mesh of 1000 μm. Then, each subsample was fractionated separately with the Motoda box. Since small objects are generally more abundant than large ones they need to be more fractionated. Separation of the small and large objects and consequent separate image acquisition of the two size classes prevents underestimation of large rare objects (Gorsky et al. 2010). The 44 subsamples were scanned after a manual separation of objects on the scanning tray. The time of the separation was limited to 20 minutes.

I.3.2.2 Imaging procedure

Sample imaging was done using the ZooScan / ZooProcess system (www.zooscan.com and fig. I.4), a laboratory instrument used for the digitization of fixed wet net samples developed at the "Laboratoire d'Océanographie de Villefranche-sur-mer" (Grosjean et al. 2003, Gorsky et al. 2010). The ZooScans used in this study were the prototype built in 2003 (used for samples from 1995 to 2006), which has a scanning surface of 7.5x18.5 cm with a pixel width of 10.56 μm (scan at 2400 dpi; 7100x17500 pixels), and the commercial model, version 2006 (used for one section in chapter II), which has a scanning surface of 15x24 cm and a pixel width of 10.56 μm (scan at 2400 dpi; 14200x22700 pixels).

Images were then analyzed by a dedicated imaging software, ZooProcess (www.zooscan.com). This software, written as a macro in java language for ImageJ (Rasband 2005), consists of a suite of procedures including calls to VueScan and ImageJ. This system (i) scans a high quality raw image,

linked with associated metadata, (ii) divide the raw image into separate valid targets, defined by the continuity of pixels with grey levels higher than a threshold of 243, and (iii) measures 46 variables for object characterization, including grey levels, fractal dimension, shape and size (Benfield et al. 2007, Gorsky et al. 2010). The present study focuses on step (iii) with a special emphasis on size variables. Basic size variables considered in this work are (i) *Area*: 2-D surface area of the object (i.e., number of pixels), (ii) *Major*: Primary axis of the best fitting ellipse for the object, and (iii) *Minor*: Secondary axis of the best fitting ellipse for the object (fig. I.5). The minor axis is computed orthogonally from the middle of the major axis, both defining the area of the best fitting ellipse (A_e), which is equal to the *Area* of the object:

$$A_e = \pi \cdot \left(\frac{Minor}{2}\right) \cdot \left(\frac{Major}{2}\right) = Area \tag{I.16}$$

All other variables were only utilized for the automatic classification of objects which is presented hereafter. ZooProcess provides an additional tool to separate touching objects on the scan image

Figure I.4 – *Picture of the ZooScan model 2006 being operated by Corinne Desnos.*

(called numerical separation in the present work). The threshold (level 243) of scanned image is displayed in black and white and the user has the possibility to draw lines to segment objects.

I.3.2.3 Automatic classification of objects

Automatic classification or prediction was performed using Plankton Identifier (Gasparini 2007), available at www.obs-vlfr.fr/~gaspari/Plankton_Identifier, which uses supervised learning algorithms implemented in TANAGRA free statistical package (Rakotomalala 2005). The supervised classification handles the learning set production and classification tasks (Benfield et al. 2007). The learning set (or training set) was produced manually by sorting objects into user-defined plankton categories. Then the automatic classification task sorted unknown objects using the human-made learning set. Automatic classification was done by building decision mechanisms (see, Sigaud & Wilson 2007, Geurts et al. 2009, Schwaighofer et al. 2009, and references therein for a detailed description and history of supervised learning) that associate variables extracted by image analysis with classifications made during the learning set production. Several decision mechanisms exist and have already been tested. An effective and widely used algorithm in terms of classification accuracy and processing time of zooplankton samples is the Random Forest Algorithm (Breiman 2001, Grosjean et al. 2003, Grosjean & Denis 2007, Gislason & Silva 2009, Gorsky et al. 2010). Recall rates (see below) of the

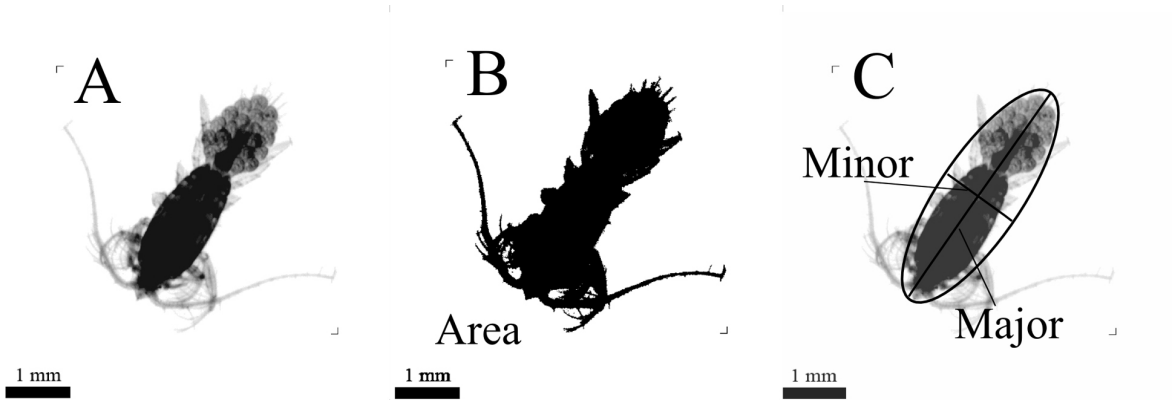

Figure I.5 – *Image analysis on objects made with ZooProcess. (A), Raw image of a copepod female with eggs. (B), same object in black and white with a threshold of 243 for the computation of the area and (C), computation of minor and major axes of the best fitting ellipse.*

Random Forest algorithm oscillates between 60% and 95%, depending on the quality of the learning set and the taxonomic resolution (Grosjean et al. 2003, Culverhouse et al. 2006, Benfield et al. 2007, Grosjean & Denis 2007, Bell & Hopcroft 2008, Irigoien et al. 2009, Gislason & Silva 2009, Gorsky et al. 2010).

To assess the performance of the classification model, confusion matrices were used. A confusion matrix is a contingency table that compares classification performed manually (observation) and by algorithmic learning (automatic prediction). The classification performed manually is considered as being 100% accurate, but see Culverhouse et al. (2003) for a critical view of the human classification. The confusion matrix was a square matrix with the number of rows and columns being the number of categories used for the classification (i.e., the categories chosen during the learning set production). Each cell contained the number of cross-classified objects, with the diagonal containing the number of correctly classified objects in each category (i.e., good agreement of man and machine classification). A global error rate, a recall rate and a contamination rate for each category were computed from the confusion matrix. The global error rate corresponded to the total percentage of misclassified objects, i.e., the proportion of objects out of the diagonal; the recall rate was the proportion of objects of a given validated category that were correctly predicted; and the contamination rate was defined as being 1-precision, where precision is the proportion of objects in a predicted category that belonged to this category according to the validation. To define the accuracy of the classification for each category, both recall and contamination are necessary (Gorsky et al. 2010).

The accuracy of the automatic classification prediction was evaluated with a confusion matrix using a manually validated set. The validated set was made with different objects from those used in the learning set. Thus the validation is the process by which the automatic prediction is corrected as defined in Gorsky et al. (2010). In this thesis (chapter II), 22 samples (containing 26027 objects) homogeneously distributed between 2003 and 2006 were fully manually classified for the validation set

into the defined 14 categories. The number of categories was chosen as a good compromise between the time spent to validate the automatic classification, the efficiency of the automatic classification — since the quality of the classification decreased with an increasing number of predicted categories (e.g., Fernandes et al. 2009, Gislason & Silva 2009, Gorsky et al. 2010) and the number of taxa necessary to study the plankton size spectrum. The number of plankton categories can be extended in the future as it is now routinely performed on other samples by automatic classification followed by manual validation.

I.3.2.4 Size-spectra computation

A size spectrum is the distribution of abundance or volume relative to the size of the organisms. The image analysis provided the major axis, minor axis and area, used to calculate the spherical (SBv) and elliptical (EBv) biovolume:

$$SBv = \frac{4}{3} \cdot \pi \cdot \left(\frac{Area}{\pi} \right)^{\frac{3}{2}} \tag{I.17}$$

$$EBv = \frac{4}{3} \cdot \pi \cdot \left(\frac{Minor}{2} \right) \cdot \left(\frac{Major}{2} \right)^{2} \tag{I.18}$$

The EBv is here the volume of a prolate ellipsoid (“rugby ball”), different from the oblate ellipsoid (“smarties candy”) used by Sprules et al. (1998). The computed biovolume used in all this work is the elliptical biovolume unless stated otherwise. The biovolume values were arranged in size classes defined by an interval on the x-axis $[\log(x_n); \log(x_{n+1})[$, with a length equal to $\log(x_{n+1}) - \log(x_n) = \log(k)$ being constant ; in this work, k was arbitrarily chosen to be equal to $2^{0.5}$. 40 size classes were used from the lowest limit of 0.014 mm^3 to the largest limit of 1050 mm^3, a range that encompasses the whole size range of zooplankters collected with the WP2 net.

Finally, the y-values (biovolume or abundance) were normalized to the length of the size class $(x_{n+1} - x_n)$, so that the resulting size spectrum was not a function of the arbitrarily-chosen value k (Platt & Denman 1977). The resulting y-value represented the exact value for a nominal size $\log(x_i)$

between $\log(x_n)$ and $\log(x_{n+1})$. The nominal values representing the size classes were defined as $\log(x_i) = (\log(x_n) + \log(x_{n+1}))/2$. The final size spectrum was presented in logarithmic scales (following Blanco et al. 1994). Units are on the y-axis in $\log(\mathrm{mm}^3\,\mathrm{m}^{-3}\,\mathrm{mm}^{-3})$ for the biovolume or $\log(\#\,\mathrm{m}^{-3}\,\mathrm{mm}^{-3})$ for the abundance and the x-axis shows individual biovolume in $\log(\mathrm{mm}^3)$. They are referred to as Normalized Biovolume Size Spectrum ("N-BSS") and Normalized Number Size Spectrum ("N-NSS"), respectively.

We characterized the size spectrum with different measures used in ecology: the mode, the total biovolume or total abundance, the slope of a linear regression to the "N-BSS" and the Shannon index (Sh) (Shannon 1948, Parsons 1969, Ruiz 1994, Brucet et al. 2006, Quintana et al. 2008):

$$Sh = -\sum(p_i \log_2(p_i)) \tag{I.19}$$

where p_i is the probability of the size class i. The Shannon index is a measurement of the equitability of size classes and is greatest if all size classes have the same value. The linear regression was made from the average mode of size spectra until the largest size class in the distribution excluding empty classes. While nonlinear functions usually produce a better fit to size distribution data (Gasol et al. 1991, Vidondo et al. 1997, Brucet et al. 2005), the ecological meaning of the model parameters is usually difficult to interpret (Quintana et al. 2008) and so, they have not been applied to the present analysis.

I.3.3 Statistical analyses

This part presents some of statistical methods that have been used for this thesis — mainly in chapter III "Inter-annual variability of the Ligurian Sea pelagic ecosystem". All followings methods were programmed using the Matlab language (the Mathworks Company, inc.). This presentation is non-exhaustive and will only present in more details the less common methods.

I.3.3.1 Identifying regime shifts

The notion that ecological and climate variations often occur in the form of "regimes" emerged in the '90s, inspired mostly by the rapid change of the North Pacific climate ca. 1977 and other abrupt shifts in the Pacific Decadal Oscillation (Kerr 1992, Mantua et al. 1997). A true regime shift implies that (Hsieh et al. 2005):

- A statistically significant difference exists between the mean value of the variable before and after a certain date based on the t-test.
- Due to "red noise" (similar to random or brownian noise) wrong regime shifts can be detected in time series ($X_t = X_{t-1} + E_t(rednoise)$) — a de-noising should be used prior to the detection.
- A regime shift appears as quasi-stationary state in measured parameters separated by periods of rapid transition.
- True regime shifts are not random features of time series but are formally associated with the ideas of non-linear amplification, alternative basins of attraction, multiple stable states, hysteresis (memory) or fold catastrophe (with a tipping point), all requiring the underlying dynamics to be non-linear in origin.

Then, several methods were developed to detect shifts or discontinuity in time series. An extensive list of these methods is available at www.beringclimate.noaa.gov/regimes/Regime_shift_methods_list.htm. Here, we will present the tests that are most commonly used, the Students T test, then the easy-to-use Cumulative Sum method (Ibañez et al. 1993), the Principal Component Analysis (PCA), which can detect shifts in the system, and the more complete Rodionov method (Rodionov 2004; 2006).

The most commonly used method to detect regime shifts is the use of the Students T test. It is a well established one but suffers from some strong disadvantages. First of all, the year of change

has to be picked up manually, which violates the assumption that the change point should not be pre-assigned (i.e., each year should be given equal weight). Then, as well as in multitude of other common methods, there is a deterioration of the test statistics toward the ends of the time series, which implies that in order to detect a regime shift with a certain degree of confidence, it is necessary to accumulate enough data (a minimum of 10 years). This results in late detection of regime shifts, generally more than ten years after the shift. Finally this method is not automatic. However, the robustness of this method makes it useful to validate the occurrence of a regime shift.

Another interesting method is the use of cumulative sums (Ibañez et al. 1993), recently used by Conversi et al. (2010). The method consists in plotting the cumulative sum of standardized values over time. First, each value of the series is subtracted from a reference value (here the mean of time series), resulting in a new time series of residuals which are used for the calculation of the cumulative sum. Then, each data point is added to the preceding data point. The interpretation is based on the slope of the line on the chart: a constant deviation from the mean of the time series shows a constant slope. Persistent changes from the mean of the time series cause a persistent change of the slope. This easy-to-use method allows the automatic detection of time in shift of the mean of a time series. Yet, this methods — as well as the Student T test — works only on the detection of shifts in the mean (not in the variance), works with anomalies and so different base periods may affect the results (Rodionov 2004). These methods are moreover, highly sensitive to trends in time series — a constant trend will be detected as a shift in the middle of the time series using the cumulative sums. In addition, the statistical significance of the observed shifts should be tested *a posteriori* by methods as the Student T test.

Another way of detecting regime shifts is PCA analysis. This method is widely used to identify coherent patterns of variability among large sets of time series (von Storch & Zwiers 1999, Mantua 2004). Datasets are previously standardized due to their different natures. Then, new synthetic vari-

ables (Principal Components, PCs) are created by minimization of the Euclidean distances among the original variables in each new projected space. In other words, new axes (PCs) are created in the multispace of *n* original variables. The first PC is the one minimizing most of the distance between variables, so it accounts for as much variability in the data as possible. The following new axes is orthogonal (independent) to one another and ordered by the minimization of distances with the original variables. This method allows to obtain the maximal common interannual variability among the studied variables and the depiction of the relationships among the variables. Although it is not a regime shift detection method *per se*, it was applied to a large set of biotic and abiotic time series to detect shifts in the entire systems, e.g., in the North Pacific to analyze the scale of regime shifts in 1977 and 1989 (Hare & Mantua 2000). The advantages of this method is that it reduces the dimensionality of the data matrix and requires no *a priori* assumption about candidate regime shift years. Yet, Additional time series analysis methods must be used to assess the statistical significance and character of temporal changes in the PCs.

New methods were then developed to suppress the previously mentioned disadvantage in the detection of regime shifts, the principal disadvantage being the need of an *a priori* hypothesis about the timing of the shift, the need of large dataset and the decrease of performance toward the end of the time series preventing early detection of shifts. A sequential algorithm was latter elaborated by (Rodionov 2004) with a further incorporation of a "pre-whitening" to deal with the autocorrelation (Rodionov 2006). The initial algorithm was set in seven steps, the only choice to be made was the empirical determination of the cut-off length l of the regimes and the level α of statistical significance. The sequential analysis proposed by Rodionov (2004; 2006) belongs to the category of exploratory or data-driven analysis that does not require an *a priori* hypothesis on the timing of regime shifts — this greatly facilitates automatic computations. It can also handle the incoming data regardless weather they are presented in the form of anomalies or absolute values (this eliminate the source of

ambiguity coming from the selection of the base period). Moreover, a comparison made with other methods shows that Rodionov (2004; 2006) dealt better than the others with the presence of trends in the time series — which often produces the detection of a false regime shift at the center of the time series. Finally it detects regime shift relatively early in time. The principal disadvantage of the method developed in 2004 (Rodionov 2004) was the absence of handling the auto-correlation (source of red-noise). The integration by Rodionov (2006) of a "pre-whitening" of time series enables the suppression of the red-noise and thus of the auto-correlation.

Finally, with the development of non-linear theories and the availability of high frequency environmental data, there were a growing interest in using non-linear techniques to deal with environmental datasets (e.g., Cushing et al. 1996, Schmitt & Seuront 2001, Dippner et al. 2002, Schmitt et al. 2006, Zaldivar et al. 2008, Vandromme et al. 2010). To deal with the non-linearity of time series the Recurrence Plot (RP) was introduced (Eckmann et al. 1987), which is based on the computation of the distance matrix between the reconstructed points in the phase space. Zbilut & Webber (1992), defined several variables to quantify RP — they call it the Recurrence Quantification Analysis (RQA) — which were used recently by Zaldivar et al. (2008) to characterize regime shifts in environmental time series. Yet, these methods seems more adapted to large datasets and were scarcely used in ecology.

To identify the main differences between the identified periods one can use methods such as simple correlations (like the Spearman rank order correlation) between parameters, principal component analysis, Student T test ... or the canonical discriminant analysis which will find the best separation between known groups (e.g., Anderson & Willis 2003, Anderson & Robinson 2003, for a review).

I.3.3.2 Computing distances between size spectra

To compute the distance between size spectra, a possibility is the well-known Kolmogorov distance, often used to compute the distance and its statistical significance between two distributions. Yet no distance seems to exist to deal with 3-D size distribution in which axes are size (x-axis), frequency, abundance, biovolume or biomass ... (y-axis), and time, depth or geographical distance ... on the new z-axis. The following paragraphs will present an adapted distance capable of dealing with 3D objects such as a year of size spectra measurements.

In the present case, the ecosystem is defined by its community size spectrum over each year. That is, the considered object is a 3-D surface, where the x-axis represents the week (or month) number, the y-axis represents the size class, and the z-axis represents the biovolume of all (or only a defined category) zooplankton organisms for a given size and a given week through the considered year. Computation of a distance between two objects of this kind was never used before in ecology. However, such a measurement exists and is used to compute the distance between, for example, two images, two dendrites or two spatial objects. The distance generally used is the Hausdorff distance (Hausdorff 1919, Rucklidge 1996) or the extended Hausdorff distance (Min et al. 2007). The Hausdorff distance between two point sets A and B is defined as:

$$H(A,B) = max\{h(A,B);h(B,A)\} \tag{I.20}$$

$$h(A,B) = \underset{p_a \in A}{max}\left\{\underset{p_b \in B}{min}\{d(p_a,p_b)\}\right\} \tag{I.21}$$

and vice-versa for $h(B,A)$. These equations expressed that the shortest distance (d, Euclidean distance) is first found from each point of A (p_a) to the set of points B or from each point of B (p_b) to the set of points A, and then the largest among the set of shortest distances is selected as the value of $h(A,B)$ or $h(B,A)$, then the maximum between $h(A,B)$ and $h(B,A)$ is selected to be the Hausdorff distance $H(A,B)$. The Hausdorff distance fulfills the properties of a distance (i.e., non-negativity,

identity, symmetry and triangle inequality). Therefore, the Hausdorff distance is a metric measure similar to the Euclidean distance. The advantage of the Hausdorff distance over the Euclidean distances is that it is able to measure the distance between two any kinds of objects (as point sets), apart from point objects. Yet, as pointed out by Min et al. (2007), the Hausdorff distance is very sensitive to outliers because the largest of the shortest individual distance is used. Moreover, the individual distances represent a distribution and one can extract a value from this distribution without changing the properties of the Hausdorff distance. Min et al. (2007) proposed to use the minimum, the maximum (classical Hausdorff distance) and the median of the distribution to fully define the distance between two spatial objects. The objects that are to be classified in the present case are not directly comparable to the one to be classified by Min et al. (2007). For example, the minimum distance is a non-sense in the present work because it will always be zero. The median is also difficult to use, the objects to be classified in our case are very close and the differences are driven by large values, the median will be too restrictive to efficiently record the distance between two 3D size spectra. To control the influence of outliers and stabilize the Hausdorff distance we look at the average of the 1% largest individual distance, which is very close to the original distance formulated by Felix Hausdorff in 1919.

Before computing the Hausdorff modified distance, the 3D size spectrum has to be modified. First of all, the units in the three axes are not the same and must be normalized. It is convenient to subtract the minimum value and divide by the remaining maximum value, so that each axis varies from 0 to 1. If one wants to give more weight to a peculiar axis it is then possible to multiply the given axis by a constant. After this normalization, the considered object is unitless in 3 dimensions and an Euclidean distance is computed between each point, hence the computation of the Hausdorff distance is feasible. A dendrogram with weighted linkage is then plotted to visualize the results of the classification made over years of size spectra. Due to the particular shape of size spectra, with high abundance of small organisms, a previous transformation is generally carried out on, here, the z-axis

to decrease the deviation between small and large organisms — it is mainly log or double squared root transformations.

I.4 Organization of the thesis

The body of the thesis is organized in three parts that will present different aspects of the analysis of zooplankton and address different issues. Chapter II "Identifying new biases from image-derived size spectra" will investigate some biases in the estimation of size spectra that are linked to the imaging methodology: the impact on the size spectrum of objects touching each other during the scanning process that are identified as a single object, the efficiency of the automatic classification within a category according to its size distribution and the use of a single, taxon-independent, model to compute individual biovolume/biomass compared to another taxon-dependent one. A short investigation of the bias due to the net selectivity is also presented. This chapter mainly introduces the notion that there are various steps from the *in situ* spectrum to the spectrum that is finally analyzed in ecological studies, each of them introducing errors that we have to take into account.

Chapter III "Inter-annual variability of the Ligurian Sea pelagic ecosystem" will present an ecological analysis of the pelagic ecosystem the Bay of Villefranche-sur-Mer, centered on zooplankton analysis. The zooplankton communities and their size spectra fluctuations are related to environmental variability and an hypothesis on the system functioning is proposed, allowing a separation between different states of zooplankton communities in relation to climatic, meteorological, hydrological and biological forcings.

Chapter IV "Continuous size-based modeling of zooplankton" will present the formulation of a size-based model for zooplankton developed in collaboration with the INRIA Sophia-Antipolis team Comore (Éric Benoît, Jonathan Rault and Jean-Luc Gouzé). This exploratory model has been used to understand the main features of the dynamics of the zooplankton size spectra and has been tested

on the main states of the zooplankton defined in chapter III. General discussion will then close the thesis.

During these three years of doctorate I was also involved in side projects that are not mentioned in the present manuscript but have deeply contributed to developed the scientific topics discussed in my thesis. Among these projects, the most enthusiastic one was the participation to the iron fertilization experiment Lohafex on board the *FS Polarstern* in the South Atlantic in January-March 2009 (co-author in Mazzocchi et al. 2009). Operating the Underwater Vision Profiler (UVP), participating to the zooplankton sampling as well as participating to discussions on carbon flux, together with the other parts mentioned in the present manuscript, gave me the opportunity to experience the complete continuum, from the measurement of size-spectra, the assessment of methodology, the various ecological analyses (coastal and offshore with different problematics) and modeling.

Besides, two original articles were written as first author during this doctorate: the first one includes most of the findings and discussion of the methodological part (chapter II) whereas the other includes the descriptive analyses and discussions about the long-term dynamics of the zooplankton communities, linked to environmental fluctuations, presented in chapter III. These two articles are currently submitted to *Journal of Experimental Biology and Ecology* and to *Biogeosciences* respectively. In addition, a third article is in preparation about the modeling part.

II IDENTIFYING NEW BIASES FROM IMAGE-DERIVED SIZE SPECTRA

II.1 Introduction to biases from image analysis of zooplankton

The traditional method to obtain data on zooplankton size spectra is the use of net collection followed by manual classification, counting and measurement of size. These steps are labor-intensive and limit the number of samples and/or organisms that can be processed. Laboratory or *in situ* imaging techniques accelerate sample processing (Wiebe & Benfield 2003, Benfield et al. 2007, and references therein). Zooplankton images obtained in the laboratory or *in situ* can be processed automatically by softwares that perform classification, counting, and size measurements (Jeffries et al. 1984, Rolke & Lenz 1984, Gorsky et al. 1989, Grosjean et al. 2003, Benfield et al. 2007, Bell & Hopcroft 2008, Gorsky et al. 2010). New datasets on zooplankton size spectra obtained by imaging techniques can be used to monitor the state of planktonic ecosystems or to assess fluxes (Yurista et al. 2005, Irigoien et al. 2009, Manriquez et al. 2009). However, the methodology used to calculate size spectra can affect ecological descriptors derived from the spectra, such as the slope or the Shannon size diversity index (Quintana et al. 2008).

These size spectra come mostly from net sampling, which also introduces a bias, yet not related to the image analysis. A net is defined by its aperture and mesh size. Nichols & Thompson (1991) demonstrated that a mesh should be at least $3/4$ of the width of the smallest organisms to be sampled in order to perform quantitative sampling. Undersampling of small organisms, which are more abundant, causes the total number of organisms caught with nets to be underestimated by a factor of 2 to 4 (Gallienne & Robins 2001, Calbet et al. 2001). On the other side of the spectrum, the maximum zooplankton size for quantitative estimates depends on the total volume sampled relative to the abun-

dance of the largest organisms and on the escape reaction of those organisms in the water column (Fleminger & Clutter 1965, McGowan & Fraundorf 1966, Laval 1974). Because larger species have generally stronger swimming capacities, net avoidance usually increases with organism size, especially when considering the crustaceans zooplankton (Thomasson et al. 2003). Thus, nets are only able to select a fraction of the whole size range of zooplankton communities, of which only a subset is quantitatively sampled.

Then, the standard size measurement procedure using imaging methods includes image acquisition, extraction of objects, automated size measurements and, recently, the ability to automatically classify objects into different categories (Benfield et al. 2007). At least three possible biases can alter the size spectra at different steps of the image processing. They have been addressed in the present thesis using an in-lab flatbed scanning system (e.g., Grosjean et al. 2003, Bell & Hopcroft 2008, Gislason & Silva 2009, Irigoien et al. 2009, Gorsky et al. 2010). The biases studied affect, to some extent, other imaging or optical instruments such as the Optical Plankton Counter (OPC, Herman 1992), the Laser-OPC (L-OPC, Herman et al. 2004) the Flow Cytometry And Microscope (FlowCAM, Sieracki et al. 1998), the Video Plankton Recorder (VPR, Davis et al. 1992) or the Underwater Video Profiler (UVP, Stemmann et al. 2008).

The first methodological bias comes from objects touching each other during the image acquisition. Touching objects (TO) are extracted as a single, large object and modifies the whole community size distribution. TO are, to some extent, equivalent to the phenomenon of coincidence observed with the in situ Optical Plankton Counter (OPC), where if two or more objects cross the viewing field simultaneously, they are classified as a single, larger object (Sprules et al. 1992; 1998, Woodd-Walker et al. 2000, Liebig et al. 2006). Scanning systems, unlike optical counters, generate images that allow a clear assessment of the number, size distribution and quality of TO. Decreasing the number of TO is generally done by decreasing the total number of objects processed at a time by scanning system

(Irigoien et al. 2009) as well as by optical counters (Woodd-Walker et al. 2000). Automated algorithms for numerical separation of TO after image acquisition are applied in medicine, chemistry or pharmacy fields (Malpica et al. 1997, Korath et al. 2008). Zooplankton shapes are highly variable and such automatic approaches are not implemented in software for automated zooplankton classification.

The second bias altering size spectra is the error in the automatic classification of objects into different plankton categories. In contrast to optical or electronic counters (Sheldon et al. 1967, Herman 1992), imaging systems provide the image of each object and thus enables to extract different taxa by means of automatic or semi-automatic classification (Grosjean et al. 2003, Irigoien et al. 2009, Gislason & Silva 2009, Manriquez et al. 2009, Gorsky et al. 2010). The efficiency of the automatic classification can be highly variable depending on the shape of organisms classified. For example, copepods are predicted as being copepods (defined as recall) with an accuracy range between about 70% (Bell & Hopcroft 2008) and 95% (Irigoien et al. 2009), yet, these values, do not take into account the percentage of wrong objects also predicted as copepods (defined as the contamination Gorsky et al. 2010). Moreover, the efficiency of automatic classification has only been estimated in terms of abundance (Grosjean et al. 2003, Bell & Hopcroft 2008, Fernandes et al. 2009, Gislason & Silva 2009, Irigoien et al. 2009, Gorsky et al. 2010). Yet, there is a lack of results about the effect of automatic classification on the size-spectrum shape of a given category.

The third bias is the choice of a single geometrical model to estimate biovolume. Most automated counting systems have used an estimated spherical diameter. Nevertheless, this tends to overestimate biovolume since most zooplankton organisms are not spherical and have very diverse morphologies (Sprules et al. 1998, Beaulieu et al. 1999). Many organisms, including the abundant copepods, are best represented by an ellipsoid (Herman 1992). Clear indication of the model used to convert from one or two dimensional size measurements to biovolume is necessary to avoid any misinterpretation when using the volume spectra in mathematical models or when calculating total plankton biovolume

in an ecosystem. Then, the choice of using a single geometrical model for the whole community will be compared to a taxonomic-based estimate of size spectra through size-biomass relations (Alcaraz et al. 2003, Hernández-León & Montero 2006, Lehette & Hernández-León 2009, Gorsky et al. 2010).

In this study, we address three main questions. (i) What is the influence of the touching objects (TO) on the shape of the size spectrum? (ii) What factors (e.g., size classes, relative and absolute abundance of zooplankton) influence the ability of automatic classification to predict reliable size spectra of a given category? And (iii), during image analysis, what is the influence of the model used to estimate individual biovolume on the shape of the size spectrum? The question of the bias due to the net sampling will be addressed briefly prior to the aforementionned three main questions. To answers these questions, a zooplankton time series from Point B (NW Mediterranean Sea) was studied using the ZooScan / ZooProcess / PlanktonIdentifier integrated system, a scanning, image analyzer and supervised classification tools following the principle proposed by Gorsky et al. (2010). This study will focus mainly, but not only, on the measurement of crustacean size spectra because (i) they have the highest rate of automatic classification, (ii) the dimensions of the body (length, width) are consistent, and (iii) they dominate the zooplankton community at this station.

II.2 Data used

Zooplankton samples were collected weekly using the WP2 net at the Point B monitoring station (see section I.3.1). For the present chapter, 22 samples collected between 2003 and 2006 and two contrasted samples from 2009 were used from the Point B time series and were analyzed with the ZooScan procedure (section I.3.2). The ZooScans used in this study were the prototype built in 2003 (samples of years 2003 and 2006) and the commercial model, version 2006 (samples of year 2009). Samples of year 2009 were scanned twice. Firstly, the aliquot was homogenously spread on the scanning tray and a scan was done without manual separation of objects. Then, a second scan was made

following a manual separation. ZooProcess provides an additional tool to separate TO on the scan image (called numerical separation in the present work) which was performed on the second scans of subsamples from year 2009 to investigate the influence of TO on the spectra (see section II.3.2). The automatic classification was run using a learning-set with 14 categories (Table II.2). The categories “fibers” and “detritus” were non biologic, “touching objects” was a composite category (see section II.3.2) and all other categories were zooplankton. The “crustaceans” category was the aggregation of categories “cladocerans”, “copepods”, “decapods”, “nauplii” and “Penilia avirostris”. The learning set was made with others scans as those used for the analysis.

II.3 IDENTIFYING NEW BIASES

The aim of the present study is to identify biases in the estimation of zooplankton size spectra directly related to their analysis with imaging systems and automatic classification of objects. Zooplankton size spectrum can be viewed at different levels defined as follows. The **real spectrum** refers to the true, in situ spectrum. The **sampled spectrum** refers to the spectrum in the net that is analyzed and subjected to the bias of net sampling. This zooplankton **sampled spectrum** is an estimate of the **real spectrum** and is the one for which we are defining a methodological framework. The **observed spectrum** refers to the spectrum obtained by an optical instrument (for example Coulter Counter or laboratory OPC) or a imaging system (the ZooScan in this study) which is subjected to additional biases such as touching objects and undesired objects such as detritus. The **predicted spectrum** is obtained from automatic classification of objects in the **observed spectrum**. Finally, the **validated spectrum** is the result of the correction made by a human expert on the **predicted spectrum**. The average **validated spectrum** is shown on fig. II.1 A and the percentage of detritus, crustaceans, other zooplankton and touching objects per size classes is presented on fig. II.1 B.

This section is organized in four subsections: the bias due to the net sampling (II.3.1), the bias

due to objects touching each other (TO) during the image acquisition (II.3.2), the bias due to misclassification of objects (II.3.3) and the bias due to the model used to estimate individual biovolume (II.3.4). II.3.1, II.3.2 and II.3.4 use validated data to avoid the bias of the automatic classification. The automatic classification is presented in section II.3.3. Standard deviation uncertainties are reported for results presented hereafter.

II.3.1 Plankton selection by nets

Average zooplankton size spectra, computed with elliptical biovolume, from 13 fully visually validated samples towed with WP2 and Régent nets during year 2003 were compared (fig. II.2). The average mode of the zooplankton WP2 N-NSS (fig. II.2 A) was 0.019 mm^3, the maximum zooplankton size class caught by the WP2 net was 27.5 mm^3, whereas it was 880 mm^3 for the Régent net. The two spectra merged at about 6.9 mm^3. Equivalent N-BSS are presented on fig. II.2 B — the mode of the WP2 N-BSS increased to 0.038 mm^3. The N-NSS of only crustaceans and their equivalent N-BSS are presented on fig. II.2 CD. The mode of the crustacean WP2 N-NSS was 0.019 mm^3. The Régent N-NSS converged with the WP2 N-NSS at 4.9 mm^3, which was also the maximum non-empty

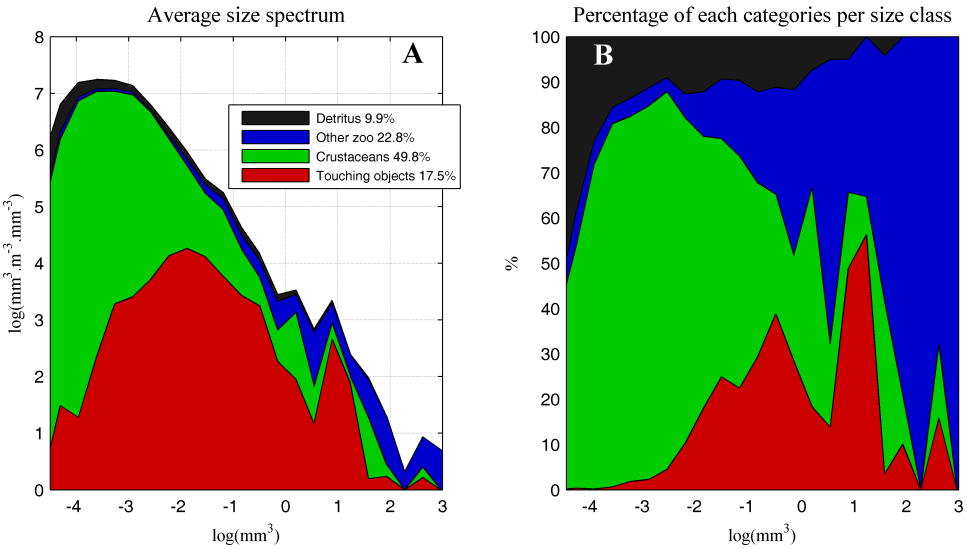

Figure II.1 – *Average validated size spectrum of the 22 samples used with the part represented by detritus, touching objects, crustaceans and other zooplankton (A). And (B), percentage of these categories per size class.*

size class in the WP2 N-NSS (fig. II.2 C, only crustaceans). The maximum size class of crustaceans captured with the Régent net was 78 mm^3. As before, the mode of the WP2 N-BSS for crustaceans increased to 0.038 mm^3. The WP2 net captured on average 1820±1740 zooplankters per cubic meter, of which 1620±1660 are crustaceans, equivalent to 220±190 mm^3 m^{-3} and 130±150 mm^3 m^{-3} of elliptical volume, respectively. The Régent net captured 28±54 zooplankton organisms per cubic meter, including 6±8 crustaceans per cubic meter, corresponding to 480±1100 mm^3 m^{-3} and 5±12 mm^3 m^{-3} of elliptical volume respectively. Taking the empirical Nichols & Thompson (1991)'s $3/4$ law of mesh selection into account, the WP2 net should quantitatively catch organisms with a width of at least 270μm. Assuming that the width of organisms was equal to the minor axis and that the major axis was on average twice the minor axis (minor axis = 48±13% of the major axis), the equivalent elliptical volume for 270 μm width is 0.0215 mm^3 (0.017 mm^3 to 0.029 mm^3 considering the standard deviation in the minor to major axis ratio). The observed mode of the WP2 N-NSS is within this range (0.019 mm^3) and the mode of the N-BSS is slightly larger (0.038 mm^3). Without normalization the modal size class of the abundance size spectra was the same as the biovolume size spectra, i.e., with a nominal size of 0.038 mm^3. In this modal size class, all organisms were theoretically quantitatively caught, which was not the case for smaller size classes. The modal size class starts at 0.032 mm^3. Considering a theoretical slope of -2 passing through the mode of the N-NSS, the WP2 underestimated the abundance of zooplankton of size ranging from 0.0057 to 0.032 mm^3 by a factor of 3.46 and the equivalent biovolume by a factor of 1.23 which is in agreement with previously published estimates (Gallienne & Robins 2001, Calbet et al. 2001). For crustaceans, the lower limit of efficient net capture was the same as when considering all zooplankton.

Quantifying the upper size limit of efficient net capture by the WP2 net is less obvious. Taking the whole zooplankton, the Régent net spectrum overlaps and lengthens the WP2 N-NSS from about 7 mm^3. This continuity is in agreement with the theoretical slope of -2 for N-NSS. However the Régent

net is supposed to be quantitative from 1.12 mm^3 (Nichols & Thompson 1991), corresponding to the mode found on fig. II.2 B. But from 1.12 mm^3 to 7 mm^3 the Régent net estimates of abundance were nearly three times lower than those of the WP2 net. Moreover, when calculating the N-NSS for only crustacean with the sizes caught by the WP2 net, the Régent net estimates were never higher than those of the WP2 net. The Régent net catches larger crustaceans than the WP2 net but with a discontinuity in the N-NSS. Larger crustaceans did not appear to be quantitatively caught by the Régent net (fig. II.2 C). Following previous results on swimming capacities (Fleminger & Clutter 1965, Laval 1974, Thomasson et al. 2003) this is probably the effect of net avoidance by active swimming and/or the result of the low concentration of large organisms in the water column. Larger crustaceans than those captured by the WP2 net are present in the water column but the comparison with the Régent net did not help to precisely quantify the upper limit of the crustaceans size distribution.

According to these results, we recommend to analyze N-BSS from their average mode. Taking into account smaller sizes would produce flatter slopes altering subsequent ecological understanding of energy flows in the plankton. This analysis did not produce a clear estimate of the upper size limit (best estimate $\approx$ 6.9 mm^3), which may depend on the concentration of large organisms in the field, on their behavior and/or on the towing speed.

II.3.2 Impact of touching objects (TO) on the shape of zooplankton observed spectrum

Differences between the observed spectrum and the sampled spectrum comes from the occurrence of objects in contact to each other, namely Touching Objects (TO, fig. II.3 C), during the scanning process. The presence of TO is related to the quality of the sample. If there is sticking material like mucus, detritus, species with large appendages and/or gelatinous bodies (e.g., remains of appendicularians houses), the probability of TO in a scan increases. Among the 22 samples from years 2003 and 2006, TO represented on average 17.5% of the total biovolume (fig. II.1 A) and approached 50%

for larger sizes (>0.6 mm^3 fig. II.1 B). Decreasing this number can be done by manual separation of objects on the scanning tray or on the image (numerical separation, see section I.3.2.2) and by decreasing the number of objects on the scanning tray. The last possibility is similar to the one used for the OPC (Woodd-Walker et al. 2000) and by Irigoien et al. (2009). Irigoien and colleagues proposed as a rule that the total area covered by objects on the scanning tray should not exceed 3% of the area of the scanning tray surface to avoid having significant effects of TO. However, this assumption was not tested by the authors and this section will address this issue. All scans used for the present work followed this recommendation and were below this proposed value of 3% (mean=1.4 $\pm$ 1.0).

To give an example of the effect of TO, we first scanned samples without separation, secondly

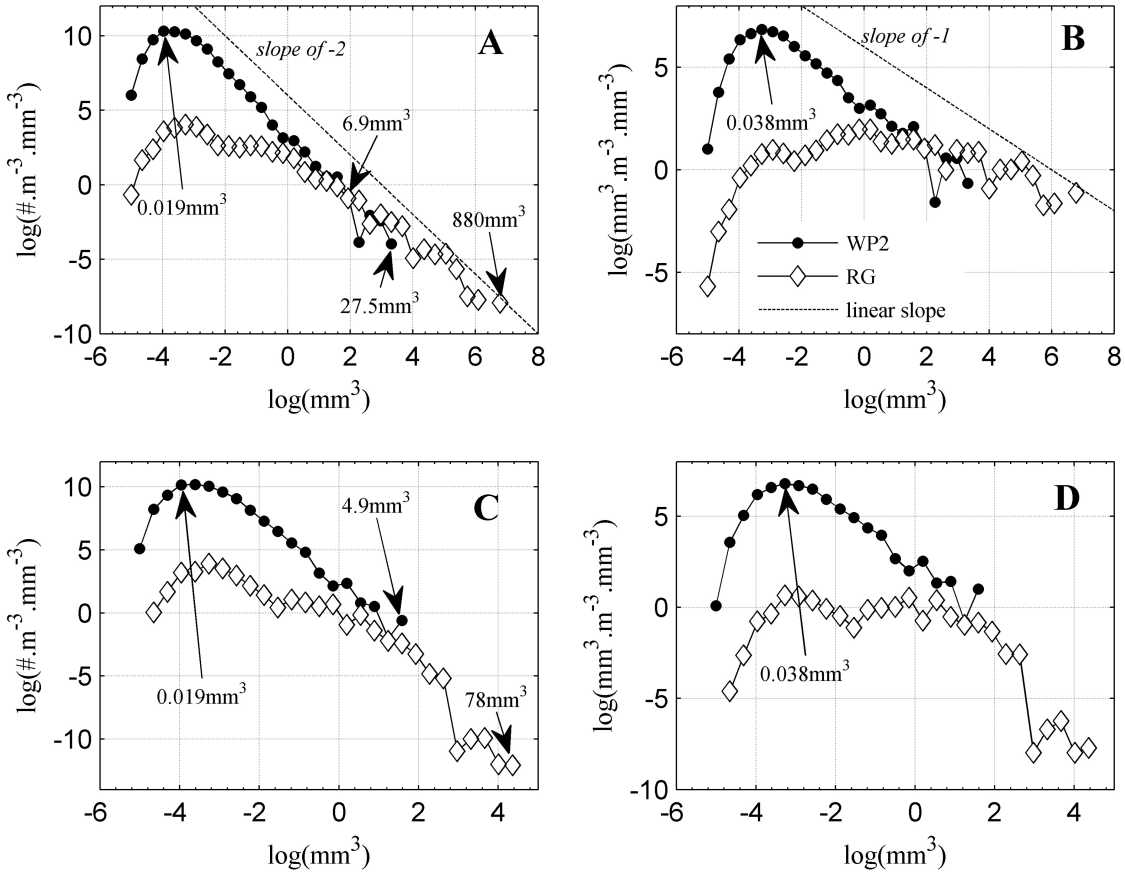

Figure II.2 – *Comparison of average size spectra measured during year 2003 with WP2 and Régent nets from visually validated samples. The size measure used is the elliptical biovolume. In (A), abundance size spectra and a linear curve with a slope of -2 are presented. (B) presents biovolume spectra and linear curve with a slope of -1. In (A) and (B) all zooplankton is presented. (C) shows the abundance size spectra and (D) the biovolume size spectra of the two nets for crustaceans only. The arrows point to particular values explained in the text.*

we performed manual separation and re-scanned the samples, and third we applied the numerical separation on the rescanned samples. All objects on the images were recognized manually and all the TO were excluded from size spectra (fig. II.3 AB). We followed the change in the plankton size spectra during the gradual separation of the TO. An increase of the abundance and biovolume of plankton is expected since we added objects previously set as TO. The process was done on two characteristic size spectra patterns (fig. II.3 AB), since doing it on the complete dataset would take too long. One spectrum had high plankton density of small size (mean individual biovolume of 0.14 mm^3) showing a unimodal distribution, while the other spectrum had lower density but larger size with two modes (mean individual biovolume of 1.13 mm^3). The spectrum obtained after numerical separation was considered as the closest estimate of the sampled spectrum. Results of these two experiments for the three categories (zooplankton, detritus and TO) are presented on table II.1. TO represented

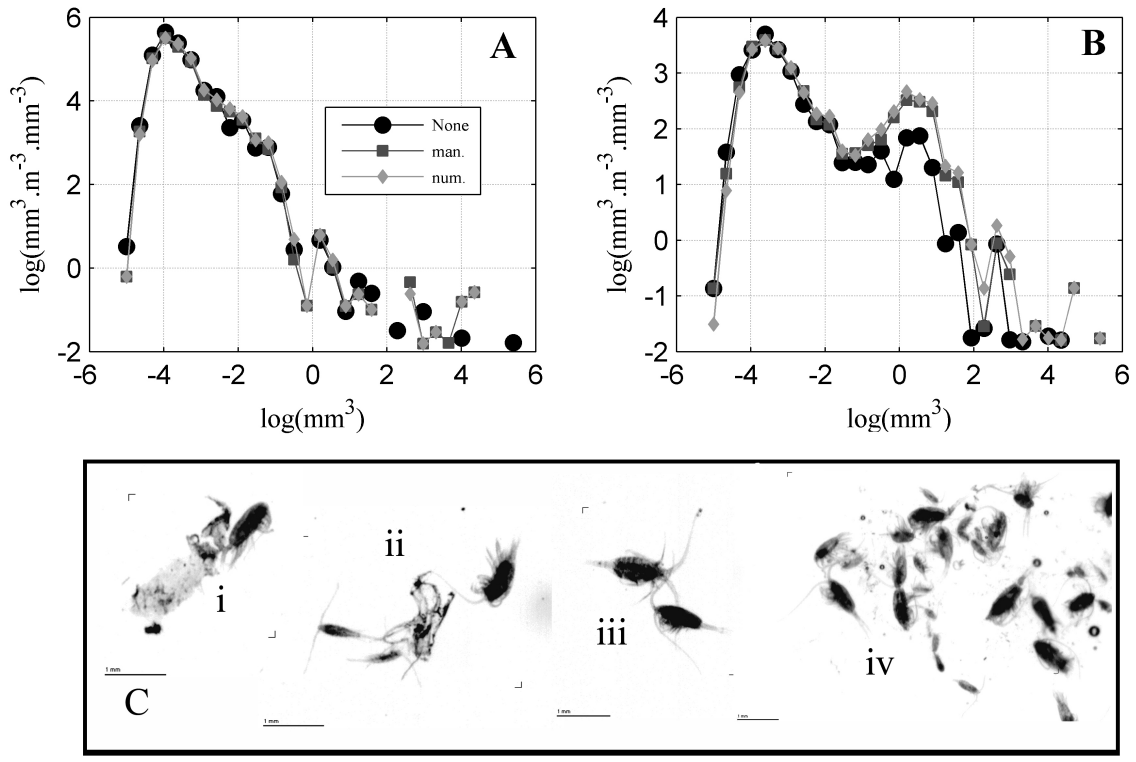

Figure II.3 – *Impact of touching objects (TO). Figures show zooplankton validated spectra in cases of no separation of TO (none), then with a manual separation on the scanning tray during 20 minutes (man.) and finally with a further numerical separation (num.). (A) experience one and (B) experience two. (C) examples of images with TO.*

respectively 46 and 85% of the total biovolume ($mm^3\ m^{-3}$) without any separation. With the manual separation these percentages decreased respectively to 14 and 19%, and with the further numerical separation they decreased to 6 and 3%. The maximum decrease of TO is observed in experiment 2 with a decrease from 85 to 3% of the total biovolume corresponding to a decrease from 217 to 4 $mm^3\ m^{-3}$ (table II.1).

In our experiment, removing the TO has the effect to decrease the total biovolume (i.e., TO + detritus + zooplankton) by 1.27 and 2.13. This result comes from the fact that the biovolume of a TO is greater than the sum of the biovolume of objects contained in the TO (i.e., according to eq. I.18, for example, the sum of the spherical biovolume of n similar objects of area a will be $n^{0.5}$ times lower than the biovolume of a TO containing these n objects and having an area $n \cdot a$). Therefore using biovolume estimates obtained with laboratory instruments which measure objects without identification and/or separation of TO may overestimate real biovolume and biomass calculated from it. Using an imaging system we can discriminate between different categories and separate TO. In the two experiments, the biovolume reduction of TO after separation contributed to increase zooplankton biovolume from 41 to 51 in the first case and from 35 to 99 $mm^3\ m^{-3}$ in the second case (respectively 19.6 and 64.7% of errors from the best estimates). With only a manual separation, the errors represented respectively 1.9 and 13.1% (table II.1). At the same time, the biovolume of non biological objects increased from 8 to 16 and from 3 to 17 $mm^3\ m^{-3}$. In both experiment the manual separation was sufficient to remove the majority of the TO. The effect of removing TO was different for the size spectra in the two experiments. In the first one, the shape of the size spectrum was rather similar, while in the second experiment a second mode at around 1.2 mm^3 was much better depicted after separation (fig. II.3 AB). For the three successive steps of separation (i.e., none, manual and numerical) the values of the slope were -0.877, -0.836 and -0.863 in the first experiment and -0.693, -0.590 and -0.620 in the second

one. The errors in the estimate of the slope without any separation were of 1.7 and 12.0% for the two experiments respectively and of 3.1 and 4.8% with a manual separation.

On the two contrasted examples chosen it first appeared that even with an area covered on the scanning tray below 3%, TO represented a large biovolume and modified the shape of the spectrum. Such results show that TO need to be identified and separated especially for a good estimate of the total zooplankton biovolume. Since a correct spectrum can already be obtained by the first step of the separation, i.e., 20 minutes of manual separation on the scanning tray, we recommend this minimum treatment before scanning samples. Using the numerical separation tool is useful if, for example, we want to extract rare large organisms from TO. In the future, automatic algorithms for the numerical separation of TO should be developed as they already exist in other fields (Malpica et al. 1997, Korath et al. 2008).

II.3.3 Biases on the shape of the predicted spectrum from automatic classification

The classical way to analyze the efficiency of the automatic classification is by considering the classification of each category as a whole (i.e., total abundance) through a confusion matrix, made on a validation set, which represents the natural proportion of each category in the field. Table II.2 synthesizes this confusion matrix. For individual categories the average recall rate was 0.77±0.13, and the

Table II.1 – *Results of the two experiments made to assess the impact of Touching Objects (TO) on the observed spectrum. The two samples were first scanned without any separation (none), then with a manual separation (man.) on the scanning tray, and finally with the further use of a numerical (num.) separation tool implemented in ZooProcess. The abundance (Ab, # m^{-3}), percentage of the abundance (% Ab), biovolume (Vol, mm^3 m^{-3}) and percentage of biovolume (% Vol) is presented for three categories, i.e., non biologic particles (detritus and fibers), touching objects and zooplankton.*

		non biologic				touching objects				zooplankton			
		Ab	%Ab	Vol	%Vol	Ab	%Ab	Vol	%Vol	Ab	%Ab	Vol	%Vol
exp. 1	none	147	27	8	9	30	5	42	46	377	68	41	45
	man.	161	29	9	13	48	9	10	14	347	63	52	74
	num.	186	33	16	22	21	4	4	06	362	63	51	72
exp. 2	none	37	30	3	1	10	8	217	85	74	61	35	14
	man.	43	32	14	11	8	6	23	19	85	63	86	70
	num.	51	36	17	14	2	2	4	3	88	63	99	83

Table II.2 – *Results of the confusion matrix based on the validation set. The number of objects in the learning set (#lr), the relative abundance in the field (p_i in %) and recall (Rec.) and contaminations (Cont.) rates are presented for each category and also for the synthetic categories all zooplankton (All zoo.) and all crustaceans.*

			Val. set	
Categories	#lr	p_i	Recall	Contam.
Fibers	1403	1.59	0.87	0.21
Touching objects	1602	5.11	0.82	0.46
Detritus	1402	21.57	0.84	0.11
Others zoo.	984	3.58	0.65	0.30
Appendicularians	1441	1.69	0.86	0.21
Chaetognaths	563	0.43	0.93	0.11
Cladocerans	596	1.30	0.64	0.45
Copepods	1686	60.72	0.92	0.02
Decapods	563	0.65	0.57	0.46
Eggs	367	0.64	0.50	0.21
Gelatinous	1245	1.53	0.82	0.40
Nauplii	547	0.65	0.82	0.42
Penilia avirostris	1158	0.16	0.80	0.87
Pteropods	518	0.38	0.73	0.84
All zoo.	9668	71.73	0.94	0.04
Crustaceans	4550	63.45	0.93	0.03

average contamination rate was 0.36±0.25. The synthetic "crustaceans" category had a recall rate of 0.93 and a contamination rate of 0.03.

Classical assessing of automatic recognition is not enough in size spectrum research. It is crucial to check if the effect of misrecognition affects homogeneously all the size classes within a category (i.e., to evaluate the bias in the predicted spectrum compared to the validated spectrum). Crustaceans were taken as example for this. This section focuses on the 22 validated crustaceans spectra through different seasons and on parameters extracted from them (i.e., total abundance and biovolume, slope and Shannon index, fig. II.4). The differences in the slope estimated from validated spectra (validated slope) and from predicted spectra represent on average 5.4±3.9 % of the validated slope. For the biovolume, the same differences, represent on average 7.4±5.3 % (fig. II.4). For all these parameters the validated and predicted spectra are significantly correlated with p values of Pearson correlation coefficients <0.001 and slope of correlation equals to 1. No statistical differences were found between parameters extracted from the validated and predicted spectra.

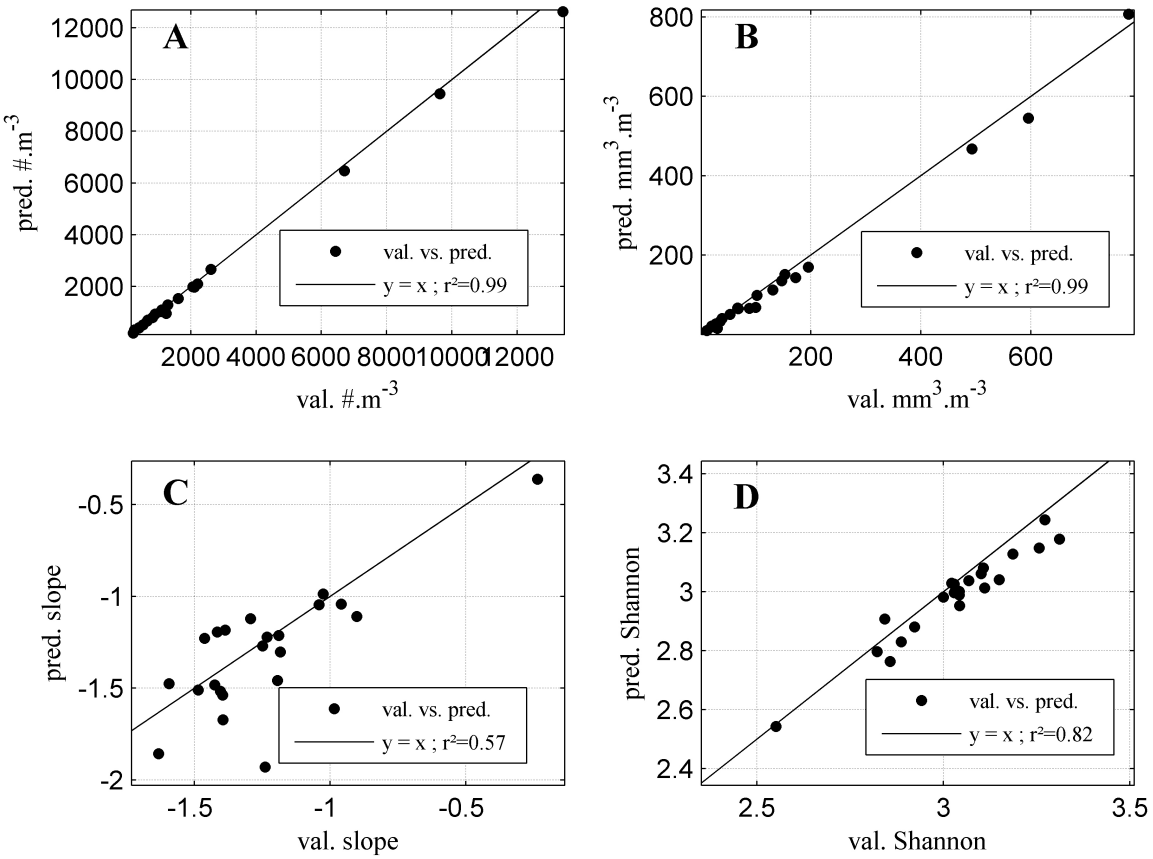

Figure II.4 – *Comparison of predicted and validated recognition of crustaceans for total abundance (A), total biovolume (B), slope of the linear regression (C) and Shannon entropy index (D) for the two years (2003 and 2006) which have been visually validated.*

The effect of size and seasonality on the recognition performance (recall and contamination rates) was also studied (table II.3, fig. II.5). A two-way ANOVA indicated that recall rates were affected by the size class but not by the season (p=0.004 and p=0.578 respectively) and that contamination rates were affected both by the size class and the season (p=0.002 and p=0.016 respectively). On average the recall rate was over 0.85 for size classes 3 to 14 and became more variable for the following classes (>0.7241 mm^3). Recall rates were significantly linked to the number of individuals in size classes in the learning set (#lr on table II.3; Pearson r^2=0.552, p=0.008). Therefore to increase the recall in the larger size classes, one should increase the number of large organisms in the learning set. However, according to the few number of large individuals, integrating enough of them (more than a hundred) in the learning set will be equivalent to make their validation, for the studied dataset. On average, contamination rates were consistently low below size class 18 and high for the large size

Table II.3 – *Recall (rec.) and Contamination (cont.) for crustaceans related to the size class and the season issued from fig. II.5. For each size class the lower (x_n) and upper (x_{n+1}) limits, the relative abundance in the field (p_i in %), the number of objects in the learning set ($\#_{lr}$) and recall (rec.) and contamination (cont.) for the four seasons and the mean are presented.*

					winter		spring		summer		autumn		**mean**	
class	x_n	x_{n+1}	p_i	$\#_{lr}$	rec.	cont.	rec.	cont.	rec.	cont.	rec.	cont.	rec.	cont.
1	0.0057	0.0080	1.0	0	0.95	0.00			1.00	0.00	0.49	0.00	0.81	0
2	0.0080	0.0113	24.4	5	0.85	0.02	0.55	0.03	0.75	0.06	0.66	0.19	0.70	0.08
3	0.0113	0.0160	43.0	91	0.92	0.02	0.91	0.01	0.93	0.08	0.84	0.03	0.90	0.04
4	0.0160	0.0226	65.8	355	0.95	0.01	0.95	0.02	0.96	0.02	0.91	0.04	0.94	0.02
5	0.0226	0.0320	77.3	544	0.97	0.01	0.96	0.01	0.96	0.03	0.93	0.05	0.96	0.03
6	0.0320	0.0453	80.0	587	0.94	0.04	0.96	0.02	0.95	0.02	0.95	0.05	0.95	0.03
7	0.0453	0.0640	77.4	599	0.95	0.05	0.94	0.02	0.95	0.04	0.94	0.06	0.95	0.04
8	0.0640	0.0905	72.7	563	0.97	0.02	0.89	0.02	0.92	0.03	0.92	0.05	0.93	0.03
9	0.0905	0.1280	63.4	625	0.93	0.06	0.89	0.06	0.92	0.06	0.71	0.17	0.86	0.09
10	0.1280	0.1810	51.4	464	0.87	0.05	0.87	0.10	0.85	0.10	0.80	0.10	0.85	0.09
11	0.1810	0.2560	38.2	248	0.79	0.05	0.82	0.02	0.80	0.09	0.79	0.32	0.80	0.12
12	0.2560	0.3620	29.4	174	0.79	0.03	0.56	0.02	0.70	0.03	0.69	0.04	0.69	0.03
13	0.3620	0.5120	20.9	110	0.67	0.14	0.62	0.10	0.81	0.18	0.64	0.20	0.69	0.16
14	0.5120	0.7241	14.4	64	0.93	0.00	0.75	0.09	0.60	0.11	1.00	0.00	0.82	0.05
15	0.7241	1.0240	13.1	51	0.60	0.00	0.35	0.00	0.65	0.00	1.00	0.49	0.65	0.12
16	1.0240	1.4482	14.7	32	0.90	0.00	0.96	0.07	0.76	0.27	0.00		0.66	0.11
17	1.4482	2.0480	16.1	15	0.88	0.00	1.00	0.00	0.42	0.35	0.00		0.58	0.13
18	2.0480	2.8963	12.7	8	0.65	0.20	0.80	0.79		1.00			0.73	0.67
19	2.8963	4.0960	10.8	8		1.00	0.00		0.53	0.00			0.27	0.50
20	4.0960	5.7926	13.4	3			0.58	0.00	0.64	0.00		1.00	0.61	0.33
21	5.7926	8.1920	9.6	1			0.00						0	
22	8.1920	11.5852	8.4	0										
23	11.5852	16.3840	5.4	3			1.00	0.00					1	0
		Mean			0.86	0.09	0.73	0.07	0.79	0.12	0.72	0.17	0.74	0.13

classes (>2.048 mm^3). In addition, the lowest mean contamination rate occurred in winter and spring (0.09 and 0.07) and was the highest in summer and autumn (0.12 and 0.17) where crustaceans show their lowest abundance. The low relative abundance of large crustaceans make them more sensitive to contamination, yet, this does not fully explain their high contamination (p_i on table II.3; r^2=-0.392, p=0.079). And the effect of low recall rates on these size classes in other categories, together with the random effect due to the rarity of large size classes, can explain the remaining variability in contamination rates.

Thus, when compared to the validated spectrum, automatic classification can be used to generate a predicted spectrum not significantly different for the extracted parameters (i.e., total abundance,

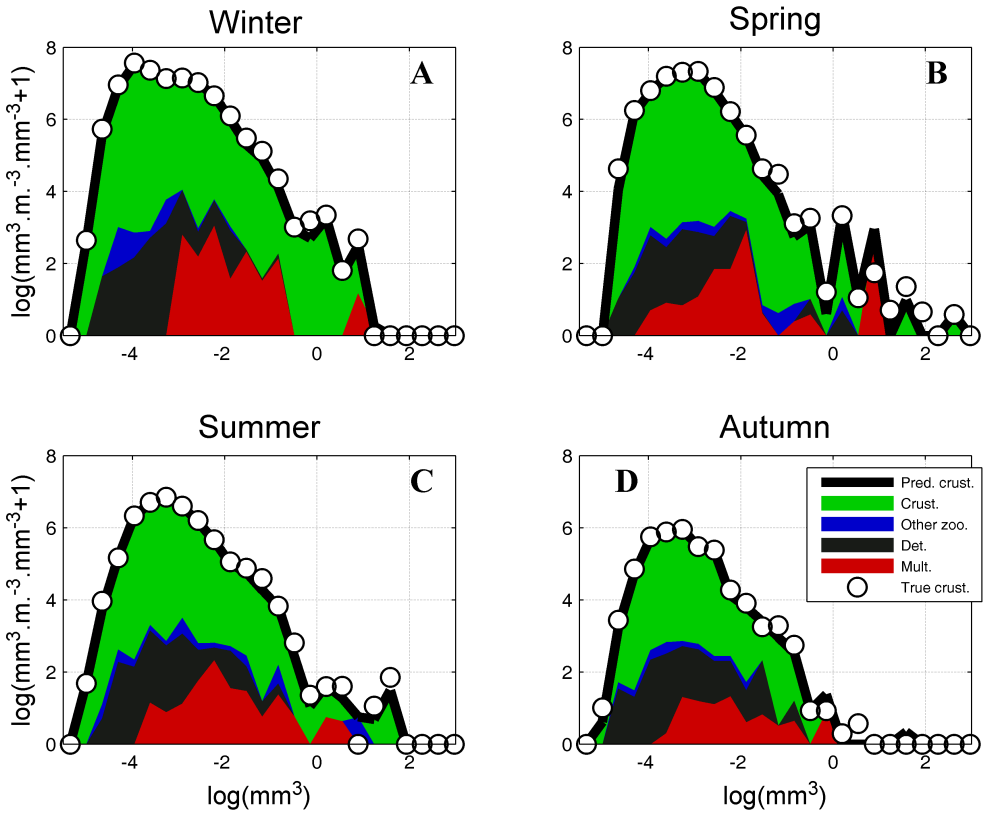

Figure II.5 – *Four seasons (A: winter, B: spring, C: summer and D: autumn) of validated crustaceans spectrum (white circle, Val. crust.), predicted crustaceans spectrum (black line, Pred. crust.) and from dark grey to light grey the composition of predicted crustaceans spectrum, which is respectively composed of crustaceans (Crust.), other zooplankters (Other zoo.), detritus (Det.) and touching objects (TO). In each figure is indicated the percentage of each of these groups inside the predicted crustaceans spectrum. The percentage of crustaceans is the value (1-contamination).*

biovolume, slope and Shannon index), even if the quality of automatic classification is not homogeneously spread throughout the spectrum. This is due to the compensation between recall and contamination (fig. II.6), i.e., "good measure for bad reasons". Nonetheless, including large size classes in the analysis is not rigorous for studies where taxonomic groups are important. For these large size classes, contamination is too high (>0.50) and recall highly variable and low (0.3-0.7, table II.3). We suggest that objects larger than 2.048 mm^3 (or 0.7241 mm^3 to be conservative, see table II.3) and smaller than 6.9 mm^3 (Fig. II.2) should be manually corrected. The manual correction of objects larger than 0.724 mm^3 decreases the average errors in the slope and biovolume from the values, mentioned above, of 5.4±3.9 and 7.4±5.3 % to the values of 2.4±1.9 % for the slope and 3.8±4.2 % for the biovolume.

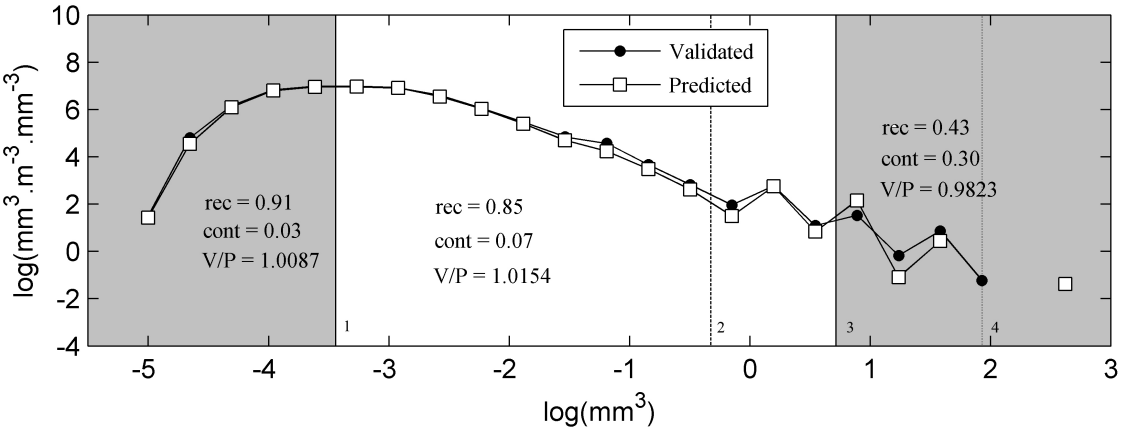

Figure II.6 – *Confidence size range of the crustaceans spectrum (white) according to the mode (1: 0.032 mm^3) and the automatic classification minimum efficiency (3: 2.048 mm^3). The more rigorous limit of the automatic classification efficiency (2: 0.724 mm^3) and the crossing point of the WP2 and Régent nets zooplankton size spectra (4: 6.9 mm^3) are also displayed. Recall (rec.), contamination (cont.) and the Validated/predicted (V/P) values are shown for three part of the spectrum.*

Beyond the gain of quality in the estimate of the slope and of the total biovolume, there is also a gain in the taxonomic classification accuracy (Gorsky et al. 2010).

II.3.4 Biases in using elliptical biovolume compared to spherical biovolume and taxonomic-based biomass estimate

Several ecological and modeling studies tend to consider zooplankton as a size structured community neglecting the taxonomic composition. Imaging systems provide tools for a fast measurement of the zooplankton size spectrum and allow the comparison of different models to compute the size spectrum using different measurements and their sensibility to the taxonomic composition of the community, which was not possible with the use of electronic or optical counters. The image analysis provides a two dimensional estimate of the individual biovolume, i.e., the Elliptical biovolume (*EBv*). Previous instruments used to measure individual biovolume gave only a one dimensional estimate, i.e., the Spherical biovolume (*SBv*), directly computed from the projected area of the object. The first part of this section will characterized the error and possible conversions due to the use of the *EBv* or the *SBv*.

Mathematically, with eq. I.16, I.18 and I.17, the *EBv* is linked to the *SBv* by:

$$EBv = SBv \cdot \sqrt{\frac{Minor}{Major}} \tag{II.1}$$

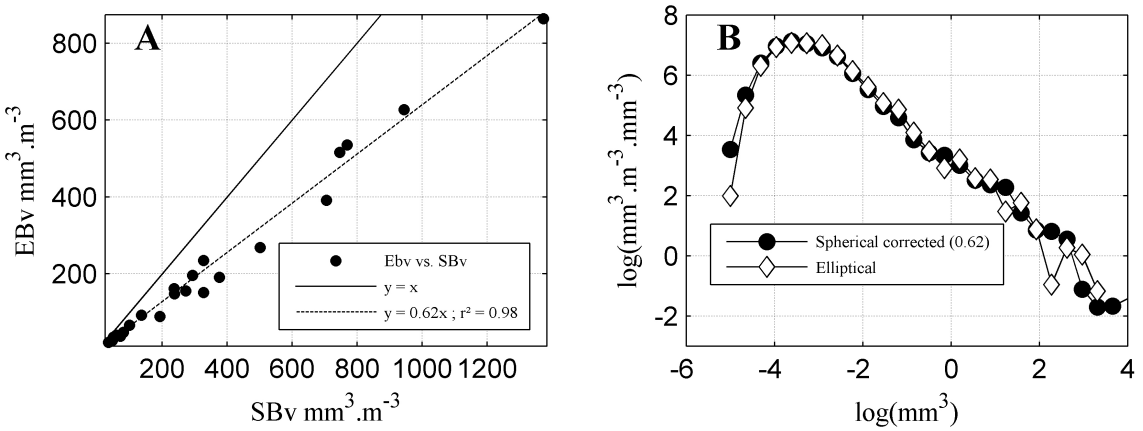

Figure II.7 – *Impact of spherical vs. elliptical biovolume measurements on the shape and parameters extracted from "N-BSS" of crustaceans. (A) total biovolume with a linear adjustment* $y = 0.62x$, r^2*=0.98. (B) average "N-BSS" calculated with an elliptical biovolume and "N-BSS" calculated with a spherical biovolume but corrected with the conversion factor 0.62 only (i.e., conversion to "N-NSS", decrease of the nominal size by 0.62, then re-conversion to "N-BSS" using the new nominal size biovolume).*

Table II.4 – *Average Minor:Major ratio (±std), slope (b) of the regression* $EBv = b \cdot SBv$, r^2 *of the regression and number of individuals used for the regression (N) for the 11 zooplankton categories.*

Categories	*Minor:Major*	$EBv = b.SBv$	r^2	*N*
Appendicularians	0.30±0.15	0.44	0.926	560
Chaetognaths	0.14±0.09	0.30	0.981	127
Cladocerans	0.75±0.10	0.85	0.979	378
Copepods	0.45±0.10	0.67	0.979	15309
Decapods	0.48±0.16	0.47	0.922	175
Eggs	0.93±0.06	0.97	0.998	129
Gelatinous	0.56±0.19	0.75	0.979	571
Nauplii	0.72±0.11	0.85	0.974	538
Penilia avirostris	0.66±0.13	0.81	0.953	345
Pteropods	0.30±0.14	0.47	0.839	293
Other zoo.	0.74±0.15	0.83	0.973	926

and thus depends on the elongation of each object. If *Major* and *Minor* axes are equal, *EBv* is equal to *SBv*. In other cases *EBv*<*SBv*. Among the validated images, it was found that the *Minor:Major* ratio was for example 0.45±0.10 for copepods. See table II.4 for *Minor:Major* ratio of the other zooplankton categories identified. According to these ratios, the total *EBv* of a community composed only of copepods will be 0.67 *SBv*. Among the 22 samples analyzed, the *EBv:SBv* was on average close to this value with an average of 0.62±0.08 (min=0.46, max=0.73) of the *SBv* (fig. II.7 A). The relationship between the total *EBv* and the total *SBv* was not highly variable and was globally significant (r^2=0.98, p<0.01, fig. II.7 A). Moreover, no relationship existed between the size of zooplankton

Table II.5 – *Relations used to computed the dry weight (in µg) from the area (in mm^3) measured by image analysis. the relation "Copepods" was used for categories copepods and nauplii — "Chaetognaths" was used for chaetognaths — "Other crustaceans" was used for decapods, cladocerans, Penilia avirostris and other crustaceans — "Gelatinous" was used for gelatinous — "Other" was used for all other categories.* $^{+}$ *is for relations from Hernández-León & Montero (2006) and* ^{o} *is for relations from Lehette & Hernández-León (2009).*

Categories	dry weight
Copepods^{+o}	$43.38 \cdot area^{1.54}$
Chaetognaths^{o}	$23.45 \cdot area^{1.19}$
Other crustaceans^{+o}	$43.97 \cdot area^{1.52}$
Gelatinous^{o}	$43.17 \cdot area^{1.02}$
Other^{+}	$36.61 \cdot area^{1.52}$

(individual *EBv*) and the *Minor:Major* ratio (r^2 <0.01), which was highly variable inside each size classes without any trend. That is to say, for Point B a single conversion factor, i.e., 0.62 (see above), can be used to convert a size spectrum computed using a spherical model to an elliptical model of biovolume. Fig. II.7 B shows the average *EBv* spectrum and the converted *SBv* spectrum. The direct comparison of these two spectra using the Kolmogorov-Smirnov test on the 22 samples used shows no statistical differences (p>0.05). Moreover, among the zooplankton of Point B, no significant relationship exists between the individual size and the *Minor:Major* ratio (r^2 <0.001). As a consequence of the non-relationship between the size and the shape of the zooplankton at this location, the global shape of spectra is not affected and the ecological parameters (i.e., slope and Shannon size diversity index) extracted from *EBv* size spectra and *SBv* size spectra show no statistical differences ($y = x$, r^2=0.86, p<0.01 and r^2=0.90, p<0.01 respectively).

Moreover, it is possible to relate biovolume estimates or size measurements provided by the image analysis to the elemental composition (mostly carbon or nitrogen content), or dry biomass with different size-biomass relationships according to the taxonomic group of each individual (Alcaraz et al. 2003, Hernández-León & Montero 2006, Lehette & Hernández-León 2009, Gorsky et al. 2010). One of the principle of the size-based analysis is to consider the zooplankton community as a unique category, structured by its size distribution. This second part will test if ecological parameters (total biovolume or biomass, slope and Shannon index) calculated on biovolume (EBv) size spectra com-

pared to the ones calculated on biomass (computed from the taxonomic origin of each objects) are significantly different. Relations of Hernández-León & Montero (2006) and Lehette & Hernández-León (2009) were used for size-biomass conversion (table II.5). These relations stand for antarctic and tropical plankton and relate to area calculated from a flatbed scanner followed by image analysis similar to these work. Relations for copepods, other crustaceans, chaetognaths, gelatinous and other zooplankton are used (table II.5). Axes of the biomass size spectrum are $\log(\mathrm{mg})$ for the x-axis and $\log(\mathrm{mg\ m^{-3}mg^{-1}})$ for the y-axis. Total biovolume and total biomass (fig. II.8 A) are significantly correlated (r=0.989, $p<0.001$). A significant correlation appears also for the slope (fig. II.8 B, r=0.946, $p<0.001$) and for the Shannon index (fig. II.8 C, r=0.797, $p<0.001$). This was also tested with the Régent net which samples more gelatinous. However, even if correlations are less strong they stay significants.

One of the strength of using a single model of biovolume estimate is the rapid measurement of the size distribution from the image analysis. In this case, the elliptical model appears more realistic since it is a function of both the projected size and the shape of each objects and not only a function of the projected size. The comparison with the taxonomic-based estimate of biomass does not show any significant differences in ecological parameters computed from size spectra. Yet, a lack of data points to the need of more experimental relationships between size and mass estimates for the different zooplankton groups. However, from a size-based analysis point of view, a single model of biovolume conversion appears sufficient to extract relevant ecological parameters and to study the underlying dynamics of the zooplankton community.

II.4 Conclusion

The present work examines some of the elements that affect the zooplankton size spectrum measured using an imaging method followed by automatic classification of objects. We studied three biases due

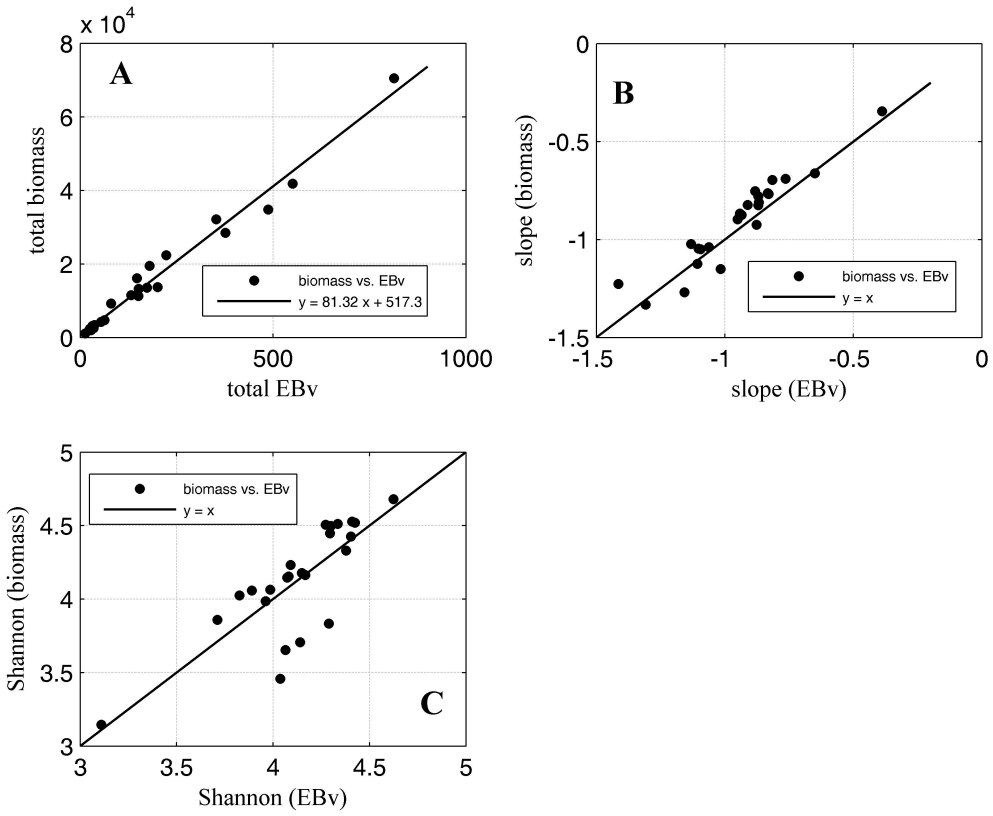

Figure II.8 – *Comparison EBv vs. biomass (in $\mu g\ m^{-3}$ calculated from relationships of Hernández-León & Montero (2006) and Lehette & Hernández-León (2009). (A) shows the relationship between the total EBv and the total biomass of the zooplankton community, (B) shows the relationship between the slopes calculated from N-$B_{biovolume}$SS and N-$B_{biomass}$SS and (C) the relationship between Shannon index calculated from both spectra.*

to imaging systems that can impact the final size spectrum: touching objects, misclassification and biovolume estimations. The bias due to the net sampling was also briefly investigated (see II.3.1 for the main conclusion).

Touching objects did not significantly affect the observed spectrum of our dataset when a short manual separation was carried out prior to the image acquisition. The predicted spectrum generated by the automatic classification of objects was most accurate for the most abundant categories (i.e., all zooplankton, all crustaceans, and all copepods), while categories with few objects were poorly classified. For a synoptic analysis of the well-recognized groups such as copepods, automatic classification accurately estimated ecological parameters extracted from size spectra and more time could be spent on the sampling effort. However, size classes with few objects were poorly classified and should be validated. For example, crustaceans >0.7241 mm^3 were poorly classified in our data set

and required manual correction of the predicted objects. Since the manual separation of touching objects prior to the scan decreased by 5 to 10 times the error in the estimate of the zooplankton biovolume and the manual correction of large objects ($>$0.724 mm^3) decreased it by around 2 times. It appeared more efficient, for a good estimate of the total zooplankton biovolume, to spent more time separating the touching objects than validating the large ones. As for the slope estimation of the zooplankton size spectra, the benefits of the manual separation of touching objects was less clear. However, the validation of large objects decreased by around 2 times the error in the slope estimates. It appears consequently relevant to spent time on both decreasing the number of TO and validating large objects.

The elliptical biovolume provided a more accurate estimate of the size of a zooplankton. Converting from a spherical to an elliptical biovolume reduced the volumes in the dataset but did not significantly change the shape of the spectrum. Then, taxonomic-based conversion of size to biomass did not change significantly the shape of the spectrum for the studied ecosystem compared to the use of a single model like the elliptical one. Yet, this will depends — like for elliptical to spherical conversion — on the taxonomic composition of the studied ecosystem. The image analysis and automatic classification (using a human-made learning set) provide relevant size spectra that can be directly used to investigate the underlying community dynamics.

These biases are common to all image-derived zooplankton spectra, whether from a scanner or *in situ* plankton imaging system. However, the impact of each bias on zooplankton spectra will depend on the characteristics of the data set (e.g., species diversity, mucus, detritus) and, for automatic classification, the training set (e.g., number of objects in a category in each size class) and the scientific objectives (focus on well automatically recognized groups in long time series or synoptic surveys). Thus, the methodology we applied to assess these biases should be used as a framework for other studies that apply laboratory or *in situ* plankton imaging systems. For example, the method applied

to minimize touching objects on a 2D imaging device (ZooScan or flatbed scanner) will differ from *in situ* instruments that sample a more complex 3D volume. On the other hand, both laboratory and *in situ* systems are affected by errors in the automatic classification of objects into categories and the choice of the model to estimate biovolume.

III Inter-annual variability of the Ligurian Sea pelagic ecosystem

III.1 Introduction

Previous time series analyses on different components of the plankton communities at Point B highlighted the correspondence between changes in the abundance and/or composition of some key species and the shift in the local climate that occurred in the late '80s (Molinero et al. 2005; 2008). In those studies, jellyfish seemed to outcompete chaetognaths and to be detrimental to copepods, whose abundance dropped from the late '80s. The authors hypothesized a trophic reorganization due to oligotrophication related to increasing stratification driven by water warming in the '90s. However, by analyzing 10 more years of the same time series but at the community level, Garcia-Comas et al. (Submitted), **?** found that total copepods and chaetognaths recovered almost the abundance of the '80s by year 2003 while jellyfish remained abundant. Instead of a long term trend, the authors proposed a quasi decadal fluctuation driven by changes in winter mixing intensity and acting through nutrients input and phytoplankton production. They suggested that dry years in the late '80s and from 1999 to 2003 would have increased surface salinity in winter and hence density close to deep values, then causing deep winter convection in the coastal Ligurian Sea. The authors hypothesized that zooplankton would have benefited from higher phytoplankton biomass. However, their study lacked date of nutrients and phytoplankton. A recent study at the observatory site Dyfamed in the open Ligurian Sea supports the hypothesis of a link between climate variability, notably precipitations, and phytoplankton production and composition (Marty & Chiavérini 2010). Convection as deep as 2000 m has been reported by Marty & Chiavérini (2010) to occur from winter 1999 to 2006 (except for 2001 and 2002) because of drier winters and reduced freshwater input from rivers.

Deep convection brought to the surface high load of nutrients that triggered an intense phytoplankton bloom of mainly diatoms (Marty & Chiavérini 2010). In addition, in the coastal zone of the Bay of Calvi (northern Corsica, Ligurian Sea), phytoplankton blooms were reported to decrease from 1978 to 1998 as a possible consequence of lower mixing related to a salinity decrease and temperature increase, which was appointed to entail less nutrient replenishment (Goffart et al. 2002). The poor sampling frequency (only 5 years in a 20 years' time series) prevented the author to determine the detailed controlling factors. From the available literature, it seems that, in the NW Mediterranean sea, surface salinity is the main determinant of the structure of the pelagic ecosystem and affects some of its components such as medusæ (Goy 1997, Buecher et al. 1997), dolioliids (Menard et al. 1997), zooplankton (Garcia-Comas et al. Submitted) and phytoplankton (Marty & Chiavérini 2010).

The aim of the present chapter is to extract the main causes of inter-annual variability of zooplankton in the Ligurian Sea and to test whether hypotheses formulated by Garcia-Comas et al. (Submitted) and Molinero et al. (2005; 2008) fit the observed dynamics. Yet, rapid changes in environmental conditions and plankton can occur at short time scales (Underwood 1989, Bustillos-Guzmán et al. 1995, Fernàndes de Puelles et al. 2007). Therefore, temporal studies based on monthly sampling or less (e.g., Goffart et al. 2002, Molinero et al. 2005; 2008, Garcia-Comas et al. Submitted, Marty & Chiavérini 2010) often miss important changes. Here, a weekly dataset that spans from 1995 to 2005 and is part of the long-term time series at Point B has been analyzed independently from the work of Molinero et al. (2008) and Garcia-Comas et al. (Submitted).

III.2 Datasets used

The sampling site was presented in section I.3.1. The environmental variables selected for the analysis are: nitrates (NO_3 μmol L^{-1}), chlorophyll-*a* (μg L^{-1}), phosphates (μmol L^{-1}), silicates (μmol L^{-1}), suspended particles, sea water temperature (°C), salinity (psu) and density (kg m^{-3}), air temperature

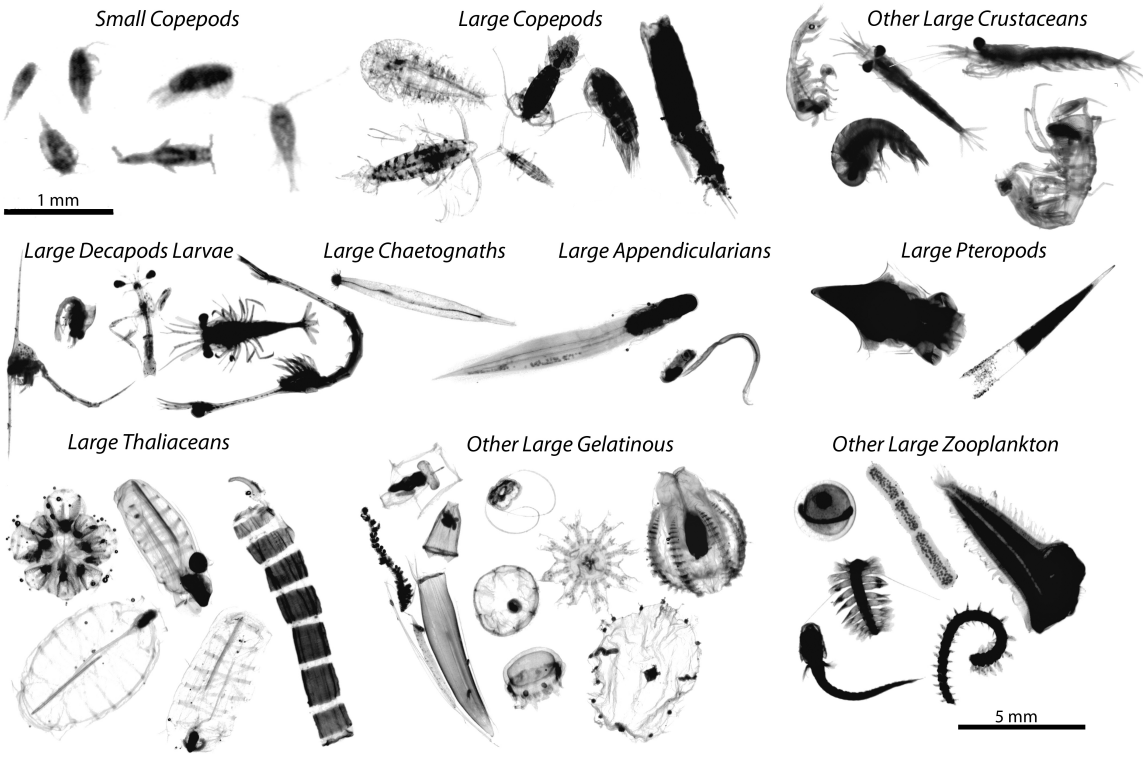

Figure III.1 – *Example of thumbnails directly issued from the ZooScan / ZooProcess of the ten identified zooplankton taxonomic groups. All thumbnails have the same scale (bottom right corner) except the small copepods which have their own scale on top left.*

(°C), precipitations (mm d^{-1}) and irradiance (J cm^{-2} d^{-1}). Water samples for suspended particles, nitrates, phosphates, silicates, and chlorophyll-*a* analysis were collected with Niskin bottles at six different depth, i.e., surface, 10, 20, 30, 50 and 75 m depth. Depth averaged values (0-75 m depth) were used in our analysis. Suspended particles were analyzed with the Coulter Counter, giving information on size distribution (slope), total biovolume and total abundance of particles from 2.9 to 92.8 μm. Nitrates were analyzed by colorimetry (Aminot & Kérouel 2004) with an autoanalyzer Technicon Alliance, chlorophyll-*a* was determined by spectrometry and fluorimetry (Strickland & Parsons 1977). A Seabird SBE25 CTD was used for weekly sea water temperature, salinity and density analysis of the water column. In the present chapter, mean values of temperature, salinity and density of the upper layer were used (10 to 40 m depth, see section III.3.2.3). Local weather came from the Sémaphore meteorological station, parameters used were temperature (mean daily temperature), precipitations and irradiation.

Zooplankton was sampled and analyzed as presented in section I.3.2. Evaluation of the accuracy of the automatic classification prediction was performed in chapter II. The zooplankton was successfully separated from non-living objects with a recall rate of 0.94 and a contamination rate of 0.04. However this is mainly due to the efficient classification of copepods (recall rate of 0.92 and contamination of 0.02). However, these rates decreased for large objects and a manual separation of objects larger than 0.724 mm^3 in "EBv" was proposed (more or less 1.5 mm length). In this chapter, all objects larger than this value were visually identified from non-living objects and classified into nine zooplankton categories: appendicularians, chaetognaths, copepods, decapods larvæ, other crustaceans, gelatinous (cnidarians an ctenophors), pteropods, thaliaceans and other zooplankton (fig. III.1 for examples of thumbnails). These large organisms (i.e., $>$0.724 mm^3 "EBv") accounted for an average of 42% of the total zooplankton apparent biovolume. Adding the small copepods automatically classified, ten zooplankton categories were defined. Percentages concerning these categories and representative species are given in table III.1. These percentages must be taken with precaution because they stand for percentages of the apparent biovolume, which is different from biomass, especially when comparing crustaceans and jellies. Yet, we focalized here on the variation of these groups and not on their absolute concentration in the field. Biases in the evaluation of their biovolume were supposed constant throughout the time lag considered.

In addition, the size structure of the crustaceans community was analyzed following the procedure presented in section I.3.2 and in chapter II. Again, crustaceans $<$0.724 mm^3 "EBv" came from the automatic identification whereas tails of spectra were visually corrected due to the poor classification of these size classes (see chapter II). From these spectra the log-linear slope was analyzed, as mentioned in section I.3.2 and in Quiñones et al. (2003), more complex measurements on size spectra (e.g. Pareto type II fitting or other) lack in having an ecological meaning and so were not analyzed.

Finally, monthly CTD casts at the DYFAMED station in the central Ligurian Sea from 1995

Table III.1 – *Large zooplankton categories (>0.724 mm^3), percentage of abundance ("Ab.") / apparent elliptical biovolume ("EBv") of these categories among zooplankton of this size range (for indication only), representative species or groups and dominant diet considered in this work. The category "Copepods (small)" comes from copepods automatically sorted from 0.032 to 0.724 mm^3 and the percentage given applies on zooplankton of this size range only. The large zooplankton (i.e., >0.724 mm^3) represent 1.8 and 31.5 % of total zooplankton abundance and apparent biovolume respectively.*

Taxonomic groups	*%Ab./EBv*	Representative species	Dominant diet
Copepods (small)	61.4 / 46.5	*Acartia spp., Oithona spp., Clausocalanus spp., Paracalanus spp., Oncaea spp., Farranula rostrata* ...	microplanktonophage
Appendicularians	1.2 / 0.5	*Oikopleura albicans, Fritillaria pelucida* ...	filter-feeders
Chaetognaths	6.1 / 4.4	*Sagitta inflata*	carnivores (copepods)
Copepods (large)	12.7 / 4.8	*Centropages spp., Temora stylifera, Calanus minor, Calanus gracilis, Pleuromamma spp., Candacia spp., Euchaeta marina* ...	omnivores
Decapods larvæ	3.3 / 2.4	Zoé, Protozoé and Metazoé larvæ of mostly crabs, langoustine and lobsters	omnivores
Crustaceans (other)	5.1 / 3.2	Euphausiids (*Meganyctiphanes norvegica, Nyctiphanes couchii*) and mysidacea	omnivores
Gelatinous predators	19.6 / 34.1	ctenophores (*Beroe sp., Pleurobrachia sp.* ...), siphonophores (*Muggia sp., Lensia sp., Agalma elegans* ...), Medusæ (Ephyrula of *Pelagia noctiluca, Rhopanolema velatum, Liriope Tetraphylla, Solmissus albecans* ...) ...	carnivores
Pteropods	4.7 / 9.3	*Cavolinia inflexa, Creseis laciculata* ...	filter-feeders / suspensivors
Thaliaceans	6.9 / 12.8	*Thalia democratica, Salpa fusiformis, Dolioleta gegenbauri, Doliolum nationalis, Pyrosoma atlanticum* ...	filter-feeders
Zooplankton (other)	1.7 / 1.2	fish larvæ, annelids ...	mixed

to 2005 were analyzed to compare the main tendency of hydrology between the coastal northern Ligurian Sea (Point B station) and this offshore station (DYFAMED). Mean seasonal values of the layer 20 to 80 m depth were taken for salinity, temperature and density.

III.3 Results

The raw data used in the present section are presented in appendix A. Time series of weekly values are presented together with bowplots made on monthly values to show the seasonality of these parameters. Results are organized in two subsections, corresponding to different ways of analysis. The first subsection presents some statistical analyses made on the data whereas the second subsection follows a descriptive analysis of the data. To deal with autocorrelation on variables, all variables used in the first subsection were de-noised before analysis (see Rodionov (2006) for the importance of de-noising). The effect of the de-noising is shown on fig. III.2 with the de-noising of the zooplankton

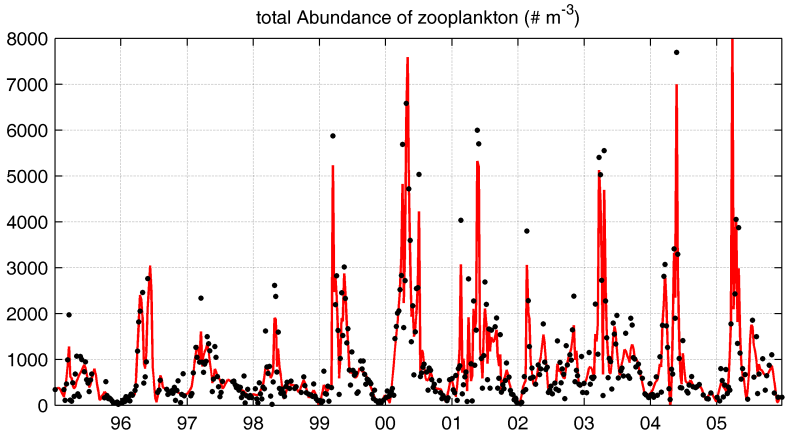

Figure III.2 – *De-noising of the zooplankton total abundance time series. Raw values are black dots and the de-noised time series in shown in red. The de-noising was made using the Matlab functions "ddencmp" and "wdencmp" of the wavelet toolbox.*

total abundance time-series. Moreover the effect of the de-noising of all parameters is presented in appendix A. The de-noising was made using the matlab function "ddencmp" and "wdencmp" (Donoho 1995).

III.3.1 Statistical analysis

In this section, "Zab" is for total abundance of zooplankton, "Zbv" is for total biovolume of zooplankton, "Zsl" is for the slope of crustaceans N-BSS, "R^2" is for the R^2 of crustaceans N-BSS, "ms" is for crustaceans mean size, "cop" is for small copepods, "Cop" is for large copepods, "dec" is for decapods larvæ, "cru" is for other crustaceans, "cha" is for chaetognaths, "app" is for appendicularians, "tha" is for thaliaceans, "pte" is for pteropods, "gel" is for gelatinous predators, "oth" is for other zooplankton, emphNO_3 is nitrates, "Pho" is phosphates, "Sil" is for silicates, "chl" is for chlorophyll-*a*, "SPab" is for suspended particles abundance, "SPbv" for their biovolume, "SPsl" for slopes of suspended particles N-BSS, "wT" is for water temperature, "wS" is for water salinity, "wD" is for water density, "T" is for air temperature, "P" is for precipitations and "I" is for solar irradiation. For hydrological ("wT", "wS" and "wD") and meteorological parameters ("T", "P", "I"), annual means of each season were taken, the number correspond to the season, "1" is for months 1,2 and 3 (winter), "2" for months 4,5 and 6 (spring) until "4" (months 10, 11, 12, autumn).

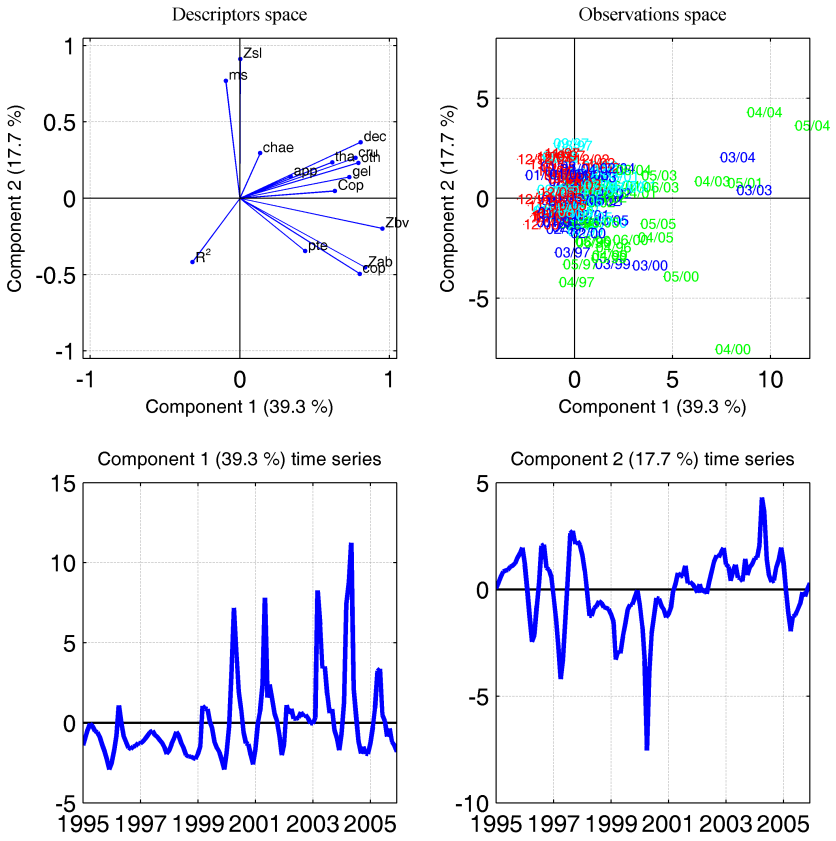

Figure III.3 – *PCA made on monthly values of zooplankton. (A) represent the space of descriptors, (B) the space of observations, (C) the time series of the first PC, and (D) of the second PC. In the space of observations (B), blue is for winter months (months 1,2 and 3), green is for spring months (4,5,6), cyan for summer months (7,8,9) and red for autumn (10, 11, 12).*

III.3.1.1 Links between parameters using Principal Components Analysis (PCA)

Four PCA were performed to investigate the relations between parameters, the first one on monthly values of zooplankton (fig. III.3) and the second one on monthly values of environmental parameters (fig. III.4). Then the third and the forth ones were made on annual values of zooplankton and environment (figs. III.5 and III.6). Each PCA presents the descriptors and observations spaces (for PC 1 and 2) as well as the time series of these two first PCs.

The first PCA, on monthly values of zooplankton parameters (i.e., total zooplankton abundance, biovolume, abundances of taxonomic groups and crustaceans size structure parameters, see fig. III.3), shows a strong correlation between the first PC (39.3% of variance) and the total zooplankton abundance, biovolume and all taxonomic groups abundances. All these parameters vary in the same direc-

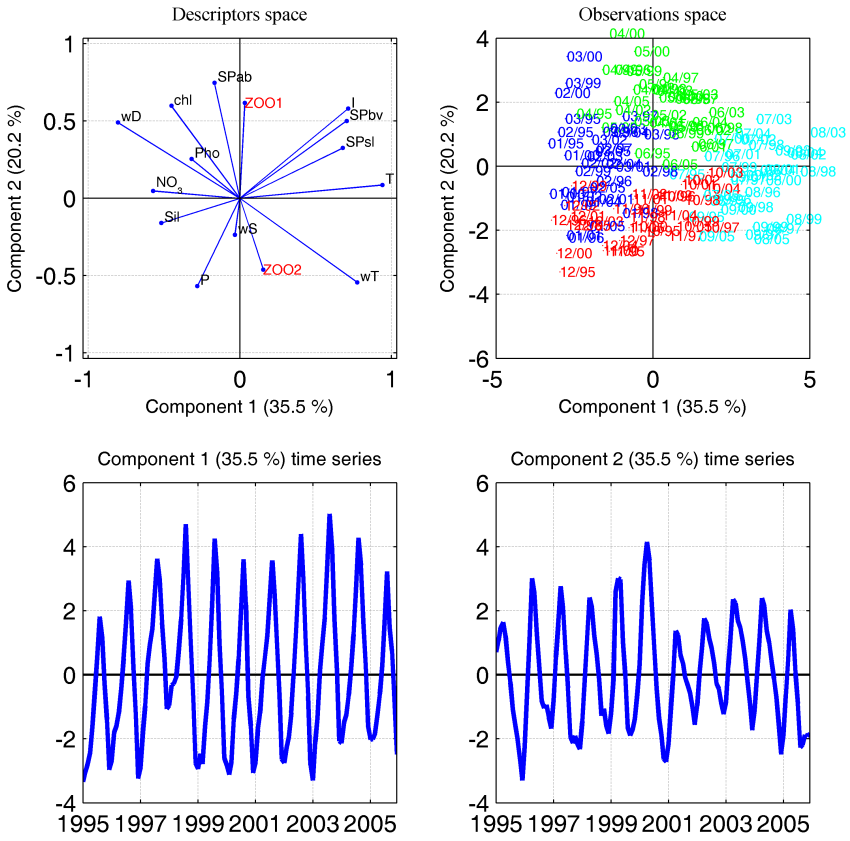

Figure III.4 – *PCA made on monthly values of environmental parameters. (A) represent the space of descriptors, (B) the space of observations, (C) the time series of the first PC, and (D) of the second PC. In the space of observations (B), blue is for winter months (months 1,2 and 3), green is for spring months (4,5,6), cyan for summer months (7,8,9) and red for autumn (10, 11, 12). The two first PC of the zooplankton (fig. III.3) were added as external variables and are shown in red.*

tion. This appears to be mainly due to March, April and May of years 2000, 2001, 2003 and 2004. The second PC (17.7% of variance) mostly represents the variability of the slope and mean size and the crustaceans community and shows a decrease around year 2000. The second PCA is on monthly values of environmental parameters (fig. III.4). The first PC (35.5% of variance) is mainly forced by the air temperature, the water density and the water temperature and represent the seasonality of these parameters. The second PC (20.2% of variance) is mainly forced by the abundance of suspended particles. The first two PCs of the zooplankton (fig. III.3) were added as external variables on the space of descriptors. None of them appears linked to the first PC of environment, but a positive link appears between the first PC of the zooplankton and the second PC of environment.

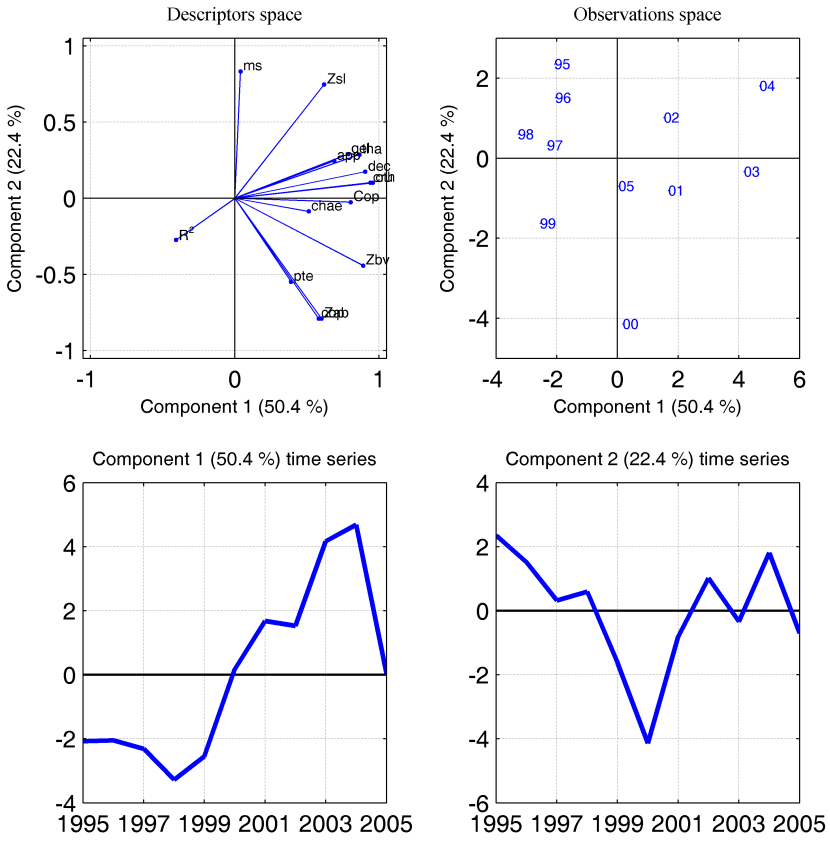

Figure III.5 – *PCA made on annual values of zooplankton. (A) represent the space of descriptors, (B) the space of observations, (C) the time series of the first PC, and (D) of the second PC.*

The third PCA based on annual values of zooplankton parameters (fig. III.5) has the first PC (50.4% of variance) positively linked to values of total zooplankton abundance and biovolume and all taxonomic groups. In this PC, a strong increase occured ca. 2000 with maximum values in 2003 and 2004. The second PC (22.4% of variance), is explained by the size structuration of the crustacean community with a main decrease ca. 2000. The last PCA is based on annual anomalies of environmental parameters (fig. III.6). Yet to account for the strong seasonality of some of these parameters and the different role played by them according to the season considered, hydrological and meteorological parameters were splitted according to the season. The annual anomalies of winter (January to March), spring (April to June), summer (July to September) and autumn (October to December) were taken for these parameters resulting in more variables considered. The first PC (24.6% of variance) is

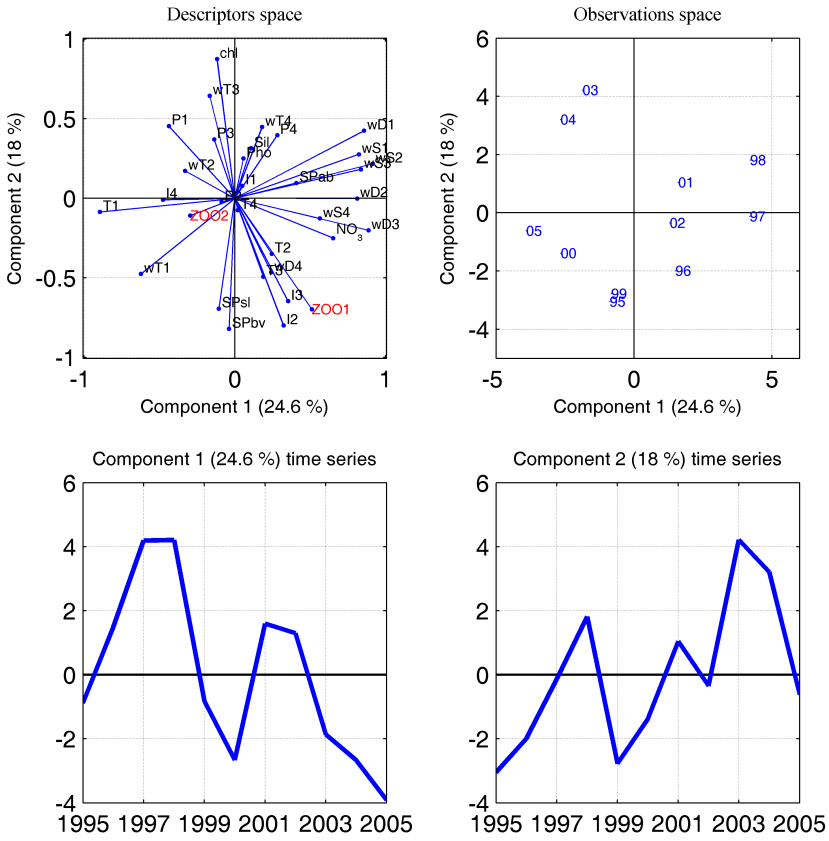

Figure III.6 – *PCA made on annual values of environmental parameters. (A) represent the space of descriptors, (B) the space of observations, (C) the time series of the first PC, and (D) of the second PC. For hydrological ("wT", "wS" and "wD") and meteorological parameters ("T", "P", "I"), annual means of each season were taken, the number correspond to the season, "1" is for months 1,2 and 3, "2" for months 4,5 and 6 until "4". The two first PC of the zooplankton (fig. III.5) were added as external variables and are shown in red.*

positively driven by salinity and density anomalies in winter, spring and summer and negatively by the air temperature in winter. The second PC (18% of variance) is driven positively by the chlorophyll-*a* and negatively by suspended particles N-BSS slopes and total biovolume and by the solar irradiation in spring and summer. The first PC shows high values in 1996, 1997, 1998, 2001 and 2002 and the second PC shows a first increase in 1998, followed by a decrease, to increase again to reach maximal values in 2003/2004. The two first PCs of the zooplankton (fig. III.5) were added. It appears that the first PC of the zooplankton is mainly linked to the second PC of environment and more specifically to the solar irradiance in spring and summer. The second PC of the zooplankton appears badly linked to both the first and second PCs of environment.

III.3.1.2 Identification of shifts using STARS

The identification of regime shift were performed using the method STARS of Rodionov (2004; 2006), with a de-noising of time series prior to shift detection. Shift were not tested on all time series available but on zooplankton monthly values of first and second PCs (see section III.3.1.1) since the first PC represents the zooplankton total biovolume and abundances as well as abundances of taxonomic groups, whereas the second PC represents the size structuration of the crustaceans community. Shift detection on environment were performed also on the first two PCs made on monthly values (see section III.3.1.1). It was not tested on the annual values due to the limited length of the time series — 11 data points being not enough to run the program. The shift detection method was applied on all available parameters (see appendix A). Results of the STARS method to detect shifts are presented on fig. **??**. The regime is represented by a magenta curve which value is the mean value of the regime. When a significant shift occurs a step is represented on the magenta curve with the new value being the mean of the new regime. To detect regime shifts the cut-off length was set at two years, the Huber weight at 1 and the significant level at 0.1 (the usual 0.05 level being too strict to detect any shift in present time series). On the time series of the first PC on zooplankton, a shift from low to high values was detected at the beginning of 2000 and lasted until mid-2004, it was followed by a small decrease from mid-2004 to the end of 2005. On the second PC, a regime change from the beginning of 1998 to the beginning of 2001, characterized by lower values was detected. The time series recovered the same mean (but with a different variability) after the beginning of 2001 until the beginning of 2005 with a second shift toward low values. On PC1 of environmental parameters no shift were detected. The decrease at the end of the time series is a possible artifact of the method, made for an early detection of regime shift. In the second PC, an increase in the mean was observed in 1998 and 1999.

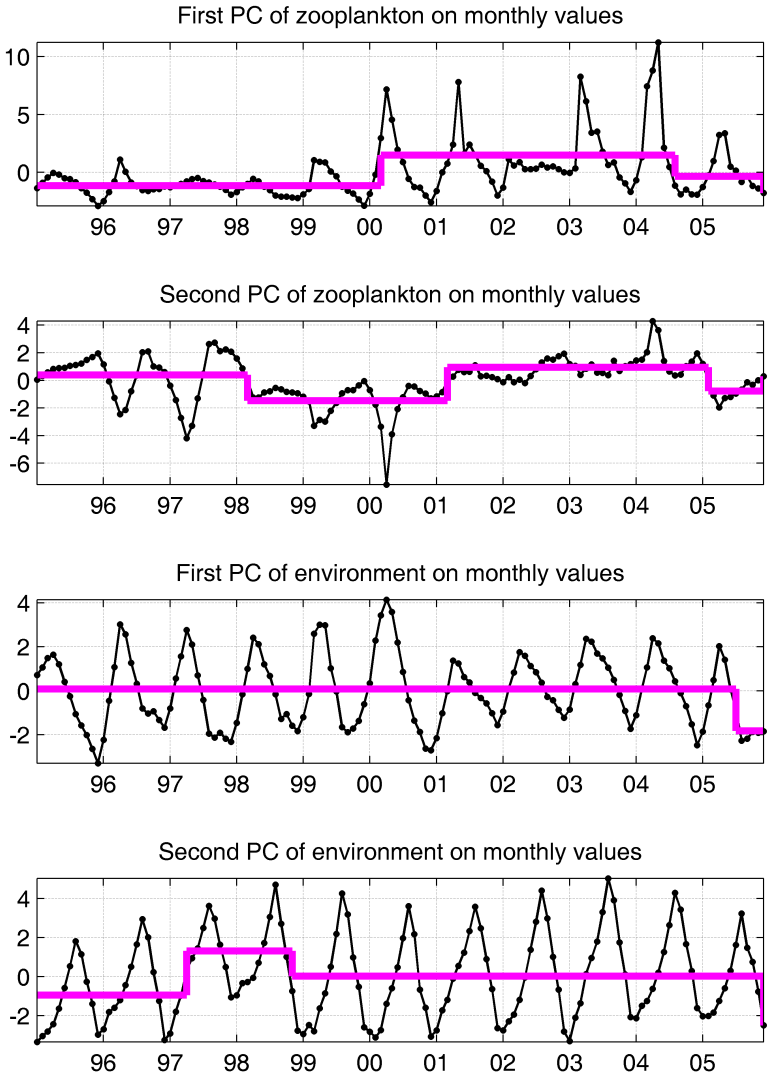

Figure III.7 – *Detection of significant regime shifts in the two first PC of zooplankton and environment monthly values (section III.3.1.1 and fig. III.3 CD, III.4 CD) computed using the STARS methods of Rodionov (2004; 2006). PC are shown in black were regimes are shown in magenta. Any step in the magenta curves indicate a significant regime shift. Parameters of the STARS method were a cut-off length of 2 years, a significant level p at 0.1, and the Huber weight at 1.*

III.3.1.3 Classification of years according to size spectra and the modified Hausdorff distance

A modified Hausdorff distance (see section I.3.3.2) was used to classify years according to the size structuration of the crustaceans community. Crustaceans size spectra were first monthly averaged, linearized and log-transformed to decrease their variability. Each object, i.e., year, is then 3 dimensional, i.e., the x-axis represents the month, the y-axis the size and the z-axis the normalized biovolume in log

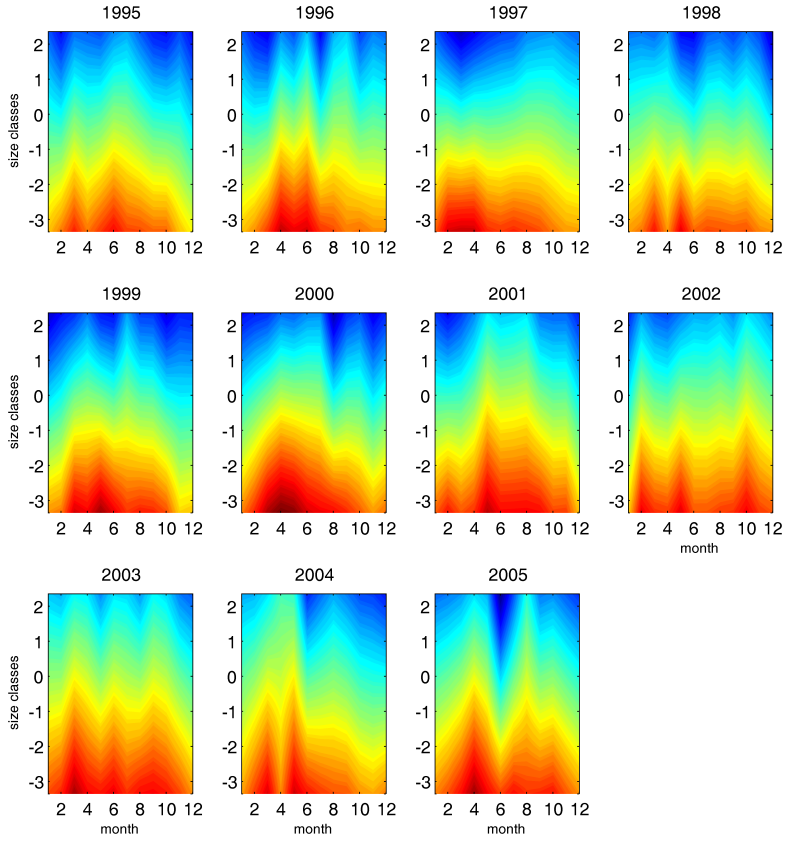

Figure III.8 – *Objects classified with the modified Hausdorff distance. Monthly averaged and linearized crustaceans N-BSS were taken. A log-transformation was then made to balance the effect of small and large size classes. Each year is considered as a single object. For the computation of the Hausdorff distance a normalisation of each axis is made to make them varying from 0 to 1. More information on the computation of the modified Hausdorff distance is in section I.3.3.2.*

scale. These objects are shown on fig. III.8. Then to compute the modified Hausdorff distance, each axis was standardized by the subtraction of the minimum value and the division by the maximum one, to make each axis varying from 0 to 1, to give the same weight to each of the 3 dimensions. At this step it is possible to give more weight to particular dimensions, this was however not tested here. A distance matrix was then computed and years were classified from these distances using the typical Unweighted average distance (UPGMA) linkage. The resulting dendrogram is presented on fig. III.9. The most similar years are 1999 and 2000, which are grouped to years 1996 and 1997 then to years 1995 and 1998. This group is then linked to years 2001, 2002 and 2003, and finally to years 2004 and 2005.

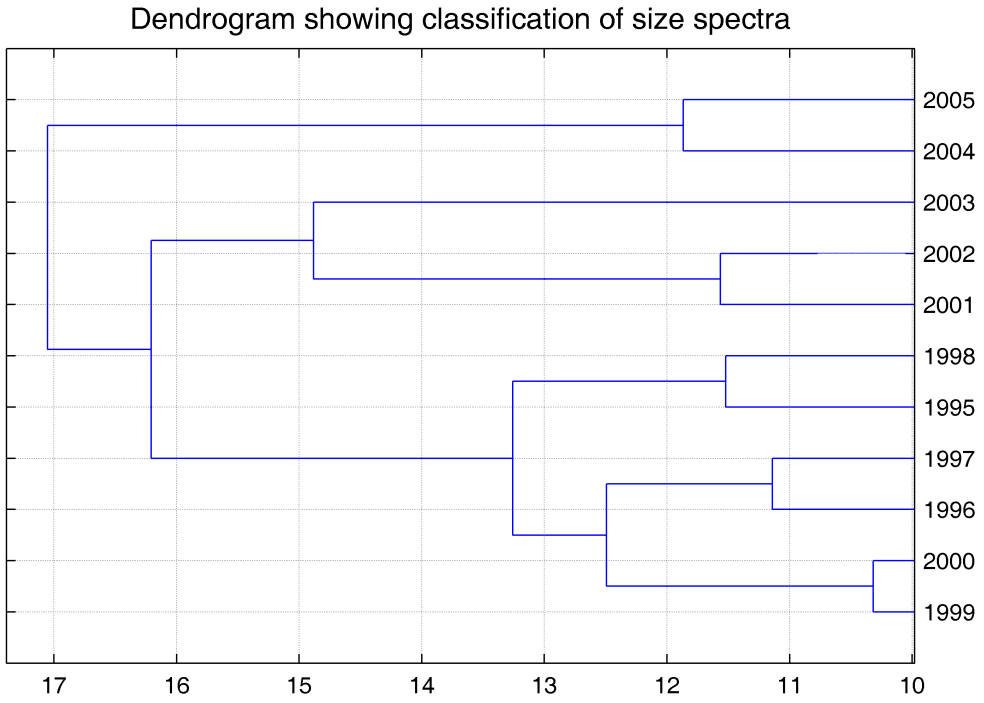

Figure III.9 – *Classification of objects of fig. III.8 according to the modified Hausdorff distance — the dendrogram was made using UPGMA linkage.*

III.3.1.4 Correlations between annual anomalies

Spearman rank order correlations were performed on all annual anomalies of various parameters and shown in fig. III.10. Strong significant correlations, i.e., $p < 0.01$, are represented by black boxes and significant correlation with $p < 0.05$ by gray boxes. When the correlation is significant but opposite, "-" appears in white in boxes. Test between dependent parameters were excluded from the analysis (e.g. total zooplankton abundance and copepod abundance). There is a total of 1005 correlations tested, among them, 32 were significant with $p < 0.01$, and 82 with $0.01 < p < 0.05$.

Yet, these correlations are not statistically valid. When testing a high number of correlations one should apply a correction to account for the fact that significant correlations can be detected at random. At the statistic level of 0.05 it is generally admitted that around 5% are false. A False Discovery Rate method (FRD) was then applied to correct for multiple correlations. The method used is the Two-stage Benjamini, Krieger, & Yekutieli FDR procedure (Benjamini et al. 2006). Correlations significant after the correction are highlighted by a red circle ($p < 0.05$) — for indication, significant

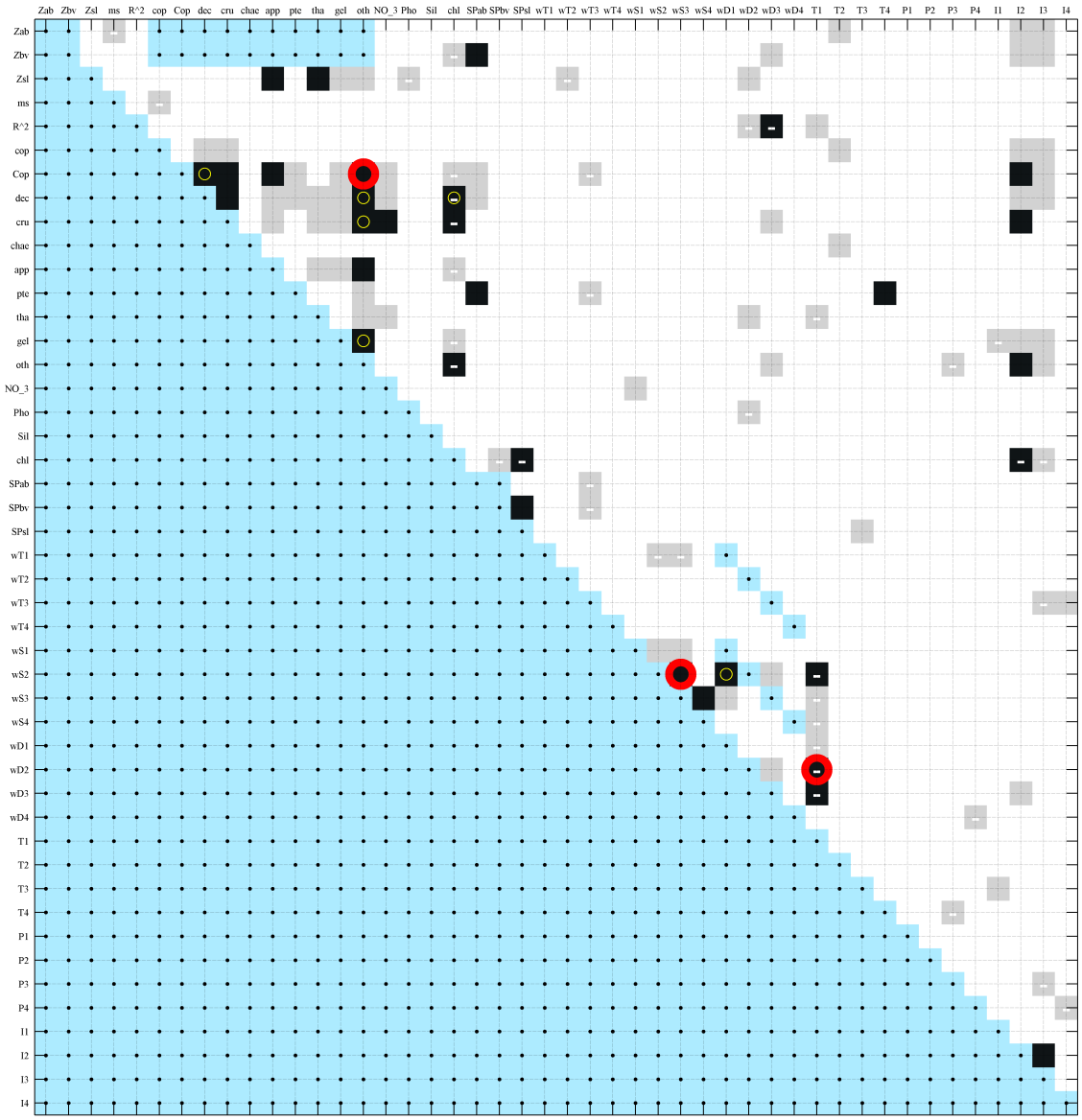

Figure III.10 – *Spearman rank order correlation between all parameters (annual anomalies). The matrix is symetrical and only the upper part is shown. correlations between non-independent parameters were discarded (see text), it is shown by light blue in the upper part of the matrix. black indicate a significant correlation <0.01 and grey <0.05. When correlations are opposite a white "-" is added. e.g. the Zooplankton total abundance anomalies (first line) are significantly correlated to zooplankton total biovolume and small copepods anomalies (p<0.01) and to crustaceans mean size (but opposed), decapods larvæ, other crustaceans, spring temperature, spring irradiation and summer irradiation (p<0.05). A correction for multiple comparison was runned (see text), correlations significant (p <0.05) after this correction are in red circles (only three). Yellow circles are from the same procedure but with p <0.3, for indication only.*

correlations at the level of $p < 0.3$ are indicated with a yellow circle. Out of 114 significant correlations before the correction only 3 remains significant (with p <0.05). At the level of p <0.2 still only the same three were significant, nine (six more) were at the level of 0.3. These numbers are

particularly low compared to the 5% generally found, it is due to the high p values of the correlations, few were below 0.001. Without corrections, correlations should not be used to detect significant links between parameters at random, but more as a space of possible correlations. The correction accounts for the possibility to detect at random a significant correlation. In the next section, III.3.2, the mentioned correlations are based on physical or ecological assumptions of a link and so, no corrections are needed. Trying to detect links by performing all possible correlations result in the detection of only three links (being statistically rigorous). These links are large copepods total abundance vs. large other zooplankton total abundance, water salinity in spring vs. water salinity in summer and water density in spring vs. air temperature in winter. Yet, other correlations give an idea of parameters which are the most linked to others despite the insignificance of these correlations.

III.3.2 Descriptive analysis

In this subsection, analyses will focus on the description of seasonal and inter-annual variations. Anomalies were computed on regularized data with linear interpolation to fill scarce gaps in time series. Correlations were Spearman rank order correlations referred to as r_s with the corresponding p value. Cumulative sums (Ibañez et al. 1993) enable a fast representation of shifts dates and were computed as the first differences of anomalies. Finally, timing of start and maximum of peaks were recorded from smoothed time series following the method of Mieruch et al. (2010) with a visual control of results.

Next, to assess the effect of light limitation on the ecosystem a combination of the model of light attenuation in the water column of Lacroix & Grégoire (2002) and Raick et al. (2005) developed for the central Ligurian Sea and of the model of phytoplankton growth of Andersen & Nival (1988) developed for the bay of Villefranche-sur-Mer was used. The light attenuation is formulated as follows

$$I_z = I_{z=0} \cdot (1 - albedo) \cdot e^{\left[-\int_0^z K_{ext}(z)\,dz\right]} \quad \text{(III.1)}$$

Table III.2 – *Timing (week number) of starting and maximum of seasonal variables, i.e., the nitrates (NO_3), the chlorophyll-a (chl-a), the zooplankton total abundance (Zoo.) and the stratification of the water column (Strat.).*

Year	NO_3		chl-*a*		Zoo.		Strat.	
	start	max	start	max	start	max	start	max
1995	3	10	6	11	9	12	17	29
1996	2	3	6	14	10	15	14	31
1997	1	2	3	8	4	10	20	32
1998	-2	1	5	10	7	11	16	33
1999	5	11	8	12	8	12	18	35
2000	3	5	3	13	8	15	15	36
2001	1	9	5	5	4	7	17	34
2002	1	9	3	7	4	7	17	30
2003	2	8	8	10	7	12	19	34
2004	2	10	4	9	9	11	19	33
2005	4	10	9	13	10	14	17	32

with $K_{ext}(z) = K_{water}(z) + K_{chl}[Chl(z,t)]$. Units and values used are the same as in Lacroix & Grégoire (2002) and Raick et al. (2005). I_z is the irradiation at depth z, K_{ext} is the light attenuation coefficient and depends on the attenuation by the water (K_{water}) and by the phytoplankton shadowing (K_{chl}) which is calculated from the measured quantity of chlorophyll-*a*. The light limitation on phytoplankton growth (I_I) is then calculated as

$$I_I = 2 \cdot (1 + \beta_I) \cdot \frac{(I_z/I_s)}{(I_z/I_s)^2 + 2 \cdot \beta_I \cdot (I_z/I_s) + 1} \tag{III.2}$$

Values of β_I and I_s (the optimal irradiance) are taken from Andersen & Nival (1988) and I_z comes from eq. III.1. This model of phytoplankton growth will be presented in more details in chapter IV.

III.3.2.1 Zooplankton community dynamics

The global average of zooplankton biovolume is 113 $mm^3\ m^{-3}$ and the abundance is 937 ind. m^{-3}. The poorest year in term of total biovolume is 1998 (66 $mm^3\ m^{-3}$) whereas the richest one is 2004 (201 $mm^3\ m^{-3}$). The less abundant year is 1995 (448 ind. m^{-3}) and the most abundant one is 2000 (1468 ind. m^{-3}). The highest biovolume and abundance values occur generally from March to May (fig. III.11 CD). Weeks of start and maximum of the spring peak were recorded from abundance time series (see Table III.2). Spring peak starts during week 7.3 $\pm$ 2.3, and is maximum during week

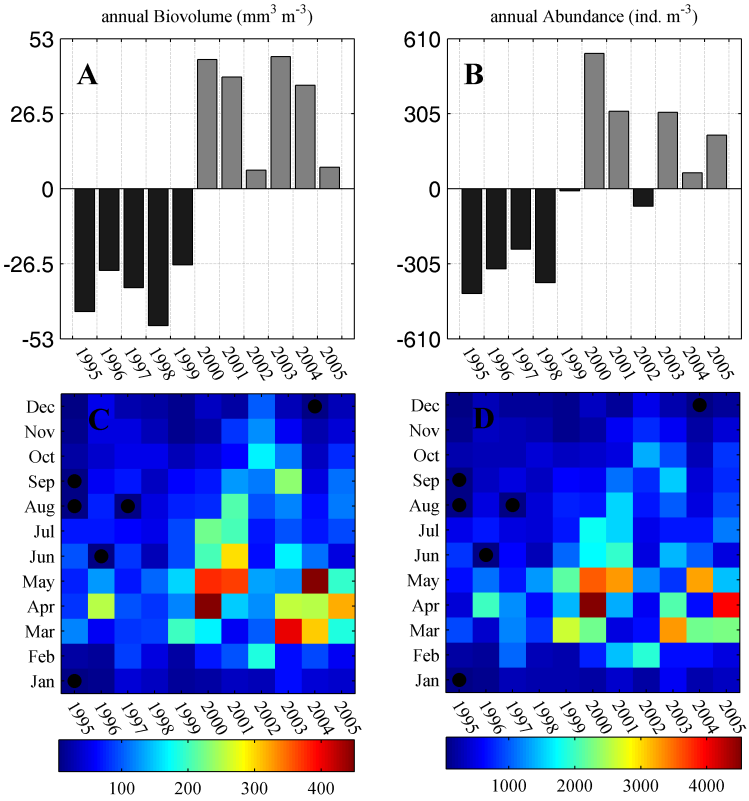

Figure III.11 – *Dynamics of total zooplankton biovolume (in mm^3 m^{-3}) and abundance (in ind. m^{-3}) from 1995 to 2005. (A) annual anomalies of total biovolume; (B) annual anomalies of total abundance; (C) monthly values of total biovolume; (D) monthly values of total abundance. Black dots represents months with no values, they were then not used for analysis, anomalies computed on years with missing months must be taken with precaution.*

11.5 $\pm$ 2.7, i.e., an average of 4.2 weeks after the start. The earliest peaks starting are detected in years 1997, 2001 and 2002 with a start on week 4, and the earliest maxima are in years 2001 and 2002 (week 7) and 1997 (week 10). A second peak in late summer / early autumn is observed only in years 2002, 2003 and 2005 — it is of the same order than the spring peak for year 2002 only.

Following the anomalies of biovolume and abundance (fig. III.11 AB), a clear opposition appears between years before and after ca. 2000. During the first period the average biovolume is 67.2 mm^3 m^{-3} and the average abundance is 614.9 ind. m^{-3}. For the second period these values have almost doubled (1.93 and 1.77 respectively) to reach 130.0 mm^3 m^{-3} and 1089.6 ind. m^{-3}. Years with the maximum annual biovolume are 2001, 2000, 2004 and 2003, followed by years 2005, 2002 and 1996 which are close to the average, then years 1998, 1995, 1999 and 1997 are the lowest. According

to annual abundance means, the pattern is almost similar (fig. III.11 B), yet anomaly of year 1999 increase and anomaly of year 2004 decrease when considering abundance instead of biovolume. This highlights changes in the average mean size, with year 1999 showing the smallest organisms with an average of 0.063 mm^3, and year 2004 showing the largest, almost 2.44 times larger, with an average of 0.154 mm^3. The maximum value of the spring peak followed a similar pattern varying between a minimum of 270 and a maximum of 1685 mm^3 m^{-3} in 1998 and 2004 according to biovolume, and between a minimum of 3676 and a maximum of 17750 ind. m^{-3} in 1997 and 2001 according to abundance (from weekly samples). From 1995 to 1999, the average value of the annual maximum is 5144 ± 323 ind. m^{-3} whereas it is 11796 ± 3623 ind. m^{-3} for the second period.

In addition, zooplankton taxonomic groups abundance globally changed from year 2000, with larger concentrations afterwards. The exact years of these changes are reported on fig. III.12 A-C with the computation of cumulative sum on yearly means for each taxonomic category. Most groups changed from negative to positive anomalies in 2001 (2000 for small copepods and pteropods, 2002 for thaliaceans, 2003 for large copepods). However, from year 2000, some differences appeared among the different categories. The biggest difference is between year 2000 and years 2001 to 2005. Years 2001 to 2005 are globally abundant in all different taxonomic groups whereas year 2000 are

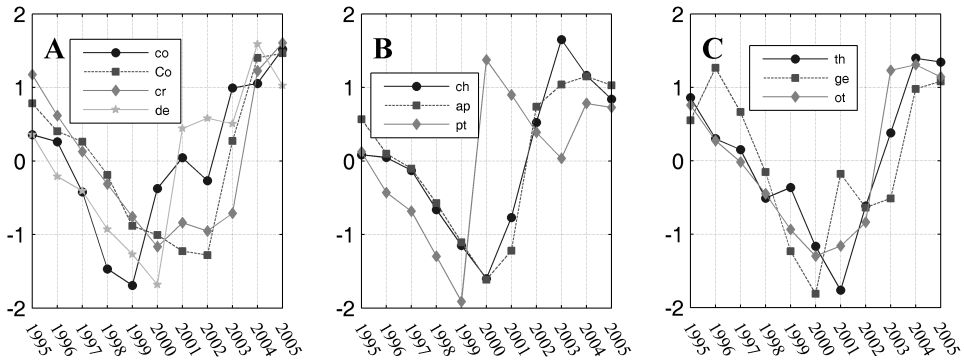

Figure III.12 – *Cumulative sum of annual anomalies of the ten identified taxonomic groups: (A) co for small copepods, Co for large copepods, de for decapods larvæ, cr for other crustaceans; (B) ch for chaetognaths, ap for appendicularians, pt for pteropods; (C) th for thaliaceans, ge for gelatinous predators, ot for other zooplankton. Small copepods account only for individuals between 0.032 and 0.724 mm^3 whereas the other groups account for individuals larger than 0.724 mm^3. The cumulative sum method was first used in ecology by Ibañez et al. (1993), a negative slope means a negative anomaly and vice-versa.*

abundant in copepods but showed negative anomalies of abundance of decapods larvæ, chaetognaths, appendicularians, thaliaceans and gelatinous predators.

III.3.2.2 Crustacean size structure

In addition to the analysis of the total zooplankton biovolume, abundance and taxonomic groups, the size structuration of the crustacean community was analyzed. The values of the log-linear slope computed from the N-BSS, the mean size and the determination coefficient between the log-linear fitting and recorded size spectra (R^2) are presented on fig. III.13. Note that the slope is calculated on the log-transformed size spectra, whereas the mean size is directly computed from all individuals, each of them having the same weight, and so this value is less sensitive than the slope to the large individuals. The slopes are on average of -1.34 with the steepest recorded in 2000 (-1.55) and the flattest in 2004 (-1.21). 1997, 1999 and 2000 showed the steepest slopes on average, whereas 2002, 2003 and 2004 showed the flattest (fig. III.13 A). No strong seasonality is observed, with however a steepness of size spectra from $\approx$ February to June in 1996, 1997, 1999 and 2000 mainly (fig. III.13 D). The years showing the lowest mean size of crustaceans are 1999, 2000, 2001 and 2005 (minimum in 1999/2000 with 0.083 mm^3), and the years with the highest mean size are 1995, 1996, 1997 and 2004 (maximum in 1996 with 0.106 mm^3). The global average is 0.094 mm^3 (fig. III.13 B). High values observed in 1995, 1996 and 1997 are mainly due to the winter period. No seasonality clearly emerge. The average value of the R^2 is 0.873 (maximum in 1998 with 0.899 and minimum in 1996 with 0.857) showing a strong linearity of recorded size spectra, yet, as for the mean size, no seasonality is observed (fig. III.13 CF).

III.3.2.3 Environmental variability

Nitrates Nitrates (NO_3) concentration (fig. III.14 A) are on average of 0.44 μmol L^{-1} with the minimum in 1996 (0.18 μmol L^{-1}) and the maximum in 2003 (0.70 μmol L^{-1}). Strong negative

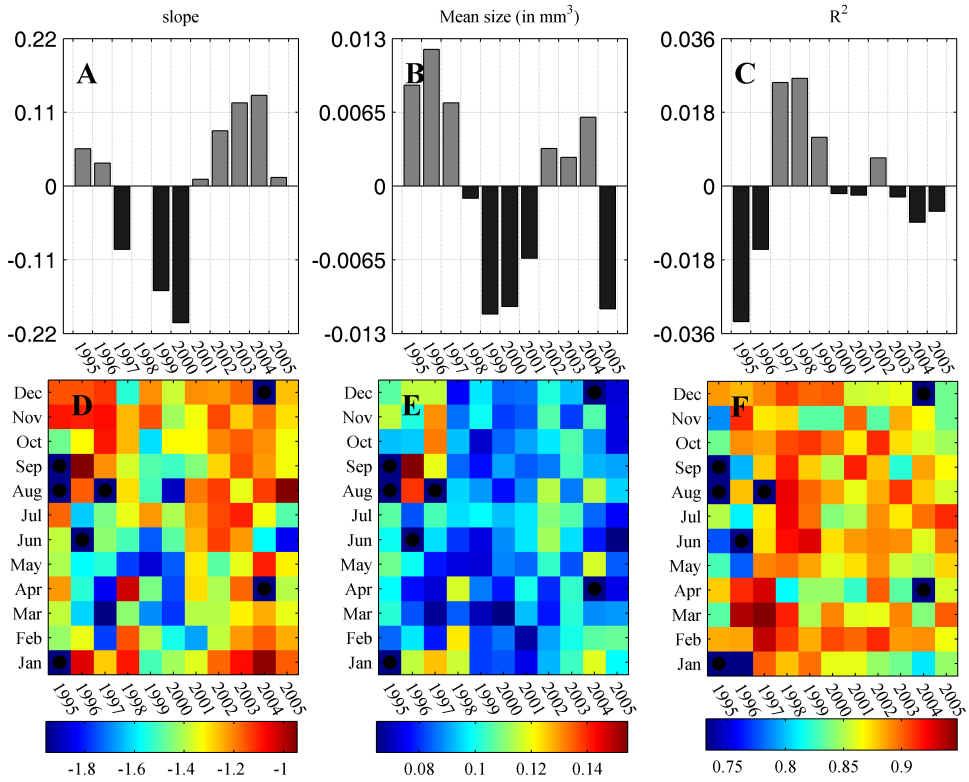

Figure III.13 – *Dynamics of crustaceans N-BSS indicators. A, B, C show the annual anomalies, where D, E and F show the monthly values. A and D are the log-linear value of the slope, B and E are Shannon index and C and F are the determination coefficient R^2 between the measured spectra and the log-linear fitting. Black dots represents months with no values, they were then not used for analysis, anomalies computed on years with missing months must be taken with precaution.*

anomalies occurred from 1995 to 1998 and in 2001, whereas strong positive anomalies occurred from 2002 to 2005, and 1999 and 2000 are close to the mean. The annual cycles as monthly means are presented on fig. III.14 C. Nitrates concentration are at maximum from January to March / April (i.e., w̃eeks 1 to 13) with maximum values reaching about 2.7 μmol L^{-1} (in 2003 from the weekly data). On these winter / spring peaks, start and maximum were measured for each year and reported in table III.2. The start of the peak of nitrates concentration occurs on average on week 2$\pm$1.8, the earliest start is recorded for year 1998 with a peak starting on week 50 (mid-December) of the previous year and the latest is recorded for year 1999, with a start during week 5. The maximum of the nitrates concentration is on average at 7.1$\pm$3.6 weeks, i.e., around five weeks after the start. The earliest and latest maxima are also for years 1998 and 1999 with a maximum during the first and eleventh weeks

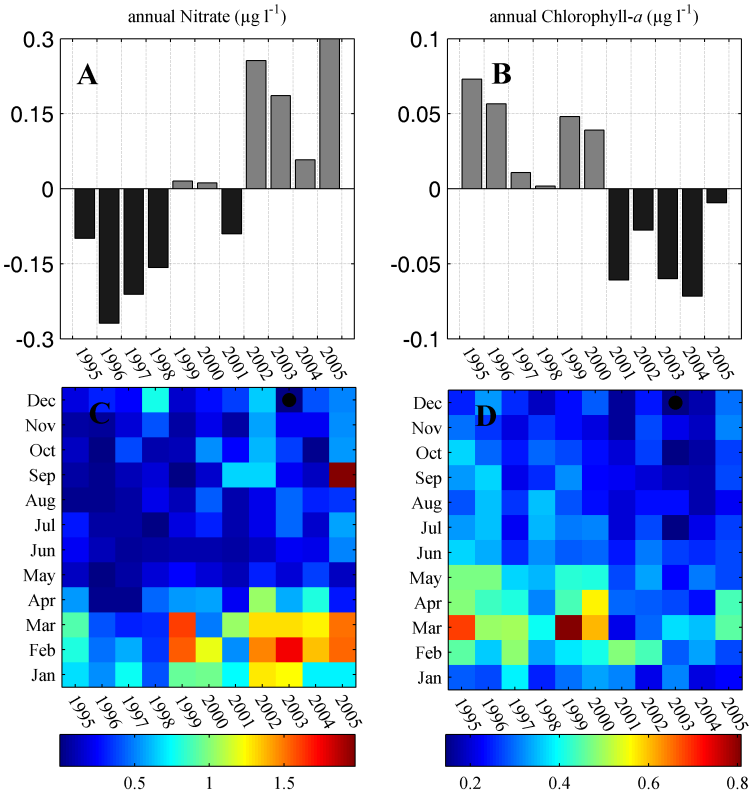

Figure III.14 – *Dynamics of nitrates (NO_3) in $\mu mol\ L^{-1}$ and chlorophyll-a in $\mu g\ L^{-1}$. (A) annual anomalies of NO_3; (B) annual anomalies of chlorophyll-a; (C) monthly values of NO_3; (D) monthly values of chlorophyll-a. Black dots represents months with no values, they were then not used for analysis, anomalies computed on years with missing months must be taken with precaution.*

of the year respectively. A high variability occurs for years before 2000 with years 1995 and 1999 having a maximum during weeks 10 and 11, and years 1996, 1997 and 1998 during weeks 3, 2, 1 which are the first three earliest nitrates concentration maxima. After this winter / spring maximum, no second peak, at the end of summer and early autumn are observed except, to some extent, in 2001, 2002 and 2005. In 2005, this second peak is even higher than the first one.

Phosphates The dynamics of phosphates is shown on fig. III.15 AC with the annual anomalies and the monthly values. The global average is of 0.023 μmol L^{-1} with the maximum in 2000 (0.067 μmol L^{-1}) and the minimum in 2005 (0.012 μmol L^{-1}). Maximum values occurred during February, March and also October of year 2000, making this particular year far above the others. Lowest values were recorded in 1995, 2004 and 2005. Maximum values generally occurred around February.

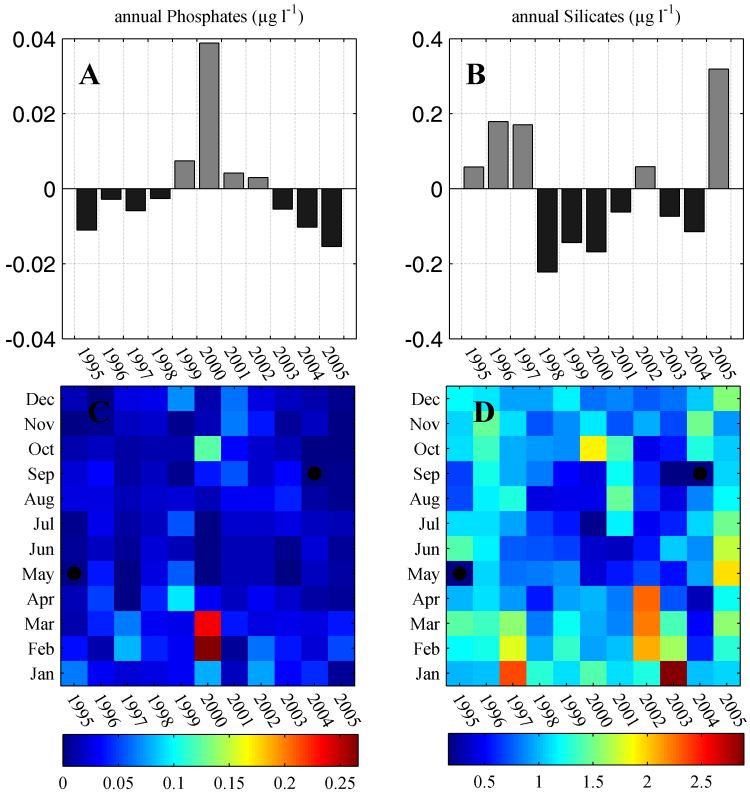

Figure III.15 – *Dynamics of phosphates (NO_3) in μmol L^{-1} and silicates () in μmol L^{-1}. (A) annual anomalies of phosphates; (B) annual anomalies of silicates; (C) monthly values of phosphates; (D) monthly values of silicates. Black dots represents months with no values, they were then not used for analysis, anomalies computed on years with missing months must be taken with precaution.*

Silicates Silicates are on average of 1.02 μmol L^{-1} with a maximum of 1.34 (2005) and a minimum of 0.80 μmol L^{-1} (1998), see fig. III.15 BD. The highest monthly value is observed in January 2003, yet the annual anomaly of this year is negative. Positive anomalies are observed in 1995, 1996, 1997, 2002 and 2005. No obvious seasonality is observed, with, yet, maximum values occurring generally from January to March, which is not always observed, e.g. year 2005.

Chlorophyll-*a* The chlorophyll-*a* concentrations (fig. III.14 B) are on average 0.301 μg L^{-1} with years 1995 to 2000 above this mean and years 2001 to 2005 below this mean. Year 2004 is the year with the minimum mean of chlorophyll-*a*(0.229 μg L^{-1}), and year 1995 is the year with the maximum (0.385 μg L^{-1}). Through the year, chlorophyll-*a* is at maximum on average from February to April / May (i.e., $\approx$ weeks 6 to 22). The start and maximum of the chlorophyll-*a* spring bloom (table III.2)

are on average at 5.5±2.2 and 10.2±2.8 weeks respectively, i.e., 3.5 and 3.1 weeks after the start and maximum of the NO_3 peaks. The earliest start of the chlorophyll-*a* peak is observed during the third week for years 1997, 2000 and 2002, and the latest start is for year 2005 during the ninth week. Earliest maximum of chlorophyll-*a* is for year 2001 and occurred during the fifth week, which is also the week of the start. The latest chlorophyll-*a* peak is for year 1996 and occurred during the fourteenth week. Second peaks in late summer / early autumn can not be identified for the different years even if years 1995, 1996 and 2002 seem to have one.

Suspended particles The suspended particles (2.9 to 92.8 μm ESD) have an average annual concentration of 2.3 10^9 ind. m^{-3} and 621 mm^3 m^{-3} with an average log-linear slope of the N-BSS of -0.68. Anomalies from these means are shown on fig. III.16 ABC. Abundance is the highest in year 2000 (3.0 10^9 ind. m^{-3}) and is the lowest in year 2005 (1.8 10^9 ind. m^{-3}). Total biovolume is the highest in year 2003 (809 mm^3 m^{-3}), and is the lowest in year 1995 (360 mm^3 m^{-3}). The high value of abundance of year 2000 appears mainly due to values recorded during June of this year. Yet, other months still show high values (fig. III.16 D). Largest abundance of suspended particles occurred mainly from February to June / July, yet, this seasonality is less marked for some years (e.g. 2003). Years with the lowest abundance are 1997, 1998 and 2005, when other years show similar values (except 2000). Peaks of suspended particles total biovolume occurred later in the year, from May to September (fig. III.16 E). In term of total biovolume, 1995 is particularly low, mainly in winter and no peak are recorded from May to August (yet, July and August are missing). Years 1998, 2002, 2003 and 2004 are the highest, other years are above the global mean. Then the size structuration of suspended particles was studied through the measurement of the log-linear slope of the N-BSS (fig. III.16 CF). The year with the steeper slopes is 1995 (-1.17) and the flatter slopes are recorded during 2003/2004 (-0.51). Slopes of year 1995 are particularly steep during the whole year, an error from the

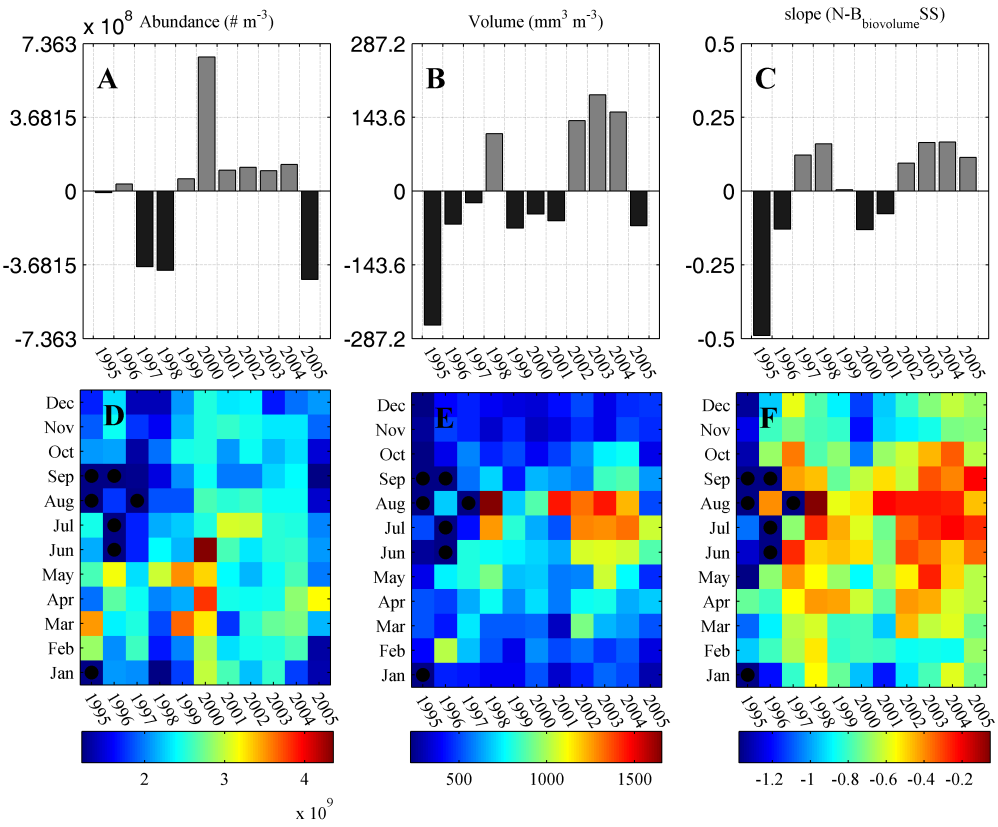

Figure III.16 – *Dynamics of Suspended particles from 2.9 to 92.8 µm ESD calculated with the Coulter Counter. A, B, C show the annual anomalies, where D, E and F show the monthly values. A and D are the total abundance of particles in # m^{-3}, B and E are the total biovolume of particles in mm^3 m^{-3} and C and F are the log-linear slope of the N-$B_{biovolume}$SS. Black dots represents months with no values, they were then not used for analysis, anomalies computed on years with missing months must be taken with precaution.*

measurement process is possible. Except for this year, the steeper slopes are observed in 1996, 2000 and 2001. The annual cycle of recorded slopes presents some similarities with the seasonal cycle of total biovolume with the steeper slopes observed mainly in winter (from November to February), slopes being flatter from March to October with maximum values generally in July and August.

Hydrology From average yearly variation of water density it appears that the density maximum occurs between the 4^{th} and 17^{th} weeks of the year reaching densities between 28.5 and 29 kg m^{-3}. During this period the water column is almost homogeneous from the surface to 80 m depth with an almost constant difference of 0.0879 kg m^{-3} between the surface layer (0-10 m) and the bottom layer (70-80 m) with a gradual increase — yet, density anomalies between all layers are significantly correlated (minimum r_s of 0.9834 and a maximum p value of 9.5 10^{-9}). Within this work, the layer

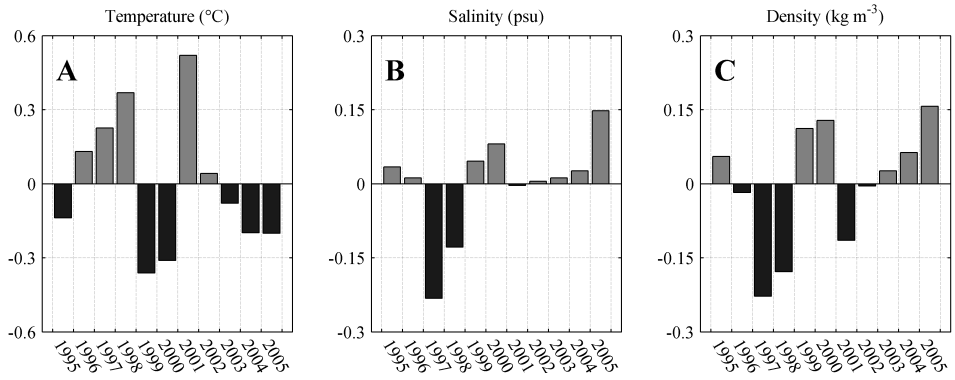

Figure III.17 – *Annual anomalies of hydrological characteristics of the water column (averaged from 10 to 40 m) during the winter period, i.e., from the 4th to the 17th weeks which showed the maximum values of sea water surface density (unpresented data). Anomalies of (A) density (in kg m^{-3}), (B) sea temperature (in °C) and (C) salinity (in psu).*

10-40 m was chosen since surface processes are analyzed (i.e., the winter convection, see section III.4.1). However, due to the strong observed correlation between all layers, another choice would not have changed the results and conclusions.

Year 2005 presents the greatest positive anomaly (fig. III.17 C) with a mean density of 28.79 kg m^{-3} whereas year 1997 is the lowest (28.41 kg m^{-3}). Years 1997, 1998 and 2001 are far below the mean, years 1995, 1999, 2000, 2004 and 2005 are above the mean, and years 1996, 2002, and 2003 are close to the mean. Density is a function of temperature and salinity and is significantly correlated to both of them (density vs. temperature: r_s=-0.923, p<0.001 ; density vs. salinity: r_s=0.972, p<0.001). Years with high densities observed in winter correspond to low water temperature (below the mean of 13.60 °C) and high salinity (above the mean of 38.04 psu) and vice versa for years with low winter densities (fig. III.17 AB). Taking the equation of state of seawater (Millero & Poisson 1981) it appears that the amplitude of variation of winter means of temperature (1.25 °C) accounts for a variation of density of about 0.39 kg m^{-3} (for a fixed salinity of 38 psu and a T_0 temperature of 13.5 °C), and that variation in winter means of salinity (0.4 psu) accounts for a variation of density of about 0.31 kg m^{-3} (fixed temperature of 13.5 °C and S_0 salinity of 38 psu) whereas the variation of winter means of density is of 0.5 kg m^{-3}. Thus temperature and salinity play an equal role in the observed density variations.

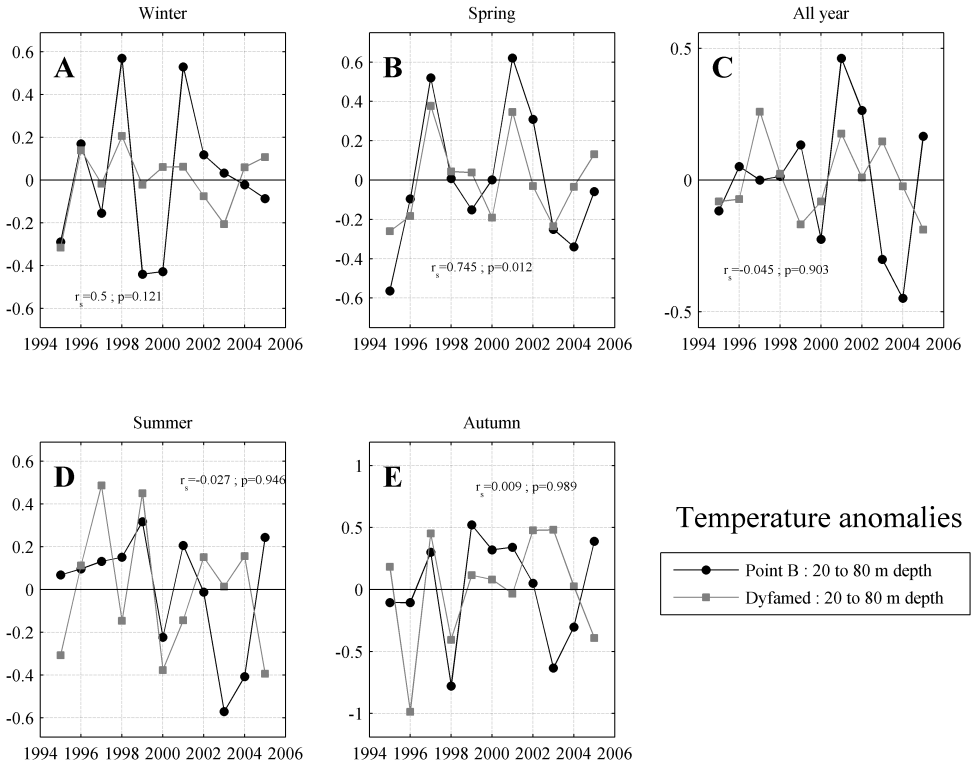

Figure III.18 – *Anomalies of temperature of the water column (averaged from 20 to 80 m) for Point B and DYFAMED stations in* °C. *(A) winter, January to March, (B) spring, April to June, (D) summer, July to September, (E) autumn, October to December and (C) all year. The Spearman r_s and p are shown on each subfigures.*

The hydrological trends at Point B were then compared to the ones recorded at the DYFAMED site (central Ligurian Sea). The DYFAMED station is only monthly sampled and so the comparison was made for each season, i.e., winter (months 1, 2, 3), spring (months 4, 5, 6), summer (months 7, 8, 9) and autumn (months 10, 11, 12) and for the whole year. To decrease the variability, mean values of 20-80 m layer were taken, both at DYFAMED and at Point B sites. Spearman correlations were computed for each comparison and shown directly on the figures. Temperature anomalies comparisons are reported on fig. III.18, salinities anomalies on fig. III.19, and densities anomalies on fig. III.20. For temperature anomalies, only spring months seem to be correlated. For salinity anomalies, winter, spring and autumn months are correlated as well as the whole years anomalies. Finally, for density anomalies, winter, spring and the whole year anomalies are correlated.

Local weather The late autumn / winter time (i.e., from November of the previous year until March of the mentioned year) precipitation, air temperature and solar irradiance means are presented on fig. III.21 A-C. The average temperature through this period is 11.13 °C, with a maximum for year 1998 (11.89 °C) and a minimum for 1999 (10.56 °C). The coldest winters are 1995, 1999 and 2005, whereas the warmest are 1997, 1998 and 2001. The precipitation are on average 2.40 mm d^{-1} during this period, with a maximum in 2001 and 5.15 mm d^{-1} on average and the minimum for 2000, with an average of 0.87 mm d^{-1}, almost 6 times less than in 2001. The driest winters are 1995, 1999, 2000, 2002, 2004 and 2005 and the rainiest are 1996, 1997 and 2001. Temperatures and precipitations during winter are correlated (r_s=0.629, p=0.026). The mean solar irradiance is 882 J cm^{-2} d^{-1} with the maximum for year 1999 (975 J cm^{-2} d^{-1}) and the minimum for 1996 (760 J cm^{-2} d^{-1}). Winters 1995, 1998, 1999, 2000 and 2002 are the sunniest and winters 1996, 2001 and 2004 the less sunny.

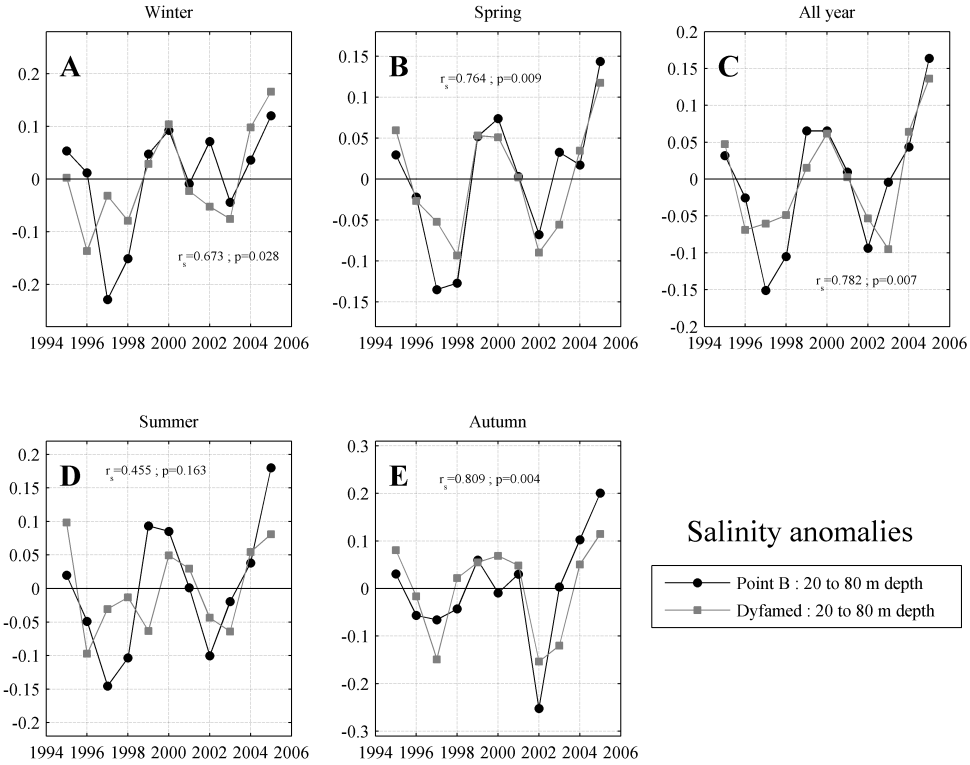

Figure III.19 – *Anomalies of salinity of the water column (averaged from 20 to 80 m) for Point B and DYFAMED stations in* °C. *(A) winter, January to March, (B) spring, April to June, (D) summer, July to September, (E) autumn, October to December and (C) all year. The Spearman r_s and p are shown on each subfigures.*

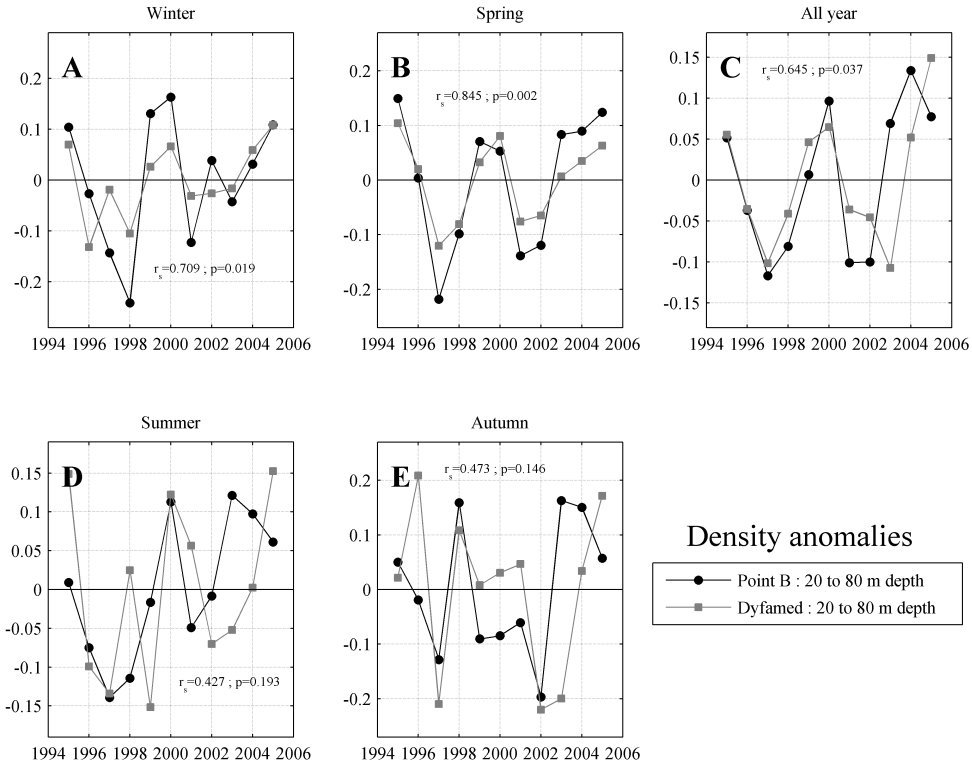

Figure III.20 – *Anomalies of density of the water column (averaged from 20 to 80 m) for Point B and DYFAMED stations in* °C. *(A) winter, January to March, (B) spring, April to June, (D) summer, July to September, (E) autumn, October to December and (C) all year. The Spearman r_s and p are shown on each subfigures.*

The spring / summer climate was also studied (April to August, fig. III.21 D-F). The average temperature during this period is 19.85 °C, year 2003 being far warmer than the others (21.69 °C, on average), and year 2004 being the coldest (19.25 °C). Precipitations during springs / summers are on average 1.23 mm d^{-1}, with 1995, 1998, 2000, 2002 and 2004 being rainy (maximum for 2002 and 2.02 mm d^{-1}), and 1996, 2001, 2003 and 2005 being the driest (minimum for 2001 and 0.57 mm d^{-1}). The springs / summers showed an average solar irradiance of 2247 J cm^{-2} d^{-1} with years 2000 to 2005, except 2002, being sunny. 2003 is the sunniest year (2365 J cm^{-2} d^{-1}). Years 1995 to 1999 and year 2002 show below average irradiance with 1999 being the less sunny (2137 J cm^{-2} d^{-1}).

Light availability and phytoplankton growth in spring / summer The average light perceived in the water column (average from 0 to 75 m depth) from April to August for the eleventh years

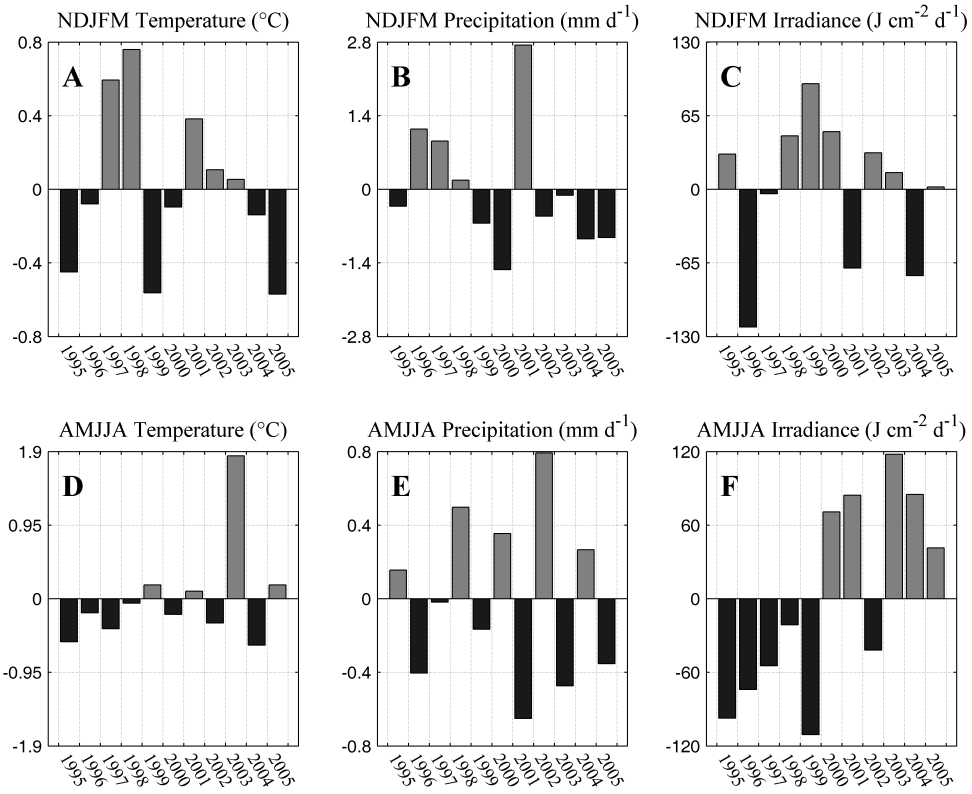

Figure III.21 – *Annual anomalies of climatic variables measured at the Sémaphore station (see fig. I.2): air temperature in* °C *(A and D), precipitation in mm* d^{-1} *(B and E) and solar irradiance in J* cm^{-2} d^{-1} *(C and F). A, B and C report anomalies from autumn and winter months, i.e., from November of the previous year to March of the current year. And D, E and F report anomalies from spring and summer months, i.e., from April to August of the current year.*

is 435 J cm^{-2} d^{-1}, with years 1995, 1996 and 1999 the lowest (respectively 373, 391 and 393 J cm^{-2} d^{-1}) and year 2001 the highest (547 J cm^{-2} d^{-1}), far ahead of year 2003, the second highest (459 J cm^{-2} d^{-1}). Years 1995 to 1999 are below the mean whereas years 2000 to 2005 are above. The light limitation factor (eq. III.2) follows a similar pattern, with an average value of 0.623, a minimum for years 1995, 1996 and 1999 (respectively 0.536, 0.566, 0.572) and the maximum for years 2001 and 2003 (0.692 and 0.673).

III.4 Discussion

III.4.1 Winter forcing on the ecosystem

In the NW Mediterranean Sea, "winter convection" (e.g., Schott et al. 1993, Marshall & Schott 1999, Soriano et al. 2004, Vage et al. 2009) occurs during continuous cooling and saltening of the surface

water by atmospheric forcing during winters (Leaman & Schott 1991, Bethoux et al. 1998; 2002). This results in an increase of density and allows surface water to sink into the deep layer, mixing the water column. Changes in sea water salinity were observed in the 11-years period considered in the present study, with less saline winter waters occurring at the beginning of the observed period until 2000 (minimum in 1997 and 1998), whereas higher salinity are observed from 2001 to 2005 (maximum in 2005). An average difference of about 0.3 psu is observed over these years. This increase of salinity is mainly related to a decrease in freshwater inputs, both due to a decrease of precipitations and rivers flow in the NW Mediterranean Sea (e.g., Skliris et al. 2007, Ludwig et al. 2009, Marty & Chiavérini 2010, Vargas-Yanez et al. 2010). Observed anomalies of precipitations in the Bay of Villefranche-sur-Mer during winters tend to confirm this hypothesis with wetter winters mainly in 1996, 1997, 1998 and 2001, corresponding to years with low anomalies of surface water salinity. However, the increase of salinity alone appears not sufficient to explain the observed increase of winter surface density and the temperature must also be taken into account (see section III.3.2.3). This appears particularly visible for year 2001, which shows low densities but close to average salinities anomalies, whereas the sea water temperature is the highest of the time series. Considering the whole time series, however, anomalies of sea water salinity and temperature are strongly correlated (r_s=-0.888, p<0.001) alike anomalies of precipitations and air temperatures (r_s=0.629, p=0.026). From the PCA analysis (fig. III.6) precipitations are poorly related to the hydrology but the air temperature in winter is, suggesting a strong effect of low winter temperature to enhance the winter convection. Yet, in the descriptive analysis (section III.3.2.3) the precipitation budget during the whole wet season, i.e., from November to March was used, in this case significant correlations between precipitations and hydrology appeared. Both air temperature and precipitations seem to determine the intensity of the winter convection in the observed ecosystem and are both strongly correlated to the winter water density (r_s= -0.804 and -0.783 respectively, p<0.001 in both cases).

Yet, the role plays by temperature in the inter-annual variability of the winter convection appears less marked, if not negligible, in the central Ligurian Sea (Dyfamed). Indeed, at the Dyfamed site, the winter temperature anomalies (fig. III.18 A) are not correlated to salinity anomalies (fig. III.19 A) with a r_s=-0.100 and a p=0.776 nor to density anomalies (fig. III.20 A) with a r_s=-0.391 and a p=0.237, whereas winter density and salinity anomalies are strongly correlated (r_s=0.864, p=0.0013). This is also shown by the absence of correlations between winter temperature anomalies at Point B and at Dyfamed whereas salinity and density are correlated between both sites (figs. III.19 A and III.20 A). Then, salinity appears to play a central role in determining the strength of the winter convection in the whole basin, whereas the role played by temperature may be more local. In any case, strength of winter convection at both Point B and DYFAMED stations seems to follow similar inter-annual variations.

The main consequence of an increase in winter convection is a stronger replenishment of nutrients through a deepening of the mixed layer (e.g., Gačić et al. 2002, Backhaus et al. 2003, Nezlin et al. 2004, Katara et al. 2008, Marty & Chiavérini 2010). This affirmation is supported by the observed strong correlation (r_s=0.726, p=0.006) between winter surface density and nitrates. Marty & Chiavérini (2010) observed in the central Ligurian Sea an increase of nitrates concentration in February of about 3 times from years with low to high convection. In the present work, years 1997/1998 show the lowest convection, and nitrates concentration is almost 7 times lower in February than for year 2005, which shows the highest convection. From the literature, such increase in nitrates and more generally nutrients availability at the end of winters are always related to a significant increase in phytoplankton productivity, and mainly diatoms in the Ligurian Sea (Goffart et al. 2002, Nezlin et al. 2004, Marty & Chiavérini 2010). In addition, the favorable conditions (dry and cold winters) and the quality of phytoplankton (i.e., more diatoms) have a positive effect on the zooplankton taxonomic groups considered in the present study (fig. III.12, except for year 2000, see III.4.2). This

is also strongly highlighted by the two PCAs performed on zooplankton (fig. III.3 and III.5) and by the STARS detection of shifts, with a significant shift from low to high zooplankton concentration detected in 2000 (fig. III.7). Such a positive forcing across different trophic levels was already observed at Point B (Garcia-Comas et al. Submitted) and in different systems (e.g., Aebischer et al. 1990, Frederiksen et al. 2006). This suggests a strong indirect response of the zooplankton community to the winter mixing and nutrients replenishment, mostly nitrates. No correlations are observed between phosphates / silicates and hydrology or biology. Only a strong input of phosphates during year 2000, where a strong convection was observed, yet other years with a strong convection did not show any increase in phosphates concentration. Yet, phosphates are mainly known to limit bacterial and dinoflagellates in summer, but not the spring bloom, which is mainly due to diatoms and more limited by nitrates and silicates. Silicates concentration shows a slight decrease during the spring time in 1998, 1999, 2000, 2001, 2003 and 2004. This can be the effect of the consumption of this nutrient by diatoms. The uncorrelation of phosphate anomalies with any other variable and the slight decrease of silicates during diatoms blooms tend to confirm the aforementioned hypothesis of a control of the ecosystem productivity mainly by the strength of diatoms blooms. In addition, the increased concentration of nitrates and of zooplankton also seem to have increased the fluxes of matter. This is detected in the analysis of suspended particle dynamics, see sections III.3.2.3 and III.3.1.1. A positive link between the slopes and total biovolume of suspended particles and zooplankton abundances is detected, with an increase of large particles (more total biovolume and flatter slopes) by the end of the time series (mainly between 2002 and 2005) during spring and summer months. This increase mainly occurs below 50 m depth (not presented) and is probably the result of the detritus and phytoplankton aggregation and give an additional support to the observed increased in zooplankton during the 2000's.

A striking result of the time series analysis is a clear opposite patterns in the inter-annual variabil-

ity between nitrates concentration and autotrophic biomass (chlorophyll-*a*) and also chlorophyll-*a* and zooplankton (fig. III.11 AB and III.14 AB but also fig. III.10 in which chlorophyll-*a* is negatively correlated to all variables). This temporal dynamics stands odd in the common conceptual model that favorable nutrient conditions result in high chlorophyll-*a* concentration. The opposite inter-annual variability betweenchlorophyll-*a* and zooplankton in periods with high nutrients concentration strongly suggests that grazers control primary producers. Therefore in addition to the "bottom-up" control hypothesis raised by Garcia-Comas et al. (Submitted), we suggest that "top-down" control by zooplankton (grazers) may be important to explain the observed variability of phytoplankton. Even if "top-down" control of phytoplankton by zooplankton at both seasonal and inter-annual scales is an accepted phenomenon (Nival et al. 1975, Graneli & Turner 2002, Gaudy et al. 2003, Sommer & Sommer 2006, Wiltshire et al. 2008), such a strong "top-down" control decreasing the whole phytoplankton community stocks has rarely been observed either in field's studies or in mesocosm experiments (Micheli et al. 1999, Shurin et al. 2002, Feuchtmayr et al. 2004, Borer et al. 2005, Sommer 2008). According to these studies, the coupling depends mainly on the sustained co-existence between zooplankton feeding on different parts of the phytoplankton size spectrum. This can be the case in oceans where, for example, a long-term coexistence of tunicates and copepods is observed, or in lakes with a co-existence of copepods and *Daphnia spp.* (Sommer 2008). Copepods will feed on large phytoplankton or on microzooplankton and so will decrease the grazing pressure on small phytoplankton, while filter-feeders (thaliaceans, appendicularians and also pteropods here) will feed on the whole size range of phytoplankton (Sommer 2008). An increased predation pressure of copepods on microzooplankton will have the effect, through a trophic cascade, to decrease the grazing pressure of microzooplankton (ciliates) on small phytoplankton and so to increase the observed phytoplankton stocks (chlorophyll-*a*). Then, the co-existence and high abundance of filter-feeders and copepods after 2000 probably explain the decline of phytoplankton stocks. Yet, year 2000 appears as an ex-

ception with high concentrations of nitrates, chlorophyll-*a* and zooplankton — the low abundance of filter-feeders during these year (only pteropods were present) seems to explain this particularity. This strong control of phytoplankton through zooplankton grazing was not observed in the central (Marty & Chiavérini 2010), nor in the southern Ligurian Sea (Goffart et al. 2002) — nutrients and chlorophyll-*a* being positively correlated. This is potentially due to lower zooplankton biomass in those locations compared to the present site (15-30 mgDW m^{-3} in Dyfamed, (Gasparini et al. 2004); 45-105 mgDW m^{-3} in Calvi, Corsica, (Hecq et al. 1981, Brohée et al. 1989, Skliris et al. 2001); compared to 20-700 mgDW m^{-3} in Point B, chapter II). Phytoplankton appears to be grazed faster than it is growing, hiding the "bottom-up" control (i.e., nutrients to phytoplankton), which can only be evidenced by rate measurements.

Finally, changes in timing of water column stratification, nitrate concentrations peaks, chlorophyll-*a* blooms and zooplankton peaks (table III.2) are not correlated to any inter-annual variability in annual anomalies of nitrates concentration, chlorophyll-*a* or zooplankton. The maximum of zooplankton, despite its variability, is always between few days to a maximum of 2 weeks after the maximum of phytoplankton. No differences in the timing of appearance of phytoplankton and zooplankton, nor in the time-lag between both peaks, are detected before and after ca. 2000. This tends to suggest that zooplankton and phytoplankton growths are determined by similar factors or that the zooplankton growth is determined by the phytoplankton one. The "match-mismatch" hypothesis (Cushing 1990, Edwards et al. 2002, Edwards & Richardson 2004, Durant et al. 2007, Bakun 2010) is, then, not supported by the present observations. A "match-mismatch" occurs when the time of appearance of different trophic levels are conditioned by different driving forces (Durant et al. 2007). Even if the "match-mismatch", among other ecological mechanisms, reviewed in Bakun (2010), may have been neglected in the present study of the Bay of Villefranche-sur-Mer, the interplay of "bottom-up" and "top-down" controls seems sufficient to explain the main observed inter-annual variability.

III.4.2 Effect of spring / summer irradiation and other patterns

The "bottom-up" control caused by nutrient replenishment by intense winter convection does not seem sufficient to explain the case of years 1995, 1999 and 2001. Indeed winter convection during 1995 and 1999 are among the strongest observed in the 11-years time series, yet, zooplankton concentrations are low. The opposite situation is observed during year 2001 with a particularly weak winter convection but a high concentration of zooplankton. These three years correspond to years in which the winter convection strength anomalies and spring / summer irradiation are opposed. For all the remaining years a strong winter convection correspond to high spring / summer irradiation and vice-versa. In addition, positive correlations are observed between zooplankton and spring / summer irradiance (r_s=0.734, p=0.005 and r_s=0.706, p=0.009 respectively for zooplankton biovolume and abundance), and also a strong link between the first PC of zooplankton and irradiation anomalies in spring and summer is detected with the PCA (section III.3.1.1, fig. III.6). A way through which solar irradiation can affect the ecosystem productivity is by light limitation on phytoplankton growth as suggested by previous studies (Andersen & Nival 1988, Sciandra et al. 1997, Duarte et al. 1999, Nezlin et al. 2004, Morán & Estrada 2005). The calculated irradiation values (eq. III.1, section III.3.2.3) do not reach saturation of phytoplankton growth generally observed (Geider et al. 1998, MacIntyre et al. 2002). Using a light limitation model (see section III.3.2.3) it appears that 1995, 1996 and 1999 are the three more limited years and 2001 is the less limited. Since the model of Andersen & Nival (1988) is multiplicative, any decrease in the light limitation factor has an effect on phytoplankton growth. In addition, the light attenuation model does not consider the turbidity from terrestrial discharge. This may be important in this coastal setting (Duarte et al. 1999) and would further decrease the available light in the water column. There is a need of adding suspended particles concentration to the light attenuation model and making new measurements of available light in the water column.

Additional experiments on light limitation on phytoplankton species from the sampling site will also be needed to validate this hypothesis.

Inter-annual variability is also observed in the time-lag between the appearances of the different taxonomic groups (see fig. III.12). This is also recorded in the size structure of the crustacean community with a steepness of recorded N-BSS slopes and decrease of the mean size (see sections III.3.1.1, III.7 and III.3.2.2). It appears that most large groups increased in 2001 whereas smaller zooplankton, mainly copepods, increased one year before, and so resulted in a steepness of crustaceans N-BSS during the shift. Such a time-lag was already observed at the same location by Garcia-Comas et al. (Submitted) in the 1981/1983 and 1999/2000 switches. The reason for the time lag is not truly understood but seems to be a constant feature in the studied area and also in various locations in the world (e.g. Cloern & Jassby 2010). A possible explanation lies in different reproductive strategies among the different taxonomic groups at the population level. Some populations may respond immediately through an increase fecundity/natality (small copepods) following a type "r" strategy. Other groups may respond with a time-lag because of longer generation time (euphausiids, amphipods), by the production of diapause eggs enabling a stronger initiation the following year (strategy of type "K"), but also because their populations reach extremely low abundances during unfavorable years, in this case a time-lag of at least one year is necessary for them to recover higher abundances. This time lag of responses of the different groups may explain the particularity of the year 2000 in which the absence of filter-feeders has reduced the "top-down" control on phytoplankton from zooplankton (section III.4.1).

III.4.3 Conceptual schematic

On the basis of the new data by Garcia-Comas et al. (Submitted) and the present work we propose an explanation whereby the climate forcing modifies the dynamics of zooplankton groups in the NW

Mediterranean Sea in four patterns (fig. III.22). In winter, precipitations and temperature control the strength of the winter convection. Years 1996, 1997, 1998 and 2001 shows a weak winter convection due to high winter precipitations and/or temperatures. Years 1995, 1999, 2000 and 2005 shows a strong winter convection, related to low precipitations and/or low temperatures in winter. Years 2002, 2003 and 2004 are intermediate. The strength of the winter convection controls the availability of nitrates, and thus phytoplankton growth. In spring / summer light limitation can counteract, or reinforce, the effect of the winter convection. Years 1995, 1996, 1997, 1998, 1999 and 2002 have an unfavorable spring / summer climate. In the case of years 1996, 1997, 1998 and 2002 the effect of

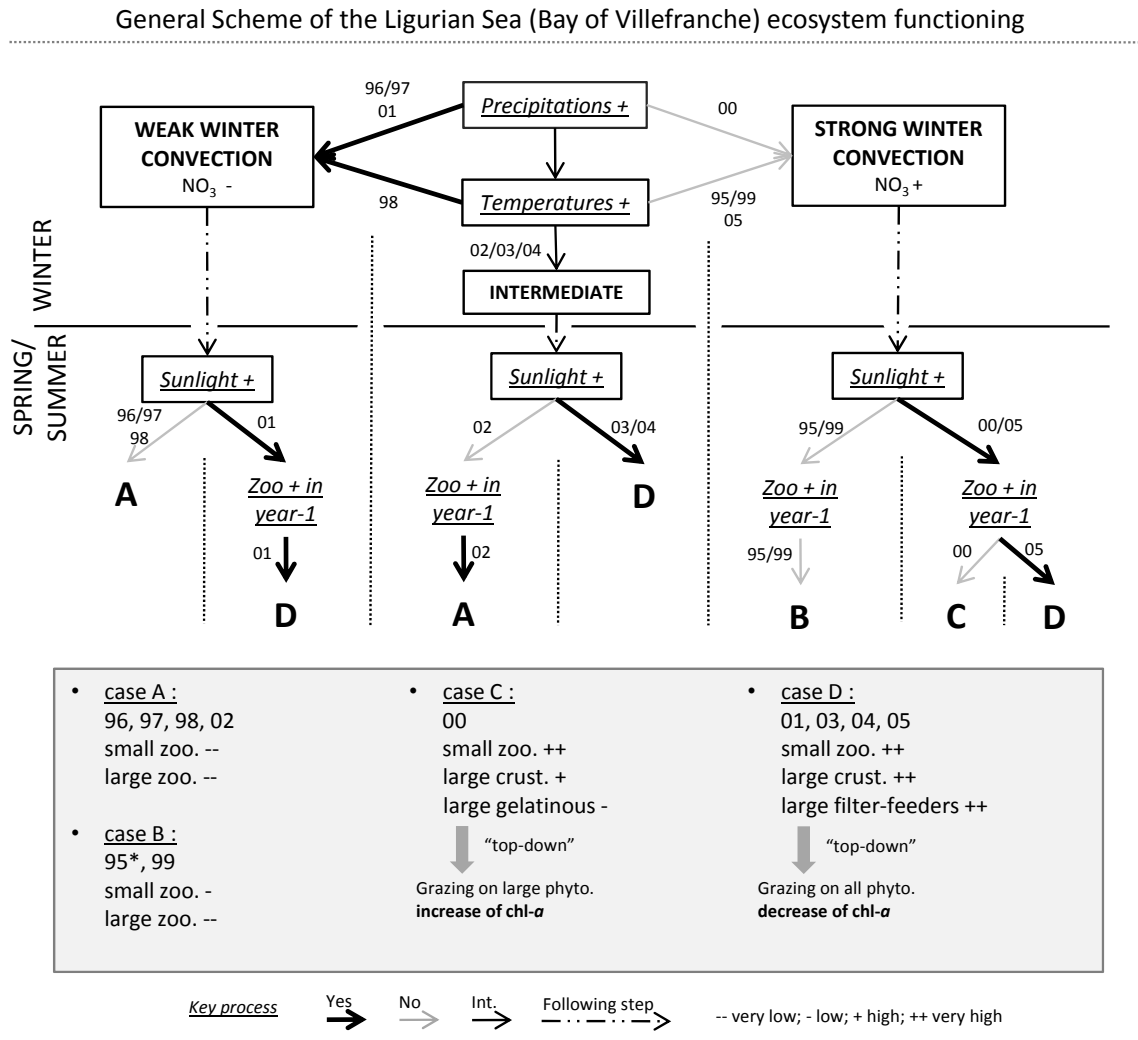

Figure III.22 – *Proposed general scheme of Ligurian Sea ecosystems dynamics, see section III.4.3 for details. The legend of line and boxes is at the bottom of the scheme (Int. is for intermediate). (*) the quantity of previous year zooplankton cannot be verified, however from Garcia-Comas et al. (Submitted) the beginning of the '90s were low in zooplankton.*

the spring / summer climate is in the same direction than the winter convection (indirect negative effect on zooplankton abundances). For year 1995 and 1999 the unfavorable spring / summer climate (i.e., low irradiance and high precipitations) may have negatively moderated the positive effect of the strong winter convection. By contrast, years 2000, 2001, 2003, 2004 and 2005 have a favorable spring / summer climate. Especially for year 2001 which is weak as regards to the winter convection but high as regard to zooplankton concentrations. This suggests again the importance of the spring / summer climate. In addition high abundances of zooplankton during the previous year would have had an impact on some taxonomic groups of zooplankton — especially the large ones. This gives an explanation of the peculiarities of the year 2000 which has a high abundance of copepods but a low abundance of gelatinous zooplankton (mainly filter-feeders) changing the characteristics of the "top-down" control from zooplankton to phytoplankton. Yet this global scheme does not take micro-zooplankton into account due to a lack of data. This can possibly modify the proposed hypotheses about the global functioning of the presented ecosystem since they are known to contribute to the grazing of phytoplankton, to represent a food resource for small copepods (especially in the bay of Villefranche-sur-Mer) and to contribute to the recycling of nutrients (Nejstgaard et al. 2001, Klaas et al. 2008). Yet, considering the microzooplankton or not will not modify the positive link between the presence of copepods only and the increase of chlorophyll-*a*. The presence of copepods feeding on large phytoplankton decreases the competitive pressure on small phytoplankton and the chloro-phyll-*a* increase. This is similar to the presence of copepods feeding on microzooplankton and so decreasing the grazing pressure on small phytoplankton by microzooplankton, which results also in an increase of chlorophyll-*a* even if the link is different. A global decrease of phytoplankton can only be reached by the massive occurrence of filter-feeders. Further studies will have, however, to deal with the microzooplankton to assess its role in the global functioning of Ligurian Sea coastal pelagic ecosystems.

In summary, dry and cold late autumns and winters are beneficial to phytoplankton growth and zooplankton development that ultimately control the biomass of phytoplankton by grazing. All groups of zooplankton are present and their concentrations are further increased if the previous year is favorable or if light availability is high. These factors seem to settle the ecosystem dynamics for the whole year.

III.4.4 Links with Global Climate indicators

Some climate indicators were previously mentioned to be strongly correlated to the climate of Europe and more precisely the NW Mediterranean. Links were found by previous authors between these climate indicators and parts of the ecosystems (e.g., Molinero et al. 2005; 2008, Fernàndes de Puelles et al. 2007, Conversi et al. 2010, Garcia-Comas et al. Submitted, ...). These patterns are mostly the North Atlantic Oscillation (NAO, Hurrell 1995, Stenseth et al. 2003, Hurrell & Deser 2010), the Atlantic Multidecadal Oscillation (AMO, Knight et al. 2005; 2006, Msadek & Frankignoul 2009), the Arctic Oscillation (AO, Thompson & Wallace 1998, Delworth & Dixon 2000, Deser 2000), the North Hemisphere Temperature (NHT, Beaugrand 2009), the El-Niño Southern Oscillation or Southern Oscillation Index (ENSO or SOI, Mariotti et al. 2002, Orfila et al. 2005, Karagiannidis et al. 2008).

Strong positive phases of the NAO (*sensu* Fernàndes de Puelles & Molinero 2008, i.e., $\pm > 1$) are known to generally drive colder and drier winters over the Western Mediterranean and vice-versa for strong negative phases. The selected NAO is the Principal Component (PC) time series of the leading EOF (Empirical Orthogonal Functions) of DJF (December through February) SLP (Sea Level Pressure) anomalies over the Atlantic sector (20-80°N, 90°W-40°E) (Hurrell 1995, Stenseth et al. 2003), and is available online at www.cgd.ucar.edu/cas/jhurrell/indices.data.html#naopcdjf. The AMO relates to the variation of Sea Surface Temperature long-term fluctuations in the tropical Atlantic (Knight et al. 2005), and is relied to diverse climate events over the Atlantic sector, such as

north eastern Brazilian and Sahel rainfalls, Atlantic hurricanes and North American and European summer climate (Goldenberg et al. 2001, Folland et al. 2001, Rowell 2003, Sutton & Hodson 2005, Knight et al. 2006, Msadek & Frankignoul 2009). Particularly, for Europe, it is known that more fre-

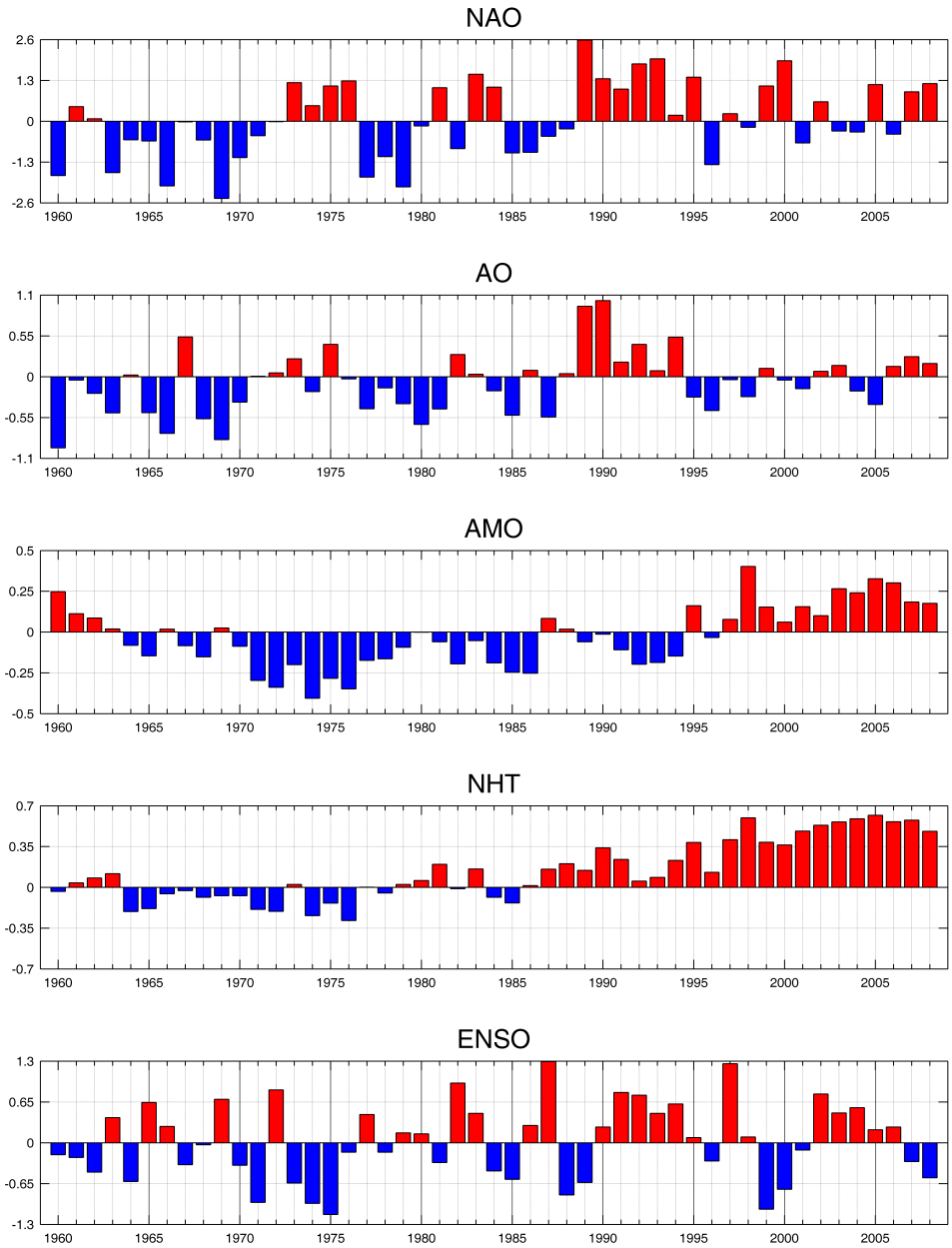

Figure III.23 – *Time series of main climate indicators with a possible influence on NW Mediterranean climate, see text for details. NAO is for North Atlantic Oscillation, AO for Arctic Oscillation, AMO for Atlantic Multi-decadal Oscillation, NHT for Northern Hemisphere Temperature and ENSO for El-Niño Southern Oscillation. The winter value of the NAO was taken whereas annual means were taken for other indicators.*

quent summer heat waves occur during positive phase of the AMO (Sutton & Hodson 2005, Msadek & Frankignoul 2009). The AMO time series comes from www.cdc.noaa.gov/Timeseries/AMO, the unsmoothed AMO SSTs were taken. The AO is a close relative of the NAO and debates exist on their separation as distinct climate indicators or not (Ambaum et al. 2001, Rogers & McHugh 2002). Ambaum et al. (2001) argue that the NAO can be identified in a more physically meaningful way. Yet, Rogers & McHugh (2002) found that these two patterns are inseparable in winter, but not in other seasons, making the AO as a standalone climate indicator. However, the effect of the AO is similar to the NAO since it drives dry air masses over the Mediterranean sector in its positive phase and vice-versa in its negative phase. The AO index can be downloaded at www.cpc.noaa.gov/products/precip/CWlink/daily_ao_index/monthly.ao.index.b50.current.ascii. The NHT is the monthly means of land and sea surface temperatures over the North Hemisphere sector that are available at www.cru.uea.ac.uk/cru/data/temperature/hadcrut3vnh.txt (Rayner et al. 2006). Variations in the NHT are related to some changes in ecosystems of the North Atlantic (Beaugrand 2009). The ENSO affects many ecosystems worldwide and is an important feature of the world climate. This oscillation of the pacific was already mentioned to influence precipitations and sea surface temperature in the Mediterranean Sea through teleconnections (Mariotti et al. 2002, Orfila et al. 2005, Karagiannidis et al. 2008). By analyzing the Ligurian Sea, Orfila et al. (2005) found a strong influence of the ENSO on sea surface temperatures with a time lag of 4 months. ENSO index is available at www.cpc.noaa.gov/products/analysis_monitoring/ensostuff/ensoyears.shtml.

Winter values were taken for the NAO, whereas the annual means were taken for other climate indicators. All these indicators are presented on fig. III.23, from 1960 to 2008. Then, correlations were made with these indicators and the important features of the Ligurian Sea ecosystems, previously identified (see fig. III.22), i.e., winter air temperature, winter precipitations, spring / summer irradiation, winter water density, water salinity and water temperature, as well as the zooplankton first

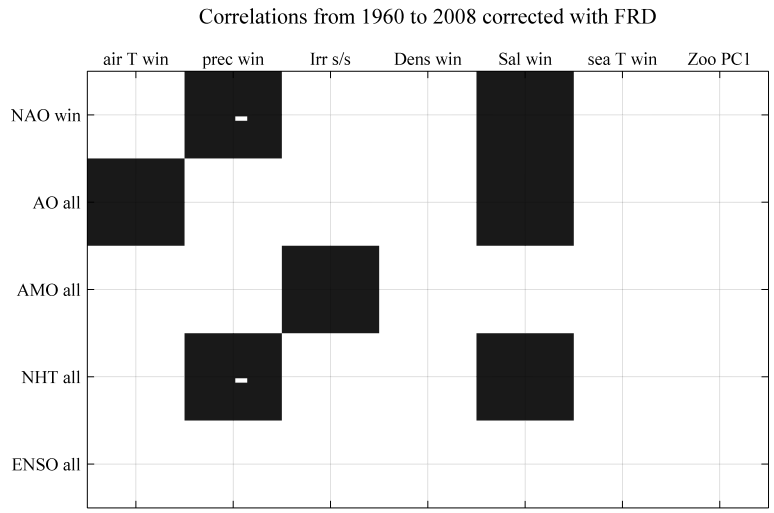

Figure III.24 – *Correlations between main climate indicators and variables of the Ligurian ecosystems previously highlighted from 1960 to 2008, i.e., "air T win" for air temperature in winter, "prec win" for winter precipitations, "Irr s/s" for spring / summer solar irradiation, "Dens win" for winter density of sea water, "Sal win" for winter salinity, "sea T win" for sea water temperature in winter and "zoo PC1" for the first PC on annual values of zooplankton (only from 1995 to 2005). Correlations were corrected using a FDR methods for multiples correlations. Only significant correlations at p<0.05 after the correction are shown, here with a black box. a white "–" in the box indicates an opposite correlation.*

PC on annual values (fig. III.5). Correlations were made on the period 1960 to 2008 (with extended datasets on local meteorology and hydrology), and on the period 1995 to 2005 (with the first PC of the zooplankton). As in section III.3.1.4 a FDR correction for multiples correlations was applied. Significant correlations are shown on fig. III.24 for the period 1960 to 2008, no significant correlations were found for the period 1995 to 2005. These results strongly highlight the need of long-term time series to detect links between local variables and global climate indicators.

From the 48 years time series (1960 to 2008), significant links were found (fig. III.24). Winter air temperatures are positively correlated to the AO, winter precipitations are negatively correlated to the winter NAO and NHT, Spring / Summer irradiation to the AMO, and winter salinities to the winter NAO, AO and NHT. No correlations were found between sea water winter densities and temperatures and any climate indicators. Considering 1995 to 2005 only no correlations were found. This confirms the findings from the comparison with the Dyfamed site in which salinities at Point B and Dyfamed were strongly correlated but not the temperatures. In the factors that determine the ecosys-

tem some seem to be local features, whereas other seem affected by the global (at least regional) climate. It appears that the winter water temperatures may be more affected by local mechanisms, maybe due to the proximity of the coast, micro-climate, or particular small scales hydrology (see also Stenseth & Mysterud 2003, for an explanation on why local climate and global indicators may not be always correlated) — yet, another possible explanation is the opposed reaction of winter sea water temperatures to NAO (cooling) and NHT (warming). Whereas winter salinities follow similar trends in the whole Ligurian Sea (see section III.3.2.3) and are strongly linked to winter precipitations, both linked to global climate indicators (NAO and NHT, AO for salinities). The increase of occurrence of positive NAO and the warming of the northern hemisphere during the last 50 years have globally decreased precipitations and increased sea water salinity during winters in the Ligurian Sea. Yet, the non-predictability (with these indicators) of the sea water temperature in winter makes the link between global indicators and winter sea water density (a proxy of the winter convection) insignificant. Then, to predict future evolutions of the strength of the winter convection in the bay of Villefranche-sur-Mer it will be needed to understand what determines, at the local scale, the sea water temperature fluctuations in winter. In addition, the other determinant factors of the inter-annual fluctuations of the Ligurian Sea ecosystems is the solar irradiation in spring / summer. This parameter seems linked on the long-term to the AMO, which is confirmed by the hypothesis that positive phase of the AMO will increase the occurrence of summer heat waves over Europe (Sutton & Hodson 2005, Msadek & Frankignoul 2009).

According to these results and the predicted rise in North Hemisphere Temperature (IPCC 2007, chapter 3.2.2.4), NAO positive phase (Woollings et al. 2010) and summer warmer and drier climate in the Mediterranean area (IPCC 2007, chapter 11.3.3), it is probable that favorable conditions for zooplankton will become more frequent — increased winter convection, increased light availability in spring / summer — leading to more periods of mesotrophy in the Ligurian Sea. Yet, the effect

of factors influenced by local climatic features is strong, and what ultimately determines these local features will have to be investigated. In addition, it will be needed to understand if the link between the strength of the winter convection, the light availability and the response of the ecosystem is linear. For example, year 2005 showed the highest positive anomalies of winter densities and also strong positive anomalies of spring / summer irradiation, but it is only the fifth year as regards to the total quantity of zooplankton. More observations of strong convections and important light availability will be needed to assess the linearity or non-linearity (optimum) of the response of the pelagic ecosystem to these features since a possible saturation or negative effect are possible. This will be essential before any projections of the future of Ligurian Sea ecosystems.

III.5 Conclusion

In this chapter an 11-years time-series of the Ligurian Sea pelagic ecosystem including zooplankton, chlorophyll-*a*, nutrients concentration, suspended particles, hydrology and local weather with weekly values was analyzed. It is presently the most complete time series analyzed in this area. The main conclusions are that (i) a recovery at ca. 2000 of the ecosystem from the oligotrophy that occurred in the '90s (Molinero et al. 2005; 2008) was found, with quasi decadal fluctuations from low to high zooplankton abundances, confirming the hypothesis of Garcia-Comas et al. (Submitted). Such a shift in ca. 2000 was also observed at diverse locations, e.g. in the central Ligurian Sea (Marty & Chiavérini 2010), in the Balearic Sea (Fernàndes de Puelles et al. 2007), in the Atlantic and British Channel French coast (Goberville et al. 2010), in Naples (Berline et al. accepted), in San-Francisco bay (Cloern & Jassby 2010) ... (ii) a one-year time lag was observed in the recovery of large zooplankton groups compared to smaller ones. (iii) a clear opposite trend in the inter-annual dynamics of nitrates and zooplankton vs. chlorophyll-*a* was observed suggesting a strong "top-down" control of phytoplankton by zooplankton. (iv) the main driving factor of these fluctuations is the strength of

the winter convection mainly determined by winter precipitations and temperature. The main consequence being a stronger replenishment in nutrients which affects zooplankton through a “bottom-up” control. (v) a second driving factor was proposed, i.e., the light limitation of phytoplankton in spring / summer, which has moderated or even reversed the effect of the winter convection. And finally, (vi) a significant links between global climate indicators and mostly winter precipitations and winter sea water salinity were found for the period 1960 to 2008. Salinity was also strongly correlated between the north coastal and central Ligurian Sea suggesting that inter-annual variability of this parameter is more regional than local, which is not the case for winter sea temperature, both determining the intensity of winter convection. There is a strong importance of local climate drivers in the control of coastal zooplankton dynamics. Yet, projected evolution of Mediterranean climate for precipitations leads to the possibility of an increased occurrence of strong winter convections, increasing the mesotrophy in the Ligurian Sea. However, the linearity or non-linearity of the ecosystem response to stronger winter convections (and also light availability) need to be investigated.

CONTINUOUS SIZE-BASED MODELING OF ZOOPLANKTON

IV

IV.1 Introduction to zooplankton models of the NW Mediterranean Sea

"*it is not energy per se that makes life go, but the flow of energy through the system*", Morowitz (1968).

Marine biogeochemistry and ecology face two major issues: the evaluation of the role of the pelagic ecosystem in biogeochemical fluxes, mainly carbon flux, and the quantification of trophic fluxes through food webs from the primary producers to top predators. In this respect, zooplankton plays a central role, at the interface of lower and upper trophic levels, influencing the pathway of matter through ecosystems, and productivity of lower and upper trophic levels. To understand the role plays by zooplankton different approach were followed, i.e., *in vitro*, *in lab*, *in situ* and finally the synthetic *in silico* one (Gentleman 2002), using computer models of ecosystems. Currently, different models are used to study the dynamics of the zooplankton with different levels of complexity and scales of application (e.g., Caparroy & Carlotti 1996, Dur et al. 2009, Lehodey et al. 2003, Fasham et al. 1990, Moloney & Field 1991, Le Quere et al. 2005).

In the Mediterranean Sea, biogeochemical models actually in use incorporate the zooplankton as a single box or as few sub-boxes. For example, in the generic Biogeochemical Flux Model (BFM Vichi et al. 2007), based on the ERSEM model (Baretta et al. 1995), the zooplankton is subdivided in heterotrophic nanoflagellates, microzooplankton and omnivorous mesozooplankton. For the Eastern Mediterranean Sea, the ALERMO model (Korres & Lascaratos 2003) adds the box "carnivorous mesozooplankton" to the BFM model. These four sub-boxes are modeled with a total of 48 param-

eters. Recently, Berline et al. (submitted) included appendicularians on the BFM model for the NW Mediterranean Sea. For the Ligurian Sea, different ecosystems models were developed, based on similar concepts, at least for the zooplankton modeling (Lacroix & Grégoire 2002, Raick et al. 2005, Skliris et al. 2001, Skliris & Djenidi 2006, for the most recent). Models of Skliris et al. (2001), Skliris & Djenidi (2006) account for the Southern Coastal Ligurian Sea (Bay of Calvi), whereas models of Lacroix & Grégoire (2002) and Raick et al. (2005) account for the central Ligurian Sea or transects from Nice to the Central Ligurian Sea (DYFAMED site). The model of Skliris et al. (2001), Skliris & Djenidi (2006) includes only a copepod box for the zooplankton. Copepods are modeled as a single differential equation including seven parameters in Skliris et al. (2001) and only three in Skliris & Djenidi (2006). A comparison of observations and model outputs was performed on data from February to April 1986. In the models of Lacroix & Grégoire (2002) and Raick et al. (2005) the zooplankton is split up into three sub-boxes based on size, the nano-, micro- and mesozooplankton, each of them having a particular differential equation. Yet, no comparison with zooplankton data were made. When comparing to observations, models skills generally decrease with increasing level of complexity, i.e., from hydrodynamic to biological compartments (Skliris et al. 2001, Holt et al. 2005, Lewis et al. 2006, Allen et al. 2007, Petihakis et al. 2009), the zooplankton being generally the less accurately represented. This seems to be due to the high spatial and temporal heterogeneity of the zooplankton, together with escape behavior from sampling instruments that make the sampling difficult, but also to the lack of experimental data on zooplankton. Hence, the zooplankton is more difficult to integrate and parametrize in models than hydrobiology for example. This may also be due to the inefficiency of box models to represent the zooplankton dynamics complexity.

To deal with the aforementioned problems (few data and need of lot of parameters), new models of zooplankton based on their size structure were developed (Baird & Suthers 2007, Maury et al. 2007a, Zhou et al. 2010). Using theoretical works and observations on the importance of the size for

zooplankton avoids, in part, these problems (see chapter I, section I.2). First of all, the development of new techniques allows fast measurements of the zooplankton size distribution (possibly in different taxa), see chapter II, and so decreases the error on the measure used to compare models outputs and observations. Then, considering the zooplankton as a single state variable but structured by size decreases the number of parameters needed for models. And finally, since the theory predicts that the size spectrum is the result of growth, mortality and predation processes within zooplankton, it allows the representation of more complex dynamics than single differential equations. The final aim being to incorporate these new models in global biogeochemical models to improve their quality of representation of the zooplankton and decrease their number of parameters and boxes.

A newly developed zooplankton continuous size-based model is presented here, and will be tested with data from the bay of Villefranche-sur-Mer, already presented in the chapter III. The model was inspired mostly by the works of Maury et al. (2007a) and Benoît & Rochet (2004) — with simplifications — and by the knowledge on the pelagic ecosystem of the Ligurian Sea. The development of the model was made in tight collaboration with the team COMORE of the INRIA Sophia-Antipolis and especially with Éric Benoît, Professor of mathematics at the INRIA and the University of La Rochelle, and Jonathan Rault, PhD student at the INRIA. Mixing of ecological and mathematical brains is a necessary and rewarding step in modern ecology.

This chapter is organized as follows. First, the ecological conceptual scheme is presented (IV.2.1), showing the main processes that will be modeled. Then the mathematical formulation is presented (IV.2.2), followed by a detailed explanation of equations and processes (IV.2.3). It was chosen here to present first the equations used and then to return on them to explain their meaning in details. To help with the understanding of the model a list of all symbols used is provided before the mathematical formulation (table IV.1). Then a review of the literature is made to find average values and the range of variation of parameters (IV.2.4). Starting from these average values a sensitivity is made on the

equilibrium solution of the model (IV.3.1). Again with average values the behavior of the model is analyzed in particular, arbitrary cases, to help getting familiar with the model and with its reactions to various inputs (IV.3.2). The last part deals with the comparison of the model to observations (IV.4). First a model of phytoplankton growth (Andersen & Nival 1988), calculated from *in situ* observations, is associated to the model to serve as the entry (IV.4.1). The model is tested on the two main scenarii (poor and rich periods of zooplankton) observed in chapter III (IV.4.2), first with default parameters from literature (IV.4.3) and then with a preliminar optimization (IV.4.4). This chapter ends with a short conclusion and perspectives (IV.5).

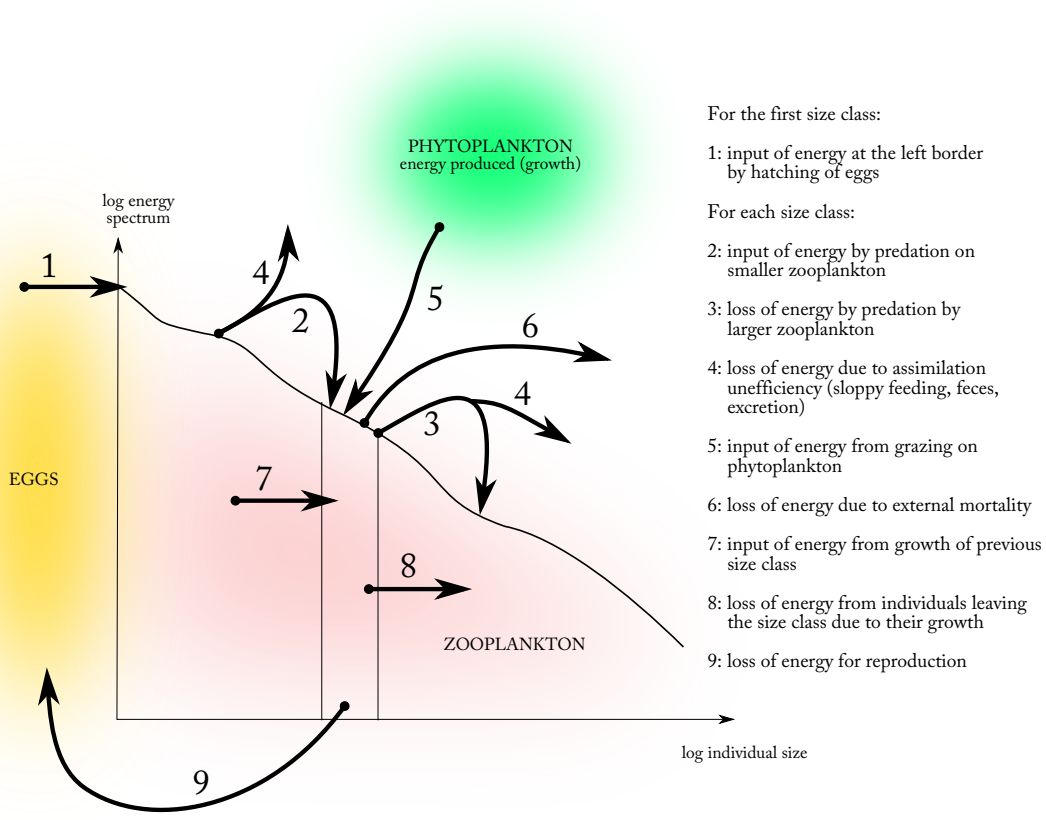

Figure IV.1 – *Conceptual scheme of the size-based model at the population scale. see text for details.*

IV.2 Presentation of the continuous size-based model

IV.2.1 Ecological conceptual scheme

The model represents the continuous evolution of the zooplankton size spectrum in time and size. The currency of the model is the energy which is assumed to be proportional to biomass and biovolume. A general scheme showing the fluxes affecting a given size class is presented on fig. IV.1. The model is continuous without any size classes in its formulation, the choice of representing the fluxes in fig. IV.1 through a size class was made for simplicity of representation (the continuity of the model corresponds to the width of size classes tending to 0). Different processes change the size distribution of the energy. First of all, individuals will feed both on phytoplankton (grazing) and on smaller zooplankton (predation). This decreases the energy content of the phytoplankton and of smaller size of zooplankton. This energy is then assimilated by organisms, with a coefficient of efficiency, the unassimilated part is lost by the system (detritus). Then the assimilated energy is used for the Soma (growth) or for the Germen (reproduction), see fig. IV.2, there is no maintenance energy. The energy used for reproduction is reallocated to an eggs pool on which a hatching success is applied: that represents the flux of energy entering at the left border of the spectrum. The energy used for growth increases the energy in the said size and allows individual to growth. An additional external mortality is applied to account for the loss due to predation by larger organisms. At the community level this results in fluxes of energy from: (i) phytoplankton which produces the primary energy for the system — the energy produced by phytoplankton (growth) is the only input of the system. (ii) Smaller to larger sizes of zooplankton through predation. (iii) Evolution of the size distribution of energy by growth. (iv) All size to the left border of the spectrum through production of eggs (with an additional hatching success). (v) All sizes to outside through external mortality, assimilation inefficiency and unhatched eggs (energy lost by the system).

IV.2.2 Mathematical formulation

A list of all symbols (variables and parameters) is provided in table IV.1. Refer to this table for units.

This part is organized as follows. First the general case of the model is presented. Then we adopt a particular solution, i.e., infinite allometric spectrum, which allows us to make choices so that the general case has an allometric equilibrium. This is convenient for both mathematical and practical reasons: it enables to simplify the number of parameters from 13 to 7 and allows more mathematical analyses.

IV.2.2.1 General case

The zooplankton organisms sizes are defined for $x \in [x_0, x_1]$, x being the logarithm of the size. The size can be the individual content of energy, biomass or biovolume — for the moment we will consider

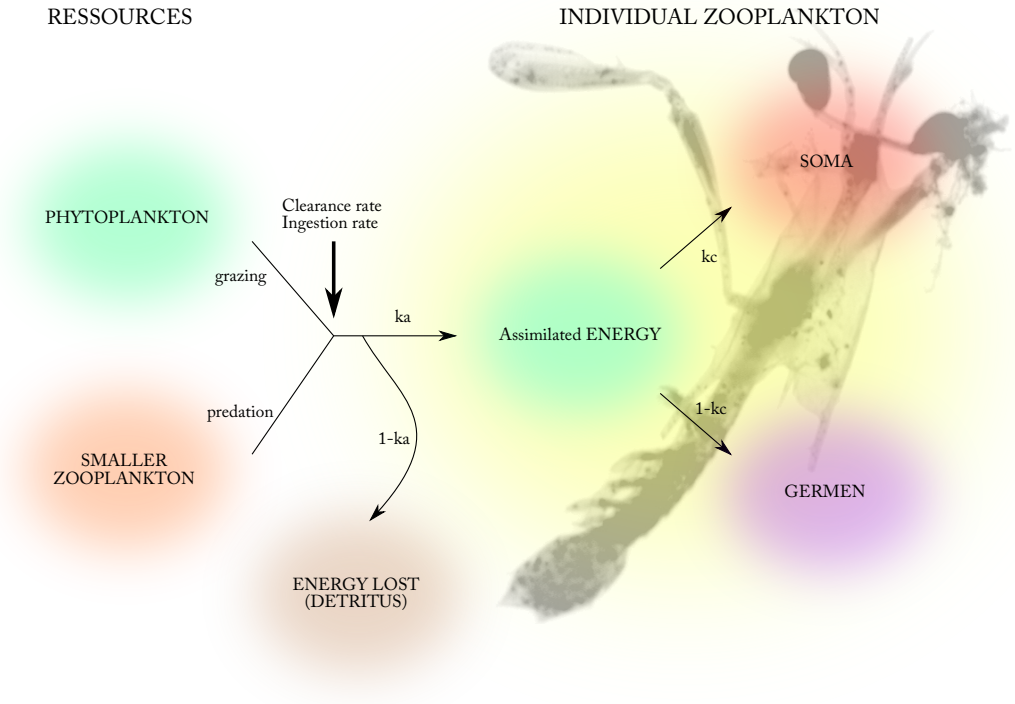

Figure IV.2 – *Conceptual scheme of the physiological modeling at the individual scale. This represents the three possible directions of food that is ingested: the unassimilated part goes to detritus, and the assimilated part goes to growth (Soma) or reproduction (Germen). see text for details.*

Table IV.1 – *Complete list of variables and parameters used in the zooplankton continuous size-based model. The currency is basically the energy and a proportional relation was assumed with biomass and biovolume. In this table we will use "mm^3" for units to be consistent with the measured made on the ecosystem.* $\underline{\ldots}$ *indicates parameters that have to be set (mean and range values are then given) and "*" indicates parameters that are calculated within the model to ensure an allometric equilibrium, see text for explanation.*

Name	Units	Mean	Range	Description
				Space
x	$\log(\mathrm{mm}^3)$	-	-	currency of the model
t	day	-	-	time
x_0	$\log(\mathrm{mm}^3)$	-7.5	-	minimal size
x_1	$\log(\mathrm{mm}^3)$	6	-	maximal size
x_a	$\log(\mathrm{mm}^3)$	-3.44	-	minimal size of zooplankton data
x_b	$\log(\mathrm{mm}^3)$	1.95	-	maximal size of zooplankton data
				State variables
$u_z(x,t)$	$\log(\mathrm{m}^{-3})$	-	-	density of zooplankton of size x at time t
$u_p(t)$	$\mathrm{mm}^3\ \mathrm{m}^{-3}$	-	-	density of phytoplankton at time t
				Entry
$e(t)$	d^{-1}	-	-	growth of phytoplankton at time t
				Processes
$\mathscr{G}(x,t)$	$\mathrm{mm}^3\ \mathrm{d}^{-1}$	-	-	biovolume used for growth of zooplankton of size x at time t
$\mathscr{M}(x,t)$	d^{-1}	-	-	rate of mortality for zooplankton of size x at time t
				Quantities
$M_p(t)$	$\mathrm{mm}^3\ \mathrm{d}^{-1}$	-	-	biovolume lost by phytoplankton due to grazing at time t
$E_r(t)$	$\mathrm{mm}^3\ \mathrm{d}^{-1}$	-	-	biovolume allocated to reproduction at time t
$R_z(x,t)$	$\mathrm{mm}^3\ \mathrm{m}^{-3}$	-	-	density of prey (zooplankton) available for zooplankton of size x at time t
$R_p(x,t)$	$\mathrm{mm}^3\ \mathrm{m}^{-3}$	-	-	density of phytoplankton available for zooplankton of size x at time t
				functions
$p_z(x,y)$	-	-	-	predatory affinity of zooplankton of size x on zooplankton of size y
$p_p(x)$	-	*	-	grazing affinity of zooplankton of size x on phytoplankton
$\mu_{ext}(x)$	-	*	-	external mortality rate for zooplankton of size x
$A(x)$	$\mathrm{m}^3\ \mathrm{d}^{-1}$	-	-	maximum clearance rate of zooplankton of size x
$D(x)$	$\mathrm{mm}^3\ \mathrm{d}^{-1}$	-	-	maximum ingestion rate of zooplankton of size x
				Parameters of the general case
α_a	-	*	-	intercept of $A(x)$
β_a	-	*	-	exponent of $A(x)$
α_d	-	*	-	intercept of $D(x)$
$\underline{\beta_d}$	-	0.75	[0.55:0.90]	exponent of $D(x)$
$\underline{\rho}$	-	3.5	[2:5]	mean of the Gaussian in log scale of p_z
$\underline{\sigma}$	-	2	[0.5:3]	variance of the Gaussian in log scale of p_z
$\underline{k_a}$	-	0.4	[0.2:0.8]	assimilation coefficient
$\underline{k_c}$	-	0.7	[0.5:0.85]	fraction of assimilated food allocated to growth
k_r	-	*	-	proportion of hatching eggs
				Parameters of the infinite case / allometric equilibrium
α	-	*	-	intercept of the allometric spectrum
β	-	*	-	exponent (slope) of the allometric spectrum
$\alpha_m(\alpha,\beta)$	-	*	-	intercept of the mortality (allometric) at equilibrium
$\alpha_g(\alpha,\beta)$	-	*	-	intercept of the growth (allometric) at equilibrium
$\alpha_r(\alpha,\beta)$	-	*	-	intercept of the total density of food (allometric) at equilibrium
				Parameters computed from the allometric equilibrium
$\underline{\varepsilon}$	-	0.75	[0.1:0.9]	fraction of available food digested at equilibrium
$\underline{T}$	day	360	[100:1080]	time to growth from size x_0 to x_1 at equilibrium

that energy = biomass = biovolume. We introduce the general evolution equation (Van Foerster like):

$$\frac{\partial u_z(x,t)}{\partial t} = -\frac{\partial e^{-x}.\mathscr{G}(x,t).u_z(x,t)}{\partial x} - \mathscr{M}(x,t).u_z(x,t) \tag{IV.1}$$

$$u_z(x_0,t) = \frac{k_r.E_r(t)}{\mathscr{G}(x_0,t)} \tag{IV.2}$$

where $u_z(x,t)$ is the density of energy for size x at time t, $\mathscr{G}$ is the growth and $\mathscr{M}$ is the mortality. To be rigorous, the terms $\mathscr{G}(x,t)$, $\mathscr{M}(x,t)$, $\mathscr{G}(x_0,t)$ and $E_r(t)$ have to be rewritten as $\mathscr{G}(x,u_z(.,t))$, $\mathscr{M}(x,u_z(.,t))$, $\mathscr{G}(x_0,u_z(.,t))$ and $E_r(u_z(.,t))$ to account for the dependence not on time t but on the state of the zooplankton spectrum at time t. The term $\mathrm{e}^{-x}.\mathscr{G}(x,t)$ accounts for the transfer of energy from size to size due to growth. $u_z(x_0,t)$ is the density of energy in the left border of the spectrum, k_r is the hatching success, $E_r(t)$ is the total energy allocated to the Germen (reproduction). That is, the density of energy in the left border is the total energy produces by larger zooplankton allocated for reproduction ($k_a \cdot (1-k_c)$, see fig. IV.2) balanced by a hatching success (that will be defined later) and divided by the growth which corresponds to the feeding of newly hatched eggs on phytoplankton.

The phytoplankton dynamics is defined as

$$\frac{d\,u_p(t)}{dt} = e(t).u_p(t) - M_p(t) \tag{IV.3}$$

The phytoplankton is not structured by size, $e(t)$ is the growth of phytoplankton (the only entry of the system) and $M_p(t)$ (or $M_p(u_z(.,t))$) is the grazing by zooplankton. We now introduce two quantities, $R_z(x,t)$ and $R_p(x,t)$:

$$R_z(x,t) = \int_{x_0}^{x_1} \mathrm{e}^{y}.p_z(x,y).u_z(y,t)dy \tag{IV.4}$$

$$R_p(x,t) = p_p(x).u_p(t) \tag{IV.5}$$

where p_z and p_p are the predation and grazing efficiencies respectively. $R_z(x,t)$ represents the total quantity of energy available for individuals of size x through predation on other zooplankton of size y. $R_p(x,t)$ represents the total quantity of energy available through grazing on phytoplankton. With these

quantities we can define the growth $\mathscr{G}$, the mortality $\mathscr{M}$, the total energy allocated to reproduction $E_r(t)$ and the total energy lost by the phytoplankton through grazing $M_p(t)$:

$$\mathscr{G}(x,t) = k_a.k_c.D(x).\frac{R_z(x,t)+R_p(x,t)}{D(x)/A(x)+R_z(x,t)+R_p(x,t)} \tag{IV.6}$$

$$\mathscr{M}(x,t) = \mu_{ext}(x,t) + \int_{x_0}^{x_1} \frac{D(y).p_z(y,x)}{D(y)/A(y)+R_z(y,t)+R_p(y,t)}.u_z(y,t)dy \tag{IV.7}$$

$$E_r(t) = k_a.(1-k_c)\int_{x_0}^{x_1} D(x).\frac{R_z(x,t)+R_p(x,t)}{D(x)/A(x)+R_z(x,t)+R_p(x,t)}.u_z(x,t).dx \tag{IV.8}$$

$$M_p(t) = \int_{x_0}^{x_1} D(x).\frac{R_p(x,t)}{D(x)/A(x)+R_z(x,t)+R_p(x,t)}.u_z(x,t).dx \tag{IV.9}$$

where $A(x)$ is the clearance rate, $D(x)$ the ingestion rate, k_a the assimilation efficiency, k_c the proportion of assimilated energy allocated to growth and μ_{ext} the external mortality. We choose the following allometric functions to define them:

$$A(x) = \alpha_a e^{\beta_a.x} \tag{IV.10}$$

$$D(x) = \alpha_d e^{\beta_d.x} \tag{IV.11}$$

$$p_z(x,y) = \mathrm{e}^{-\frac{(x-y-\rho)^2}{2.\sigma^2}} \tag{IV.12}$$

Then a total of 13 parameters are needed for this general case: p_p and μ_{ext} are curves and need at least two parameters each to be defined, then α_a, β_a, α_d, β_d, ρ, σ, k_a, k_c and k_r. In the following section we will use properties of the allometric equilibrium of the model in a particular case to calculate p_p, μ_{ext}, α_a, β_a, α_d and k_r within the model to ensure an allometric equilibrium. For this, two new parameters ε and T will be defined at the end of the next section.

IV.2.2.2 Infinite case

To reduce the number of parameters of the general case we decided to ensure that the model has an allometric equilibrium for a particular case. We will then find some formulations of parameters that will ensure the general model to have the same allometric equilibrium. This particular case is

named the "infinite case", i.e., on $x \in [-\infty : +\infty]$. Because of this there is no external mortality, no phytoplankton and no closure on reproduction. The philosophy is to extend the formulation of the predation on this infinite spectrum. Then the grazing on phytoplankton will be defined as the predation of individuals from x_0 to $+\infty$ on individuals from $-\infty$ to x_0, the external mortality as the predation of individuals from x_1 to $+\infty$ on individuals from x_0 to x_1, and the closure on reproduction, i.e., k_r the proportion of hatching eggs, as the coefficient to be applied on the total energy allocated to reproduction by individuals from x_1 to x_0 so that it equals the density of the allometric spectrum at x_0 ($u_z^*(x_0)$). At the end, this will reduce the number of parameters from 13 to 7 and will ensure the general case to have an allometric equilibrium which is mathematically more convenient. This part details the mathematical steps followed.

The general allometric form of the spectrum is:

$$u_z(x) = \alpha \mathrm{e}^{\beta x} \tag{IV.13}$$

We look now for sufficient conditions of existence of this allometric equilibrium. We suppose that

$$\beta_a = \beta_d - \beta - 1 \tag{IV.14}$$

β_a and β_d being the exponents of clearance and ingestion rates respectively and β the exponent of the equilibrium we are looking for. With this equality it becomes possible to calculate the available resources, the growth and the mortality at equilibrium:

$$R_z(x) = \underbrace{\alpha.\sigma\sqrt{2\pi}.\mathrm{e}^{\frac{(\beta+1)^2\sigma^2}{2}}.\mathrm{e}^{-(\beta+1)\rho}}_{\alpha_r(\alpha,\beta)}.\mathrm{e}^{(\beta+1).x} \tag{IV.15}$$

$$\mathscr{G}(x) = \underbrace{k_a.k_c.\alpha_d.\frac{\alpha_r(\alpha,\beta)}{\frac{\alpha_d}{\alpha_a}+\alpha_r(\alpha,\beta)}}_{\alpha_g(\alpha,\beta)}.\mathrm{e}^{\beta_d.x} \tag{IV.16}$$

$$\mathscr{M}(x) = \underbrace{\frac{\alpha.\alpha_d}{\frac{\alpha_d}{\alpha_a}+\alpha_r(\alpha,\beta)}.\sigma\sqrt{2\pi}.\mathrm{e}^{\frac{(\beta_d-1)^2\sigma^2}{2}}.\mathrm{e}^{(\beta_d-1)\rho}}_{\alpha_m(\alpha,\beta)}.\mathrm{e}^{(\beta_d-1).x} \tag{IV.17}$$

We define three new intercepts: α_r, α_g and α_m, intercepts of the available food quantity, growth and mortality at equilibrium.

A necessary and sufficient condition of existence of an allometric equilibrium appears:

$$\alpha_g(\alpha,\beta).(\beta_d+\beta-1)+\alpha_m(\alpha,\beta)=0 \tag{IV.18}$$

If we introduce:

$$y=\beta+\beta_D-1 \qquad \text{and} \qquad \lambda=2\beta_D-4+\frac{2\rho}{\sigma^2} \tag{IV.19}$$

We have then:

$$IV.18 \qquad \Longleftrightarrow \qquad f(y)=y.\mathrm{e}^{\frac{\sigma^2}{2}\left(y^2-\lambda y-(\lambda+1)\right)}+\frac{1}{k_c.k_a}=0 \tag{IV.20}$$

We look now for the solutions of $f(y)$. Because α is not in this equation, there is the existence of a family of equilibrium for each solution of this equation. We can derive:

$$f'(y)=\mathrm{e}^{\frac{\sigma^2}{2}\left(y^2-\lambda y-(\lambda+1)\right)}\sigma^2\left[y^2-\frac{\lambda}{2}y+\frac{1}{\sigma^2}\right] \tag{IV.21}$$

and look for roots:

$$\Delta=\frac{\lambda^2}{4}-\frac{4}{\sigma^2} \tag{IV.22}$$

If $\Delta\leq 0$, then a single solution of $f(y)=0$, else we calculate the roots of the polynomial :

$$y_1=\frac{\lambda}{4}-\frac{1}{2}\sqrt{\Delta} \tag{IV.23}$$

$$y_2=\frac{\lambda}{4}+\frac{1}{2}\sqrt{\Delta} \tag{IV.24}$$

leading to different cases:

- $f(y_1)>0$ and $f(y_2)<0$ then 3 solutions
- $f(y_1)<0$ and $f(y_2)<0$ then 1 solution
- $f(y_1)>0$ and $f(y_2)>0$ then 1 solution

- $f(y_1) = 0$ or $f(y_2) = 0$ then 2 solutions (critical case)

We have just seen that there is always at least one solution of the equilibrium to the infinite scenario. We have then a value of β so that all spectra are solutions of the stationary "infinite" case:

$$u(x) = \alpha.\mathrm{e}^{\beta x} \qquad \alpha \in \mathbb{R}_+^* \tag{IV.25}$$

Choices on external mortality and grazing on phytoplankton will allow the case with border (general case), to have this (these) same equilibrium(a). We make the following choice:

$$\mu_{ext}(x) = \alpha.\int_{\mathbb{R}\setminus[x_0,x_1]} \frac{D(y).p_z(y,x)}{D(y)/A(y) + \alpha_r(\alpha,\beta).\mathrm{e}^{(\beta+1)y}}.\mathrm{e}^{\beta y}.dy \tag{IV.26}$$

$$= \frac{\alpha_m(\alpha,\beta)}{2}.\Big[2 + \mathrm{erf}\big(\hat{v_1}(x)\big) - \mathrm{erf}\big(\hat{v_0}(x)\big)\Big].\mathrm{e}^{(\beta_d-1).x} \tag{IV.27}$$

with:

$$\hat{v_0}(x) = \frac{x - x_0 + \rho + (\beta_d - 1)\sigma^2}{\sigma\sqrt{2}} \qquad \text{and} \qquad \hat{v_1}(x) = \frac{x - x_1 + \rho + (\beta_d - 1)\sigma^2}{\sigma\sqrt{2}} \tag{IV.28}$$

$$R_p^\star(x) = \alpha.\int_{\mathbb{R}\setminus[x_0,x_1]} \mathrm{e}^y.p_z(x,y).\mathrm{e}^{\beta y}.dy \tag{IV.29}$$

$$= \frac{\alpha_r(\alpha,\beta)}{2}.\Big[2 + \mathrm{erf}\big(\bar{v_1}(x,\beta)\big) - \mathrm{erf}\big(\bar{v_0}(x,\beta)\big)\Big].\mathrm{e}^{(\beta+1).x} \tag{IV.30}$$

with:

$$\bar{v_0}(x,\beta) = \frac{x - x_0 - \rho + (\beta + 1)\sigma^2}{\sigma\sqrt{2}} \qquad \text{and} \qquad \bar{v_1}(x,\beta) = \frac{x - x_1 - \rho + (\beta + 1)\sigma^2}{\sigma\sqrt{2}} \tag{IV.31}$$

and with the error function:

$$\mathrm{erf}(x) = \frac{2}{\sqrt{\pi}}\int_0^x \mathrm{e}^{-x^2}.dx \tag{IV.32}$$

which accounts for the error of calculating the area of an infinite function on a discrete window compared to the complete area of the function.

Processes are then formulated at the equilibrium (* indicate equilibrium). The total energy allocated to reproduction is (case of $\beta_d \neq \beta$) :

$$E_r^*(x) = \frac{(1-k_c)}{k_c}.\frac{\alpha.\alpha_g(\alpha,\beta)}{\beta_d + \beta}\left[\mathrm{e}^{(\beta_d+\beta)x_1} - \mathrm{e}^{(\beta_d+\beta)x_0}\right] \tag{IV.33}$$

Which corresponds to the border condition:

$$u_z^*(x_0) = \frac{k_r.(1-k_c)}{k_c}.\frac{\alpha}{\beta_d+\beta}.\mathrm{e}^{-\beta_d.x_0}\left[\mathrm{e}^{(\beta_d+\beta)x_1} - \mathrm{e}^{(\beta_d+\beta)x_0}\right] \quad \left(=\alpha.\mathrm{e}^{\beta.x_0}\right) \tag{IV.34}$$

We loose here a degree of freedom by imposing:

$$k_r = \frac{k_c}{(1-k_c)}.(\beta_d+\beta).\frac{1}{\left[\mathrm{e}^{(\beta_d+\beta)(x_1-x_0)}-1\right]} \tag{IV.35}$$

with $k_r \leq 1$. The total mortality of phytoplankton becomes:

$$M_p^* = \frac{\alpha.\alpha_g(\alpha,\beta)}{2.k_a.k_c}\int_{x_0}^{x_1}\left[2+\mathrm{erf}\left(\bar{v_1}(x,\beta)\right)-\mathrm{erf}\left(\bar{v_0}(x,\beta)\right)\right]\mathrm{e}^{(\beta_d+\beta)x}dx \tag{IV.36}$$

Moreover, for the phytoplankton to be at the equilibrium, it needs:

$$\mathrm{e}^*.u_p^* - M_p^* = 0 \tag{IV.37}$$

Parameters defined for equilibrium are difficult to use in an ecological sense, yet, it is possible to derive ecologically pertinent ones from them:

- the maximal fraction of energy that is ingested at equilibrium

$$\varepsilon = \frac{\alpha_r(\alpha,\beta)}{\frac{\alpha_d}{\alpha_a}+\alpha_r(\alpha,\beta)} < 1 \tag{IV.38}$$

- time to go from size x_0 to size x_1

$$T = \int_{x_0}^{x_1}\frac{dx}{\mathrm{e}^{-x}.\mathscr{G}^*(x)} = \frac{1}{\varepsilon.\alpha_d.k_a.k_c(1-\beta_d)}\left[\mathrm{e}^{(1-\beta_d)x_1}-\mathrm{e}^{(1-\beta_d)x_0}\right] \tag{IV.39}$$

The maximal fraction of energy that is ingested at equilibrium ε, is the ratio between the intercept of the energy available at equilibrium (α_r), divided by the sum of α_r and the ratio of the intercepts of the ingestion rate (α_d) and the clearance rate (α_a), hence it is the ratio between the available energy and the maximum energy that is ingested due to physiological constraints. T represents the time, at equilibrium, an individual of size x_0 needs to reach size x_1. These two parameters are used to compute α_a and α_d, so that an allometric equilibrium exists.

The model contains then a single input, i.e., $e(t)$ the growth of phytoplankton, and a total of seven parameters that need to be set: k_a the assimilation coefficient, k_c the proportion of energy allocated to growth, ρ the logarithm of the predator/prey size ratio, σ the logarithm of the variance of the predator/prey size ratio, β_d the coefficient of the ingestion rate, ε the maximal fraction of energy that is ingested at equilibrium, T the time to go from the first size class x_0, eggs, to size x_1. These parameters are underlined in table IV.1.

IV.2.3 Discussion on model formulation

IV.2.3.1 Grazing, predation and growth

The growth is the result of grazing on phytoplankton and predation on zooplankton with an assimilation coefficient and a fraction allocated to growth, the other part being used for reproduction (presented after in IV.2.3.3). First of all, two quantities were introduced, i.e., R_z and R_p eq. IV.4 and IV.5. These two quantities represent the total quantity of zooplankton and phytoplankton individuals of size x can prey upon. R_z is the integrate over the whole spectrum of the available energy of zooplankton multiplied by an affinity coefficient (p_z, eq. IV.12). This affinity coefficient p_z is defined as a Gaussian in the logarithmic space with two coefficients, ρ which is the average predator/prey size ratio and σ which is the variance of the Gaussian. This equation is presented on fig. IV.3 with ρ equals 4 and σ equals 2 (example values). This modeling of predation implies that a predator can potentially reach all the available prey within its preferences, in this sense the model is more similar to the one of Maury et al. (2007a) than of Baird & Suthers (2007) which used an aggregation model to explicitly model encounters in the system. Here encounter rates are not modeled.

Then, the quantity R_p, is the available phytoplankton, i.e., the total phytoplankton balanced by an affinity coefficient p_p. Equation IV.36 — the mortality of phytoplankton — can also be viewed as the integral on each $p_p(x) * u_z(x)$ at the equilibrium, x being the size of individuals — in the allometric

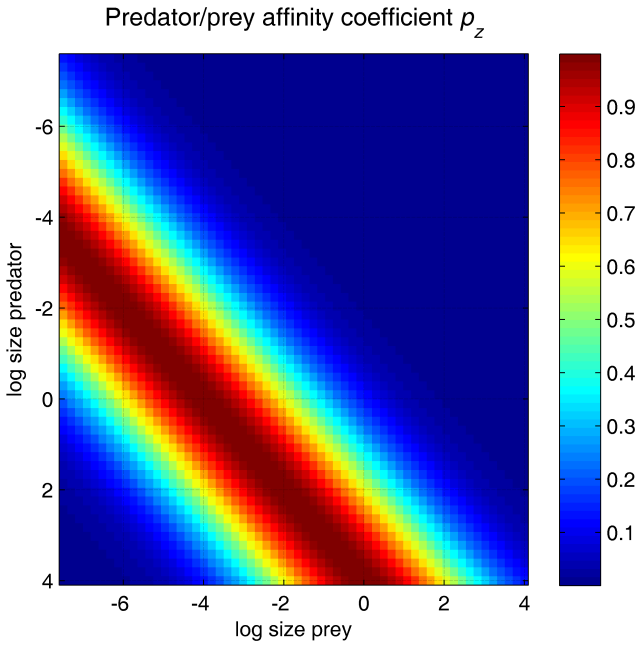

Figure IV.3 – *Predator/prey affinity coefficient p_z with $\rho = 4$ and $\sigma = 2$ taken as example values to illustrate the general shape of p_z.*

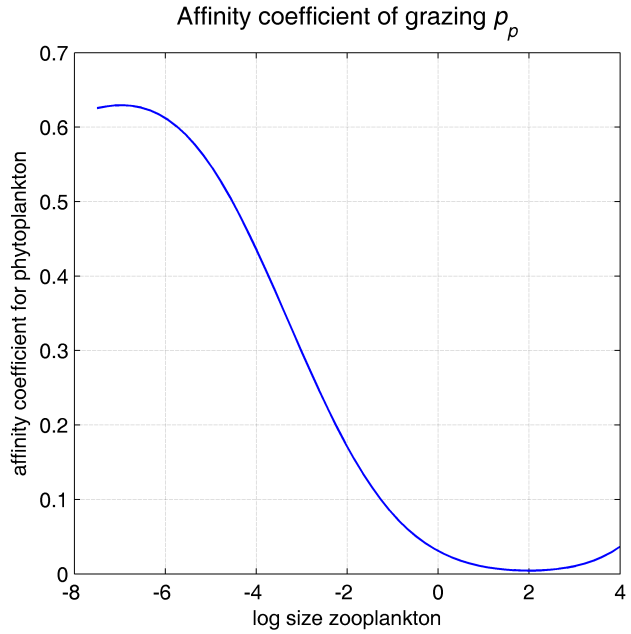

Figure IV.4 – *Example of the shape of the grazing affinity coefficient p_p.*

equilibrium case, x has an infinite range of variation, and so does not represent only the zooplankton. The general shape of p_p is on the form $ax \cdot e^{bx}$, an example is shown on fig. IV.4.

The sum of the two quantities R_z and R_p represents the total quantity of food available for zooplankton. In previous models, such as the one of Benoît & Rochet (2004), this quantity was directly

used by organisms, this was a "supply" vision of the ecosystem. This vision introduced however a potentially infinite growth of organisms (Benoît & Rochet 2004). Here we use a symmetric vision of the ecosystem based on "supply" and "needs" of organisms. This vision is similar to the one used by Maury et al. (2007a) with a different formulation. We define a clearance rate A (volume of water explored per day) and a ingestion rate D (quantity of energy potentially ingested per day) that will be applied to the quantity $R_z + R_p$. The digestion rate D represents the maximum quantity of food an individual can ingest each day (not to be confused with the assimilated food). Both A and D are on the form of allometric relationships depending on the size of zooplankton. The quantity ingested is then on the form, with $R = R_z + R_p$:

$$\frac{D \cdot R}{(D/A) + R} \tag{IV.40}$$

which is an Holling type II relationship and appears in eqs. IV.6, IV.7, IV.8, IV.9 of the general model. The value of D represents the maximal quantity of food that can be ingested, and the value of D/A is similar to a "half saturation constant". An example with hypothetical values of $D = 10$ and $A = 1$ is shown on fig. IV.5 to illustrate the general shape. This relationship stabilizes the system by limiting the quantity of food effectively ingested — organisms are limited by their physiology. Then, a part of this ingested food is assimilated, with the coefficient k_a, and a part of the assimilated food is used for growth (fraction k_c), whereas the other part is used for reproduction (fraction $1 - k_c$). The fraction k_c used for growth allows individuals to increase their size (with the transfer term in eq. IV.1). The fraction $1 - k_c$ used for reproduction is allocated to an eggs pool determining $u_z(x_0)$. This part of the model is inspired by the "Dynamic Energy Budget DEB" theory (Kooijman 2001) as in Maury et al. (2007a). However, metabolic costs are not modeled here.

IV.2.3.2 Mortality on zooplankton

The mortality of the zooplankton is the sum of predation by larger zooplankton, second term of eq. IV.7 (see IV.2.3.1), and external mortality. The latter is computed within the system (eq. IV.26). In the allometric equilibrium in the case of an infinite spectrum the external mortality does not exist. Yet, the modeled spectrum is not infinite and border conditions should be defined. Within the infinite spectrum, the mortality at equilibrium is defined by eq. IV.17 and is allometric (i.e., on the form ae^{bx}), calculated as predation by organisms larger than x_1 and depends on parameters ρ and σ of the predator/prey size relationship, on parameters α and β of the spectrum at equilibrium and on β_d the exponent of the clearance rate. The external mortality is necessary to avoid the last size class to increase and exert an unrealistic predation pressure on smaller zooplankton. Such process will propagate a false and uncontrollable trophic cascade from the right border of the spectrum. It is suppressed by an external mortality constraint.

IV.2.3.3 Closure on reproduction

As the external mortality, the reproduction represents the border condition, but on the left side of the spectrum (x_0). It is the recruitment. The choice was made to include in the physiology a proportion

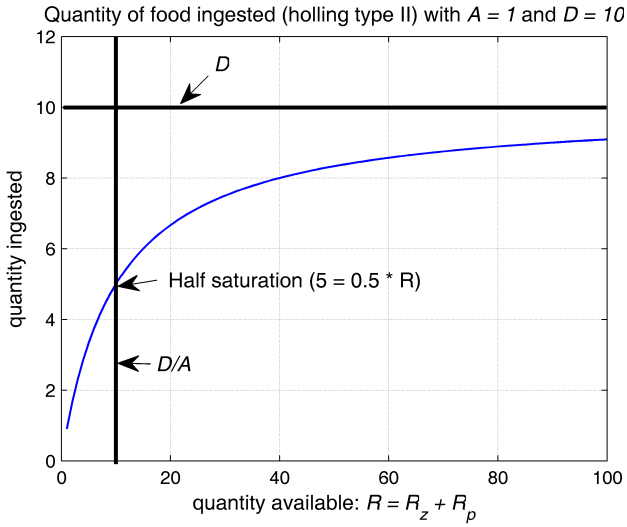

Figure IV.5 – *Example of the food effectively ingested vs. available food.*

of assimilated energy that is used for reproduction. The proportion allocated to reproduction is $k_a * (1 - k_c)$ of the ingested food quantity. This biomass represents the total production of eggs. Then a hatching success k_r is applied on this quantity. k_r is computed at the equilibrium as the coefficient to add to the total production of energy for reproduction of individuals x_0 to x_1 and equals $u_z^*(x_0,t)$: the density of energy of the allometric equilibrium spectrum at x_0. The value of k_r is imposed to be a function of k_c, β_d and β, see eq. IV.35 and must be ≤ 1.

IV.2.3.4 Phytoplankton dynamics

To model the phytoplankton, a simple equation including a growth rate and a mortality by zooplankton is used (eq. IV.3). The growth rate is the only input of the model, it represents the energy produced by the phytoplankton. For the comparison with observations that will be done later in this chapter, the growth rate was computed using the model of Andersen & Nival (1988) and will be a function of temperature, nitrates and solar irradiation. Parameters for the mortality of phytoplankton by zooplankton grazing, see eq. IV.9, are also calculated to ensure an allometric equilibrium.

IV.2.4 Values for parameters

A total of seven parameters have to be set, i.e., k_a, k_c, β_d, ρ, σ, ε and T. In addition, the lower size x_0 and the maximum size x_1 need also to be set. For the model the currency used is not important, yet parameter units chosen for simulation and comparison with data need to be homogeneous. Since the data are mostly in biovolume, we will choose biovolume (in mm^3) as the currency of the model. Parameter values set within this section are summarized on table IV.2 but were already mentioned on table IV.1.

First of all, the lower size x_0 and the maximum size x_1 were chosen to globally cover the size range of crustaceans because they dominate the zooplankton in the bay of Villefranche-sur-Mer. x_0 is set to -7.5 in $\log(mm^3)$, which is equivalent, using average relationships (see chapter II) to 100

μm ESD, which is approximately the size of nauplii. The upper limit x_1 was set to 6 (in log(mm^3)), equivalent to 1 cm ESD, which is the approximate size of larger amphipods, euphausiids and mysiids found in the bay of Villefranche-sur-Mer.

The assimilation coefficient k_a is generally set around 0.7 (e.g., Andersen & Nival 1988). Maury et al. (2007a) used values from 0.65 to 0.99 with an average at 0.8. Values used by Raick et al. (2005) were on the same order, with assimilation efficiencies of 0.77 for the nitrogen and 0.64 for the carbon. From the physiological literature it was found that the assimilation efficiency for copepods varies from 0.10 to 0.95. For example, *Acartia tonsa* was found to have assimilation efficiency from 0.10 to 0.55 (Roman 1977), *Centropages typicus* of around 0.34 (Person-Le Ruyet et al. 1975), *Temora longicornis* from 0.10 to 0.40 (Harris & Paffenhöfer 1976) and *Temora stylifera* of around 0.28 (Person-Le Ruyet et al. 1975). Species with higher assimilation efficiency (up to 0.9), e.g., *Calanus finmarchicus, Calanus hyperboreus, Chiridius armatus, Metridia gerlachei, Pareuchaeta norvegica* ... are not abundant in the NW Mediterranean Sea. We will then use the value 0.4 as a starting point because it may represent better the physiology of organisms locally present. Then the fraction allocated to growth k_c was set by Maury et al. (2007a) as varying from 0.65 to 0.88 with a mean at 0.7, and was set by Raick et al. (2005) to 0.8.

The average predator/prey size ratio was found to vary from 3 to 150 in the literature (Hansen et al. 1994, Straile 1997, Baird & Suthers 2007, Maury et al. 2007a, Barnes et al. 2010, see references herein for the last three). These ratio are calculated on individual biomass, yet since the relationship between biomass and biovolume is linear (see chapter II), the ratio remains the same. From Straile (1997) this ratio varies from 50 to 135 for copepods with a mean of 80, yet from Hansen et al. (1994) the mean ratio for copepods is closer to 20. The mean ratio (ρ) has to be set in logarithm. We choose to make it vary from 2 to 5 (i.e., $\approx$ 10 to 150). The average value is 4.4 according to Straile (1997) and 3 according to Hansen et al. (1994). We decided to take the average value of 3.5 as a mean between

the studies previously mentioned. The variance σ is poorly mentioned in the literature. In Benoît & Rochet (2004) it was guessed from the distribution of prey size in a predator (fish) stomach, the value varied from 1 to 10 with a mean at 5. This gives a mean value of 1.6 in logarithm scale. We arbitrarily set σ to vary from 0.5 to 3.

The coefficient β_d represents the exponent of the ingestion rate. This coefficient was found by Saiz & Calbet (2007), on marine calanoids copepods, to be on average 0.703 with a confidence interval of 0.59 to 0.82. This value is close to the 3/4 law predicted by the metabolic theory. Yet, Glazier (2005) reported that metabolic scaling of copepods on general and of pelagic species was generally closer to 0.85. According to this, we will make this parameter vary from 0.55 to 0.90 to cover this range with a mean value of 0.75 (3/4 law).

Then, ε, the maximal proportion of energy used at equilibrium, can vary between 0 and 1. A value close to 1 will decrease the constraints due to clearance and ingestion rates (A and D), and a value close to 0 will increase it. We will make this parameter to vary from 0.1 to 0.9 with a mean at 0.75. Finally, T represents the time needed at equilibrium for energy to go from size x_0 to size x_1. It can be as short as few weeks for copepods to go from eggs to adults, but as long as few years for larger organisms such as amphipods, euphausiids or mysiids. Yet, this parameter depends on the choice made for x_0 and x_1. Since we have chosen the minimum size as equivalent to 100 μm ESD and the maximum to 1 cm ESD, we will made T varying from few months (i.e., 100 days), to three years (1080 days) which corresponds to the maximum time lag observed in chapter III between the increase of small copepods and of larger categories.

IV.3 Behavior of the model

IV.3.1 Sensitivity at equilibrium

With the previously mentioned average parameters the model gives the following values of the derived parameters (i.e., parameters calculated from the allometric equilibrium in the infinite case, section IV.2.2.2):

- one allometric equilibrium
- $\beta = -1.0325$ and $\alpha = 3.3688$, the slope and intercept of the allometric spectrum at equilibrium
- $\beta_a = 0.7325$ and $\alpha_a = 0.0224$, the coefficients (exponent and intercept) of the allometric relationship between size and clearance rate $A(x)$
- $\alpha_d = 0.1417$, the intercept of the allometric relationship between size and digestion rate $D(x)$
- $k_r = 0.7932 < 1$, the proportion of hatching eggs
- see fig. IV.6 A for p_p the affinity on phytoplankton, and B for μ_{ext} the rate of external mortality

The value of the slope of the spectrum at equilibrium appears close to -1, the allometric exponent of the clearance rate β_a is close to 0.75 and the proportion of hatching eggs is lower than 1. The affinity for phytoplankton decreases with size and the external mortality is high for both small and large

Table IV.2 – *Parameters default values (mean) and range of variation (min to max) determined from literature. See section IV.2.4.*

Parameter	min	max	**mean**
x_0 (mm^3)	-	-	-7.5
x_1 (mm^3)	-	-	6
k_a	0.20	0.80	0.40
k_c	0.50	0.85	0.70
ρ	2	5	3.5
σ	0.5	3	2
β_d	0.55	0.90	0.75
ε	0.1	0.9	0.75
T (days)	100	1080	360

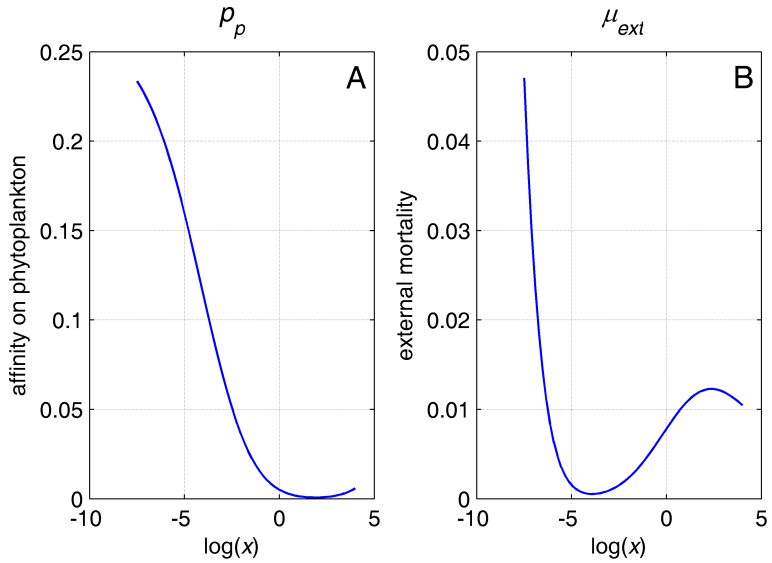

Figure IV.6 – *Value of p_p and μ_{ext} with average parameters.*

organisms. The high external mortality appears evident for large organisms but not for small ones. Yet, it is computed following mathematical constraints, i.e., so as to ensure an allometric equilibrium, and not following ecological realism in this case.

Nevertheless, these derived parameters are realistic. We will then test the effect of changing these parameters on the equilibrium. We will fix the parameters at their average values and then change the values of each of them separately. the sensitivity is shown on figs. IV.7, IV.8, IV.9, IV.10, IV.11, IV.12 and IV.13. On each figure the sensibilities of β, α, β_a, α_a, α_d, k_r, p_p and μ_{ext} are shown.

β, which is the slope of the allometric spectrum at equilibrium, is an important parameter, it represents the average slope, and so the shape of the spectrum. From the literature it is generally found to be close to -1 (e.g., Sheldon et al. 1972, Quiñones et al. 2003). The value of β ranges here from -1.2 to -0.85 (with parameters varying one by one). It is strongly sensitive to k_a, ρ and β_d. Increasing the assimilation coefficient k_a and the predator/prey size ratio ρ will flatter the spectrum, where increasing the allometric exponent of the ingestion rate β_d will steepens it. It is also sensitive, in a lower extent, to k_c and σ. The other parameters of the stationnary spectrum, the intercept α, is principally sensitive to k_a (in the range of variation of parameters which is meaningful). An increase

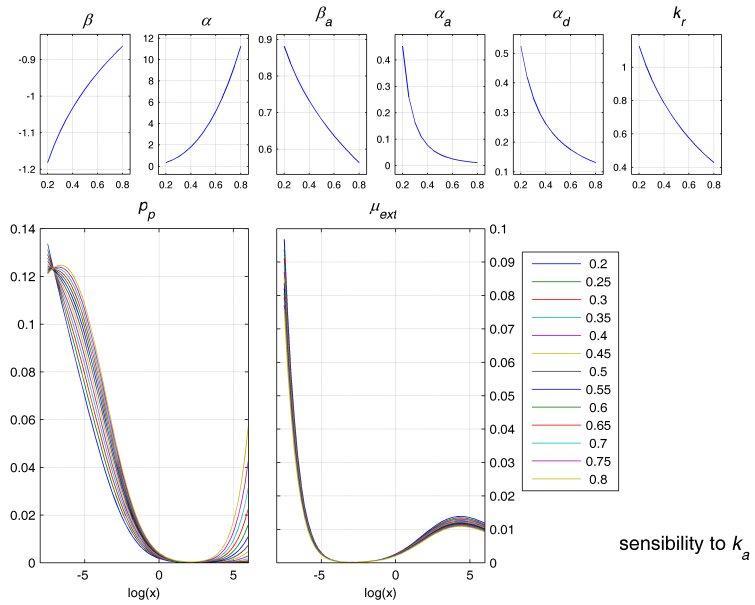

Figure IV.7 – *Sentivity of derived parameters and equilibrium on variation in k_a, the assimilation coefficient.*

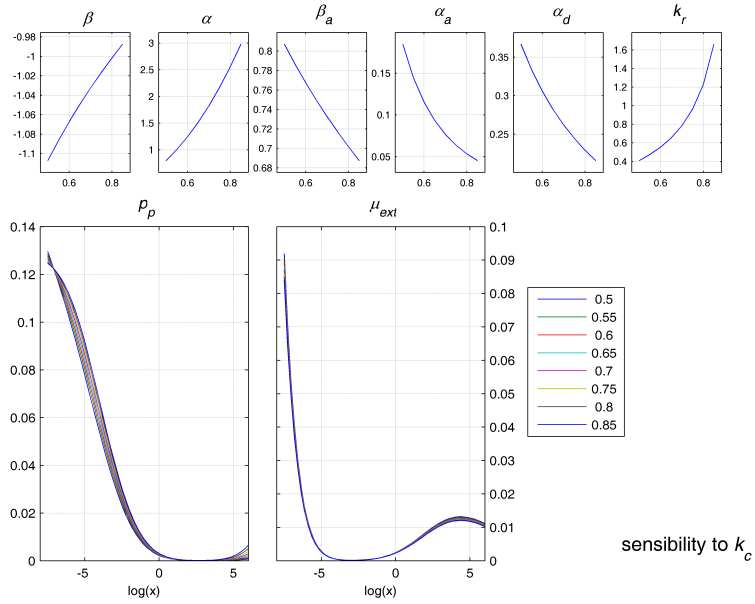

Figure IV.8 – *Sentivity of derived parameters and equilibrium on variation in k_c, the proportion of assimilated food allocated to growth.*

of k_a from 0.2 to 0.8 will make α to vary from 0.5 to 11. That is, a low assimilation coefficient will dramatically decrease the total energy / biomass / biovolume contained in the spectrum — a low k_a means that an important fraction is lost by the system in detritus.

The exponent β_a and the intercept α_a of the clearance rate A are mostly sensitive to k_a and ρ for β_a and k_a, β_d and principally T for α_a. Increase in k_a will decrease the exponent and the intercept, it

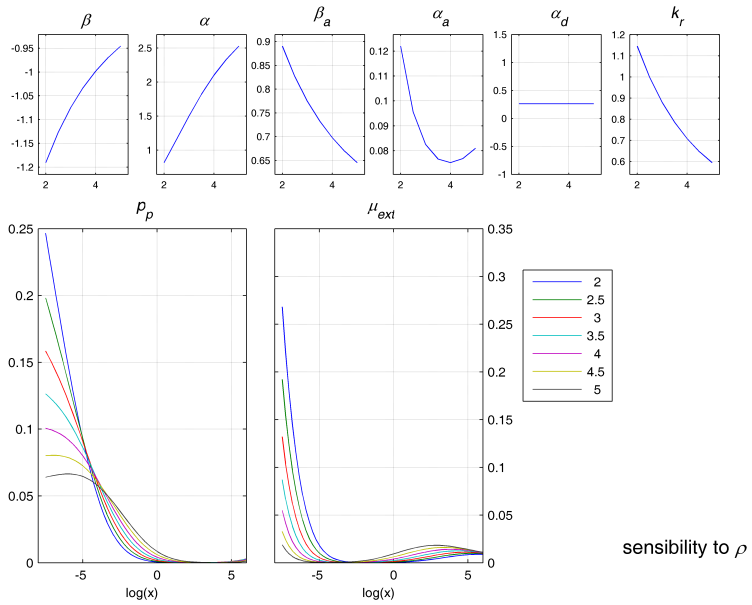

Figure IV.9 – *Sentivity of derived parameters and equilibrium on variation in* ρ*, the mean predator/prey size ratio.*

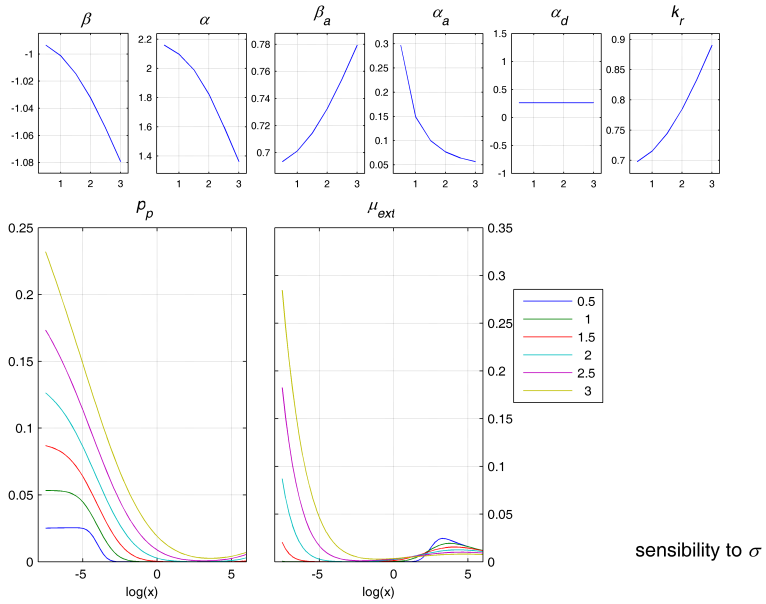

Figure IV.10 – *Sentivity of derived parameters and equilibrium on variation in* σ*, the variance of the predator/prey size ratio.*

will so decrease the clearance rate and the differences between size. Increase in ρ will decrease the exponent but have a limited effect on the intercept. Then increase in β_d and especially T will strongly decrease the intercept and so the total quantity organisms can filter per day.

Then, α_d, the intercept of the ingestion rate, is principally sensitive to variations in ε and T, increase in these parameters resulting in a decrease of α_d, and thus of an increase in the constraint

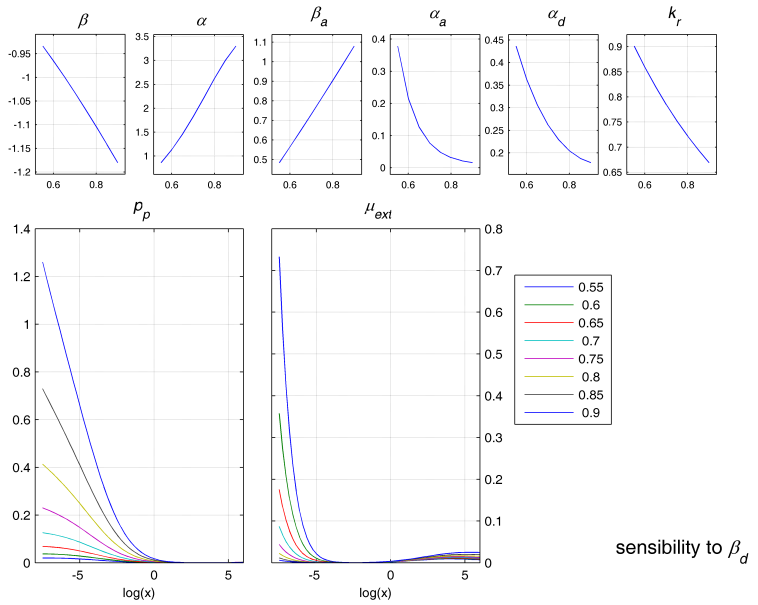

Figure IV.11 – *Sentivity of derived parameters and equilibrium on variation in β_d, the exponent of the digestion rate $D(x)$.*

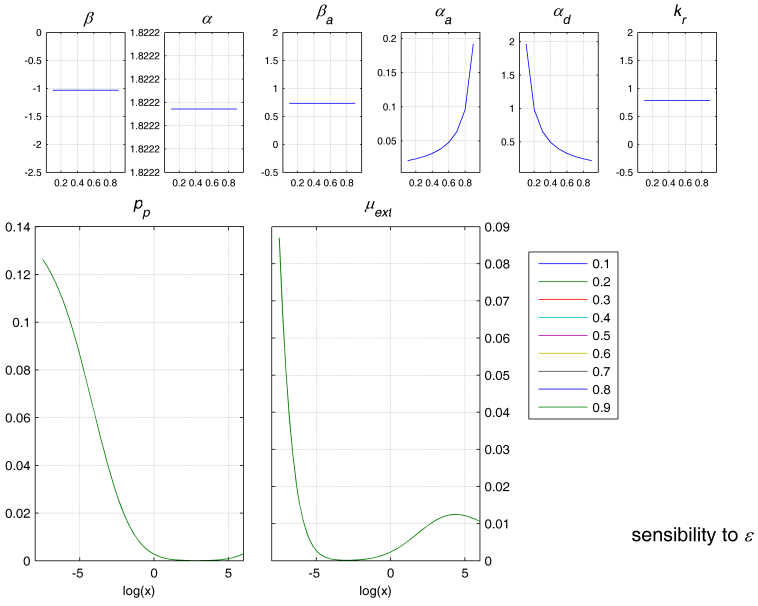

Figure IV.12 – *Sentivity of derived parameters and equilibrium on variation in ε, the maximum fraction of ingested food at equilibrium.*

due to ingestion rate. When ε increases, α_a increases and α_d decreases, so the ratio α_d / α_a decreases. When T increases, it means that it will take more time for organisms to grow, resulting in a decrease in α_d meaning that organisms can digest less food per day.

k_r, the proportion of hatching eggs, is extremely sensitive to k_a, k_c and ρ. Some values of these parameters drive to values of k_r higher than 1 which is ecologically impossible but not forced by

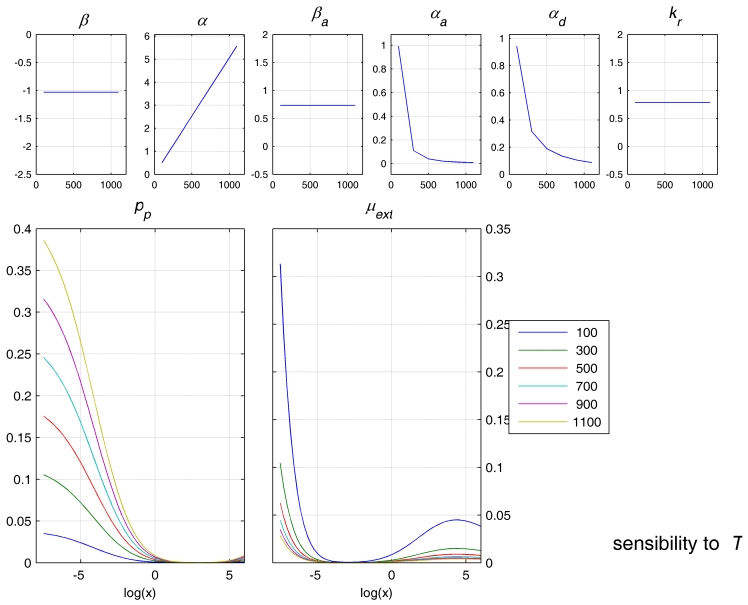

Figure IV.13 – *Sentivity of derived parameters and equilibrium on variation in T, the time to growth from the minimum size x_0 to the maximum size x_1 at equilibrium, T is in days.*

the model. This happened here for values of $k_a < 0.3$, $k_c > 0.75$ and $\rho < 2.5$ (approximatively). It will then be important to check before any simulation that the set of parameters chosen drives to a k_r lower than 1. Increase in k_a and ρ decreases k_r. An increasing assimilation efficiency will increase the overall energy allocated to eggs and so, to ensure a stationnary equilibrium, the ratio of hatching eggs will decrease.

p_p is strongly sensitive to β_d but also to ρ, σ and T to a lower extent. Increase in β_d strongly increases the affinity of smaller zooplankton to phytoplankton. Increase in ρ decreases p_p for small zooplankton, increase in σ increases p_p and increase in T increases p_p. All these parameters, except T, impact the slope β of the spectrum. Steep slopes are related to high p_p and vice-versa. When the spectrum is steep at equilibrium this will increase the quantity of food lower than x_0, organisms larger than x_0 have to prey to ensure the allometric stationary equilibrium. Note that for some values the curve p_p increases again for larger organisms, close to x_1, this is due to the way p_p is computed, i.e., to ensure the allometric equilibrium. This property is then due to mathematical constraints on the model and not to ecological choice.

μ_{ext} is sensitive to the same parameters as p_p is, i.e., to β_d, ρ, σ and T. The shape of μ_{ext} is particular, with high values for sizes close to x_0, then a decrease and again an increase for large size classes (close to x_1). The right part of μ_{ext} represents the quantity removed at equilibrium by organisms larger than x_1. This quantity will decrease by decreasing β_d, decreasing ρ, increasing σ and decreasing T. The left part of μ_{ext} is due to the mathematical formulation and constraints on the model. Ecologically it can be viewed as the need to decrease the quantity of juveniles for the model to have an allometric equilibrium. The response of this part is opposite to the right part, except for T.

IV.3.2 Behavior of outputs in particular cases

We will then look at the response of models outputs. The numerical simulations that will be performed afterward are made on a period of one year, identically repeated ten times for the model to stabilize. The integration is an eulerian one, the unit is the day and the $\Delta(t)$ is set to 0.1. The initial condition is the allometric equilibrium. Here, parameters are set to their default value and we will only modify the entry, i.e., $e(t)$. Results are presented on fig. IV.14.

A total of six well different cases were simulated. The first case (A on fig. IV.14), represents a constant and low growth rate of phytoplankton $e(t) = 0.1$ d^{-1}. The second case (B) represents a constant but higher growth rate, $e(t) = 0.4$ d^{-1}. The third case (C) represents low growth rate (0.1) with a peak at day 100 up to 0.4. This peak is short in time, starting at day 50 to end at day 150. The forth case (D) represents a peak lower in its maximal value (0.3) but longer in time, it reaches its maximal value at day 150 but spreads almost on the whole year. The fifth case (E) represents two peaks, reaching 0.3, the first one at day 100 and the second at day 200. Finally, the sixth case (F) represents the same two peaks but with the first one reaching 0.4 and the second one 0.05.

Without any dynamics (cases A and B), the zooplankton biovolume and slope are stable. An increase of the phytoplankton by 4 increases the total biovolume of zooplankton by 4 also (from 25

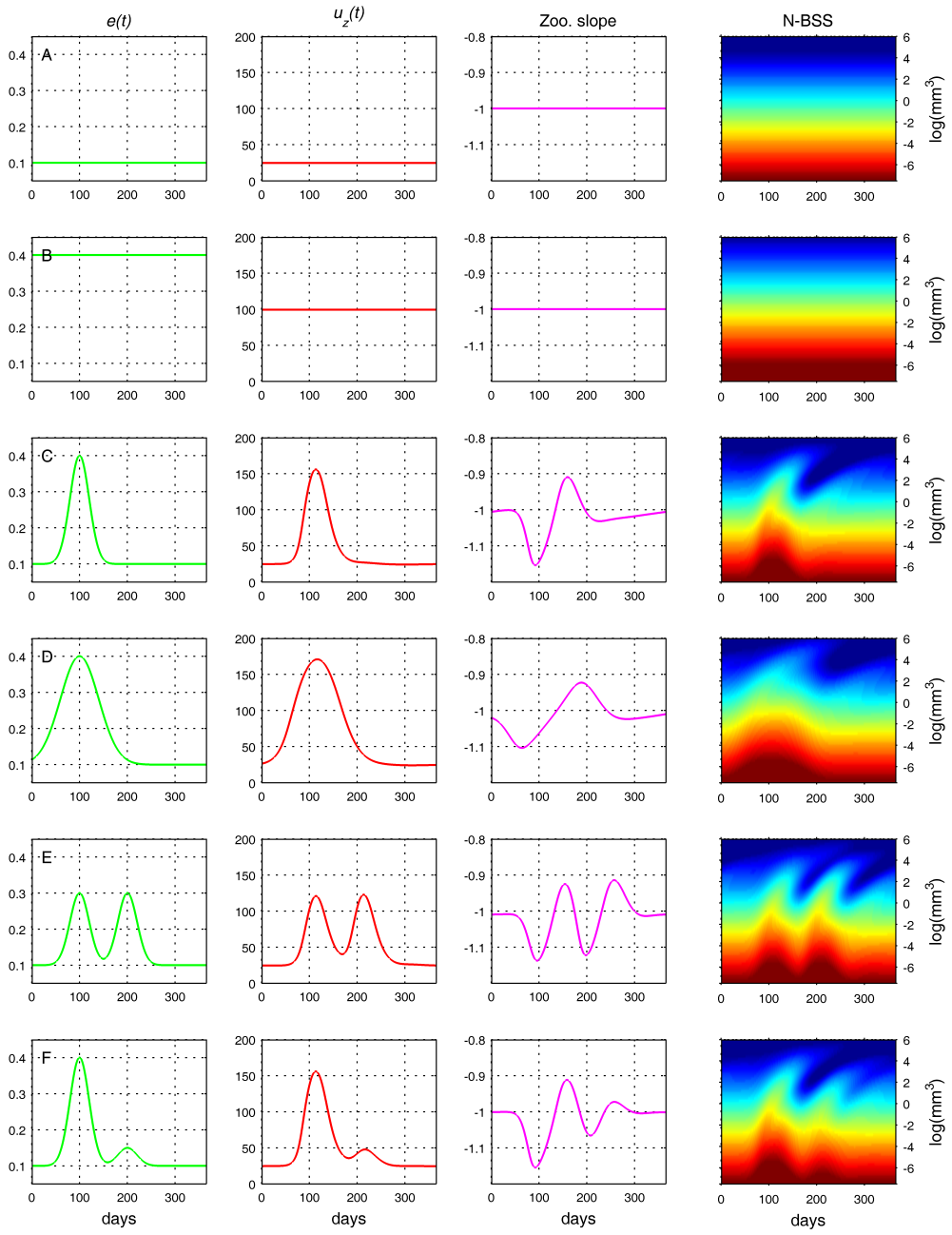

Figure IV.14 – *Simulations of the model for particular cases of the phytoplankton growth. The first column represents the input $e(t)$, the growth rate of phytoplankton which is in d^{-1}, the second is the total biovolume of zooplankton in $mm^3.m^{-3}$, the third one is the slopes of the N-BSS and the third is the N-BSS in* $\log(mm^3 m^{-3} mm^{-3})$. *For the last three columns it is for size from x_0 to x_1. The different scenarii are: (A) constant and low, (B) constant and high , (C) Short and high peak, (D) long and lower peak, (E) two short and identical peaks and (F) one high peak followed by a smaller one.*

mm^3 m^{-3} to 100 mm^3 m^{-3}). The slope is constant at -1.0325 in both cases. Adding then a peak in the phytoplankton growth (case C) reaching 0.4 and maximal at day 100 results in a peak in the

zooplankton total biovolume with the maximum at day 115. This maximum of zooplankton reaches 150 mm^3 m^{-3}, which is higher than with a constant growth of phytoplankton of 0.4. The system is not at the equilibrium. This is viewed in the dynamics of the slope which starts decreasing (minimum in day 95) down to -1.15, then increases again up to day 160 and the value -0.9 to decrease again to a value lower than -1 (minimum on day 225) and then increases gradually to reach the value -1 by the end of the year. On the whole spectra we clearly see a second peak composed mainly by large zooplankton. This is due to the delay in the increase of size classes, the small one responding first to the increase of phytoplankton. A wave is created on the spectrum that will flow up to the large individuals. When the phytoplankton growth decreases this affects first the small individuals and so flattens the spectrum (max at day 160 here) since larger individuals still benefit from the peak of phytoplankton growth. Then the predation by large organisms propagates in the spectrum — even in the first size classes which show they lowest value just before day 200. The further disappearance of large organisms to the right end of the spectrum will then create steeper size spectra (day 160 to day 225 here) with values of slope lower than -1 (the equilibrium). These values lower than -1 are due to the previous decrease (due to predation) of the smallest size classes which are then lower than they must be from the input by phytoplankton. The decrease of predation on these size classes will then make them return to their equilibrium value, which has the effect to create a second wave in the spectrum. The spectrum then slowly reaches its equilibrium (from day 225 to 360 here). In case D, the amplitude of the peak of phytoplankton growth is increased. The maximum of zooplankton is still 15 days after the maximum of phytoplankton growth. The dynamics of the biovolume and the slope are similar as in case C, with yet lower extremes of the slope, the zooplankton spectrum having more time to adapt to changes. In cases E and F, i.e., with two peaks, the behavior is also similar but with two peaks here, both in the biovolume and the slope dynamics. The second peak appears similar to the first one, in a lower extent in case F.

Table IV.3 – *Units and values used for computing the irradiance at depth z.*

Parameter	Units	Value
I_z	W m^{-2}	-
$I_{z=0}$	W m^{-2}	data from MétéoFrance
$albedo$	-	0.085
$K_{ext}(z)$	m^{-1}	-
$K_{water}(z)$	m^{-1}	$f(z)$[tab. IV.4]
K_{chl}	(mgChl m^2)$^{-1}$	0.02
$Chl(z,t)$	mgChl m^{-3}	data from PointB

IV.4 Comparison with observations

We now analyze the behavior of the model with data as inputs, and compare the outputs of the model with observations on crustaceans size spectra dynamics (see chapter III). The two main states of the ecosystem identified in chapter III, i.e., low zooplankton (years 1996, 1997, 1998) and high zooplankton (years 2001, 2003, 2004, 2005) are chosen. Years of changes (1999 and 2000) are not taken as well as years 1995 and 2002 which showed less marked pattern. Hereafter the mean of years 1996, 1997 and 1998 will be considered as scenario 1 and the mean of 2001, 2003, 2004, 2005 as scenario 2. The first step will be to integrate a model of the growth of phytoplankton, since we do not have direct measure of this variable. Then a comparison with recorded size spectra will be made. For this part a sub-part only of the modeled size-spectrum is taken since data do not cover the range $[x_0 = -7.5 : x_1 = 6]$. From results of chapter II the ZooScan and the WP2 net cover the range $[x_a = -3.44 : x_b = 1.95]$ (i.e., from 0.032 to 7 mm^3). Total biovolume and slope will be calculated on this range to compare with data. At the end of this section, a preliminary optimization on parameters will be presented. A complete optimization is currently underway but is not presented in this manuscript. As in the previous section, simulations are made using an Eulerian numerical integration with a $\Delta t = 0.1$, one year is repeated ten times for the model to stabilize and the initial condition is the allometric equilibrium.

Table IV.4 – $K_{water}(z)$

depth	0-1	1-2	2-3	3-5	5-10	10-20	>20
$K_{water}(z)$	0.8	0.25	0.14	0.12	0.08	0.07	0.04

IV.4.1 Integration of a phytoplankton growth model

The growth of phytoplankton, as a function of nitrates (NO_3), irradiance and temperature was calculated using the model of Andersen & Nival (1988) made for the same location, i.e., Point B. NO_3 and temperature were computed as the 0-75 m depth integrated values, whereas irradiance (I_z 0-75 m depth integrated) were calculated using the model of Raick et al. (2005) and Lacroix & Grégoire (2002):

$$I_z = I_{z=0} \cdot (1 - albedo) \cdot e^{[-\int_0^z K_{ext}(z)dz]} \tag{IV.41}$$

where,

$$K_{ext}(z) = K_{water}(z) + K_{chl}\left[Chl(z,t)\right] \tag{IV.42}$$

The units and values used are described in table IV.3. Then the growth of phytoplankton (μ) is calculated following:

$$\mu = \mu_{max} \cdot I_N \cdot I_I \cdot I_T \tag{IV.43}$$

$$I_N = \frac{N}{K_N + N} \tag{IV.44}$$

$$I_I = 2 \cdot (1 + \beta_I) \cdot \frac{x_I}{{x_I}^2 + 2 \cdot \beta_I \cdot x_I + 1} \Rightarrow x_I = \frac{I_z}{I_s} \tag{IV.45}$$

$$I_T = 2 \cdot (1 + \beta_T) \cdot \frac{x_T}{{x_T}^2 + 2 \cdot \beta_T \cdot x_T + 1} \Rightarrow x_T = \frac{T - T_E}{T_S - T_E} \tag{IV.46}$$

Where units and values used are described in table IV.5.

This model of phytoplankton growth include three limitations: by light, by temperature and by nutrients. Variables used for, and result from, this model are presented below.

Table IV.5 – *Units and values used for computing phytoplankton growth μ at depth z*

Parameter	Units	Value
μ_{max}	d^{-1}	2.16
K_N	-	1
N	$\mu g\ L^{-1}$	NO_3 / data from PointB
I_S	ly d^{-1}	200
I_Z	ly d^{-1}	see eq. IV.41
β_I	-	-0.6
T	°C	Temp(z) / data from PointB
T_S	°C	15.5
T_E	°C	11
β_T	-	-0.8

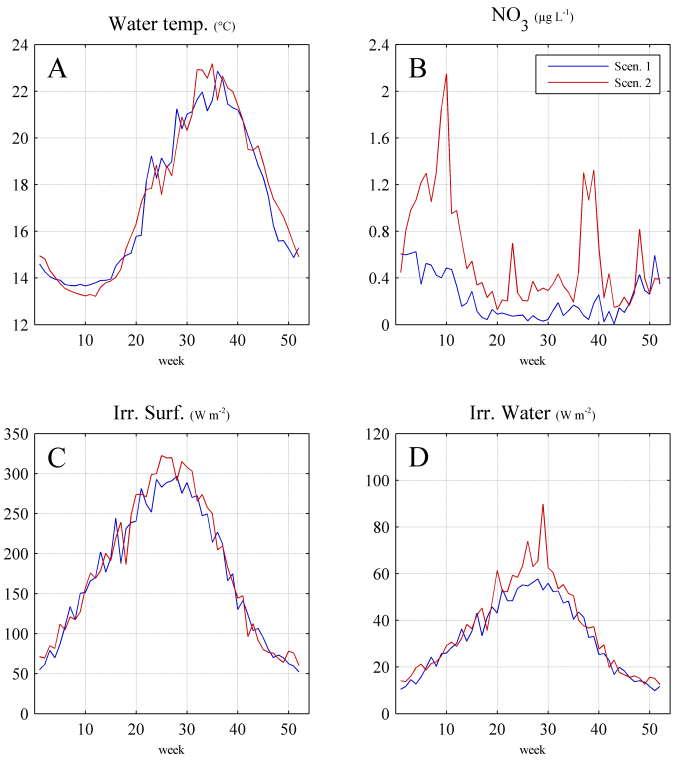

Figure IV.15 – *Data used to compute the phytoplankton growth in the two scenarii (1: years 1996, 1997 and 1998, 2: years 2001, 2003, 2004 and 2005). (A) is the water temperature, (B) the nitrates, (C) the surface irradiation and (D) the irradiation in water computed with eq. IV.41. A, B and D are depth integrated values from surface to 75 m depth.*

IV.4.2 Data presentation

We present here the data used to compute the growth of the phytoplankton, i.e., the nutrients, temperature, light in surface and integrated over the water column (fig. IV.15) during the two scenarii previously mentioned. In fig. IV.16 A the total phytoplankton is presented in biovolume. The conver-

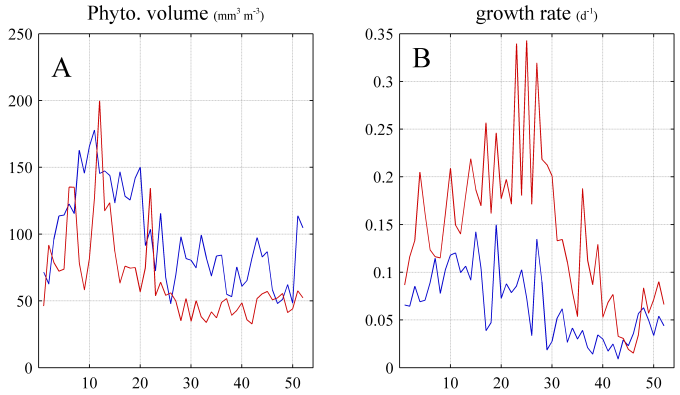

Figure IV.16 – *Phytoplankton biovolume (A) and growth (B) in the two scenarii (1: years 1996, 1997 and 1998, 2: years 2001, 2003, 2004 and 2005). A and B are depth integrated values from surface to 75 m depth.*

sion was made from chlorophyll-*a* using relationships from Jimenez et al. (1987):

$$log(Vol) = \frac{log(chla) - 0.44}{0.66} \tag{IV.47}$$

where *Vol* is in mm^3 m^{-3} and *chla* in mg L^{-1}. Finally, the result, i.e., the growth of phytoplankton for the two scenarii is presented on fig. IV.16 B.

Then data on crustacean dynamics, i.e., the total biovolume and the slope of the N-BSS, is presented on fig. IV.17. These two variables will be compared to the outputs of the model computed on the restricted size range, i.e., from $x_a = -3.44$ and $x_b = 1.95$, which corresponds to 0.032 and 7 mm^3 (see chapter II).

The first scenario (1996, 1997 and 1998) is characterized by lower values of nutrients but also lower values of irradiation. The temperature is higher in scenario 1 during winter time but slightly lower afterward. The total phytoplankton biovolume (and chlorophyll-*a*) is higher in scenario 1 with maximum values from 100 to 150 mm^3 m^{-3} but the modeled growth is lower which corresponds to the findings of chapter III. The growth is the highest from $\approx$ weeks 5 to 25, reaching values around 0.1 d^{-1}, to decrease after to values below 0.05 d^{-1} in summer and autumn. Crustaceans biovolume is maximum around week 20 with values close to 100 mm^3 m^{-3}. The slopes of crustaceans N-BSS first decrease from values close to -1.2 to -1.7/-1.8 — the minimum is observed from weeks 10 to 20. Then the slopes gradually increased to reach -1.2 around week 35.

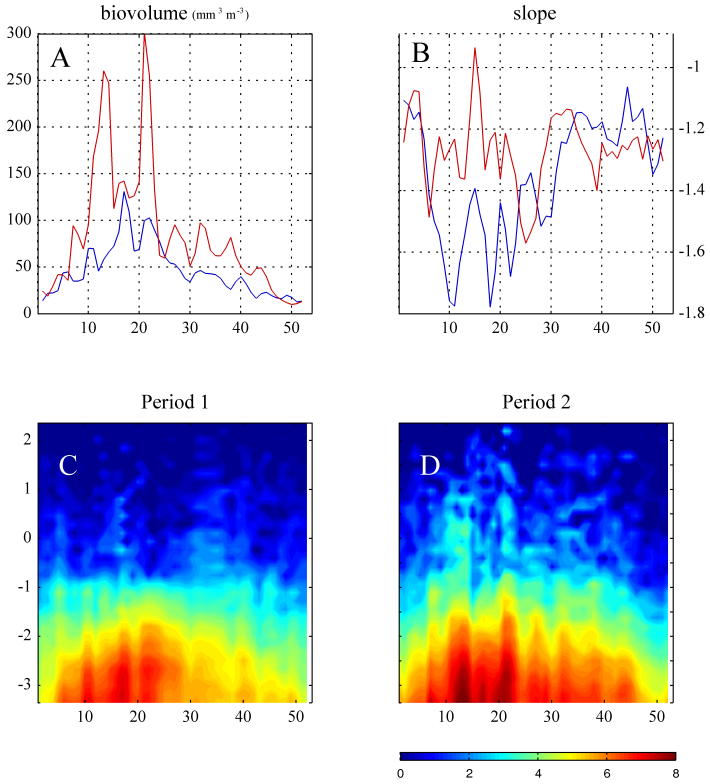

Figure IV.17 – *Crustaceans biovolume (A) and slope (B) in the two scenarii (1: years 1996, 1997 and 1998, 2: years 2001, 2003, 2004 and 2005). C and D represent the observed spectrum for the two scenarii.*

The second scenario (2001, 2003, 2004 and 2005) is characterized by higher values of nutrients and irradiation, lower value of temperature during winter but slightly higher the rest of the year. The total phytoplankton biovolume is lower, yet with short peaks reaching values of the same order (i.e., 150/200 mm^3 m^{-3}). The growth of phytoplankton is higher than during scenario 1 during the whole years, with maximal values of 0.3 d^{-1} from weeks 20 to 30. The maximal growth rate of phytoplankton occurs then almost 15 weeks after the peaks of biovolume. Looking at the crustaceans, the total biovolume reaches values of 250/300 mm^3 m^{-3} from weeks 10 to 25 and is higher than in scenario 1 during the whole year. The crustaceans N-BSS slopes have a less obvious annual cycle with the decrease in spring being less marked (see also chapter III), yet the values during winter and autumn are similar, i.e., around -1.2.

IV.4.3 Comparison with default parameters

First of all, the two scenarii were compared to simulation without changing the values of parameters. Results of the comparison are shown on fig. IV.18 for the first scenario and on fig. IV.19 for the second one. Each figure shows the comparison of the observed and modeled total biovolume, the observed and modeled N-BSS slopes, the phytoplankton biovolume modeled and observed, the biovolume of hatched eggs (i.e., fraction $k_a \cdot (1-k_c) \cdot k_r$), the total lost of biovolume (i.e., unassimilated food $1-k_a$, un-hatched eggs $k_a \cdot (1-k_c) \cdot (1-k_r)$, external mortality), and the modeled N-BSS on the total range. On the last one the size restrictions, i.e., x_a and x_b, are shown. The biovolume and the slopes are calculated on this range for comparison with observations.

For the two scenarii the default parameters underestimate the total biovolume. Yet, for the first scenario the timing of the peak was similar (around day 100). It was not in the second scenario with a late peak (before day 200). This late peak is also in the modeled growth of phytoplankton (fig. IV.16) but not in the observed phytoplankton biovolume. This seems to be due to the high observed values of nitrates at this time which resulted in an increase of the growth in the model, yet this did not seem to occur in observations. This peak occurring between days 150 and 200 may be false, probably due to a too simplistic phytoplankton growth model which does not consider the season and so the composition of the phytoplankton community that changes the specific limitations — nitrates mainly limits diatoms which are present during the spring bloom, dinoflagellates present after may be not limited by nitrates but more by phosphates (e.g., Thingstad et al. 2005, Tanaka et al. 2004).

According to the dynamics of the slope, it is overestimated (flatter spectra) by the model. In the first scenario, the slope oscillates around -1 and does not show the tendency of a global decrease up to day 200. Yet, increases and decreases of the slope seem somewhat to occur at the same timing, for example in days 100, 125, 225 ... In the second scenario the modeled slopes dynamics is more

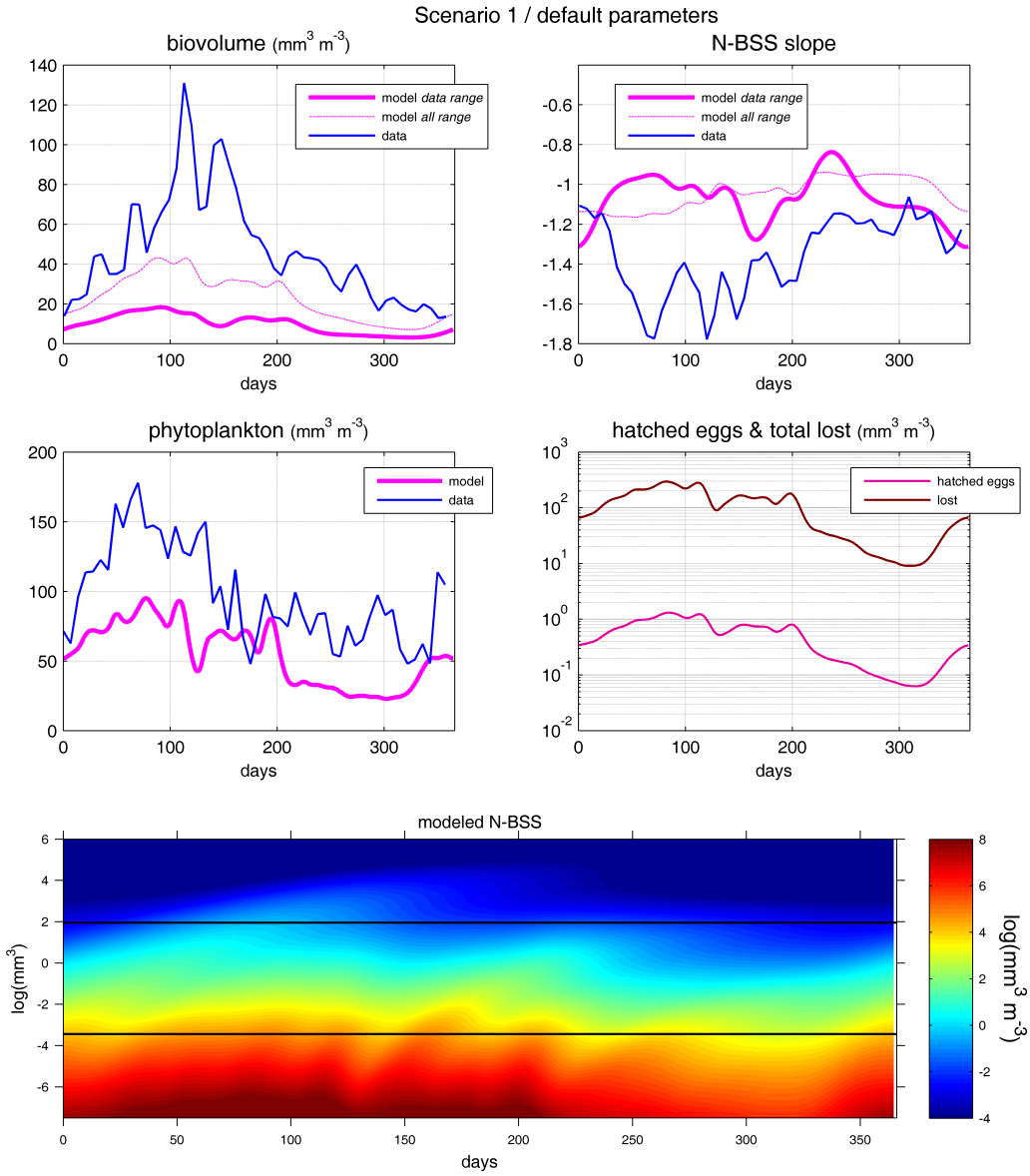

Figure IV.18 – *Comparison of observations and model outputs for the first scenario with default values of parameters, i.e.,* $k_a = 0.4$, $k_c = 0.7$, $\rho = 3.5$, $\sigma = 2$, $\beta_d = 0.75$, $\varepsilon = 0.75$ *and* $T = 360$.

variable, again oscillating around -1 with a certain (slight) tendency to decrease and increase at same periods of the year.

The modeled phytoplankton biovolume appears to be of the same order than the observed one, especially in scenario 1 in which the modeled dynamics is extremely close. For the second scenario, the phytoplankton biovolume is less close to the observed one, especially because of the peak in the

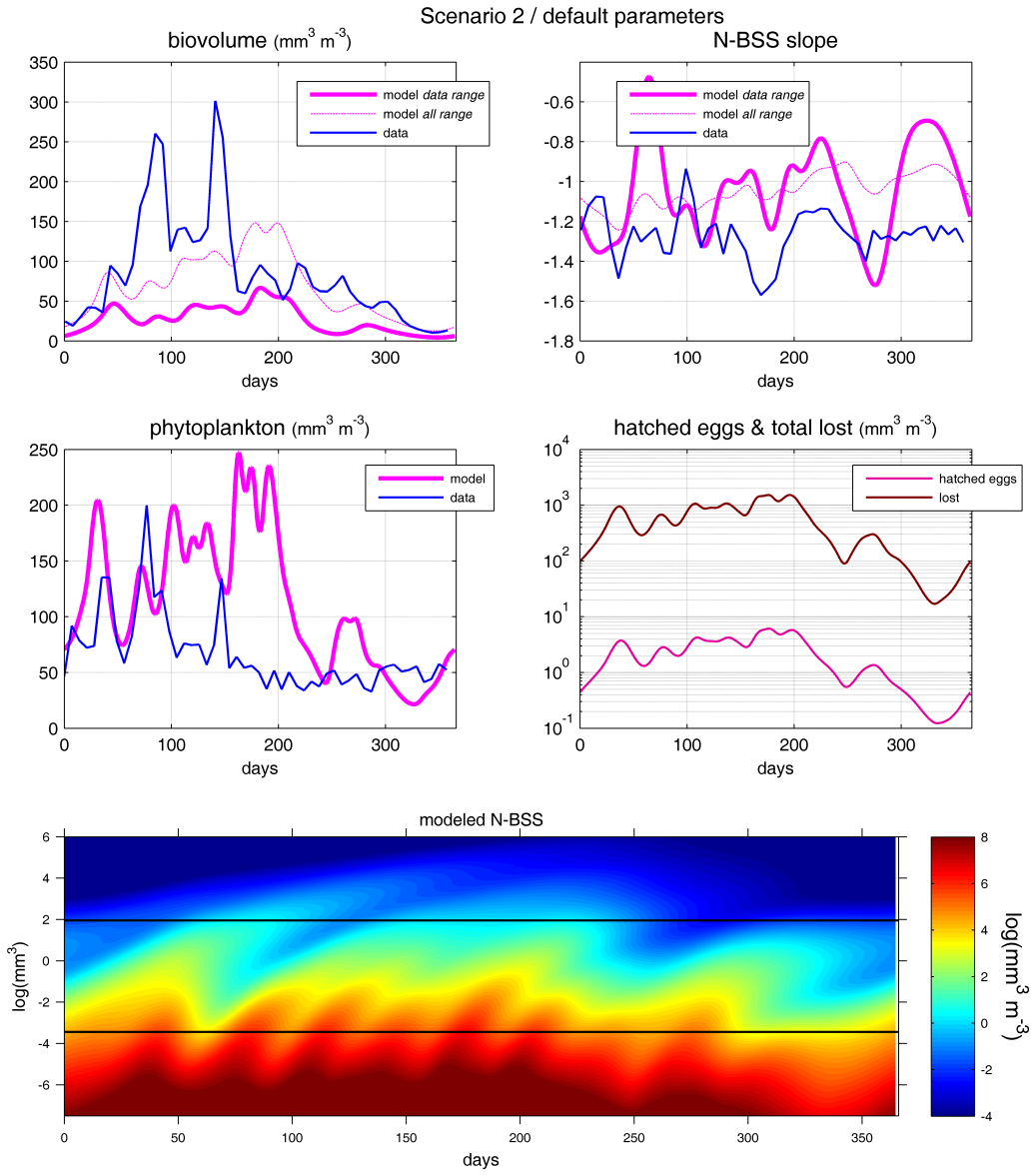

Figure IV.19 – *Comparison of observations and model outputs for the second scenario with default values of parameters, i.e.,* $k_a = 0.4$, $k_c = 0.7$, $\rho = 3.5$, $\sigma = 2$, $\beta_d = 0.75$, $\varepsilon = 0.75$ *and* $T = 360$.

mid-year, already mentioned (see above) as a possible false peak due to some inadequations between the phytoplankton growth model and the observations.

IV.4.4 Preliminary results of optimization

We will now perform a preliminary optimization "by hand". An optimization is currently underway to find the best set of parameters to represent the dynamics of biovolume and slopes. Yet, by explor-

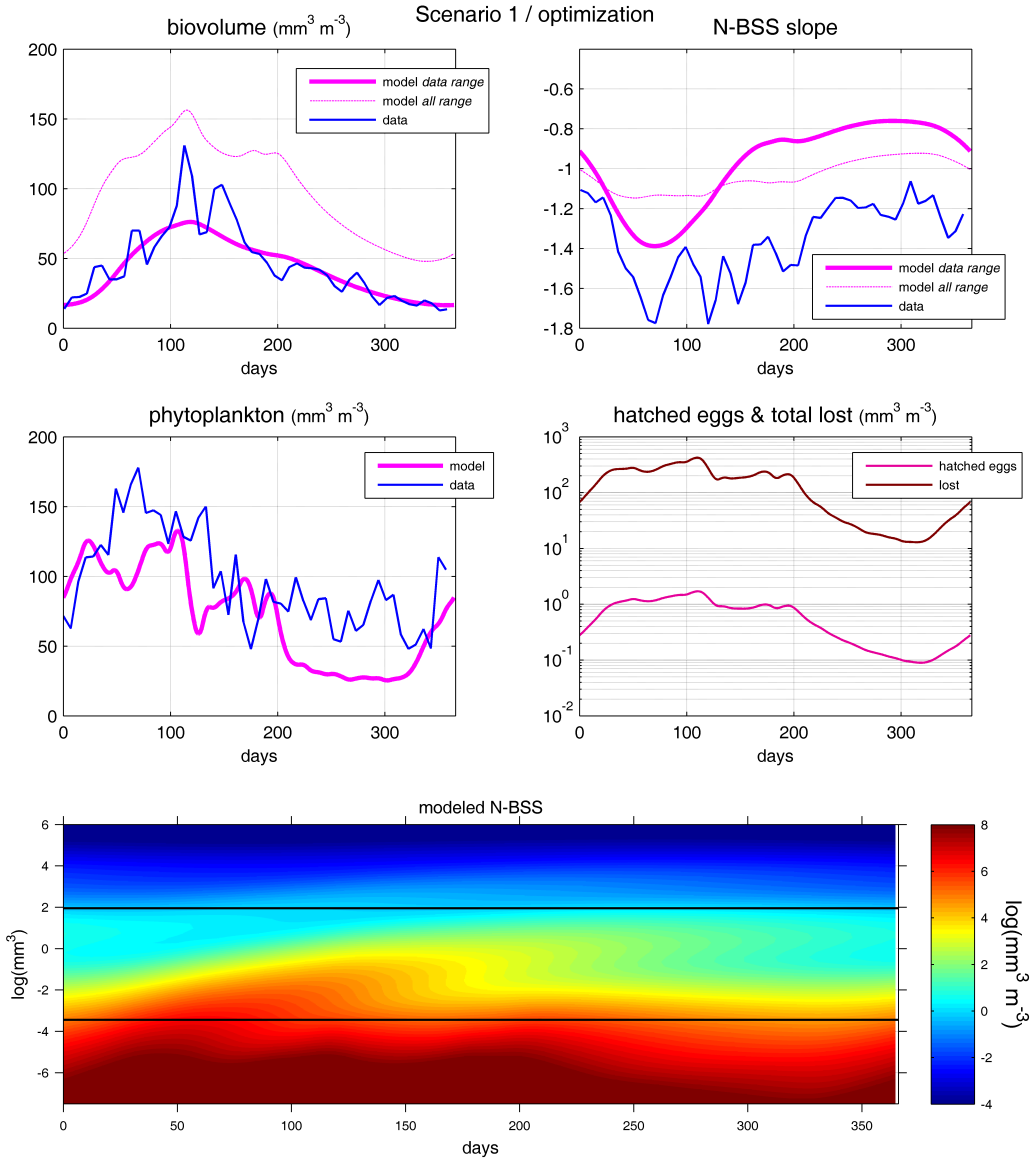

Figure IV.20 – *Comparison of observations and model outputs for the first scenario with a preliminary optimization on parameters which gave* $k_a = 0.4$, $k_c = 0.7$, $\rho = 3.5$, $\sigma = 2$, $\beta_d = 0.75$, $\varepsilon = 0.3$ *and* $T = 1080$.

ing manually the effects of parameters on inputs of the model a set of them was found that gives interesting insights into the comprehension of the model and of the ecosystem.

The best set of parameters that was found is: $k_a = 0.4$, $k_c = 0.7$, $\rho = 3.5$, $\sigma = 2$, $\beta_d = 0.75$, $\varepsilon = 0.3$ ($\searrow 0.45$) and $T = 1080$ ($\nearrow 720$).

We have increased the value of T and decreased the value of ε. The result is shown on fig. IV.20 for the first scenario and on fig. IV.21 for the second one. The same set of parameters is used for both

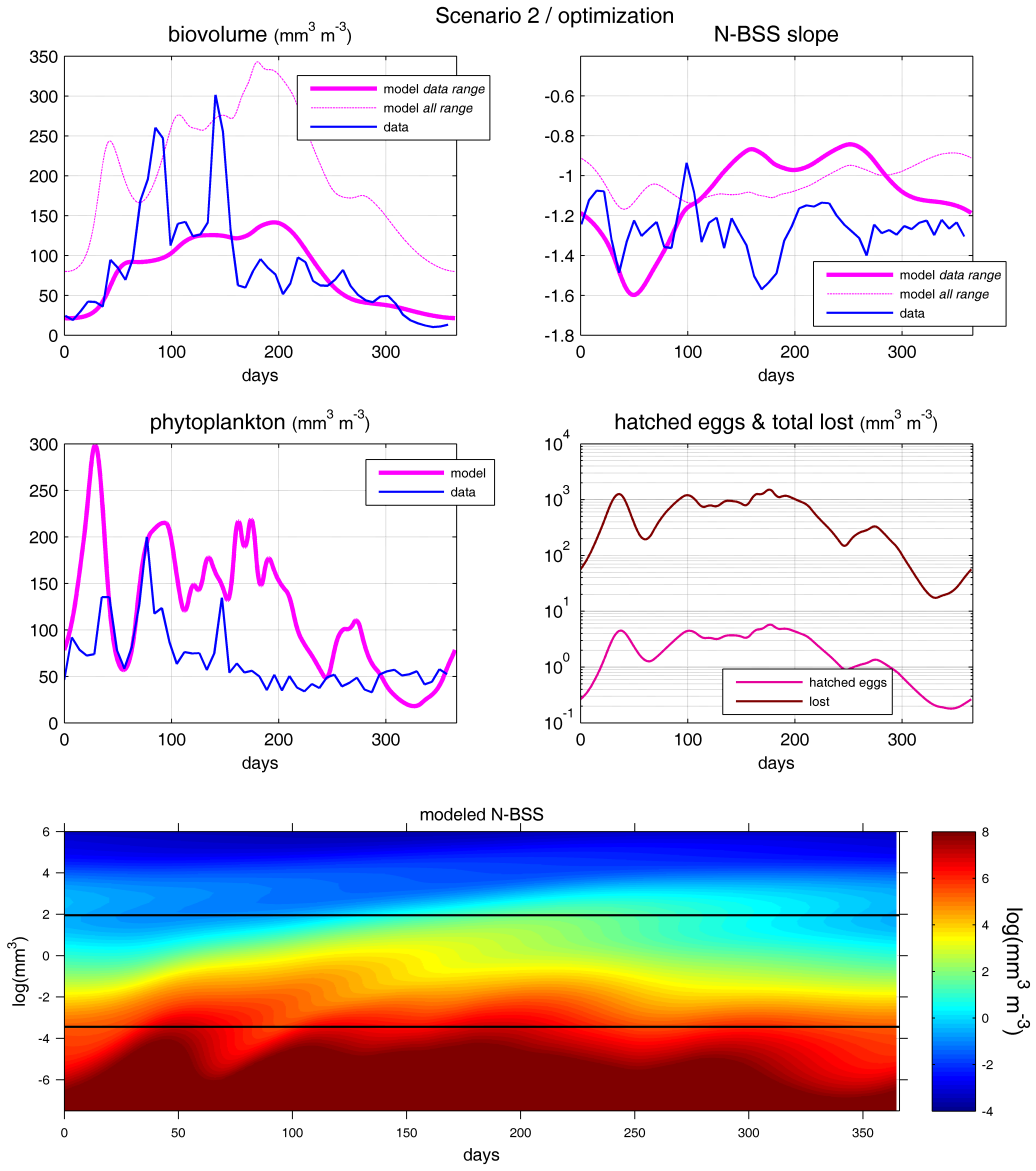

Figure IV.21 – *Comparison of observations and model outputs for the second scenario with a preliminary optimization on parameters which gave* $k_a = 0.4$, $k_c = 0.7$, $\rho = 3.5$, $\sigma = 2$, $\beta_d = 0.75$, $\varepsilon = 0.3$ *and* $T = 1080$.

scenarii, the only change is the input $e(t)$ (fig. IV.16). With these parameters we find one equilibrium, $\beta = -1.0679$ and $\alpha = 4.4942$, $\beta_a = 0.8179$ and $\alpha_a = 0.0238$, $\alpha_d = 0.2290$, $k_r = 0.7521 < 1$ and see fig. IV.22 A for p_p and B for $\mu_e xt$.

For the first scenario, this slight optimization leads to a good representation of the biovolume general dynamics during the year. Values are on the same order, but the high temporal variability and peaks are not represented. The general tendency of the slope is similar with a first decrease from

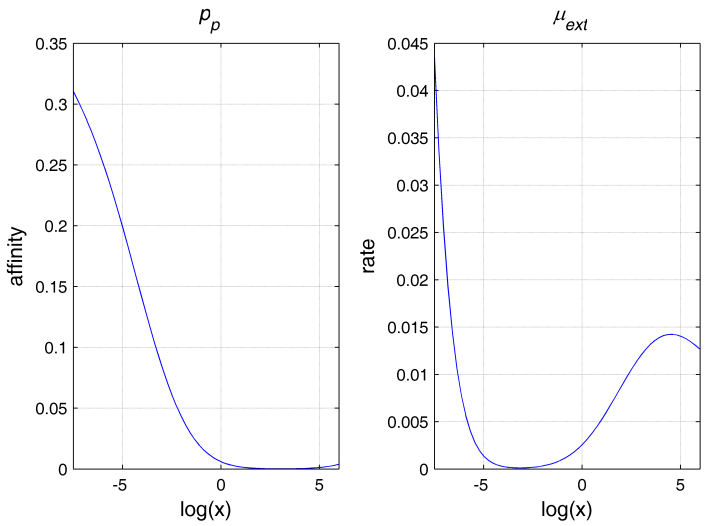

Figure IV.22 – *Value of p_p and μ_{ext} with a preliminary optimization on parameters ($k_a = 0.4$, $k_c = 0.7$, $\rho = 3.5$, $\sigma = 2$, $\beta_d = 0.75$, $\varepsilon = 0.3$ and $T = 1080$).*

days 0 to 150 (minimum $\approx$ day 75) followed by a stabilization. This decrease of slopes lasting $\approx$ 150 days was enabled by the increase of T. Yet the values of the modeled slopes are higher by 0.2 at the beginning of the year and up to 0.4 afterward. Finally, the modeled phytoplankton biovolume is of the same order than the observed one, with yet a different timing of peaks.

In the second scenario, the modeled biovolume has similar values to the observed ones in winter and autumn, but failed in representing the high peaks in spring. Moreover the model is higher in summer around day 200, and as already mentioned this is due to the false peak in modeled growth of phytoplankton because of observed peaks in nitrates. The modeled slopes show again a first decrease at the beginning of the year, the minimum reaches values as low as -1.6 (i.e., lower than in scenario 1) to then peaks at high values (i.e., -0.8). The dynamics is here more variable with a higher amplitude of variation than in scenario 1. Yet, the values of the model are still higher than the observed one (by 0.3/0.4), except at the beginning of the year for which the values are similar. Finally, the modeled phytoplankton is higher than the observed one. The increased zooplankton (crustaceans) biovolume does not result in a global decrease of the phytoplankton one as was observed in chapter III. Yet the preliminary optimization was only made to increase the representation of crustaceans and the only differences between the two scenarii is the input $e(t)$, i.e., the modeled growth of phytoplankton.

IV.5 Conclusion & Perspectives

The main objective of developing a size-based model for zooplankton (here crustaceans) was to explore if this new kinds of models are efficient in representing the dynamics of a zooplankton community, both in term of total biovolume and in term of shape of spectra (i.e., slopes). Several size-based models were already developed but only one was tested with zooplankton data (Zhou et al. 2010). Yet the model of Zhou et al. (2010) has a very different philosophy. This model considers the slopes as inputs and tries to represent the total biovolume of zooplankton. In the location it was tested (Marseille, Coastal Gulf of Lion), they considered the slopes as stationary along the year and so they took a constant value, that was used to compute the mortality in the model. This appears similar to what is currently made in size-based models of fish dynamics (e.g., Andersen & Beyer 2006). Here we based our model on assumptions about physiology and predation and slopes are considered as a result of the model. This is more similar to the philosophy of Baird & Suthers (2007) and Maury et al. (2007a), which however do not compare with observations. A key point of the model is the mathematical choice to compute parameters from others to ensure the model to have an allometric equilibrium. This is necessary for the model to be mathematically exploitable and to decrease the numbers of parameters that need to be fixed to only 7 (compared to 13 without). By taking typical values from literature and changing only two parameters (the time to grow from eggs to maximal size T and the fraction of food ingested on the total available food at equilibrium ε), we are able to fairly well represent the dynamics of the total biovolume and the general shape of the slopes with yet an overestimation. As discussed in Zhou et al. (2010) it is not necessary the model that is false but maybe the measurement methodology itself. We overestimate here the slopes, i.e., there are more large organisms in the model that in observations as compared to small organisms. However it is known that size selection by nets (escape, heterogeneity, scarcity) but also biases from the imaging methodology

(touching objects, estimate of biovolume ... see chapter II) affect more large organisms and so these large organisms are less accurately sampled than smaller ones. It is also due in part to the fact that the comparison was only made on crustaceans. The mean value of crustaceans slopes is -1.3470 whereas it is -1.1443 for the total zooplankton (0.2 higher — less than the overestimation). Nevertheless, these preliminary results show that such models are able to reproduce fairly well the observations with few parameters. Yet, the value of T (3 years) might be too large to be realistic, but until now we have only performed a basic comparison with observations and much work has still to be carried on. First, a complete optimization, using numerical techniques, is currently underway. It will be interesting to see if it is possible to reach good approximations with other changes in the parameters (i.e., with lower values of T). It will also be interesting to perform a different optimization on the two scenariii and to see the main differences between them, if there are some. The next step will then be to improve the quality of the representation of phytoplankton and to use this model to test the effect of nutrients and light limitation on phytoplankton and its impact on zooplankton (see chapter III). The top-down control identified in chapter III of zooplankton on phytoplankton is also an interesting feature of the ecosystem. This is not modeled with the actual set of parameters and formulation, the total phytoplankton being higher in scenario 2 (no anti-correlation between phytoplankton and zooplankton). It will be necessary to identify if it is possible, and in the affirmative, with which sets of parameters. This model has a final aim to be integrated in larger models representing the biogeochemical fluxes of matter (mainly carbon) through ecosystems or production of larger organisms such as fish. To do so it will be necessary to explicitly link this model to higher trophic levels, to the detritus pool but also to the microbial loop. It may also be necessary to simplify the model, to reduce simulation times. A discrete version of the model is currently being developed at the INRIA, it will be interesting to test if the same features are retrieved from a simpler model. This chapter opens up a lot of perspectives and has set up a framework that will be used in future studies.

General discussion and perspectives

V

Along this manuscript, three main issues were investigated, covering different levels of analysis. The first level (chapter II) is the observation one, i.e., which part of the ecosystem we are really observing and analyzing. It deals here with imaging systems, mainly flatbed scanner of zooplankton net samples, and their effects on the observed size spectrum. Main conclusions from this chapter are given below in section V.1. Then, knowing the advantages and limits of our methodology we shifted to the second level of analysis that is the ecological one (chapter III). From available data at the monitoring station Point B (North Ligurian Sea) covering the period 1995-2005 we propose a general scheme of inter-annual fluctuations in this area. Different states of the zooplankton community were found (main conclusions in section V.2). The two major states are then compared to the outputs of a continuous size-based zooplankton model developed in chapter IV, which constitutes the third level of analysis: the modeling. The main conclusions of this part are presented in section V.3. Finally an extension of the zooplankton time series with recent analysis of various nets is presented. The reconstructed time series is 45 years long (from 1966 to 2010) making it one of the longest in the world. In the the light of the findings of previous chapters we will comment this time series and extend findings and expectations for the future of the Ligurian Sea ecosystems (section V.4).

V.1 Measurement of size spectra from imaging methods

In the first chapter (II), we explored the effect of sampling and sample analyzing on the zooplankton size spectra. We have focused on crustaceans, the most locally abundant group and best predicted by automated techniques. A general scheme is presented on fig. V.1. Different biases will affect spectra so we have differentiated spectra at different levels. First, there is the *in situ* spectrum, the one we

want to estimate the most accurately with techniques, time and money constraints. To estimate this spectrum we followed a methodology based on net sampling followed by image acquisition and analysis. The philosophy was here to analyze 22 samples with maximum effort so as to assess the error due to the different biases and hence to determine which steps are necessary since it would be technically impossible to spend this effort on each sample. Among the possible biases we focused on four: the size selection by nets, the impact of touching objects, the efficiency of the automatic classification and the choice of the model to estimate biovolume/biomass. The three latter are directly related to imaging procedure.

The first bias occurs from the *in situ* to the sampled spectrum. Because of the net used there is an underestimation of small and large objects. It is then necessary to study only the size range which is

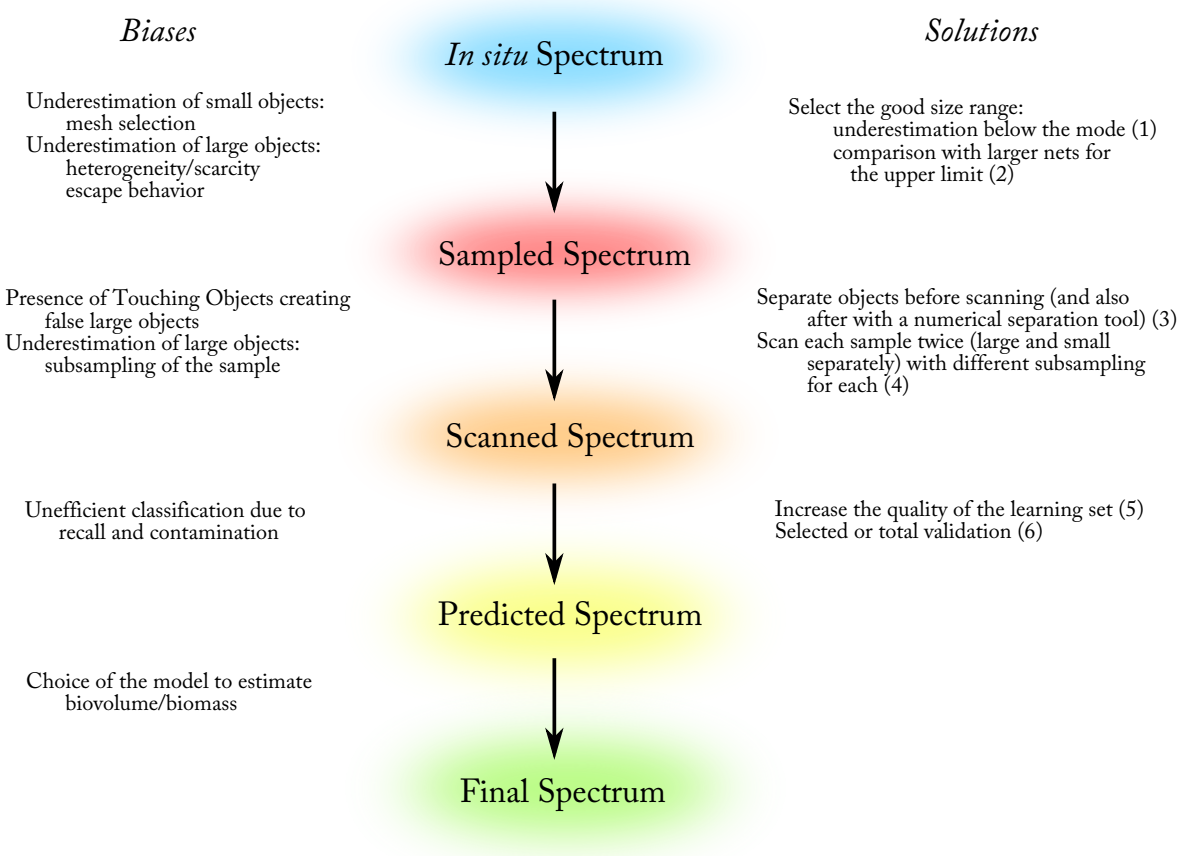

Figure V.1 – *General scheme of biases and solutions in the measurement of zooplankton size spectra. See text for explanation on numbers.*

not underestimated. From Nichols & Thompson (1991) it is known that a net underestimates objects which have a width lower than 4/3 of the mesh size. We tested this relationship and found that the mode of the spectrum was in the size class just above this value. For the WP2 this is 0.032 mm^3 (solution (1) in fig. V.1). For the upper limit, the solution is to compare with a larger net: sampling a higher volume with a larger aperture decreases the possibilities for swimmers to escape and increases the probability to sample large, rare, objects. We compared here the WP2 net to a Régent net and found that the Régent net started giving a higher estimate for sizes of 6.9 mm^3. This is a first estimate of the upper limit of the WP2 net in the bay of Villefranche-sur-Mer (solution (2) in fig. V.1). Yet, this upper limit may be highly sensitive to the composition of zooplankton, their heterogeneity in the field and their abundance (they all change with the seasons), and so is extremely difficult to make an accurate determination. Further comparison with various nets and at different seasons are consequently needed.

The second bias occurs from the sampled spectrum to the scanned one. At this step the sample is spread on a scanning tray and the image is acquired. During this acquisition objects in contact to each other are recognized as a single object. We call "Touching Objects" (TO) these false, larger objects. Their presence modifies the size distribution and thus the spectrum characteristics. The impact of TO was investigated previously with other sizing instruments such as the Optical Plankton Counter (OPC) and is known as the coincidence effect (Sprules et al. 1992; 1998, Woodd-Walker et al. 2000, Liebig et al. 2006). Error due to this effect is relied to the total concentration of objects. It was used by Irigoien et al. (2009) on flatbed scanner. They argued that if the total area covered by the objects on the scanning tray does not exceed 3%, then TO have a negligeable influence. Here we stayed below this level of 3% and tested the effect of touching objects by scanning the sample directly, then after 20 minutes of manual separation and finally, after an *a posteriori* numerical separation tool to decrease again their number. Even below 3%, and without any separation, touching objects have an effect on

the spectrum. This effect is almost eliminated after a prior manual separation on the scanning tray during an average of 20 minutes (solution (3) in fig. V.1). This increases again the processing time but appears necessary to obtain a good estimate of the size spectrum.

The third bias is due to the efficiency of the automatic classification of objects. A strong advance from imaging systems is the possibility to classify objects as a function of their origins (taxonomic group). Looking at a group *A*: the part of objects *A* effectively classified as *A* represents the recall, and the part of objects classified as *A* but which are not *A* represents the contamination. It is necessary to consider both recall and contamination when evaluating the effect of the automatic classification. Yet this was not performed in many studies of this kind (e.g., Bell & Hopcroft 2008, Gislason & Silva 2009, Irigoien et al. 2009). Moreover, the efficiency of the automatic classification was never studied before on size spectrum — it was only tested on whole categories as in Gorsky et al. (2010). We found that by increasing the quality of the learning set it is possible to increase the recall, yet the contamination is more a function of the relative abundance of each group. A group which is not abundant will be strongly affected by contamination from abundant groups — if only 1% of the copepods are badly classified this will be dramatic for some rare groups in which the contamination represents often more than 50%. Results of automatic classification should be taken as it is only for the most abundant groups. This appears to be similar within a group. Poorly abundant size classes, even of the most abundant group, will be affected by contamination. It is then necessary to perform a visual correction of larger objects, here > 0.724 mm^3 (solution (6) in fig. V.1), since increasing the quality of the learning set, which will never be absolutely perfect, will not be enough to decrease the contamination. Moreover, for a taxonomic analysis on the whole community it would be necessary to visually correct all objects (Gorsky et al. 2010).

Finally, we tested the choice of the model to compute individual biovolume/biomass. First we compared the spherical model to the elliptical one, and finally we compared the elliptical model to

a taxon-dependent one of biomass (Hernández-León & Montero 2006, Lehette & Hernández-León 2009). No strong effects are detected, even using a taxon-dependent model. The zooplankton community of the monitoring station is mainly dominated by crustaceans which have similar shapes, regardless of the sizes. No relationships are then found in the community between sizes and shapes, and the differences between taxa in estimating biomass are not sufficient to affect size spectra. This bias should however impact zooplankton communities with strong differences in composition or shape between size classes. The effect was higher with other nets (i.e., the Régent net which is larger and samples more gelatinous) but still not significant.

To have relevant measures of the size of the organisms and thereby the size spectra of the zooplankton community, time to adequately process the sample is required. Following the fastest process, which is no separate scans of large and small objects, no manual separation of objects, no visual correction of automatic classification of presorted samples on a sieve then errors in the estimate of the real shape of the size spectrum will appear. Automatization of some of these steps should be explored in the future, for example the possibility to automatically detect and numerically separate the touching objects, as it is done in other fields (Malpica et al. 1997, Korath et al. 2008), or to continue to increase the quality of automatic classification methods to facilitate the correction. Nevertheless, imaging systems, with their limits, appear to be rapid and efficient tools to study both the taxonomic and the size distribution of communities.

V.2 Fluctuations of the Ligurian Sea ecosystem

The aim of chapter III was to explore the relations between zooplankton and its environment by using available datasets of the bay of Villefranche-sur-Mer monitoring station (Point B). We analyzed the weekly sampled 1995-2005 time series, period with the most available data. For the environment we used data from the CTD sonde: water temperature, salinity and density from surface to 80 m depth;

from Niskin bottles at six depths (surface up to 75 m depth): nitrates, phosphates, silicates, chlorophyll-*a* and suspended particles (data from Coulter Counter, particles from $\approx$ 3 to 90 μm); from the meteorological station Sémaphore (1.2 km away from Point B): air temperature, precipitation and irradiation. We also used time series of global climate indicators, and also hydrological data from another monitoring station in the central Ligurian Sea, Dyfamed. For the zooplankton we used data from the WP2 net (200 μm meshsize, 0.25 m^2 mouth opening), trawled vertically from 60 m depth to the surface. Samples were analyzed following the ZooScan methodology and automatic classification (see chapter II). Large objects, larger than 0.724 mm^3, were visually corrected and classified into 9 taxonomic categories. With small copepods automatically classified this made a total of 10 categories. In addition to these taxonomic groups the total zooplankton biovolume and abundance were taken. Finally, the crustaceans size spectra were analyzed: slopes, mean size and the determination coefficient of the linear fitting.

We found that the predicted trend toward more oligotrophy in the Ligurian Sea did not yet occur. This trend was suggested from the analysis of zooplankton time series ending in early '90s (Molinero et al. 2005; 2008, at Point B) and was assumed to be due to rising temperature and earlier stratification in the year. We showed that low abundances of zooplankton observed here from 1995 to 1999 shifted in 2000 toward higher abundances of almost all categories — a time lag of $\approx$ one/two years being observed for some large zooplankton groups. This recovery of the ecosystem trophic state was not due to later stratifications or to a global increase of temperature. It was more likely due to an increase in the strength of the winter convection and to high irradiation in spring / summer. We stress here the importance of the winter climate in determining the state of the ecosystem. Two major meteorological features are implicated in the winter convection: the air temperature and precipitations, both during the wet Mediterranean season, i.e., from $\approx$ November to March. Low temperature and low precipitations act on the water surface temperature and salinity and increase the surface density. Vice-

versa as for high temperature and high precipitations. A high surface density increases the convection and, by a chain reaction, increases the winter mixing, nutrients replenishment, phytoplankton and zooplankton growths. The ecosystem seems then to be determined by a strong "bottom-up" control. Air temperature and precipitations in winter varied almost together during the 11-years of the survey, showing a strong correlation. In addition to the winter forcing, another major meteorological forcing was detected: the spring / summer irradiation. It varied most of the years in the same direction as the winter convection except for 1995, 1999 and 2001. The first two showing high winter convection but low spring / summer irradiation, and the opposite for year 2001. In these three cases the winter initiation was reversed. We hypothesized that the irradiation in spring / summer act on phytoplankton growth by determining its light limitation in spring / summer. It is however impossible for the moment to test this hypothesis. Other ones are possible, e.g., an indirect effect on stratification due to sunnier weather leading to a more stable water column, in this case the stratification is beneficial for zooplankton (possible optimum stratification).

Comparisons made with the central Ligurian Sea (Dyfamed) and with global climate indicators gave interesting insights. Trends in salinity and density at Point B and Dyfamed during winters are strongly correlated. The correlation with temperatures is weaker. Moreover, on a longer period (1960-2008) significant correlations appear between global climatic indicators (mainly NAO and NHT) and salinity and precipitations trends during winter, but not with winter temperature and density. It seems that precipitations and salinities — strongly linked — are affected by more basin scale forcings than temperature is. Temperature may be more likely affected by local factors. It is then impossible to rely linearly global climate indicators to the productivity of the ecosystem. The three main climatic factors that we hypothesized to play a role on the determination of the state of the ecosystem act together, and what is important is their combination. Three factors having two possible states will drive to eight possibilities: this makes the response of the ecosystem strongly non-linear and may explain why none

of them is significantly linked or is clearly isolated by statistical techniques. Longer time series will be needed to use non-linear approaches. Nevertheless, on a longer scale, constant changes on one of them (or more) is likely to affect the ecosystem. The winter salinity have increased together with the NHT and the NAO. If NHT and NAO continue to increase, then this is likely to increase the occurrence of strong convection in the future. This aspect will be discussed later in section V.4.

Going back to the local scale, Point B, another extremely interesting result is the clear opposite trend in chlorophyll-*a* compared to nitrates and zooplankton that suggests that grazers exert a strong "top-down" control on the phytoplankton observed at the inter-annual time scale. This strong "top-down" control seems to be due to the co-existence of both copepods and filter-feeders (tunicates) from 2001 to 2005 (see Sommer 2008, for explanation and examples of this kind of trophic cascades). In chapter IV we used a model of phytoplankton growth (Andersen & Nival 1988), and taken data on nitrates, temperatures and irradiation, it appeared that the growth of phytoplankton was higher when its total biomass (chlorophyll-*a*) was lower. Such an opposite relation was recently discussed by Behrenfeld (2010) in the explanation of the initiation of phytoplankton spring blooms in the North Atlantic. He jeopardized the Sverdrup's hypothesis on critical depth, arguing (among other) that it did not consider the grazing pressure. Here, we are in the same direction, the total chlorophyll-*a* may not be an efficient indicator of the productivity of an ecosystem, at least for the area studied. This gives also insight in the "Mediterranean paradox" that biomass of higher trophic levels are higher than expected from chlorophyll-*a* measurements only (Fiorentini et al. 1997, Estrada 1996, Siokou-Frangou et al. 2010). This has strong implications for the vision of the Ligurian Sea productivity and mitigates the concept of its central highly productive zone and coastal deserts (e.g., Nezlin et al. 2004, Barale et al. 2008, D'Ortenzio & d'Alcala 2009). Coastal zooplankton may be important in controlling the phytoplankton. It also questions suggested trends toward oligotrophication of the Mediterranean Sea inferred from chlorophyll-*a* analysis (e.g., Barale et al. 2008, Mozetic et al. 2010, Steinacher et al.

2010) at least for some coastal areas. This strongly highlights the need of considering zooplankton when studying marine ecosystems.

A global scheme of the links between climatic, hydrological and biological variables is presented on fig. V.2 as a global resume of the previously mentioned findings.

Our analysis was however not exhaustive and missed highly relevant parts of the ecosystem. The first one being the non-availability of data on microplankton, which are known to play a major role as grazers of phytoplankton, food for copepods (small copepods being mainly microplanktonophage in the bay of Villefranche-sur-Mer) and in the microbial loop for the recycling of nutrients (e.g.,

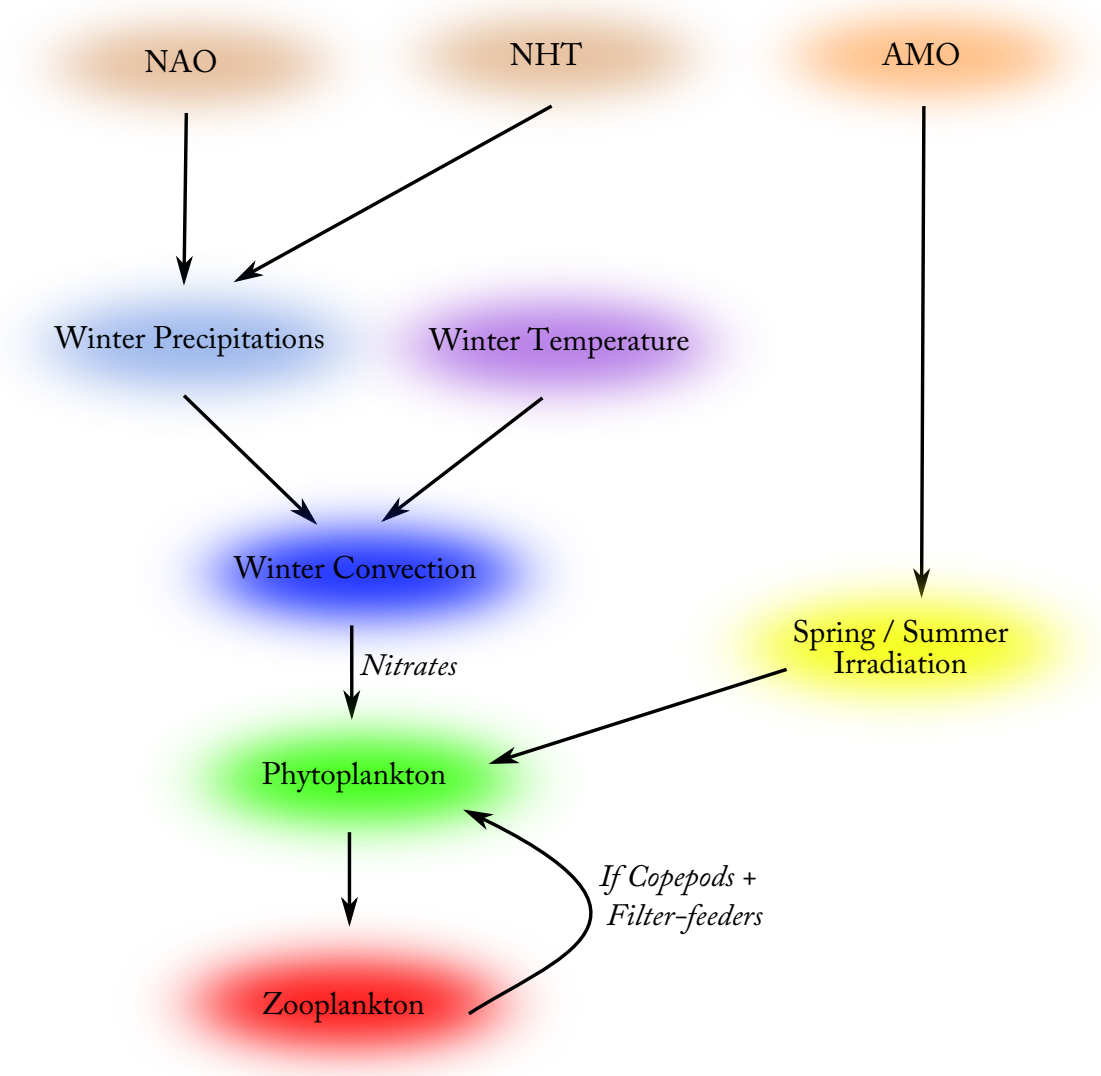

Figure V.2 – *General scheme of links between climate, hydrology and biology in the Ligurian Sea from present findings. NAO is for North Atlantic Oscillation, NHT for Northern Hemisphere Temperature and AMO for Atlantic Multidecadal Oscillation.*

Thingstad et al. 2005). Then, the phytoplankton was only described using chlorophyll-*a*, no long-term data being available on its taxonomic composition. From Marty & Chiavérini (2010) we know that around ca. 2000 the dominance of diatoms increased in Dyfamed (especially during the spring bloom), yet we do not have this information at Point B. We do not have either *in situ* data about the phytoplankton growth rate and its limitation which is strongly needed to validate our hypothesis. Another relevant compartment to have data on is the higher trophic levels such as fish and medusæ. We do not know if they exert a "top-down" control on zooplankton (as zooplankton do on phytoplankton) and we do not clearly know their response to the increase of periods of mesotrophy. From observations made on the bay of Villefranche-sur-Mer by divers, generally non-scientific, it seems that total abundance of fish and medusæ have increased (Goy 1997, for medusæ). Yet, it may not be beneficial for all species. This is also true for the zooplankton, and even if we have observed a positive response of all groups, there is a needed to classify these groups in more details to look at the species levels. Exhaustive "end-to-end" analyses of Ligurian Sea ecosystems are needed for the future.

V.3 Size-based modeling

As compared to the previous chapters, the work carried out on modeling is more preliminary. In this chapter (IV) a size-based model of zooplankton dynamics is developed. It is the result of a collaboration initiated with a mathematicians team of the INRIA lab in Sophia-Antipolis. The main aims of developing a model were to explore possible ways of improving the representation of zooplankton in models since it is often a critical point (Skliris et al. 2001, Holt et al. 2005, Lewis et al. 2006, Allen et al. 2007, Petihakis et al. 2009) and to run the model with locally measured data to test the assumptions made on the functioning of zooplankton, especially assumptions on growth and predation.

Structuring the zooplankton community only by its size was chosen for several reasons, notably the fact that many physiological and inter-individuals processes scale with the size of zooplankton

individuals (e.g., Brown et al. 2004, Glazier 2005, Saiz & Calbet 2007), that considering only a size structuration will reduce the number of parameters compared to a taxa-based structuration, and that it allows a complex dynamics. Such models were previously developed for zooplankton by Baird & Suthers (2007), Maury et al. (2007a) and Zhou et al. (2010), yet only the later made a direct comparison with data. The model developed here is mostly inspired by the one of Maury et al. (2007a) but also by a model made by Benoît & Rochet (2004) on fish. The present model appears more simple than the previous ones.

This present model is a continuous size-based model of zooplankton dynamics, i.e., the formulation does not consider size classes. The entry of the model is the energy created by the phytoplankton (the growth rate) and the output is the size spectrum of the zooplankton on which we measured the integrate (the total biovolume) and the log-linear slope, a relevant ecological measure used in previous chapters and in many zooplankton studies. This makes the model different from the one of Zhou et al. (2010) on which the log-linear slope of the zooplankton size spectrum is considered as an entry. From the growth of phytoplankton to the structuration by size of the zooplankton different processes are included: grazing, predation, growth, external mortality and reproduction. For the grazing an affinity coefficient is defined and is a function of the size of zooplankton, according to it certain size of zooplankton will grazed on phytoplankton. Then, for the predation, an affinity coefficient is also defined and depends on the predator and prey sizes. It is represented as a Gaussian in the log-scale which is centered on an average predator/prey size ratio and has a constant variance. These two affinity coefficients apply to the quantity of phytoplankton and zooplankton determine the total quantity of food a zooplankton of a certain size can prey upon. Yet physiological constraints were added. This part was in some way inspired by the DEB theory (Kooijman 2001). To the total available quantity of food only a part will be ingested; this is determined by a maximum volume zooplankton can sample per day and by a maximum quantity of food zooplankton can ingest per day. This leads to an Holling

type II relationship between the available and the ingested quantities of food. On this ingested food, a fraction is assimilated whereas the other is lost (detritus production), and on the assimilated fraction another fraction is devoted to growth whereas the other is for reproduction. The fraction used for growth enables zooplankton to increase their sizes. The fraction used for reproduction is injected at the left border (smallest size) of the spectrum to represent an egg pool on which a hatching success is applied. In addition an external mortality, representing predation by higher trophic levels is added to the system.

A key point of the model is the use of a particular mathematical case to ensure some mathematical properties and to reduce the number of parameters that need to be set. The particular case is called the "infinite case" on which the spectrum is infinite in both directions. In this case there is no phytoplankton and no external mortality: we extend the predation formulation to infinity and then predation upon the extended left side is used to calculate the grazing affinity. It is similar to the right side of the spectrum on which the predation by the right extent (up to infinity) is used to compute the external mortality rates. By looking at solutions for an allometric equilibrium we reduce the number of parameters from 13 to 7 and ensure the model to have an allometric equilibrium.

The comparison with data was made on the two main scenarii identified in the previous chapter, i.e., low zooplankton (years 1996, 1997 and 1998) and high zooplankton (years 2001, 2003, 2004 and 2005). To compute the entry of the model, i.e., the growth rate of phytoplankton, we used the model of Andersen & Nival (1988) made for the same location. It was not possible, as was done by Zhou et al. (2010), to use directly the chlorophyll-*a* values since we have suggested a strong effect of grazing, due to coexistence of copepods and tunicates, that made this variable not representative of the trophic state of the local ecosystem. Only a basic optimization has been performed up to now. It appears that by changing only two parameters from their typical values obtained from literature we are able to represent fairly well the observed dynamics of the zooplankton in the two main scenarii,

notably a particular seasonal shape of the dynamics of the slopes as well as the seasonality of total biovolume of zooplankton. This tends to confirm that size-based models of zooplankton are efficient tools to represent realistic and complex dynamics with a limited number of parameters.

This chapter is only preliminary but opens a lot of perspectives for future studies on zooplankton size-spectra in response to climate changes. Among them the most immediate and already underway is to perform a complete optimization on the two scenarii. This will give us relevant indications on the physiological properties of the zooplankton community in the studied location and also between both scenarii. Notably if it necessary to change the parametrization of the model or if the change in the growth rate of phytoplankton is sufficient to explain the observed differences. This optimization is strongly needed for the future use of the model as a tool to infer poorly known mechanisms of the ecosystem such as the detritus production.

V.4 Horizon: Insights from past and expectations for future evolutions of the Ligurian Sea pelagic ecosystems

In this part we present some recently analyzed data on zooplankton in the bay of Villefranche-sur-Mer, extending the time series from 1966 to 2010. These 45 years of zooplankton data make this time series one of the longest in the world — see the SCOR WG125 wg125.net. The 45 years time series is made from four different time series, methodological aspects of this cumulation is presented in annexe B. Here we will only present this final time series, for copepods only. It stands for the moment as a first comparison, all future discussions and hypotheses must be taken cautiously. Conceptual schematics which raised up mainly from chapter III will then help us toward some debates on possible futures for Ligurian Sea ecosystems based on past evolutions. This part needs to be viewed as an extension and deepening of conclusions previously made based on assumptions and extrapolations.

Within this frame, and with respect to future validations that will be made on the data, few things

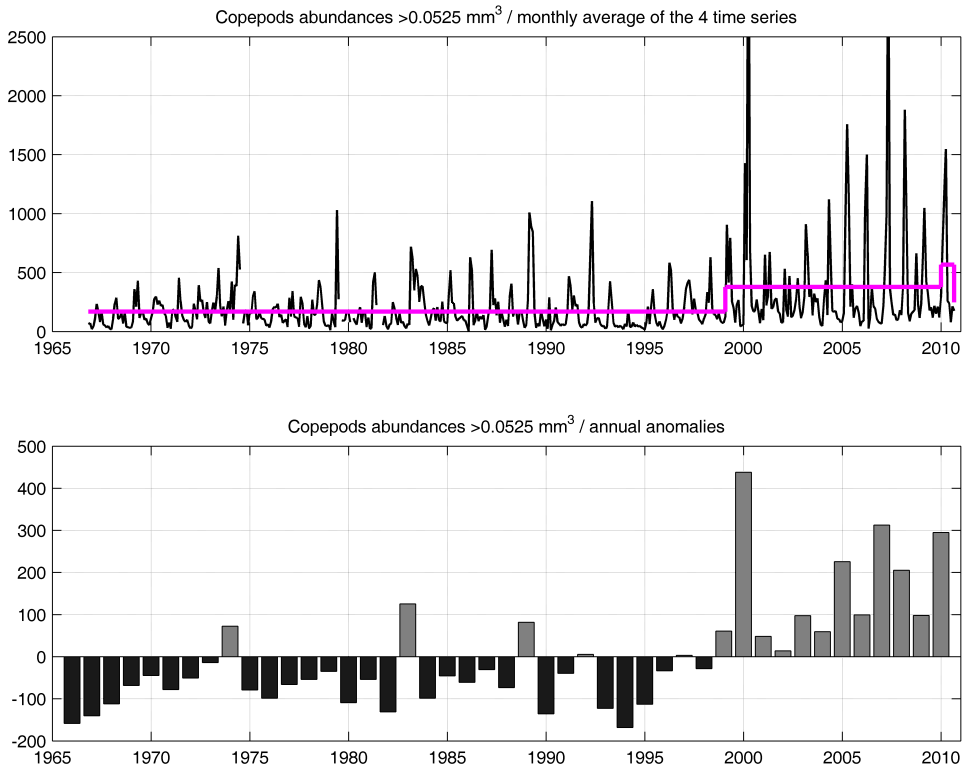

Figure V.3 – *Monthly average of copepods abundances of all time series from 1966 to 2010, see fig. B.3. The first graph shows the monthly values of the new composite time series together with the application of the STARS methods to detect shifts (see chapter III). The second graph shows annual anomalies of copepods abundances.*

are observed that give interesting insights in the long-term dynamics of Ligurian Sea ecosystems. We present only here the dynamics of copepods, yet it was observed in this thesis on the period 1995-2005, and in Garcia-Comas et al. (Submitted) on the period 1974-2003 that groups tend to vary together, with a time lag between small and large. Copepods represent the most abundant group and can be used as an indicator of the quantity of zooplankton in the ecosystem. The first thing that appears is the strong increase of copepods abundances from 1999/2000 in both nets and both sampling strategies, reaching abundances far higher than every year before. Year 2000 is the highest of the 45 years of copepods abundances. On a log scale, this increase occurs early, i.e., ca. 1996, and the years 2000 and 2008 are the highest (2010 is not complete). The log scale is more efficient to detect changes in the baseline and not only in the amplitude of peaks since it reduces ratio between large and small values. On this log scale, we observe a first increase in the first half of the ’70s, then a decrease

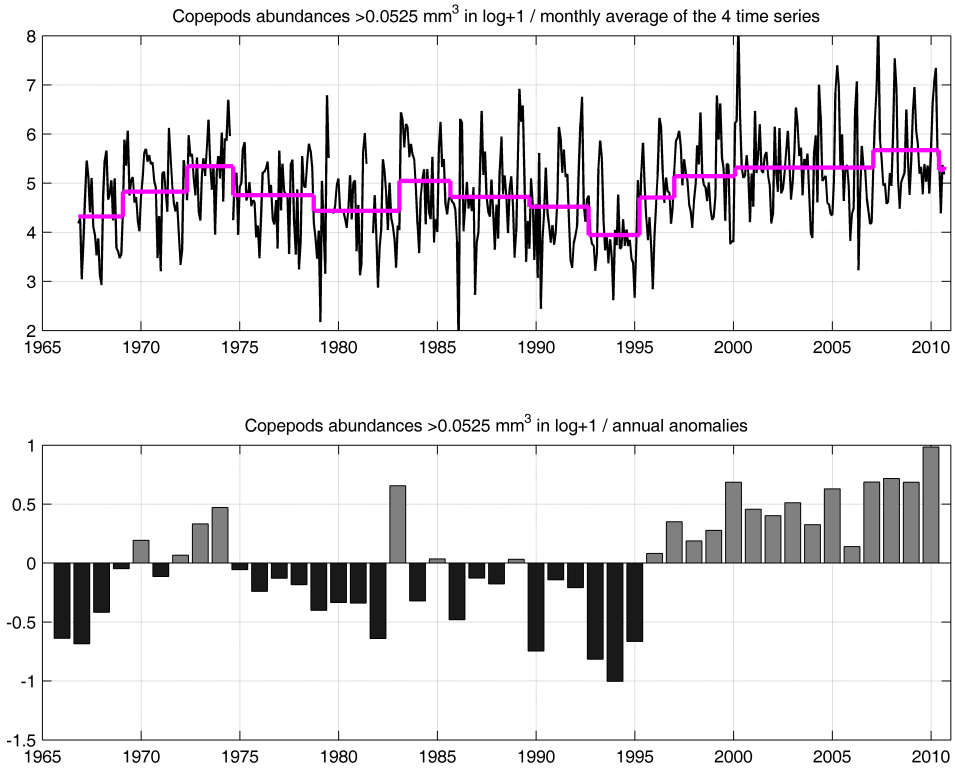

Figure V.4 – *Same as in fig. V.3 but on log(abundances +1).*

followed by higher values in the mid '80s — corresponding to what was observed in Garcia-Comas et al. (Submitted) — but nothing comparable to the high values observed in the last 10/14 years.

Looking at the correlations that were identified in chapter III with hydrology and climatic indicators from 1960 to 2008 (AMO, NAO and NHT), we tested these climatic indicators over the 45 years of copepods. Abundances anomalies in normal scale are significantly correlated (using Pearson correlations) to AMO (r_p=0.455, p=0.002), to NAO (r_p=0.351, p=0.021) and to NHT (r_p=0.543, p <0.001). The log of abundances anomalies are only significantly correlated to AMO (r_p=0.402, p=0.008) and to NHT (r_p=0.435, p=0.004), the correlation with the NAO is not any more significant (r_p=0.169, p=0.279). The main implications in the previously mentioned findings are:

- The refutation made in chapter III and in Garcia-Comas et al. (Submitted) of the oligotrophy that was predicted to occur from the '90s by Molinero et al. (2005; 2008) is confirmed. The ecosystem recovers the state before the '90s and exceeds previous values. The last decade is

the highest ever observed in the bay of Villefranche-sur-Mer for 45 years in terms of copepods abundance and probably of other groups according to the parallelism reported in this thesis.

- In Garcia-Comas et al. (Submitted) a quasi decadal oscillation was proposed between rich and poor periods of zooplankton abundances. Yet, even if an oscillation is observed (mainly on the log scale), it is not comparable to the global increase that has occurred from the late '90s.

- From previous studies, the NAO was suggested as a main forcing on Ligurian Sea ecosystems (e.g., Gomez & Gorsky 2003, Molinero et al. 2005; 2008, Garcia-Comas et al. Submitted, Conversi et al. 2010), yet, even if some links were found between the NAO and variables of the ecosystem, on a long-term scale the influence of the NAO is less than the ones of the AMO and of the NHT which seems to have a major impact on the ecosystem.

The mechanistic links between the AMO/NHT and the ecosystem will then be a key to understand the past and actual functioning, and to try to predict the possible futures of the Ligurian Sea pelagic ecosystems. The AMO and the NHT have different implications. The AMO is known to influence the frequency of summer heat waves in Europe (Sutton & Hodson 2005, Msadek & Frankignoul 2009) and was here significantly correlated to the spring / summer irradiation, whereas the NHT was significantly linked to winter precipitations (negative correlation) and to winter salinities (positive correlation).

The AMO shows an oscillation between positive and negative values, each period lasting 20 to 30 years. The last negative period occurred from $\approx$ 1964 to 1996/1998 then we have been in the positive period since 1995. This corresponds strongly to the change in copepods abundances observed on the log scale. Sadly the time series started at the beginning of the negative period and we do not have any observation of zooplankton in the last positive period that occurred from $\approx$ 1926 to 1963. It is then not possible for the moment to know if the quantity of zooplankton, or the trophic state of the ecosystem,

was at the same level before 1963 and after 1998. This will be a key question to discriminate the effect of the AMO and so of the spring / summer irradiation, together with the effect of the NHT but also NAO (winter climate). A possibility that may be explored to get an idea of the trophic state before 1963 is to look it up in the biological archives. In other locations, like in the bay of Brest, France, estimates of daily and yearly growths of bivalves (e.g., *Pecten maximus*), "printed" in their shells, were related to environmental conditions and the global present and past trophic states of the ecosystem (Chauvaud et al. 1998; 2005). In the bay of Villefranche-sur-Mer we have the noble pen shell, *Pinna nobilis*, which is the second largest bivalve in the world: it can reach a length of about 1 meter with a longevity of more than 20 years and is planktonophage (pinnanobilis.free.fr). It is a possibility, by studying dead shells, to go back in the past and have an idea of the trophic state of the Ligurian Sea pelagic ecosystems in the last positive phase of AMO.

Mechanistic links between the NHT and the ecosystem may be more indirect. On the studied period the NHT has increased and was then related to the observed increase in winter salinities and decrease in winter precipitations. Yet, these two features were also linked to the NAO, which showed also a tendency to increase in these last 45 years. Other changes, like the decrease of river run-off due to damming (Skliris et al. 2007), are related to the increase of salinities (but not of precipitations). It is a question of the relative importance of the winter forcing and of the spring / summer forcing. During the last 45 years these two forcings have followed a similar trend. Yet, their future trends may be strongly different. Where the NHT and maybe the NAO are expected to increase (IPCC 2007, Woollings et al. 2010), there is no indications of possible increase of positive phases of the AMO, and so it should retrieve its negative phase within 15 to 20 years.

This, with other previously mentioned key points, raise some questions that we cannot be answered at the moment. First, directly from the preceding paragraphs, there is a question on the exact link between the AMO, so the spring / summer climate, and the ecosystem, and of its relative im-

portance in the long-term compared to the winter forcing. In this thesis we made the hypothesis of an enhanced phytoplankton growth due to more light. Yet, the spring / summer irradiation can also act on other parts of the ecosystem, directly on zooplankton or on the hydrodynamics (stratification). Measures of phytoplankton *in situ* growth will be needed to test the hypothesis of the light limitation. On the long-term dynamics, the relative importance of the spring / summer irradiation compared to the winter climate is difficult to test since they followed similar trends. Yet, over the detailed 11 years study it appears that the three times when a conflict occurred, the spring / summer irradiation seemed to have outcompeted the winter initiation of the ecosystem (years 1995, 1999 and 2001). It will be however essential to get proxies or approximation of the ecosystem productivity before 1963 as it is possible by looking in biological archives. Other questions that will also have to be answered are the impact of the observed increase toward mesotrophy at the species level and also on higher trophic levels (e.g., on *Pelagia noctiluca*), the linearity of the response of the ecosystem to this increase (is there an optimum? see discussion in chapter III.4.4 about year 2005), the impact on lower trophic levels (microzooplankton) and on the composition of the phytoplankton ...

From this we can however make an attempt to forecast possible state of the Ligurian Sea pelagic ecosystem. In the next decade it is strongly probable that the salinity will continue to increase and that the AMO will stay high. In this case it is likely that the productivity will continue to increase leading to an increase of the zooplankton, and possibly of the jellyfish *Pelagia noctiluca* which are reported to be strongly abundant since ca. 2001. The effect on fish will have to be studied. Then, in more than 15/20 years, with the expected decrease of AMO and probably of the spring / summer irradiation, it is possible that the ecosystem productivity will decrease. Yet, salinities but also temperatures will be higher (if the trend continues) than before 2000, and so the productivity will possibly stay higher than before 2000. Will the ecosystem continue to respond linearly to increase in productivity? Or will

we observe an inhibition? What will be the impact on communities diversity and on higher trophic levels? These are key questions for the future of the Ligurian Sea pelagic ecosystems.

Appendix

RAW GRAPHICS OF DATA USED IN CHAPTER III

A

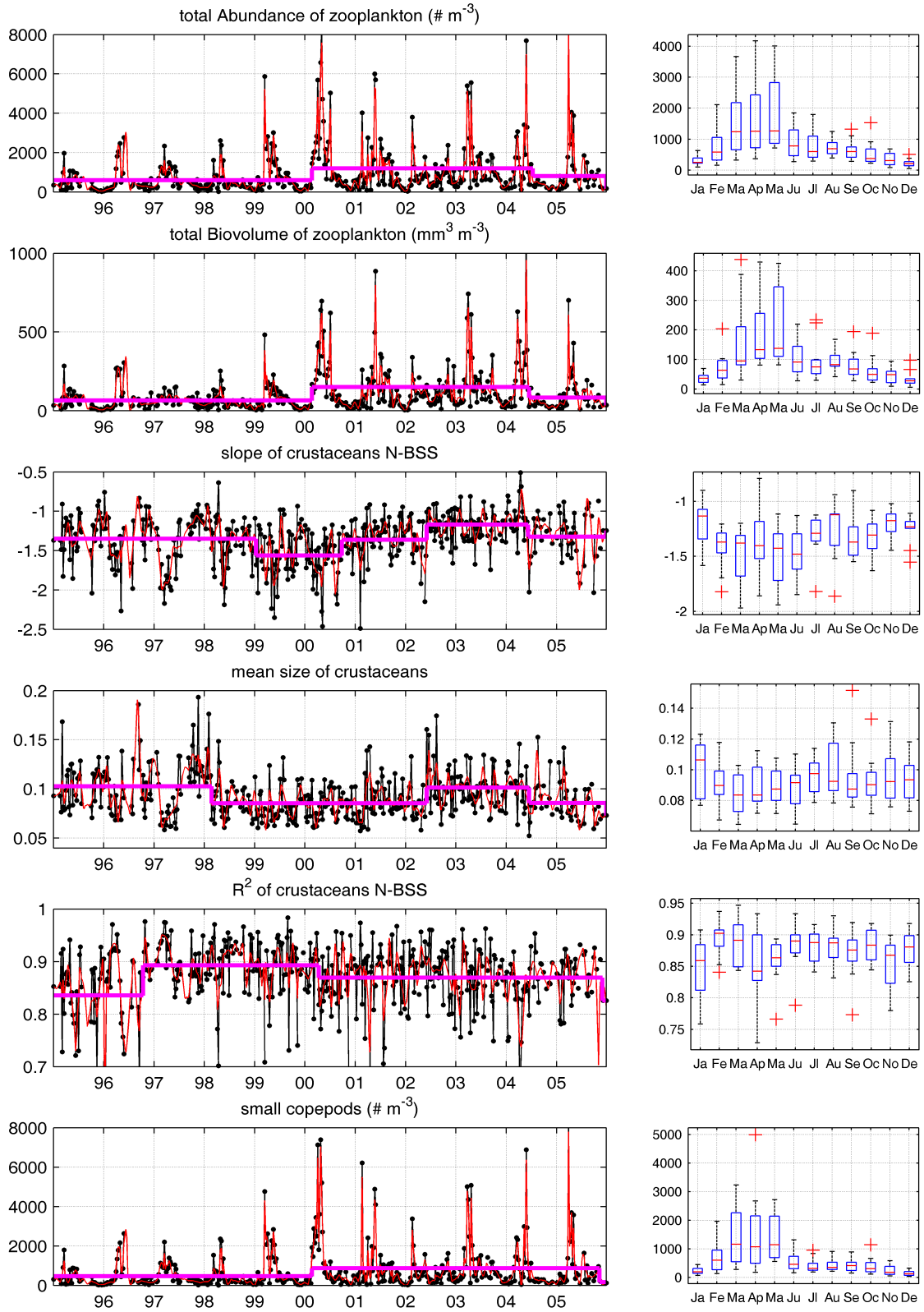

Figure A.1 – *Raw zoological, biological, hydrological and meteorological data from Point B and Sémaphore stations used in this chapter. For all parameters the complete raw time series is shown together with a boxplot made on month values. Zooplankton data come from WP2 sampling from 60 m depth to surface. Biological and suspended particles come from NISKIN bottles at 6 different depths, shown values are depth averaged. Hydrological data come from CTD casts, average value from 10 to 40 m were taken. Meteorological data come from daily measurements, the average weekly values were taken. Red curves present the de-noised time series using the matlab function "ddencmp" and "wdencmp". Finally, the magenta curves represent the results of shifts detection following the STARS method of Rodionov (2004; 2006), any step in these curves indicates a significant change (at the threshold of 0.1) in the mean with the cut-off length being set to two years.*

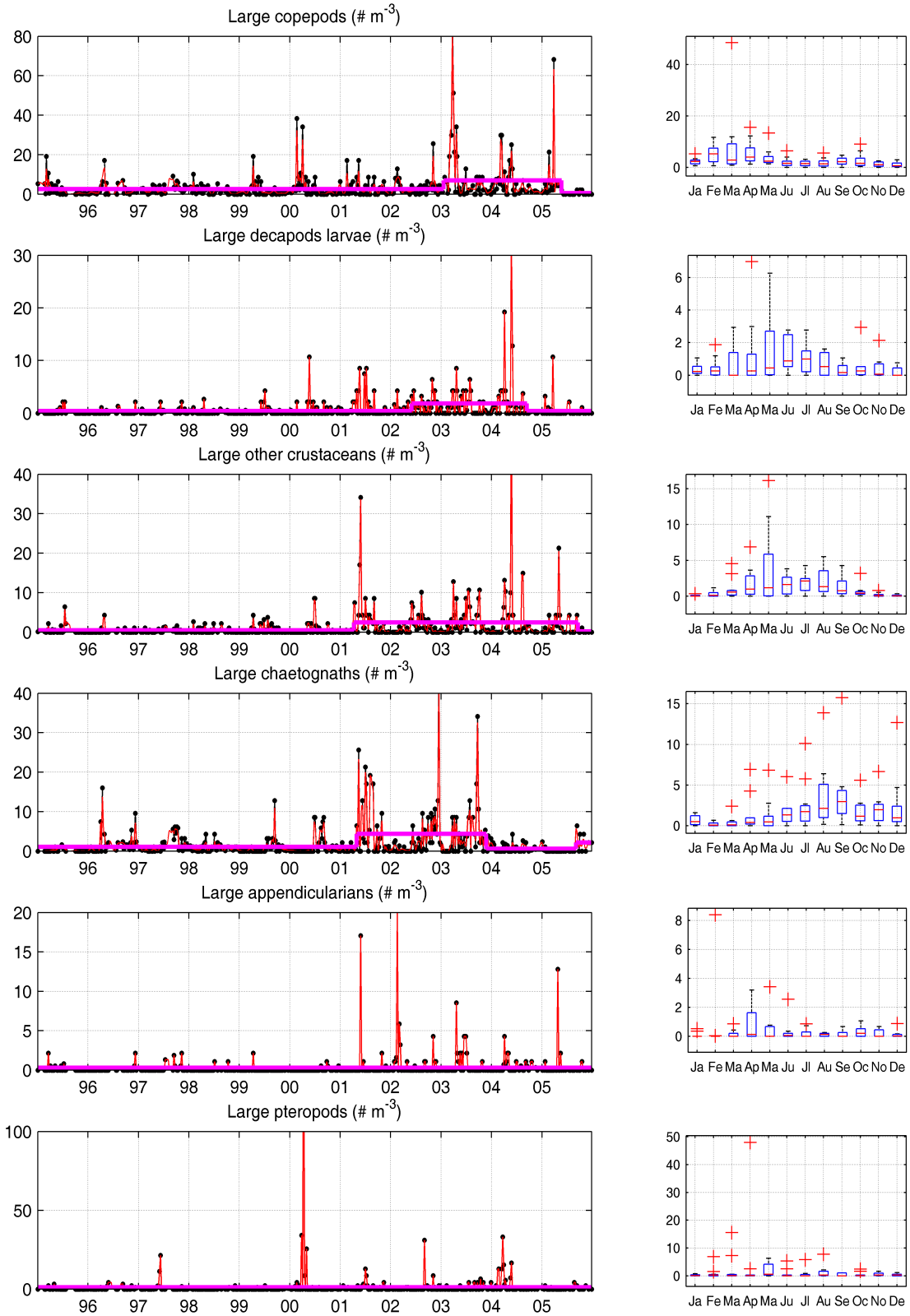

Figure A.1 – *suite.*

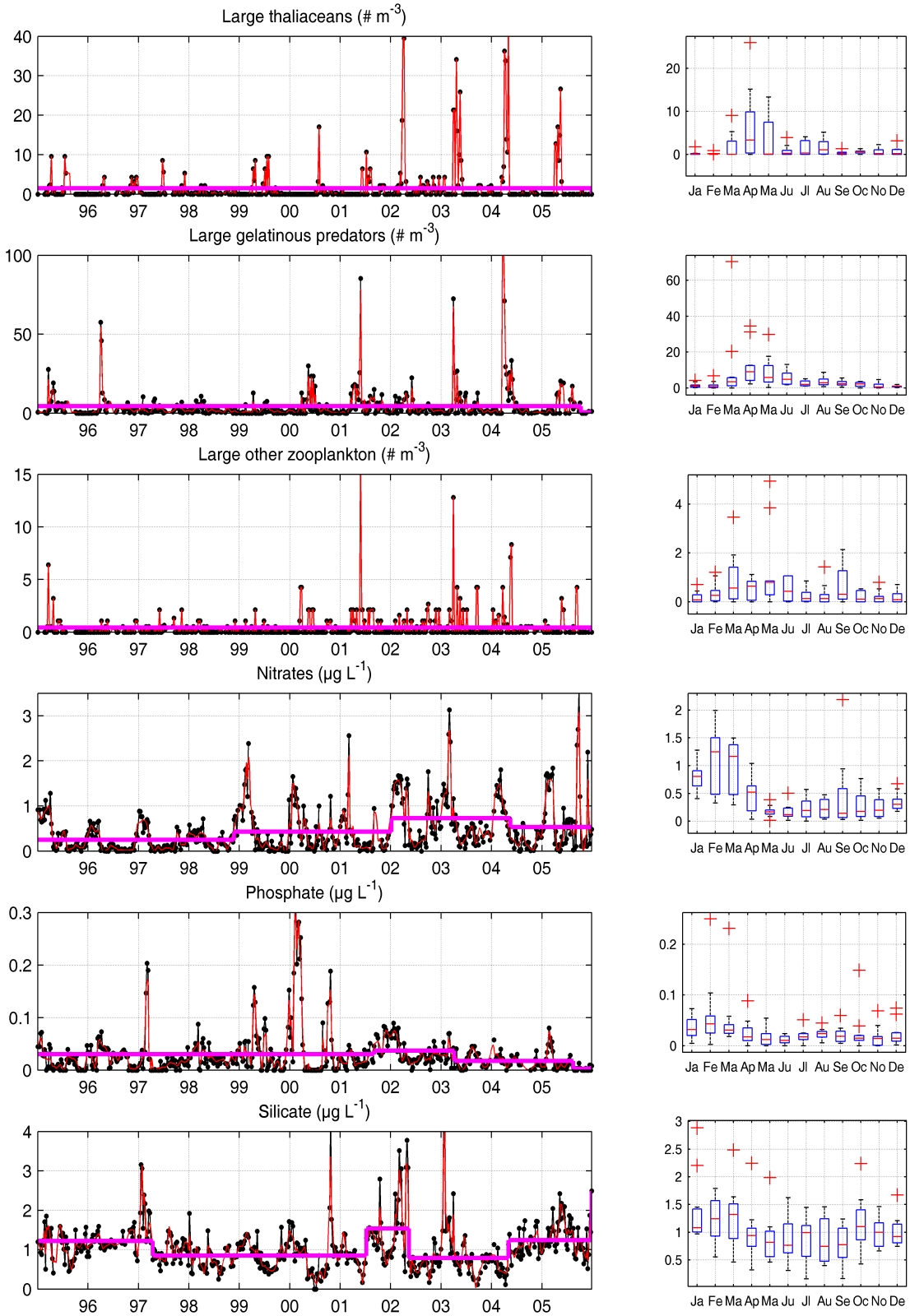

Figure A.1 – *suite.*

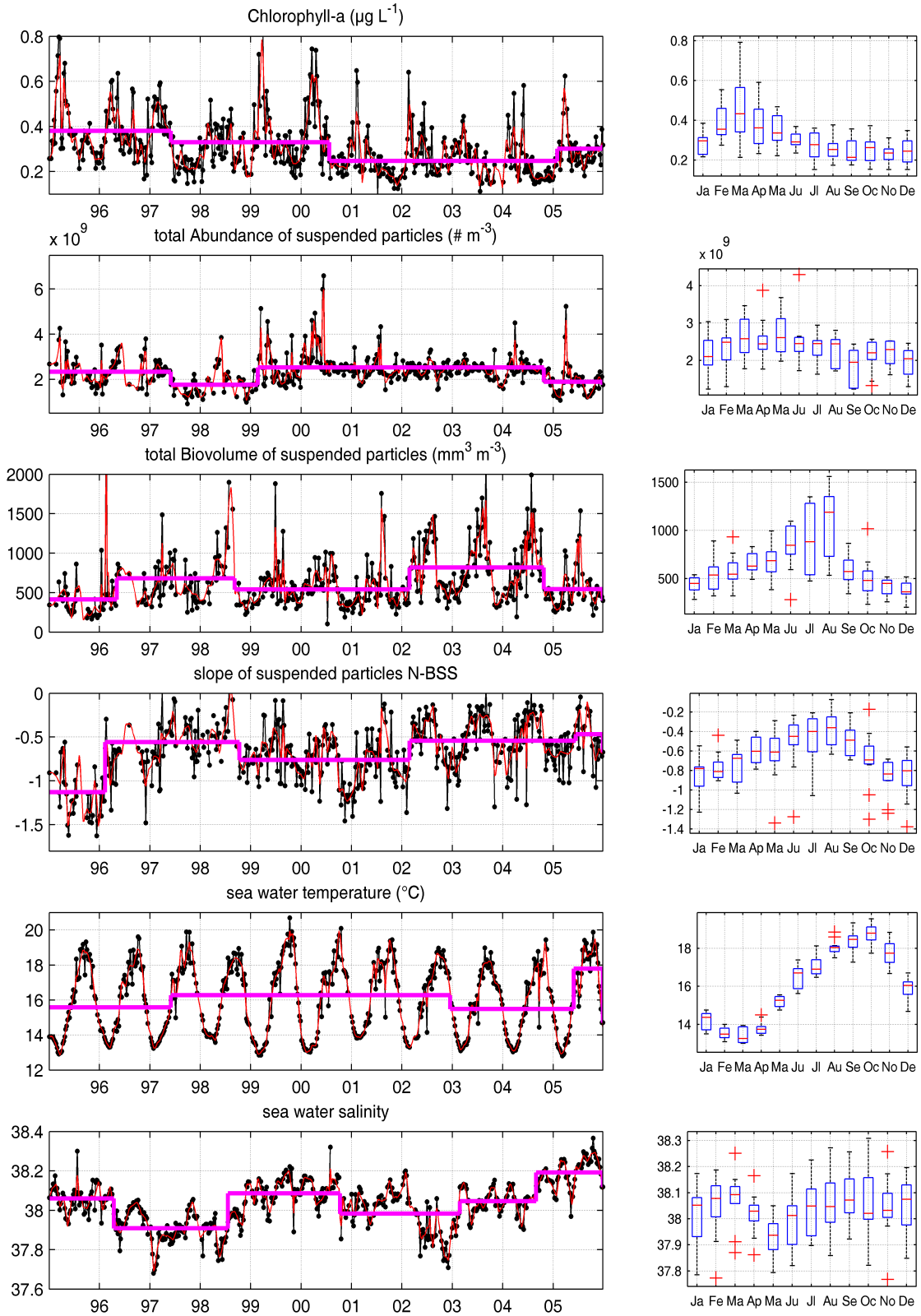

Figure A.1 – *suite.*

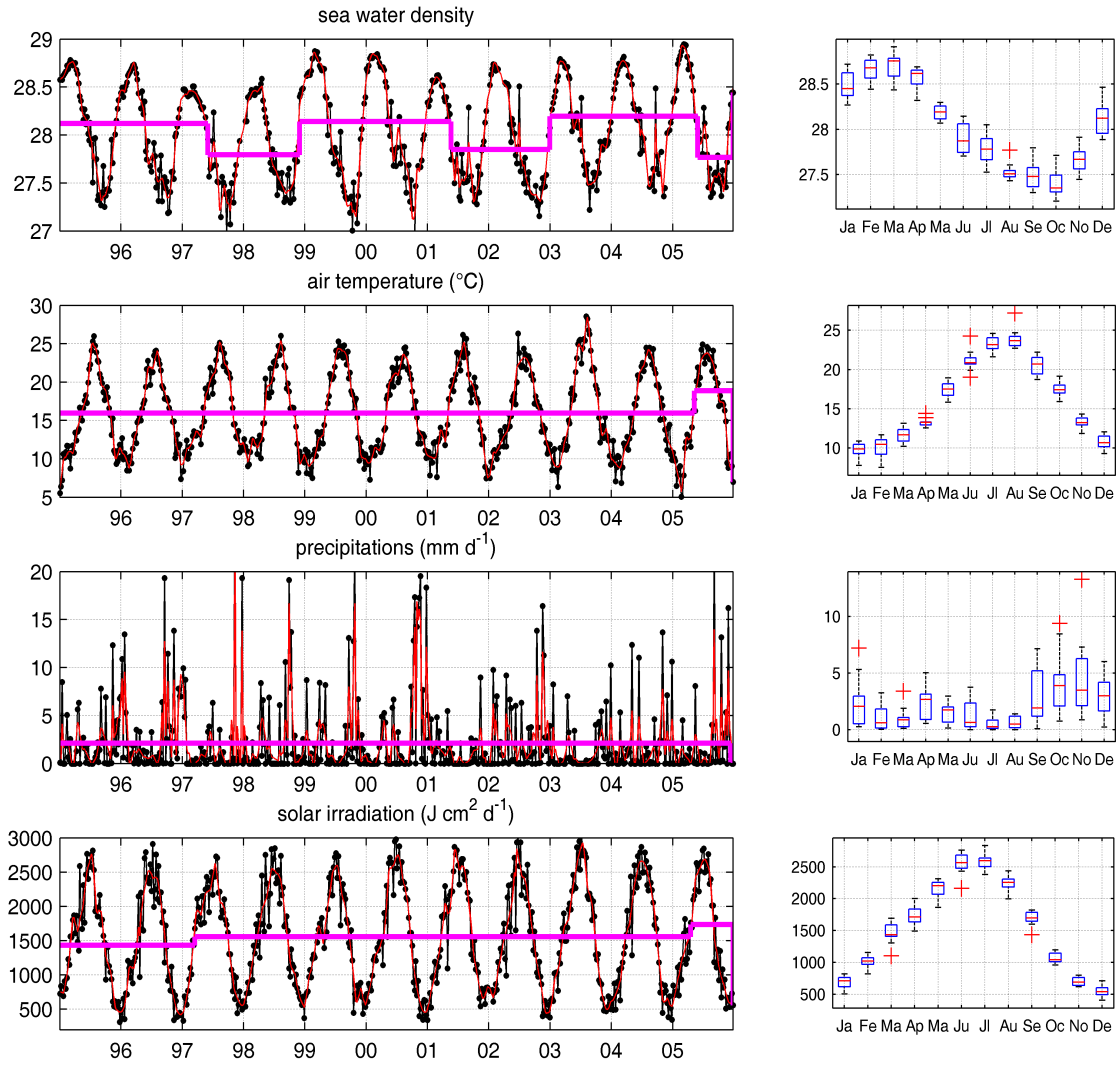

Figure A.1 – *suite.*

45 YEARS OF COPEPODS TIME SERIES

B

With the recently processed samples of diverse time series from Point B we now have the possibility to cumulate them to form one of the longest zooplankton time series in the world, from 1966 to 2010. These time series are:

- Juday-Bogorov (330 μm mesh size, 0.25 m^2 mouth aperture) daily samples from 1966 to 2003 and from 75 m depth to surface. Daily samples were pooled together each week. One per month was scanned with the ZooScan prototype 2003 (time series presented in Garcia-Comas et al. Submitted), called here JB 1, and two per month were recently scanned with the ZooScan model 2006 (see chapter II) and called JB 2. This makes 3 points per months (on average) — each point being the cumul of 7 net tows (on average).

- WP2 (200 μm mesh size, 0.25 m^2 mouth aperture) time series analyzed here (chapter III, called here WP2 1), weekly sampled from 1995 to 2005 and from 60 m depth to the surface, analyzed with the ZooScan 2003. Each point is here only one net tow.

- WP2 daily samples from 2004 to present (sample of the 1st September 2010 was the last one used here) and from 75 m depth to surface called here WP2 2. As for the Juday-Bogorov daily samples were pooled together each week. Samples were scanned with the ZooScan 2006.

The total number of weeks sampled per month for these different time series is shown on fig. B.1, and the total number of tows cumulated per month on fig. B.2.

An automatic prediction (see chapter II) was then applied to the scans. Here we will present the results for Copepods abundances — the best predicted and the most abundant. The visual validation of other groups, to include them, was not done for Juday-Bogorov samples scanned with the ZooScan 2006. For the comparison between the different nets we used the Nichols & Thompson (1991) 3/4 relation, see chapter II. For the Juday-Bogorov it then appeared that copepods were quantitatively sampled from 0.0525 mm^3 (it was 0.0320 for the WP2). Since Juday-Bogorov and WP2 net had the

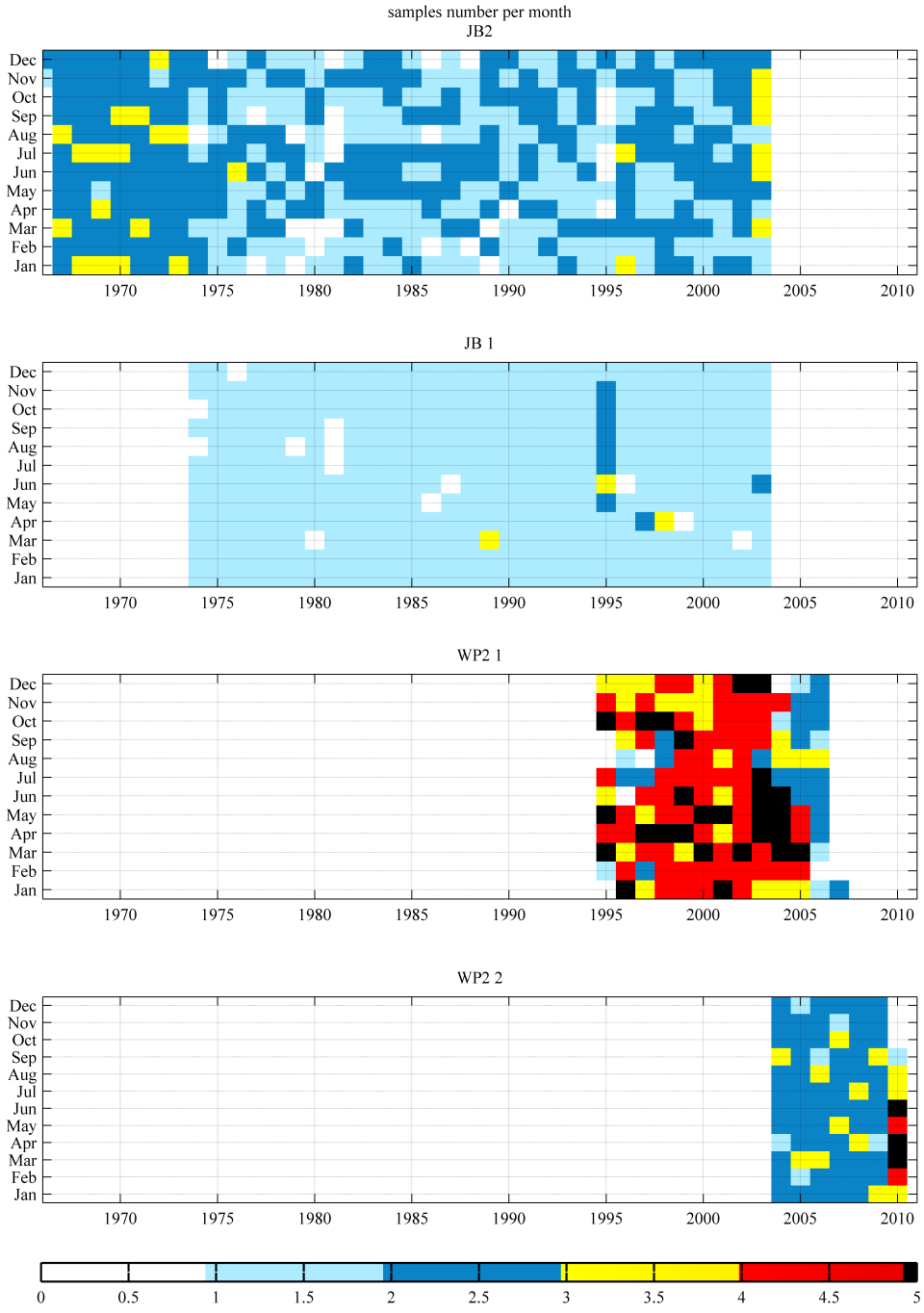

Figure B.1 – *Number of weeks sampled per month, from 0 to 5, for the four time series: JB 1, JB 2, WP2 1, WP2 2.*

same opening area and were trawled the same way it is unlikely that they exhibit a difference in the sampling of larger objects. So for all time series only individuals larger than 0.0525 mm^3 were taken. Moreover, to decrease the variability and to study the long-term trends, monthly averaging of the different time series was done. These different time series are shown on fig. B.3.

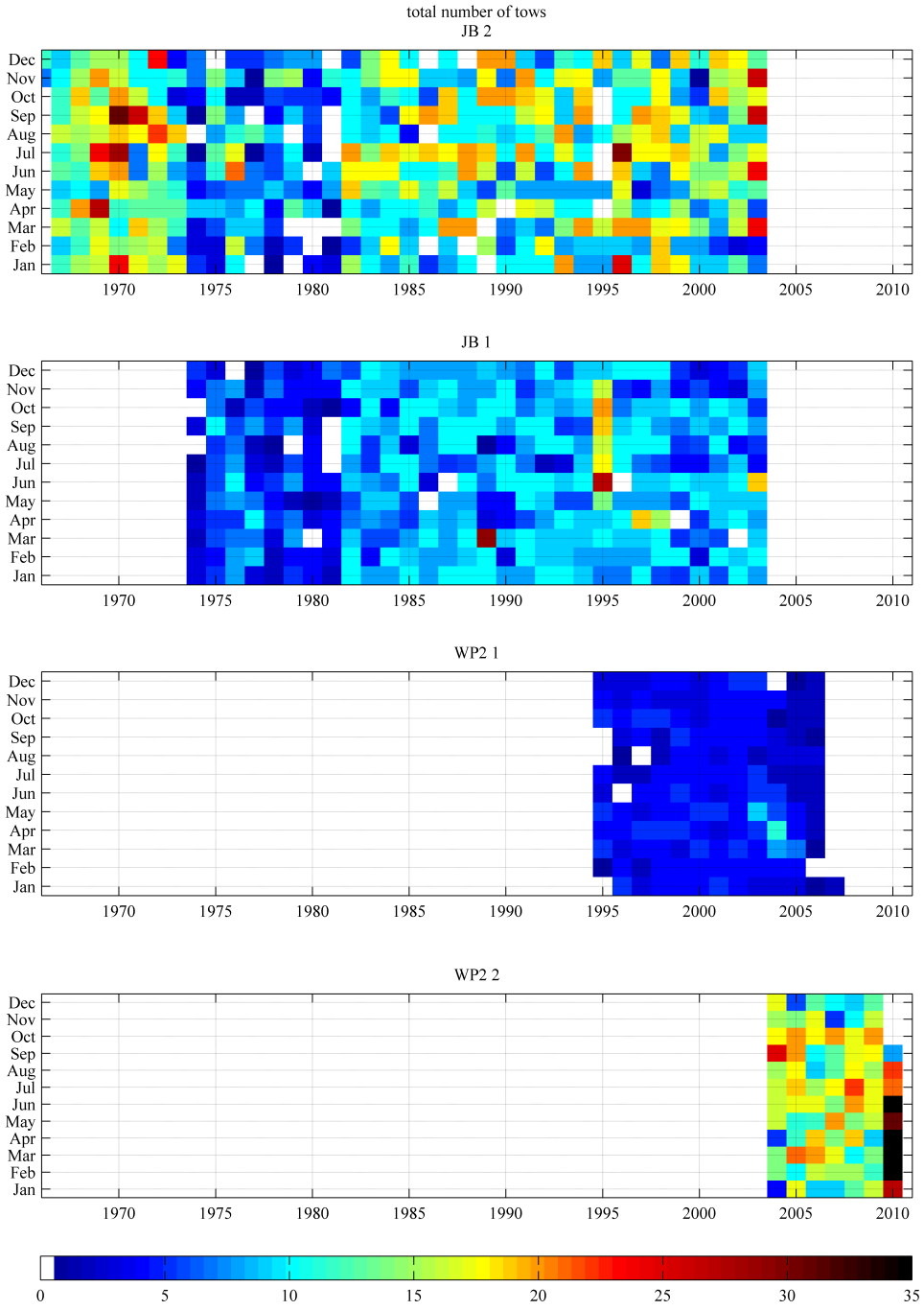

Figure B.2 – *Number of tows per month, from 0 to 35, for the four time series: JB 1, JB 2, WP2 1, WP2 2.*

It represents for the moment a first comparison, based only on a size selection by a lower limit (0.0525 mm^3) using the 3/4 relation of Nichols & Thompson (1991) that showed interesting results in chapter II. We also choose to present only the copepods since they are systematically well automatically predicted by the different learning sets that were used. Yet a deeper calibration of the different

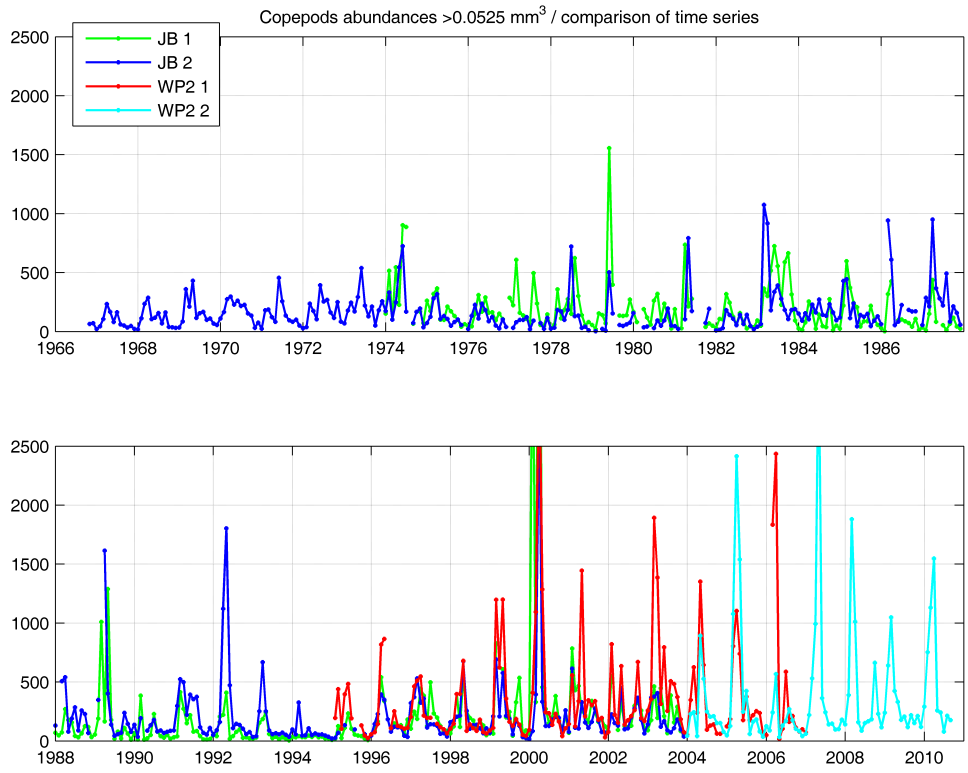

Figure B.3 – *Copepods abundances of all time series from 1966 to 2010 shown together — it is displayed on two graphs for more clarity. See text for significance of JB 1, JB 2, WP2 1 and WP2 2. The time series analyzed in chapter III is WP2 1.*

time series will be needed in the future, not only because of the two different nets used but also because of different sampling strategies: pooling of all samples of the week or doing only one. Because of this all future discussions and hypotheses made in section V.4 must be taken cautiously.

Yet, this first comparison based on the lower size selection is already enthusiastic. Comparisons of same months of the JB 1 and 2 and the WP2 1 and 2 with linear regression (model $y = a.x$, standardized major axis regression) give, in the log scale (N indicates number of months that could be compared):

- $\log(\mathrm{WP2}_1) = 1.081 \cdot \log(\mathrm{JB}_2)$, $r^2 = 0.9846$, $p < 0.001$, N = 99;
- $\log(\mathrm{WP2}_1) = 1.037 \cdot \log(\mathrm{JB}_1)$, $r^2 = 0.9802$, $p < 0.001$, N = 101;
- $\log(\mathrm{WP2}_1) = 1.026 \cdot \log(\mathrm{WP2}_2)$, $r^2 = 0.9781$, $p < 0.001$, N = 35;

- $\log(\mathrm{JB}_2) = 0.988 \cdot \log(\mathrm{JB}_1)$, r^2 = 0.9573, $p < 0.001$, N = 325;

The coefficient is always close to 1 indicating that all nets and sampling strategies gave copepods abundances of the same order, there is no constant over or under estimations. Yet, only the coefficient of WP2 1 vs. WP2 2 and WP2 1 vs. JB 2 are not significantly different from 1 (test of the slope). In addition all comparisons gave significant correlations with p <0.001. Yet χ^2 tests were not significant for all of them (p values from 0.23 to 0.29). However, since the exact date of sampling does not always overlap (for example between JB 1 and JB 2, in which dates of sampling are always different), sampling strategies and nets are different, and the comparison was made with only a single constraint (lower limit): these comparisons are already good.

BIBLIOGRAPHY

Aebischer, N. J., Coulson, J. C., & Colebrook, J. M. (1990). Parallel long-term trends across 4 marine trophic levels and weather. *Nature*, *347*(6295), 753–755. (Cited pages 3 and 101.)

Alcaraz, M., Saiz, E., Calbet, A., Trepat, I., & Broglio, E. (2003). Estimating zooplankton biomass through image analysis. *Marine Biology*, *143*(2), 307–315. (Cited pages 46 and 61.)

Allen, J. I., Holt, J. T., Blackford, J., & Proctor, R. (2007). Error quantification of a high-resolution coupled hydrodynamic-ecosystem coastal-ocean model: Part 2. chlorophyll-a, nutrients and spm. *Journal of Marine Systems*, *68*(3-4), 381–404. (Cited pages 120 and 174.)

Ambaum, M. H. P., Hoskins, B. J., & Stephenson, D. B. (2001). Arctic oscillation or north atlantic oscillation? *Journal of Climate*, *14*(16), 3495–3507. (Cited page 110.)

Aminot, A., & Kérouel, R. (2004). Dissolved organic carbon, nitrogen and phosphorus in the n-e atlantic and the n-w mediterranean with particular reference to non-refractory fractions and degradation. *Deep-sea Research Part I-oceanographic Research Papers*, *51*(12), 1975–1999. (Cited page 71.)

Andersen, K. H., & Beyer, J. E. (2006). Asymptotic size determines species abundance in the marine size spectrum. *American Naturalist*, *168*(1), 54–61. (Cited pages 17, 19, and 159.)

Andersen, V., & Nival, P. (1988). A pelagic ecosystem model simulating production and sedimentation of biogenic particles - role of salps and copepods. *Marine Ecology-progress Series*, *44*(1), 37–50. (Cited pages 84, 85, 104, 122, 136, 137, 149, 172, and 176.)

Anderson, M. J., & Robinson, J. (2003). Generalized discriminant analysis based on distances. *Australian & New Zealand Journal of Statistics*, *45*(3), 301–318. (Cited page 35.)

Anderson, M. J., & Willis, T. J. (2003). Canonical analysis of principal coordinates: A useful method of constrained ordination for ecology. *Ecology*, *84*(2), 511–525. (Cited page 35.)

Armstrong, R. A. (1999). Stable model structures for representing biogeochemical diversity and size spectra in plankton communities. *Journal of Plankton Research*, *21*(3), 445–464. (Cited page 8.)

Backhaus, J. O., Hegseth, E. N., Wehde, H., Irigoien, X., Hatten, K., & Logemann, K. (2003). Convection and primary production in winter. *Marine Ecology-progress Series*, *251*, 1–14. (Cited page 100.)

Baird, M. E., & Suthers, I. M. (2007). A size-resolved pelagic ecosystem model. *Ecological Modelling*, *203*(3-4), 185–203. (Cited pages 8, 10, 19, 20, 23, 120, 132, 137, 159, and 175.)

Bakun, A. (2010). Linking climate to population variability in marine ecosystems characterized by non-simple dynamics: Conceptual templates and schematic constructs. *Journal of Marine Systems*, *79*(3-4), 361–373. (Cited page 103.)

Banse, K. (1995). Zooplankton - Pivotal Role in the Control of Ocean Production. *Ices Journal of Marine Science*, *52*(3-4), 265–277. (Cited page 3.)

Barale, V., Jaquet, J. M., & Ndiaye, M. (2008). Algal blooming patterns and anomalies in the mediterranean sea as derived from the seawifs data set (1998-2003). *Remote Sensing of Environment*, *112*(8), 3300–3313. (Cited pages 5 and 172.)

Baretta, J. W., Ebenhoh, W., & Ruardij, P. (1995). The european-regional-seas-ecosystem-model, a complex marine ecosystem model. *Netherlands Journal of Sea Research*, *33*(3-4), 233–246. (Cited page 119.)

Barnes, C., Maxwell, D., Reuman, D. C., & Jennings, S. (2010). Global patterns in predator-prey size relationships reveal size dependency of trophic transfer efficiency. *Ecology*, *91*(1), 222–232. (Cited page 137.)

Beaugrand, G. (2004). The north sea regime shift: evidence, causes, mechanisms and consequences. *Progress In Oceanography*, *60*(2-4), 245–262. (Cited page 5.)

Beaugrand, G. (2009). Decadal changes in climate and ecosystems in the north atlantic ocean and adjacent seas. *Deep-sea Research Part Ii-topical Studies In Oceanography*, *56*(8-10), 656–673. (Cited pages 108 and 110.)

Beaugrand, G., Edwards, M., Brander, K., Luczak, C., & Ibañez, F. (2008). Causes and projections of abrupt climate-driven ecosystem shifts in the North Atlantic. *Ecology Letters*, *11*(11), 1157–1168. (Cited page 5.)

Beaugrand, G., & Ibañez, F. (2002). Spatial dependence of calanoid copepod diversity in the North Atlantic Ocean. *Marine Ecology-Progress Series*, *232*, 197–211. (Cited page 3.)

Beaulieu, S. E., Mullin, M. M., Tang, V. T., Pyne, S. M., King, A. L., & Twining, B. S. (1999). Using an optical plankton counter to determine the size distributions of preserved zooplankton samples. *Journal of Plankton Research*, *21*(10), 1939–1956. (Cited page 45.)

Behrenfeld, M. J. (2010). Abandoning sverdrup's critical depth hypothesis on phytoplankton blooms. *Ecology*, *91*(4), 977–989. (Cited page 172.)

Bell, J. L., & Hopcroft, R. R. (2008). Assessment of ZooImage as a tool for the classification of zooplankton. *Journal of Plankton Research*, *30*(12), 1351–1367. (Cited pages 11, 29, 43, 44, 45, and 168.)

Benfield, M. C., Grosjean, P., Culverhouse, P. F., Irigoien, X., Sieracki, M. E., Lopez-Urrutia, A., Dam, H. G., Hu, Q., Davis, C. S., Hansen, A., Pilskaln, C. H., Riseman, E. M., Schultz, H., Utgoff, P. E., & Gorsky, G. (2007). RAPID Research on Automated Plankton Identification. *Oceanography*, *20*(2), 172–187. (Cited pages 11, 12, 27, 28, 29, 43, and 44.)

Benjamini, Y., Krieger, A. M., & Yekutieli, D. (2006). Adaptive linear step-up procedures that control the false discovery rate. *Biometrika*, *93*(3), 491–507. (Cited page 82.)

Benoît, E., & Rochet, M.-J. (2004). A continuous model of biomass size spectra governed by predation and the effects of fishing on them. *Journal of Theoretical Biology*, *226*, 9–21. (Cited pages 8, 19, 21, 121, 133, 134, 138, and 175.)

Berline, L., Siokou-Frangou, I., Marasović, I., Vidjak, O., Fernàndes de Puelles, M. L., Mazzocchi, M. G., Assimakopoulou, G., Zervoudaki, S., Fonda Umani, S., Conversi, A., Garcia-Comas, C., Ibañez, F., Gasparini, S., Stemmann, L., & Gorsky, G. (accepted). Intercomparison of six mediterranean zooplankton time series. *Progress In Oceanography*. (Cited pages 3, 6, and 113.)

Berline, L., Stemmann, L., Vichi, M., Lombard, F., & Gorsky, G. (submitted). Impact of appendicularians on detritus and export fluxes: a model approach at dyfamed site. *Journal of Plankton Research*. (Cited page 120.)

Bertalanffy, L. v. (1957). Quantitative laws in metabolism and growth. *Quarterly Review of Biology*, *32*, 217–231. (Cited pages 7 and 8.)

Bethoux, J. P., de Madron, X. D., Nyffeler, F., & Tailliez, D. (2002). Deep water in the western Mediterranean: peculiar 1999 and 2000 characteristics, shelf formation hypothesis, variability since 1970 and geochemical inferences. *Journal of Marine Systems*, *33*, 117–131. (Cited page 99.)

Bethoux, J. P., Gentili, B., & Tailliez, D. (1998). Warming and freshwater budget change in the Mediterranean since the 1940s, their possible relation to the greenhouse effect. *Geophysical Research Letters*, *25*(7), 1023–1026. (Cited page 99.)

Blanco, J. M., Echevarrìa, F., & Garcia, C. M. (1994). Dealing with size-spectra: some conceptual and mathematical problems. *Scienta Marina*, *58*(1-2). (Cited pages 13 and 31.)

Borer, E. T., Seabloom, E. W., Shurin, J. B., Anderson, K. E., Blanchette, C. A., Broitman, B., Cooper, S. D., & Halpern, B. S. (2005). What determines the strength of a trophic cascade? *Ecology*, *86*(2), 528–537. (Cited page 102.)

Borgmann, U. (1982). Particle-size-conversion efficiency and total animal production in pelagic ecosystems. *Canadian Journal of Fisheries and Aquatic Sciences*, *39*(5), 668–674. (Cited pages 12 and 14.)

Borgmann, U. (1987). Models on the Slope of, and Biomass Flow up, the Biomass Size Spectrum. *Canadian Journal of Fisheries and Aquatic Sciences*, *44*, 136–140. (Cited pages 12 and 14.)

Breiman, L. (2001). Random forests. *Machine Learning*, *45*(1), 5–32. (Cited page 28.)

Brohée, M., Goffart, A., Frankignoul, C., Henri, V., Mouchet, A., & Hecq, J. H. (1989). Variations printanières des communautés planctoniques en baie de calvi (corse) en relation avec les contraintes physiques locales. *Cahiers De Biologie Marine*, *30*, 321–328. (Cited page 103.)

Brown, J. H., Gillooly, J. F., Allen, A. P., Savage, V. M., & West, G. B. (2004). Toward a metabolic theory of ecology. *Ecology*, *85*(7), 1771–1789. (Cited pages 8, 9, 17, and 175.)

Brucet, S., Boix, D., Lopez-Flores, R., Badosa, A., Moreno-Amich, R., & Quintana, X. D. (2005). Zooplankton structure and dynamics in permanent and temporary Mediterranean salt marshes:

taxon-based and size-based approaches. *Archiv Fur Hydrobiologie*, *162*(4), 535–555. (Cited page 31.)

Brucet, S., Boix, D., Lopez-Flores, R., Badosa, A., & Quintana, X. D. (2006). Size and species diversity of zooplankton communities in fluctuating Mediterranean salt marshes. *Estuarine Coastal and Shelf Science*, *67*(3), 424–432. (Cited page 31.)

Buecher, E., Goy, J., Planque, B., Etienne, M., & Dallot, S. (1997). Long-term fluctuations of liriope tetraphylla in villefranche bay between 1966 and 1993 compared to pelagia noctiluca populations. *Oceanologica Acta*, *20*(1), 145–157. (Cited page 70.)

Bustillos-Guzmán, J., Claustre, H., & Marty, J. C. (1995). Specific phytoplankton signatures and their relationship to hydrographic conditions in the coastal northwestern mediterranean-sea. *Marine Ecology-progress Series*, *124*(1-3), 247–258. (Cited page 70.)

Calbet, A., Garrido, S., Saiz, E., Alcaraz, M., & Duarte, C. M. (2001). Annual zooplankton succession in coastal NW Mediterranean waters: the importance of the smaller size fractions. *Journal of Plankton Research*, *23*(3), 319–331. (Cited pages 43 and 49.)

Camacho, J., & Solé, R. V. (2001). Scaling in ecological size-spectra. *Europhysics Letters*, *55*(6), 774–780. (Cited page 17.)

Caparroy, P., & Carlotti, F. (1996). A model for acartia tonsa: Effect of turbulence and consequences for the related physiological processes. *Journal of Plankton Research*, *18*(11), 2139–2177. (Cited page 119.)

Carlotti, F., & Poggiale, J. C. (2010). Towards methodological approaches to implement the zooplankton component in "end to end" food-web models. *Progress In Oceanography*, *84*(1-2), 20–38. (Cited pages 8 and 19.)

Chaui-Berlinck, J. G. (2006). A critical understanding of the fractal model of metabolic scaling. *Journal of Experimental Biology*, *209*, 3045–3054. (Cited page 8.)

Chauvaud, L., Lorrain, A., Dunbar, R. B., Paulet, Y. M., Thouzeau, G., Jean, F., Guarini, J. M., & Mucciarone, D. (2005). Shell of the great scallop pecten maximus as a high-frequency archive of paleoenvironmental changes. *Geochemistry Geophysics Geosystems*, *6*. (Cited page 181.)

Chauvaud, L., Thouzeau, G., & Paulet, Y. M. (1998). Effects of environmental factors on the daily growth rate of pecten maximus juveniles in the bay of brest (france). *Journal of Experimental Marine Biology and Ecology*, *227*(1), 83–111. (Cited page 181.)

Choi, J. S., Mazumder, A., & Hansell, R. I. C. (1999). Measuring perturbation in a complicated, thermodynamic world. *Ecological Modelling*, *117*(1), 143–158. (Cited page 18.)

Cloern, J. E., & Jassby, A. D. (2010). Patterns and scales of phytoplankton variability in estuarine-coastal ecosystems. *Estuaries and Coasts*, *33*(2), 230–241. (Cited pages 105 and 113.)

Conversi, A., Fonda Umani, S., Peluso, T., Molinero, J. C., Santojanni, A., & Edwards, M. (2010). The Mediterranean Sea regime shift at the end of the 1980s, and intriguing parallelisms with other european basins. *PLoS ONE*, *5*(5), e10633. (Cited pages 6, 33, 108, and 180.)

Culverhouse, P. F., Williams, R., Benfield, M., Flood, P. R., Sell, A. F., Mazzocchi, M. G., Buttino, I., & Sieracki, M. (2006). Automatic image analysis of plankton: future perspectives. *Marine Ecology Progress Series*, *312*, 297–309. (Cited page 29.)

Culverhouse, P. F., Williams, R., Reguera, B., Herry, V., & Gonzalez-Gil, S. (2003). Do experts make mistakes? A comparison of human and machine identification of dinoflagellates. *Marine Ecology-Progress Series*, *247*, 17–25. (Cited page 29.)

Cushing, D. H. (1990). Plankton production and year-class strength in fish populations - an update of the match mismatch hypothesis. *Advances In Marine Biology*, *26*, 249–293. (Cited page 103.)

Cushing, J. M., Dennis, B., Desharnais, R. A., & Costantino, R. F. (1996). An interdisciplinary approach to understanding nonlinear ecological dynamics. *Ecological Modelling*, *92*(2-3), 111–119. (Cited page 35.)

da Silva, J. K. L., Barbosa, L. A., & Silva, P. R. (2007). Unified theory of interspecific allometric scaling. *Journal of Physics a-Mathematical and Theoretical*, *40*(44), F953–F959. (Cited page 9.)

Davis, C. S., Gallager, S. M., Berman, M. S., Haury, L. R., & Strickler, J. R. (1992). The Video Plankton Recorder (VPR): design and initial results. *Ergebnisse der Limnologie ERLIA6*, *36*, 67–81. (Cited page 44.)

De Eyto, E., & Irvine, K. (2007). Assessing the status of shallow lakes using an additive model of biomass size spectra. *Aquatic Conservation: Marine and Freshwater Ecosystems*, *17*(7), 724–736. (Cited page 8.)

Delworth, T. L., & Dixon, K. W. (2000). Implications of the recent trend in the arctic/north atlantic oscillation for the north atlantic thermohaline circulation. *Journal of Climate*, *13*(21), 3721–3727. (Cited page 108.)

Demetrius, L. (2006). The origin of allometric scaling laws in biology. *Journal of Theoretical Biology*, *243*(4), 455–467. (Cited pages 9 and 17.)

Deser, C. (2000). On the teleconnectivity of the "arctic oscillation". *Geophysical Research Letters*, *27*(6), 779–782. (Cited page 108.)

Dippner, J. W., Heerkloss, R., & Zbilut, J. P. (2002). Recurrence quantification analysis as a tool for characterization of non-linear mesocosm dynamics. *Marine Ecology-progress Series*, *242*, 29–37. (Cited page 35.)

Donoho, D. L. (1995). De-noising by soft-thresholding. *IEEE, Transactions on Information Theory*, *41*(3), 613–627. (Cited page 74.)

D'Ortenzio, F., & d'Alcala, M. R. (2009). On the trophic regimes of the mediterranean sea: a satellite analysis. *Biogeosciences*, *6*(2), 139–148. (Cited pages 4 and 172.)

Drinkwater, K. F., Belgrano, A., Borja, A., Conversi, A., Edwards, M., Greene, C. H., Ottersen, G., Pershing, A. J., & Walker, H. (2003). The Response of Marine Ecosystems to Climate Variability Associated With the North Atlantic Oscillation. *Geophysical Monograph*, *134*, 211–234. (Cited page 3.)

Duarte, C. M., Agusti, S., Kennedy, H., & Vaque, D. (1999). The Mediterranean climate as a template for Mediterranean marine ecosystems: the example of the northeast Spanish littoral. *Progress in Oceanography*, *44*(1-3), 245–270. (Cited page 104.)

Dur, G., Souissi, S., Devreker, D., Ginot, V., Schmitt, F. G., & Hwang, J. S. (2009). An individual-based model to study the reproduction of egg bearing copepods: Application to eurytemora affinis

(copepoda calanoida) from the seine estuary, france. *Ecological Modelling*, *220*(8), 1073–1089. (Cited page 119.)

Durant, J. M., Hjermann, D. O., Ottersen, G., & Stenseth, N. C. (2007). Climate and the match or mismatch between predator requirements and resource availability. *Climate Research*, *33*(3), 271–283. (Cited page 103.)

Eckmann, J. P., Kamphorst, S. O., & Ruelle, D. (1987). Recurrence plots of dynamic-systems. *Europhysics Letters*, *4*(9), 973–977. (Cited page 35.)

Edvardsen, A., Zhou, M., Tande, K. S., & Zhu, Y. (2002). Zooplankton population dynamics: measuring in situ growth and mortality rates using an Optical Plankton Counter. *Marine Ecology Progress Series*, *227*, 205–219. (Cited pages 8 and 16.)

Edwards, M., Beaugrand, G., Reid, P. C., Rowden, A. A., & Jones, M. B. (2002). Ocean climate anomalies and the ecology of the north sea. *Marine Ecology-progress Series*, *239*, 1–10. (Cited page 103.)

Edwards, M., & Richardson, A. J. (2004). Impact of climate change on marine pelagic phenology and trophic mismatch. *Nature*, *430*(7002), 881–884. (Cited page 103.)

Elton, C. S. (1924). Periodic fluctuations in the numbers of animals - Their causes and effects. *British Journal of Experimental Biology*, *2*(1), 119–163. (Cited page 3.)

Estrada, M. (1996). Primary production in the northwestern mediterranean. *Scientia Marina*, *60*, 55–64. (Cited pages 5 and 172.)

Fasham, M. J. R., Ducklow, H. W., & McKelvie, S. M. (1990). A Nitrogen-Based Model of Plankton Dynamics in the Oceanic Mixed Layer. *Journal of Marine Research*, *48*(3), 591–639. (Cited pages 7 and 119.)

Fenchel, T. (1974). Intrinsic Rate of Natural Increase - Relationship with Body Size. *Oecologia*, *14*(4), 317–326. (Cited pages 8 and 14.)

Fernandes, J. A., Irigoien, X., Boyra, G., Lozano, J. A., & Inza, I. (2009). Optimizing the number of classes in automated zooplankton classification. *Journal of Plankton Research*, *31*(1), 19–29. (Cited pages 30 and 45.)

Fernàndes de Puelles, M. L., Alemany, F., & Jansa, J. (2007). Zooplankton time-series in the Balearic Sea (Western Mediterranean): Variability during the decade 1994-2003. *Progress in Oceanography*, *74*(2-3), 329–354. (Cited pages 6, 70, 108, and 113.)

Fernàndes de Puelles, M. L., & Molinero, J. C. (2008). Decadal changes in hydrographic and ecological time-series in the Balearic Sea (western Mediterranean), identifying links between climate and zooplankton. *ICES Journal of Marine Science*, *65*(3), 311–317. (Cited pages 6 and 108.)

Feuchtmayr, H., Zollner, E., Santer, B., Sommer, U., & Grey, J. (2004). Zooplankton interactions in an enclosure experiment: insights from stable isotope analyses. *Freshwater Biology*, *49*(11), 1495–1504. (Cited page 102.)

Fiorentini, L., Caddy, J. F., & De Leiva, J. I. (1997). Long- and short-term trends of mediterranean fishery resources. *Studies and Reviews*, *69, Food and Agriculture Organization for the United Nations*, 72 pp. (Cited pages 5 and 172.)

Fleminger, A., & Clutter, R. I. (1965). Avoidance of Towed Nets by Zooplankton. *Limnology and Oceanography*, *10*(1), 96–104. (Cited pages 44 and 50.)

Folland, C. K., Colman, A. W., Rowell, D. P., & Davey, M. K. (2001). Predictability of northeast brazil rainfall and real-time forecast skill, 1987-98. *Journal of Climate*, *14*(9), 1937–1958. (Cited page 109.)

Frederiksen, M., Edwards, M., Richardson, A. J., Halliday, N. C., & Wanless, S. (2006). From plankton to top predators: bottom-up control of a marine food web across four trophic levels. *Journal of Animal Ecology*, *75*(6), 1259–1268. (Cited page 101.)

Fromentin, J. M., & Planque, B. (1996). Calanus and environment in the eastern North Atlantic .2. Influence of the North Atlantic Oscillation on C-finmarchicus and C-helgolandicus. *Marine Ecology-Progress Series*, *134*(1-3), 111–118. (Cited page 3.)

Gallienne, C. P., & Robins, D. B. (2001). Is Oithona the most important copepod in the world's oceans? *Journal of Plankton Research*, *23*(12), 1421–1432. (Cited pages 43 and 49.)

Garcia-Comas, C., Stemmann, L., Ibañez, F., Gasparini, S., Mazzocchi, M. G., Berline, L., Picheral, M., & Gorsky, G. (Submitted). Zooplankton long-term changes in the nw mediterranean sea:

Decadal periodicity forced by large-scale atmospheric changes? *Journal of Marine Systems*. (Cited pages xxix, 6, 69, 70, 101, 102, 105, 106, 108, 113, 178, 179, 180, and 197.)

Gasol, J. M., Guerrero, R., & Pedrosalio, C. (1991). Seasonal-variations in size structure and prokaryotic dominance in sulfurous lake Ciso. *Limnology and Oceanography*, *36*(5), 860–872. (Cited page 31.)

Gasparini, S. (2007). PLANKTON IDENTIFIER: a software for automatic recognition of planktonic organisms. http://www.obs-vlfr.fr/∼gaspari/Plankton_Identifier/index.php. *user manual*. (Cited page 28.)

Gasparini, S., Mousseau, L., & Marty, J. C. (2004). Zooplankton biomass at dyfamed time series station. http://doi.pangaea.de/10.1594/PANGAEA.183618. *Pangaea*, (p. doi:10.1594/PANGAEA.183618). (Cited page 103.)

Gaudy, R., Youssara, F., Diaz, F., & Raimbault, P. (2003). Biomass, metabolism and nutrition of zooplankton in the gulf of lions (nw mediterranean). *Oceanologica Acta*, *26*(4), 357–372. (Cited page 102.)

Gačić, M., Civitarese, G., Miserocchi, S., Cardin, V., Crise, A., & Mauri, E. (2002). The open-ocean convection in the Southern Adriatic: a controlling mechanism of the spring phytoplankton bloom. *Continental Shelf Research*, *22*(14), 1897–1908. (Cited page 100.)

Geider, R. J., MacIntyre, H. L., & Kana, T. M. (1998). A dynamic regulatory model of phytoplanktonic acclimation to light, nutrients, and temperature. *Limnology and Oceanography*, *43*(4), 679–694. (Cited page 104.)

Gentleman, W. (2002). A chronology of plankton dynamics in silico: how computer models have been used to study marine ecosystems. *Hydrobiologia*, *480*(1-3), 69–85. (Cited page 119.)

Geurts, P., Irrthum, A., & Wehenkel, L. (2009). Supervised learning with decision tree-based methods in computational and systems biology. *Molecular BioSystems*, *5*(12), 1593–1605. (Cited page 28.)

Gin, K. Y. H., Guo, J., & Cheong, H.-F. (1998). A size-based ecosystem model for pelagic waters. *Ecological Modelling*, *112*, 53–72. (Cited page 8.)

Gislason, A., & Silva, T. (2009). Comparison between automated analysis of zooplankton using ZooImage and traditional methodology. *Journal of Plankton Research*, *31*(12), 1505–1516. (Cited pages 28, 29, 30, 44, 45, and 168.)

Glazier, D. S. (2005). Beyond the '3/4-power law': variation in the intra- and interspecific scaling of metabolic rate in animals. *Biological Review*, *80*, 611–662. (Cited pages 8, 9, 17, 138, and 175.)

Goberville, E., Beaugrand, G., Sautour, B., Tréguer, P., & SOMLIT-Team (2010). Climate-driven changes in coastal marine systems of western europe. *Marine Ecology Progress Series*, *408*, 129–148. (Cited pages 3 and 113.)

Goffart, A., Hecq, J. H., & Legendre, L. (2002). Changes in the development of the winter-spring phytoplankton bloom in the bay of calvi (nw mediterranean) over the last two decades: a response to changing climate? *Marine Ecology-progress Series*, *236*, 45–60. (Cited pages 7, 70, 100, and 103.)

Goldenberg, S. B., Landsea, C. W., Mestas-Nunez, A. M., & Gray, W. M. (2001). The recent increase in atlantic hurricane activity: Causes and implications. *Science*, *293*(5529), 474–479. (Cited page 109.)

Gomez, F., & Gorsky, G. (2003). Annual microplankton cycles in Villefranche Bay, Ligurian Sea, NW Mediterranean. *Journal of Plankton Research*, *25*(4), 323–339. (Cited page 180.)

Gorsky, G., Aldorf, C., Kage, M., Picheral, M., Garcia, Y., & Favole, J. (1992). Vertical-Distribution of Suspended Aggregates Determined by a New Underwater Video Profiler. *Annales De L Institut Oceanographique*, *68*(1-2), 275–280. (Cited page 12.)

Gorsky, G., Guilbert, P., & Valenta, E. (1989). The Autonomous Image Analyzer - Enumeration, Measurement and Identification of Marine-Phytoplankton. *Marine Ecology Progress Series*, *58*(1-2), 133–142. (Cited pages 11 and 43.)

Gorsky, G., Ohman, M. D., Picheral, M., Gasparini, S., Stemmann, L., Romagnan, J.-B., Cawood, A., Pesant, S., Garcia-Comas, C., & Prejger, F. (2010). Digital zooplankton image analysis using the ZooScan integrated system. *Journal of Plankton Research*, *32*(3). (Cited pages 12, 26, 27, 28, 29, 30, 43, 44, 45, 46, 59, 61, and 168.)

Goy, J. (1997). The medusae (cnidaria, hydrozoa) and their trophic environment: An example in the north-western mediterranean. *Annales De L'Institut Océanographique*, *73*(2), 159–171. (Cited pages 70 and 174.)

Graneli, E., & Turner, J. T. (2002). Top-down regulation in ctenophore-copepod-ciliate-diatom-phytoflagellate communities in coastal waters: a mesocosm study. *Marine Ecology-Progress Series*, *239*, 57–68. (Cited page 102.)

Grosjean, P., & Denis, K. (2007). Zoo/phytoimage version 1.2-0. Tech. rep. (Cited pages 28 and 29.)

Grosjean, P., Picheral, M., Warembourg, C., & Gorsky, G. (2003). Enumeration, measurement, and identification of net zooplankton samples using the ZOOSCAN digital imaging system. In *3rd International Zooplankton Production Symposium*, (pp. 518–525). Gijon, SPAIN. (Cited pages 11, 12, 26, 28, 29, 43, 44, and 45.)

Hansen, B., Bjornsen, P. K., & Hansen, P. J. (1994). The size ratio between planktonic predators and their prey. *Limnology and Oceanography*, *39*(2), 395–403. (Cited page 137.)

Hansen, P. J., Bjornsen, P. K., & Hansen, B. W. (1997). Zooplankton grazing and growth: Scaling within the 2-2,000-mu m body size range. *Limnology and Oceanography*, *42*(4), 687–704. (Cited page 19.)

Hare, S. R., & Mantua, N. J. (2000). Empirical evidence for north pacific regime shifts in 1977 and 1989. *Progress In Oceanography*, *47*(2-4), 103–145. (Cited page 34.)

Harris, R. P., & Paffenhöfer, G. A. (1976). Feeding, growth and reproduction of marine planktonic copepod temora-longicornis muller. *Journal of the Marine Biological Association of the United Kingdom*, *56*(3), 675–690. (Cited page 137.)

Hausdorff, F. (1919). Dimension and outer dimension. *Mathematische Annalen*, *79*, 157–179. (Cited page 36.)

Hays, G. C., Richardson, A. J., & Robinson, C. (2005). Climate change and marine plankton. *Trends in Ecology & Evolution*, *20*(6), 337–344. (Cited page 4.)

Heath, M. R. (1995). Size spectrum dynamics and the planktonic ecosystem of Loch Linnhe. *ICES Journal of Marine Science*, *52*, 627–642. (Cited pages 7, 12, and 15.)

Hecq, J. H., Gaspar, A., & Dauby, P. (1981). Caractéristiques écologiques et biochimiques de l'écosystème planctonique en baie de calvi (corse). *Bulletin de la Société Royale Scientifique de Liège 50e année (11-12)*, (pp. 440–445). (Cited page 103.)

Hendriks, A. J. (2007). The power of size: A meta-analysis reveals consistency of allometric regressions. *Ecological Modelling*, *205*(1-2), 196–208. (Cited pages 8 and 9.)

Herman, A. W. (1992). Design and Calibration of a New Optical Plankton Counter Capable of Sizing Small Zooplankton. *Deep-Sea Research Part A Oceanographic Research Papers*, *39*(3-4A), 395–415. (Cited pages 11, 44, and 45.)

Herman, A. W., Beanlands, B., & Phillips, E. F. (2004). The next generation of Optical Plankton Counter: the Laser-OPC. *Journal of Plankton Research*, *26*(10), 1135–1145. (Cited pages 11 and 44.)

Hernández-León, S., & Montero, I. (2006). Zooplankton biomass estimated from digitalized images in Antarctic waters: A calibration exercise. *Journal of Geophysical Research-Oceans*, *111*(C5). (Cited pages xxvi, xxxiii, 46, 61, 62, 63, and 169.)

Hirst, A. G., & Bunker, A. J. (2003). Growth of marine planktonic copepods: Global rates and patterns in relation to chlorophyll a, temperature, and body weight. *Limnology and Oceanography*, *48*(5), 1988–2010. (Cited page 22.)

Holt, J. T., Allen, J. I., Proctor, R., & Gilbert, F. (2005). Error quantification of a high-resolution coupled hydrodynamic-ecosystem coastal-ocean model: Part 1 model overview and assessment of the hydrodynamics. *Journal of Marine Systems*, *57*(1-2), 167–188. (Cited pages 120 and 174.)

Hsieh, C. H., Glaser, S. M., Lucas, A. J., & Sugihara, G. (2005). Distinguishing random environmental fluctuations from ecological catastrophes for the north pacific ocean. *Nature*, *435*(7040), 336–340. (Cited page 32.)

Huntley, M., & Boyd, C. (1984). Food-limited growth of marine zooplankton. *American Naturalist*, *124*(4), 455–478. (Cited page 22.)

Hurrell, J. W. (1995). Decadal Trends in the North Atlantic Oscillation - Regional temperature and precipitations. *Science*, *269*(5224), 676–679. (Cited page 108.)

Hurrell, J. W., & Deser, C. (2010). North Atlantic climate variability: The role of the North Atlantic Oscillation. *Journal of Marine Systems*, *79*(3-4), 231–244. (Cited pages 5 and 108.)

Ibañez, F., Fromentin, J. M., & Castel, J. (1993). Application of the cumulated function to the processing of chronological data in oceanography. *Comptes Rendus De L Academie Des Sciences Serie Iii-sciences De La Vie-life Sciences*, *316*(8), 745–748. (Cited pages xxviii, 32, 33, 84, and 87.)

IPCC (2007). *Contribution of Working Group I to the Fourth Assessment Report of the Intergovernmental Panel on Climate Change*. Cambridge University Press. (Cited pages 112 and 181.)

Irigoien, X., Fernandes, J. A., Grosjean, P., Denis, K., Albaina, A., & Santos, M. (2009). Spring zooplankton distribution in the bay of biscay from 1998 to 2006 in relation with anchovy recruitment. *Journal of Plankton Research*, *31*(1), 1–17. (Cited pages 29, 43, 44, 45, 51, 167, and 168.)

Jackson, G. A. (1990). A Model of the Formation of Marine Algal Flocs by Physical Coagulation Processes. *Deep-Sea Research Part a-Oceanographic Research Papers*, *37*(8), 1197–1211. (Cited page 10.)

Jackson, G. A., & Burd, A. B. (1998). Aggregation in the marine environment. *Environmental Science & Technology*, *32*(19), 2805–2814. (Cited page 10.)

Jackson, G. A., & Kiorboe, T. (2004). Zooplankton use of chemodetection to find and eat particles. *Marine Ecology-Progress Series*, *269*, 153–162. (Cited page 10.)

Jackson, G. A., Logan, B. E., Alldredge, A. L., & Dam, H. G. (1995). Combining Particle-Size Spectra from a Mesocosm Experiment Measured Using Photographic and Aperture Impedance (Coulter and Elzone) Techniques. *Deep-Sea Research Part Ii-Topical Studies in Oceanography*, *42*(1), 139–157. (Cited pages 10, 11, and 19.)

Jeffries, H. P., Berman, M. S., Poularikas, A. D., Katsinis, C., Melas, I., Sherman, K., & Bivins, L. (1984). Automated Sizing, Counting and Identification of Zooplankton by Pattern-Recognition. *Marine Biology*, *78*(3), 329–334. (Cited pages 11 and 43.)

Jennings, S., Greenstreet, S. P. R., Hill, L., Piet, G. J., Pinnegar, J. K., & Warr, K. J. (2002). Long-term trends in the trophic structure of the north sea fish community: evidence from stable-isotope analysis, size-spectra and community metrics. *Marine Biology*, *141*, 1085–1097. (Cited page 19.)

Jimenez, F., Rodriguez, J., Bautista, B., & Rodriguez, V. (1987). Relations between chlorophyll, phytoplankton cell abundance and biovolume during a winter bloom in mediterranean coastal waters. *Journal of Experimental Marine Biology and Ecology*, *105*(2-3), 161–173. (Cited page 151.)

Karagiannidis, A. F., Bloutsos, A. A., Maheras, P., & Sachsamanoglou, C. (2008). Some statistical characteristics of precipitation in Europe. *Theoretical and Applied Climatology*, *91*(1-4), 193–204. (Cited pages 108 and 110.)

Katara, I., Illian, J., Pierce, G. J., Scott, B., & Wang, J. J. (2008). Atmospheric forcing on chlorophyll concentration in the Mediterranean. *Hydrobiologia*, *612*, 33–48. (Cited page 100.)

Kerr, R. A. (1992). Unmasking a shifty climate system. *Science*, *255*(5051), 1508–1510. (Cited page 32.)

Kiorboe, T. (2001). Formation and fate of marine snow: small-scale processes with large-scale implications. *Scientia Marina*, *65*, 57–71. (Cited page 10.)

Kirby, R. R., & Beaugrand, G. (2009). Trophic amplification of climate warming. *Proceedings of the Royal Society B-Biological Sciences*, *276*(1676), 4095–4103. (Cited page 3.)

Klaas, C., Verity, P. G., & Schultes, S. (2008). Determination of copepod grazing on natural plankton communities: correcting for trophic cascade effects. *Marine Ecology-progress Series*, *357*, 195–206. (Cited page 107.)

Knight, J. R., Allan, R. J., Folland, C. K., Vellinga, M., & Mann, M. E. (2005). A signature of persistent natural thermohaline circulation cycles in observed climate. *Geophysical Research Letters*, *32*(20). (Cited page 108.)

Knight, J. R., Folland, C. K., & Scaife, A. A. (2006). Climate impacts of the Atlantic Multidecadal Oscillation. *Geophysical Research Letters*, *33*(17). (Cited pages 108 and 109.)

Kooijman, S. A. L. M. (1986). Energy budgets can explain body size relations. *Journal of Theoretical Biology*, *121*(3), 269–282. (Cited pages 9 and 20.)

Kooijman, S. A. L. M. (2001). Quantitative aspects of metabolic organization: a discussion of concepts. *Philosophical Transactions of the Royal Society of London Series B-biological Sciences*, *356*(1407), 331–349. (Cited pages 9, 19, 20, 21, 134, and 175.)

Korath, J. M., Abbas, A., & Romagnoli, J. A. (2008). A clustering approach for the separation of touching edges in particle images. *Particle & Particle Systems Characterization*, *25*(2), 142–153. (Cited pages 45, 54, and 169.)

Korres, G., & Lascaratos, A. (2003). A one-way nested eddy resolving model of the aegean and levantine basins: implementation and climatological runs. *Annales Geophysicae*, *21*(1), 205–220. (Cited page 119.)

Kriest, I., & Evans, G. T. (2000). A vertically resolved model for phytoplankton aggregation. *Proceedings of the Indian Academy of Sciences-Earth and Planetary Sciences*, *109*(4), 453–469. (Cited page 10.)

Lacroix, G., & Grégoire, A. (2002). Revisited ecosystem model (modecogel) of the ligurian sea: seasonal and interannual variability due to atmospheric forcing. *Journal of Marine Systems*, *37*(4), 229–258. (Cited pages 84, 85, 120, and 149.)

Laval, P. (1974). Mathematical-Model for Avoidance of Net by Plankton, Its Practical Application, and Its Indirect Verification in Recurrence of Parasitism of Pelagic Amphipod Vibilia-Armata Bovallius. *Journal of Experimental Marine Biology and Ecology*, *14*(1), 57–87. (Cited pages 44 and 50.)

Le Quere, C., Harrison, S. P., Prentice, I. C., Buitenhuis, E. T., Aumont, O., Bopp, L., Claustre, H., Da Cunha, L. C., Geider, R., Giraud, X., Klaas, C., Kohfeld, K. E., Legendre, L., Manizza, M., Platt, T., Rivkin, R. B., Sathyendranath, S., Uitz, J., Watson, A. J., & Wolf-Gladrow, D. (2005). Ecosystem dynamics based on plankton functional types for global ocean biogeochemistry models. *Global Change Biology*, *11*(11), 2016–2040. (Cited pages 18 and 119.)

Leaman, K. D., & Schott, F. A. (1991). Hydrographic structure of the convection regime in the gulf of lions - winter 1987. *Journal of Physical Oceanography*, *21*(4), 575–598. (Cited page 99.)

Lehette, P., & Hernández-León, S. (2009). Zooplankton biomass estimation from digitized images: a comparison between subtropical and Antarctic organisms. *Limnology and Oceanography: Methods*, *7*, 304–308. (Cited pages xxvi, xxxiii, 46, 61, 62, 63, and 169.)

Lehodey, P., Chai, F., & Hampton, J. (2003). Modelling climate-related variability of tuna populations from a coupled ocean-biogeochemical-populations dynamics model. *Fisheries Oceanography*, *12*(4-5), 483–494. (Cited page 119.)

Levy, M., Memery, L., & Madec, G. (1998). The onset of a bloom after deep winter convection in the northwestern mediterranean sea: mesoscale process study with a primitive equation model. *Journal of Marine Systems*, *16*(1-2), 7–21. (Cited page 4.)

Lewis, K., Allen, J. I., Richardson, A. J., & Holte, J. T. (2006). Error quantification of a high resolution coupled hydrodynamic-ecosystem coastal-ocean model: Part3, validation with continuous plankton recorder data. *Journal of Marine Systems*, *63*(3-4), 209–224. (Cited pages 120 and 174.)

Liebig, J. R., Vanderploeg, H. A., & Ruberg, S. A. (2006). Factors affecting the performance of the optical plankton counter in large lakes: Insights from Lake Michigan and laboratory studies. *Journal of Geophysical Research-Oceans*, *111*(C5), 10. (Cited pages 44 and 167.)

Ludwig, W., Dumont, E., Meybeck, M., & Heussner, S. (2009). River discharges of water and nutrients to the mediterranean and black sea: Major drivers for ecosystem changes during past and future decades? *Progress In Oceanography*, *80*(3-4), 199–217. (Cited page 99.)

MacIntyre, H. L., Kana, T. M., Anning, T., & Geider, R. J. (2002). Photoacclimation of photosynthesis irradiance response curves and photosynthetic pigments in microalgae and cyanobacteria. *Journal of Phycology*, *38*(1), 17–38. (Cited page 104.)

Mackas, D. L., & Beaugrand, G. (2010). Comparisons of zooplankton time series. *Journal of Marine Systems*, *79*(3-4), 286–304. (Cited page 3.)

Malpica, N., deSolorzano, C. O., Vaquero, J. J., Santos, A., Vallcorba, I., GarciaSagredo, J. M., & delPozo, F. (1997). Applying watershed algorithms to the segmentation of clustered nuclei. *Cytometry*, *28*(4), 289–297. (Cited pages 45, 54, and 169.)

Manriquez, K., Escribano, R., & Hidalgo, P. (2009). The influence of coastal upwelling on the mesozooplankton community structure in the coastal zone off Central/Southern Chile as assessed by automated image analysis. *Journal of Plankton Research*, *31*(9), 1075–1088. (Cited pages 43 and 45.)

Mantua, N. J. (2004). Methods for detecting regime shifts in large marine ecosystems: a review with approaches applied to north pacific data. *Progress In Oceanography*, *60*, 165–182. (Cited page 33.)

Mantua, N. J., Hare, S. R., Zhang, Y., Wallace, J. M., & Francis, R. C. (1997). A pacific interdecadal climate oscillation with impacts on salmon production. *Bulletin of the American Meteorological Society*, *78*(6), 1069–1079. (Cited page 32.)

Mariotti, A., Zeng, N., & Lau, K. M. (2002). Euro-Mediterranean rainfall and ENSO - a seasonally varying relationship. *Geophysical Research Letters*, *29*(12), 4. (Cited pages 108 and 110.)

Marquet, P. A., Quiñones, R. A., Abades, S., Labra, F., Tognelli, M., Arim, M., & Rivadeneira, M. (2005). Scaling and power-laws in ecological systems. *The Journal of Experimental Biology*, *208*, 1749–1769. (Cited page 8.)

Marshall, J., & Schott, F. (1999). Open-ocean convection: Observations, theory, and models. *Reviews of Geophysics*, *37*(1), 1–64. (Cited page 98.)

Marty, J. C. (2002). The DYFAMED time-series program (French-JGOFS) - Preface. *Deep-Sea Research Part Ii-Topical Studies in Oceanography*, *49*(11), 1963–1964. (Cited page 24.)

Marty, J. C., & Chiavérini, J. (2010). Hydrological changes in the Ligurian Sea (NW Mediterranean, DYFAMED site) during 1995-2007 and biogeochemical consequences. *Biogeosciences Discuss.*, *7*, 1377–1406. (Cited pages 7, 24, 69, 70, 99, 100, 103, 113, and 174.)

Mauchline, J. (1998). The biology of calanoid copepods. *Advances In Marine Biology*, *33*, 710 pp. (Cited page 3.)

Maury, O., Faugeras, B., Shin, Y.-J., Poggiale, J.-C., Ari, T. B., & Marsac, F. (2007a). Modeling environmental effects on the size-structured energy flow through marine ecosystems. Part 1: The model. *Progress In Oceanography*, *74*(4), 479–499. (Cited pages 8, 10, 19, 20, 23, 120, 121, 132, 134, 137, 159, and 175.)

Maury, O., Shin, Y.-J., Faugeras, B., Ari, B. T., & Marsac, F. (2007b). Modeling environmental effects on the size-structured energy flow through marine ecosystems. Part 2: Simulations. *Progress In Oceanography*, *74*(4), 500–514. (Cited pages 8, 20, and 21.)

Mazzocchi, M. G., Christou, E. D., Di Capua, I., de Puelles, M. L. F., Fonda-Umani, S., Molinero, J. C., Nival, P., & Siokou-Frangou, I. (2007). Temporal variability of Centropages typicus in the Mediterranean Sea over seasonal-to-decadal scales. *Progress in Oceanography*, *72*(2-3), 214–232. (Cited page 5.)

Mazzocchi, M. G., González, H. E., Vandromme, P., Borrione, I., Ribera d'Alcala, M. R., Gauns, M., Assmy, P., Fuchs, B., Klaas, C., Martin, P., Montresor, M., Ramaiah, N., Naqvi, S. W. A., & Smetacek, V. (2009). A non-diatom plankton bloom controlled by copepod grazing and amphipod predation: Preliminary results from the lohafex iron-fertilisation experiment. *Globec International Newsletter*, *15*(2), 3–6. (Cited page 39.)

McGowan, J. A., & Fraundorf, V. J. (1966). The Relationship Between Size of Net Used and Estimates of Zooplankton Diversity. *Limnology and Oceanography*, *11*(4), 456–469. (Cited page 44.)

Menard, F., Fromentin, J. M., Goy, J., & Dallot, S. (1997). Temporal fluctuations of doliolid abundance in the bay of villefranche-sur-mer (northwestern mediterranean sea) from 1967 to 1990. *Oceanologica Acta*, *20*(5), 733–742. (Cited page 70.)

Meybeck, M., Durr, H. H., Roussennac, S., & Ludwig, W. (2007). Regional seas and their interception of riverine fluxes to oceans. *Marine Chemistry*, *106*(1-2), 301–325. (Cited page 4.)

Micheli, F., Cottingham, K. L., Bascompte, J., Bjornstad, O. N., Eckert, G. L., Fischer, J. M., Keitt, T. H., Kendall, B. E., Klug, J. L., & Rusak, J. A. (1999). The dual nature of community variability. *Oikos*, *85*(1), 161–169. (Cited page 102.)

Mieruch, S., Freund, J. A., Feudel, U., Boersma, M., Janisch, S., & Wiltshire, K. H. (2010). A new method of describing phytoplankton blooms: Examples from helgoland roads. *Journal of Marine Systems*, *79*(1-2), 36–43. (Cited page 84.)

Millero, F. J., & Poisson, A. (1981). International one-atmosphere equation of state of seawater. *Deep-Sea Research Part a-Oceanographic Research Papers*, *28*(6), 625–629. (Cited page 94.)

Millot, C. (1999). Circulation in the Western Mediterranean Sea. *Journal of Marine Systems*, *20*(1-4), 423–442. (Cited pages 4 and 23.)

Min, D., Zhilin, L., & Xiaoyong, C. (2007). Extended Hausdorff distance for spatial objects in GIS. *International Journal of Geographical Information Science*, *21*(4), 459–475. (Cited pages 36 and 37.)

Molinero, J. C., Ibañez, F., Nival, P., Buecher, E., & Souissi, S. (2005). North Atlantic climate and northwestern Mediterranean plankton variability. *Limnology and Oceanography*, *50*(4), 1213–1220. (Cited pages 5, 69, 70, 108, 113, 170, 179, and 180.)

Molinero, J. C., Ibañez, F., Souissi, S., Buecher, E., Dallot, S., & Nival, P. (2008). Climate control on the long-term anomalous changes of zooplankton communities in the Northwestern Mediterranean. *Global Change Biology*, *14*(1), 11–26. (Cited pages 5, 6, 69, 70, 108, 113, 170, 179, and 180.)

Moloney, C. L., & Field, J. G. (1991). The Size-Based Dynamics of Plankton Food Webs .1. a Simulation-Model of Carbon and Nitrogen Flows. *Journal of Plankton Research*, *13*(5), 1003–1038. (Cited pages 7, 8, 19, and 119.)

Moloney, C. L., Field, J. G., & Lucas, M. I. (1991). The Size-Based Dynamics of Plankton Food Webs .2. Simulations of 3 Contrasting Southern Benguela Food Webs. *Journal of Plankton Research*, *13*(5), 1039–1092. (Cited page 8.)

Morán, X. A. G., & Estrada, M. (2005). Winter pelagic photosynthesis in the NW Mediterranean. *Deep-Sea Research Part I-Oceanographic Research Papers*, *52*(10), 1806–1822. (Cited page 104.)

Morowitz, H. J. (1968). *Energy flow in biology*. Academic Press, New-York and London. (Cited page 119.)

Mozetic, P., Solidoro, C., Cossarini, G., Socal, G., Precali, R., France, J., Bianchi, F., De Vittor, C., Smodlaka, N., & Umani, S. (2010). Recent trends towards oligotrophication of the northern adriatic: Evidence from chlorophyll a time series. *Estuaries and Coasts*, *33*(2), 362–375. (Cited pages 5 and 172.)

Msadek, R., & Frankignoul, C. (2009). Atlantic multidecadal oceanic variability and its influence on the atmosphere in a climate model. *Climate Dynamics*, *33*(1), 45–62. (Cited pages 108, 109, 110, 112, and 180.)

Mysterud, A., Stenseth, N. C., Yoccoz, N. G., Ottersen, G., & Langvatn, R. (2003). The response of the terrestrial ecosystems to climate variability associated with the North Atlantic Oscillation. In J. W. Hurrell, Y. Kushnir, G. Ottersen, & M. Visbeck (Eds.) *The North Atlantic Oscillation*, (pp. 235–262). Washington: American Geophysical Union. (Cited page 3.)

Nejstgaard, J. C., Hygum, B. H., Naustvoll, L. J., & Bamstedt, U. (2001). Zooplankton growth, diet and reproductive success compared in simultaneous diatom- and flagellate-microzooplankton-dominated plankton blooms. *Marine Ecology-progress Series*, *221*, 77–91. (Cited page 107.)

Nezlin, N. P., Lacroix, G., Kostianoy, A. G., & Djenidi, S. (2004). Remotely sensed seasonal dynamics of phytoplankton in the Ligurian Sea in 1997-1999. *Journal of Geophysical Research-Oceans*, *109*(C7). (Cited pages 7, 100, 104, and 172.)

Nichols, J. H., & Thompson, A. B. (1991). Mesh Selection of Copepodite and Nauplius Stages of 4 Calanoid Copepod Species. *Journal of Plankton Research*, *13*(3), 661–671. (Cited pages 43, 49, 50, 167, 197, and 199.)

Nisbet, R. M., Muller, E. B., Lika, K., & Kooijman, S. (2000). From molecules to ecosystems through dynamic energy budget models. *Journal of Animal Ecology*, *69*(6), 913–926. (Cited pages 9, 10, and 20.)

Nival, P., Nival, S., & Thiriot, A. (1975). Influence des conditions hivernales sur les productions phyto- et zooplanctoniques en méditerranée nord-occidentale. *Marine Biology*, *31*, 249–270. (Cited page 102.)

O'Connor, M. P., Kemp, S. J., Agosta, S. J., Hansen, F., Sieg, A. E., Wallace, B. P., McNair, J. N., & Dunham, A. E. (2007). Reconsidering the mechanistic basis of the metabolic theory of ecology. *Oikos*, *116*(6), 1058–1072. (Cited page 8.)

Orfila, A., Alvarez, A., Tintore, J., Jordi, A., & Basterretxea, G. (2005). Climate teleconnections at monthly time scales in the Ligurian Sea inferred from satellite data. *Progress in Oceanography*, *66*(2-4), 157–170. (Cited pages 108 and 110.)

Ortner, P. B., Cummings, S. R., & Aftring, R. P. (1979). Silhouette Photography of Oceanic Zooplankton. *Nature*, *277*(5691), 50–51. (Cited page 12.)

Parsons, T. R. (1969). The use of particle size spectra in determining the structure of plankton community. *J. Oceanogr. Soc. Japan*, *25*, 172–181. (Cited pages 11 and 31.)

Perry, R. I., Batchelder, H. P., Mackas, D. L., Chiba, S., Durbin, E., Greve, W., & Verheye, H. M. (2004). Identifying global synchronies in marine zooplankton populations: issues and opportunities. *Ices Journal of Marine Science*, *61*(4), 445–456. (Cited page 4.)

Person-Le Ruyet, J., Razouls, C., & Razouls, S. (1975). Biologie comparée entre espèces vicariantes et communes de copépodes dans un écosystème néritique en méditerranée et en manche. *Vie et Milieu*, *25 B*, 283–312. (Cited page 137.)

Peters, R. H., & Wassenberg, K. (1983). The effect of body size on animal abundance. *Oecologia*, *60*(1), 89–96. (Cited pages 7, 8, and 9.)

Petihakis, G., Triantafyllou, G., Tsiaras, K., Korres, G., Pollani, A., & Hoteit, I. (2009). Eastern mediterranean biogeochemical flux model - simulations of the pelagic ecosystem. *Ocean Science*, *5*(1), 29–46. (Cited pages 120 and 174.)

Pinardi, N., & Masetti, E. (2000). Variability of the large scale general circulation of the mediterranean sea from observations and modelling: a review. *Palaeogeography Palaeoclimatology Palaeoecology*, *158*(3-4), 153–174. (Cited page 4.)

Platt, T., & Denman, K. (1977). Organization in Pelagic Ecosystem. *Helgolander Wissenschaftliche Meeresuntersuchungen*, *30*(1-4), 575–581. (Cited pages 7, 12, 14, 15, 20, and 30.)

Prieur, L., Bethoux, J. P., Bong, J. H., & Tailliez, D. (1983). Particularités hydrologiques et formation d'eau profonde dans le basin liguro-provençal en 1981-1982. *Rapport Commission Internationale sur la Mer Méditerranée*, *28*, 51–53. (Cited page 23.)

Quiñones, R. A., Platt, T., & Rodriguez, J. (2003). Patterns of biomass-size spectra from oligotrophic waters of the Northwest Atlantic. *Progress in Oceanography*, *57*, 405–427. (Cited pages 72 and 140.)

Quintana, X. D., Brucet, S., Boix, D., Lopez-Flores, R., Gascon, S., Badosa, A., Sala, J., Moreno-Amich, R., & Egozcue, J. J. (2008). A nonparametric method for the measurement of size diversity

with emphasis on data standardization. *Limnology and Oceanography: Methods*, *6*, 75–86. (Cited pages 31 and 43.)

Raick, C., Delhez, E. J. M., Soetaert, K., & Gregoire, M. (2005). Study of the seasonal cycle of the biogeochemical processes in the ligurian sea using a id interdisciplinary model. *Journal of Marine Systems*, *55*(3-4), 177–203. (Cited pages 84, 85, 120, 137, and 149.)

Rakotomalala, R. (2005). TANAGRA : une plate-forme d'expérimentation pour la fouille de données. *MODULAD*, *32*, 71–85. (Cited page 28.)

Rasband, W. S. (2005). ImageJ http://rsb.info.nih.gov/ij/. *U. S. National Institutes of Health*. (Cited page 26.)

Rayner, N. A., Brohan, P., Parker, D. E., Folland, C. K., Kennedy, J. J., Vanicek, M., Ansell, T. J., & Tett, S. F. B. (2006). Improved analyses of changes and uncertainties in sea surface temperature measured in situ sice the mid-nineteenth century: The hadsst2 dataset. *Journal of Climate*, *19*(3), 446–469. (Cited page 110.)

Reid, P. C., Borges, M. D., & Svendsen, E. (2001). A regime shift in the north sea circa 1988 linked to changes in the north sea horse mackerel fishery. *Fisheries Research*, *50*(1-2), 163–171. (Cited page 5.)

Reid, P. C., Edwards, M., Beaugrand, G., Skogen, M., & Stevens, D. (2003). Periodic changes in the zooplankton of the north sea during the twentieth century linked to oceanic inflow. *Fisheries Oceanography*, *12*(4-5), 260–269. (Cited page 5.)

Richardson, A. J. (2008). In hot water: zooplankton and climate change. *Ices Journal of Marine Science*, *65*(3), 279–295. (Cited page 3.)

Rodionov, S. N. (2004). A sequential algorithm for testing climate regime shifts. *Geophysical Research Letters*, *31*(9), L09204. (Cited pages xxvii, xxxii, 32, 33, 34, 35, 79, 80, and 189.)

Rodionov, S. N. (2006). Use of prewhitening in climate regime shift detection. *Geophysical Research Letters*, *33*(12). (Cited pages xxvii, xxxii, 32, 34, 35, 73, 79, 80, and 189.)

Rogers, J. C., & McHugh, M. J. (2002). On the separability of the north atlantic oscillation and arctic oscillation. *Climate Dynamics*, *19*(7), 599–608. (Cited page 110.)

Rolke, M., & Lenz, J. (1984). Size Structure-Analysis of Zooplankton Samples by Means of an Automated Image Analyzing System. *Journal of Plankton Research*, *6*(4), 637–645. (Cited pages 11 and 43.)

Roman, M. R. (1977). Feeding of copepod acartia-tonsa on diatom nitzschia-closterium and brown-algae (fucus-vesiculosus) detritus. *Marine Biology*, *42*(2), 149–155. (Cited page 137.)

Rowell, D. P. (2003). The impact of mediterranean ssts on the sahelian rainfall season. *Journal of Climate*, *16*(5), 849–862. (Cited page 109.)

Rucklidge, W. J. (1996). Lower bounds for the complexity of the graph of the hausdorff distance as a function of transformation. *Discrete & Computational Geometry*, *16*(2), 135–153. (Cited page 36.)

Ruiz, J. (1994). The measurement of size diversity in the pelagic ecosystem. *Scienta Marina*, *58*(1-2), 103–107. (Cited page 31.)

Saiz, E., & Calbet, A. (2007). Scaling of feeding in marine calanoid copepods. *Limnology and Oceanography*, *52*(2), 668–675. (Cited pages 138 and 175.)

Schmitt, F. G., & Seuront, L. (2001). Multifractal random walk in copepod behavior. *Physica a-Statistical Mechanics and Its Applications*, *301*(1-4), 375–396. (Cited pages 10 and 35.)

Schmitt, F. G., Seuront, L., Hwang, J. S., Souissi, S., & Tseng, L. C. (2006). Scaling of swimming sequences in copepod behavior: Data analysis and simulation. *Physica A-statistical Mechanics and Its Applications*, *364*, 287–296. (Cited pages 10 and 35.)

Schneider, E. D., & Kay, J. J. (1994). Life as a Manifestation of the 2nd Law of Thermodynamics. *Mathematical and Computer Modelling*, *19*(6-8), 25–48. (Cited pages 17 and 18.)

Schott, F., Visbeck, M., & Fischer, J. (1993). Observations of vertical currents and convection in the central greenland sea during the winter of 1988-1989. *Journal of Geophysical Research-oceans*, *98*(C8), 14401–14421. (Cited page 98.)

Schwaighofer, A., Schroeter, T., Mika, S., & Blanchard, G. (2009). How Wrong Can We Get? A Review of Machine Learning Approaches and Error Bars. *Combinatorial Chemistry & High Throughput Screening*, *12*(5), 453–468. (Cited page 28.)

Sciandra, A., Gostan, J., Collos, Y., Descolas-Gros, C., Leboulanger, C., Martin-Jezequel, V., Denis, M., Lefevre, D., Copin-Montegut, C., & Avril, B. (1997). Growth-compensating phenomena in continuous cultures of Dunaliella tertiolecta limited simultaneously by light and nitrate. *Limnology and Oceanography*, *42*(6), 1325–1339. (Cited page 104.)

Shannon, C. E. (1948). A Mathematical Theory of Communication. *Bell System Technical Journal*, *27*(3), 379–423. (Cited page 31.)

Sheldon, R. W., Evelyn, T. P. T., & Parsons, T. R. (1967). On Occurrence and Formation of Small Particles in Seawater. *Limnology and Oceanography*, *12*(3), 367–&. (Cited page 45.)

Sheldon, R. W., & Kerr, S. R. (1972). Population-Density of Monsters in Loch-Ness. *Limnology and Oceanography*, *17*(5), 796–798. (Cited page 7.)

Sheldon, R. W., Sutcliffe, W. H., & Paranjape, M. A. (1977). Structure of Pelagic Food-Chain and Relationship between Plankton and Fish Production. *Journal of the Fisheries Research Board of Canada*, *34*(12), 2344–2353. (Cited pages 12 and 14.)

Sheldon, R. W., Sutcliffe, W. H., & Prakash, A. (1972). Size Distribution of Particles in Ocean. *Limnology and Oceanography*, *17*(3), 327–&. (Cited pages 7, 17, and 140.)

Shurin, J. B., Borer, E. T., Seabloom, E. W., Anderson, K., Blanchette, C. A., Broitman, B., Cooper, S. D., & Halpern, B. S. (2002). A cross-ecosystem comparison of the strength of trophic cascades. *Ecology Letters*, *5*(6), 785–791. (Cited page 102.)

Sieracki, C. K., Sieracki, M. E., & Yentsch, C. S. (1998). An imaging-in-flow system for automated analysis of marine microplankton. *Marine Ecology Progress Series*, *168*, 285–296. (Cited pages 12 and 44.)

Sigaud, O., & Wilson, S. W. (2007). Learning classifier systems: a survey. *Soft Computing*, *11*(11), 1065–1078. (Cited page 28.)

Silvert, W., & Platt, T. (1978). Energy flux in the pelagic ecosystem: a time dependent equation. *Limnology and Oceanography*, *23*(4), 813–816. (Cited pages 12, 14, and 15.)

Siokou-Frangou, I., Christaki, U., Mazzocchi, M. G., Montresor, M., d'Alcala, M. R., Vaque, D., & Zingone, A. (2010). Plankton in the open mediterranean sea: a review. *Biogeosciences*, *7*(5), 1543–1586. (Cited pages 4, 5, and 172.)

Skliris, N., & Djenidi, S. (2006). Plankton dynamics controlled by hydrodynamic processes near a submarine canyon off NW corsican coast: A numerical modelling study. *Continental Shelf Research*, *26*(11), 1336–1358. (Cited page 120.)

Skliris, N., Elkalay, K., Goffart, A., Frangoulis, C., & Hecq, J. H. (2001). One-dimensional modelling of the plankton ecosystem of the north-western Corsican coastal area in relation to meteorological constraints. *Journal of Marine Systems*, *27*(4), 337–362. (Cited pages 103, 120, and 174.)

Skliris, N., Sofianos, S., & Lascaratos, A. (2007). Hydrological changes in the Mediterranean Sea in relation to changes in the freshwater budget: A numerical modelling study. *Journal of Marine Systems*, *65*(1-4), 400–416. (Cited pages 99 and 181.)

Smetacek, V. S. (1985). Role of Sinking in Diatom Life-History Cycles - Ecological, Evolutionary and Geological Significance. *Marine Biology*, *84*(3), 239–251. (Cited page 3.)

Sommer, U. (2008). Trophic Cascades in Marine and Freshwater Plankton. *International Review of Hydrobiology*, *93*(4-5), 506–516. (Cited pages 102 and 172.)

Sommer, U., & Sommer, F. (2006). Cladocerans versus copepods: the cause of contrasting top-down controls on freshwater and marine phytoplankton. *Oecologia*, *147*(2), 183–194. (Cited page 102.)

Soriano, L. R., De Pablo, F., & Tomas, C. (2004). Impact of the north atlantic oscillation on winter convection: Convective precipitation and cloud-to-ground lightning. *International Journal of Climatology*, *24*(10), 1241–1247. (Cited page 98.)

Sournia, A. (1973). La production primaire planctonique en méditerranée; essai de mise à jour. *Cybium, Cooperative investigation in the Mediterranean*, *81*. (Cited page 5.)

Sousa, T., Domingos, T., & Kooijman, S. (2008). From empirical patterns to theory: a formal metabolic theory of life. *Phylosophical Transactions of the Royal Society B*. (Cited page 9.)

Sousa, T., Mota, R., Domingos, T., & Kooijman, S. (2006). Thermodynamics of organisms in the context of dynamic energy budget theory. *Physical Review E*, *74*(5). (Cited page 9.)

Sprules, W. G., Bergstrom, B., Cyr, H., Hargraves, B. R., Kilham, S. S., MacIsaac, H. J., Matsushita, K., Stemberger, R. S., & Williams, R. (1992). Non-video optical instruments for studying zooplankton distribution and abundance. *Archiv für Hydrobiologie Beiheft Ergebnisse der Limnologie*, *36*, 45–58. (Cited pages 44 and 167.)

Sprules, W. G., Jin, E. H., Herman, A. W., & Stockwell, J. D. (1998). Calibration of an optical plankton counter for use in fresh water. *Limnology and Oceanography*, *43*(4), 726–733. (Cited pages 30, 44, 45, and 167.)

Stanley, E. H. (1995). Power laws and universality. *Nature*, *378*, 554. (Cited page 8.)

Steinacher, M., Joos, F., Frolicher, T. L., Bopp, L., Cadule, P., Cocco, V., Doney, S. C., Gehlen, M., Lindsay, K., Moore, J. K., Schneider, B., & Segschneider, J. (2010). Projected 21st century decrease in marine productivity: a multi-model analysis. *Biogeosciences*, *7*(3), 979–1005. (Cited pages 5 and 172.)

Stemmann, L., Eloire, D., Sciandra, A., Jackson, G. A., Guidi, L., Picheral, M., & Gorsky, G. (2008). Volume distribution for particles between 3.5 to 2000 mu m in the upper 200 m region of the South Pacific Gyre. *Biogeosciences*, *5*(2), 299–310. (Cited page 44.)

Stemmann, L., Jackson, G. A., & Gorsky, G. (2004a). A vertical model of particle size distributions and fluxes in the midwater column that includes biological and physical processes - Part II: application to a three year survey in the NW Mediterranean Sea. *Deep-Sea Research Part I-Oceanographic Research Papers*, *51*(7), 885–908. (Cited page 10.)

Stemmann, L., Jackson, G. A., & Ianson, D. (2004b). A vertical model of particle size distributions and fluxes in the midwater column that includes biological and physical processes - Part I: model formulation. *Deep-Sea Research Part I-Oceanographic Research Papers*, *51*(7), 865–884. (Cited page 10.)

Stenseth, N. C., & Mysterud, A. (2003). Adaptive herbivore ecology - From resources to populations in variable environments. *Science*, *299*(5606), 518–518. (Cited pages 3 and 112.)

Stenseth, N. C., Ottersen, G., Hurrell, J. W., Mysterud, A., Lima, M., Chan, K. S., Yoccoz, N. G., & Adlandsvik, B. (2003). Studying climate effects on ecology through the use of climate indices: the

North Atlantic Oscillation, El Nino Southern Oscillation and beyond. *Proceedings of the Royal Society of London Series B-Biological Sciences*, *270*(1529), 2087–2096. (Cited page 108.)

Stock, C. A., Powell, T. M., & Levin, S. A. (2008). Bottom-up and top-down forcing in a simple size-structured plankton dynamics model. *Journal of Marine Systems*, *74*(1-2), 134–152. (Cited page 8.)

Straile, D. (1997). Gross growth efficiencies of protozoan and metazoan zooplankton and their dependence on food concentration, predator-prey weight ratio, and taxonomic group. *Limnology and Oceanography*, *42*(6), 1375–1385. (Cited page 137.)

Strickland, J. D. H., & Parsons, T. R. (1977). *A practical handbook of seawater analysis*. Queen's Printer, Ottawa. (Cited page 71.)

Sutton, R. T., & Hodson, D. L. R. (2005). Atlantic ocean forcing of north american and european summer climate. *Science*, *309*(5731), 115–118. (Cited pages 109, 110, 112, and 180.)

Tanaka, T., Rassoulzadegan, F., & Thingstad, T. F. (2004). Orthophosphate uptake by heterotrophic bacteria, cyanobacteria, and autotrophic nanoflagellates in Villefranche Bay, northwestern Mediterranean: Vertical, seasonal, and short-term variations of the competitive relationship for phosphorus. *Limnology and Oceanography*, *49*(4), 1063–1072. (Cited page 153.)

Taylor, A. H., Allen, J. I., & Clark, P. A. (2002). Extraction of a weak climatic signal by an ecosystem. *Nature*, *416*(6881), 629–632. (Cited page 4.)

Thiebaux, M. L., & Dickie, L. M. (1993). Structure of the body-size spectrum of the biomass in aquatic ecosystems - a consequence of allometry in predator-prey interactions. *Canadian Journal of Fisheries and Aquatic Sciences*, *50*(6), 1308–1317. (Cited page 15.)

Thingstad, T. F., Krom, M. D., Mantoura, R. F. C., Flaten, G. A. F., Groom, S., Herut, B., Kress, N., Law, C. S., Pasternak, A., Pitta, P., Psarra, S., Rassoulzadegan, F., Tanaka, T., Tselepides, A., Wassmann, P., Woodward, E. M. S., Riser, C. W., Zodiatis, G., & Zohary, T. (2005). Nature of phosphorus limitation in the ultraoligotrophic eastern mediterranean. *Science*, *309*(5737), 1068–1071. (Cited pages 5, 153, and 174.)

Thomasson, M. A., Johnson, M. L., Stromberg, J. O., & Gaten, E. (2003). Swimming capacity and pleopod beat rate as a function of sex, size and moult stage in northern krill meganyctiphanes norvegica. *Marine Ecology-progress Series*, *250*, 205–213. (Cited pages 44 and 50.)

Thompson, D. W. J., & Wallace, J. M. (1998). The arctic oscillation signature in the wintertime geopotential height and temperature fields. *Geophysical Research Letters*, *25*(9), 1297–1300. (Cited page 108.)

Underwood, A. J. (1989). The analysis of stress in natural-populations. *Biological Journal of the Linnean Society*, *37*(1-2), 51–78. (Cited page 70.)

Vage, K., Pickart, R. S., Thierry, V., Reverdin, G., Lee, C. M., Petrie, B., Agnew, T. A., Wong, A., & Ribergaard, M. H. (2009). Surprising return of deep convection to the subpolar north atlantic ocean in winter 2007-2008. *Nature Geoscience*, *2*(1), 67–72. (Cited page 98.)

van der Meer, J. (2006). An introduction to Dynamic Energy Budget (DEB) models with special emphasis on parameter estimation. *Journal of Sea Research*, *56*(2), 85–102. (Cited page 9.)

Vandromme, P., Schmitt, F., Souissi, S., Buskey, E. G., Strikler, R. J., Wu, C.-H., & Hwang, J.-S. (2010). Symbolic Analysis of Plankton Swimming Trajectories: Case Study of Strobilidium sp. (PROTISTA) Helical Walk under Various Food Conditions. *Zoological Studies*, *49*(3), 289–303. (Cited pages 10 and 35.)

Vargas-Yanez, M., Zunino, P., Benali, A., Delpy, M., Pastre, F., Moya, F., Garcia-Martinez, M. D., & Tel, E. (2010). How much is the western mediterranean really warming and salting? *Journal of Geophysical Research-oceans*, *115*. (Cited page 99.)

Verity, P. G., & Smetacek, V. (1996). Organism life cycles, predation, and the structure of marine pelagic ecosystems. *Marine Ecology-Progress Series*, *130*(1-3), 277–293. (Cited page 3.)

Vichi, M., Pinardi, N., & Masina, S. (2007). A generalized model of pelagic biogeochemistry.for the global ocean ecosystem. Part I: Theory. *Journal of Marine Systems*, *64*(1-4), 89–109. (Cited pages 18 and 119.)

Vidondo, B., Prairie, Y. T., Blanco, J. M., & Duarte, C. M. (1997). Some aspects of the analysis of size spectra in aquatic ecology. *Limnology and Oceanography*, *42*(1), 184–192. (Cited page 31.)

Visser, A. W. (2001). Hydromechanical signals in the plankton. *Marine Ecology-progress Series*, *222*, 1–24. (Cited page 10.)

Visser, A. W. (2007). Motility of zooplankton: fitness, foraging and predation. *Journal of Plankton Research*, *29*(5), 447–461. (Cited page 10.)

Visser, A. W., & Kiorboe, T. (2006). Plankton motility patterns and encounter rates. *Oecologia*, *148*(3), 538–546. (Cited page 10.)

von Storch, H., & Zwiers, F. W. (1999). *Statistical Analysis in Climate Research*. Cambridge University Press, New York. (Cited page 33.)

West, G. B., Savage, V. M., Gillooly, J., Enquist, B. J., Woodruff, W. H., & Brown, J. H. (2003). Why does metabolic rate scale with body size? *Nature*, *421*(6924), 713–713. (Cited page 8.)

Wiebe, P. H., & Benfield, M. C. (2003). From the Hensen net toward four-dimensional biological oceanography. *Progress in Oceanography*, *56*(1), 7–136. (Cited pages 11, 12, and 43.)

Wiltshire, K. H., Malzahn, A. M., Wirtz, K., Greve, W., Janisch, S., Mangelsdorf, P., Manly, B. F. J., & Boersma, M. (2008). Resilience of North Sea phytoplankton spring bloom dynamics: An analysis of long-term data at Helgoland Roads. *Limnology and Oceanography*, *53*(4), 1294–1302. (Cited page 102.)

Woodd-Walker, R. S., Gallienne, C. P., & Robins, D. B. (2000). A test model for optical plankton counter (OPC) coincidence and a comparison of OPC-derived and conventional measures of plankton abundance. *Journal of Plankton Research*, *22*(3), 473–483. (Cited pages 44, 45, 51, and 167.)

Woollings, T., Hannachi, A., Hoskins, B., & Turner, A. (2010). A regime view of the north atlantic oscillation and its response to anthropogenic forcing. *Journal of Climate*, *23*(6), 1291–1307. (Cited pages 112 and 181.)

Yurista, P., Kelly, J. R., & Miller, S. (2005). Evaluation of optically acquired zooplankton size-spectrum data as a potential tool for assessment of condition in the Great Lakes. *Environmental Management*, *35*(1), 34–44. (Cited page 43.)

Zaldivar, J. M., Strozzi, F., Dueri, S., Marinov, D., & Zbilut, J. P. (2008). Characterization of regime shifts in environmental time series with recurrence quantification analysis. *Ecological Modelling*, *210*(1-2), 58–70. (Cited page 35.)

Zavatarelli, M., & Mellor, G. L. (1995). A numerical study of the mediterranean-sea circulation. *Journal of Physical Oceanography*, *25*(6), 1384–1414. (Cited page 4.)

Zbilut, J. P., & Webber, C. L. (1992). Embeddings and delays as derived from quantification of recurrence plots. *Physics Letters A*, *171*(3-4), 199–203. (Cited page 35.)

Zhou, M. (2006). What determine the slope of a plankton biomass spectrum? *Journal of Plankton Research*, *28*(5), 437–448. (Cited pages 8, 12, 16, and 22.)

Zhou, M., Carlotti, F., & Zhu, Y. W. (2010). A size-spectrum zooplankton closure model for ecosystem modelling. *Journal of Plankton Research*, *32*(8), 1147–1165. (Cited pages 8, 12, 19, 22, 23, 120, 159, 175, and 176.)

Zhou, M., & Huntley, M. E. (1997). Population dynamics theory of plankton based on biomass spectra. *Marine Ecology Progress Series*, *159*, 61–73. (Cited pages 12, 15, 16, 19, 22, and 23.)

Titre Évolution décennale du zooplancton de la Mer Ligure en relation avec les fluctuations environnementales. De l'imagerie à la modélisation basée en taille.

Résumé L'imagerie a récemment émergée comme outil de mesure de la dynamique du zooplancton en donnant des informations à la fois taxonomiques et de structure en taille de la communauté — nécessaires à la bonne compréhension de la dynamique du zooplancton au sein de l'ecosystème pélagique. Ce travail est cependant davantage centré sur l'étude de la structure en taille du zooplancton dont différents aspects seront examinés au cours de trois chapitres: méthodes, analyse et description écologique d'une série temporelle de 11 ans, modélisation. Le chapitre méthodologique évalue la validité de l'imagerie en examinant l'effet de nouveaux biais, directement issus de l'imagerie, sur ledit spectre de taille (objets en contact au cours de l'acquisition d'image, efficacitée de la classification automatique, modèle utilisé pour le calcul des biovolumes et biomasses). Il s'agit d'une discussion sur ce que le scientifique veut mesurer et sur ce qu'il analyse finalement compte tenu des contraintes méthodologiques. Le second chapitre est consacré à l'évolution temporelle (1995-2005) de l'écosystème pélagique de la mer Ligure — plus spécifiquement de la station d'observation côtière de la rade de Villefranche-sur-Mer. Par l'étude combinée des données disponibles (taxonomie, structure en taille, climat, météorologie locale, hydrologie et biologie), les facteurs physiques, chimiques et biologiques déterminant pour l'écosystème sont extraits. Il s'agit principalement du climat hivernal, précipitations et températures, ainsi que de l'irradiation solaire reçu au printemps et en été. Les interactions entre ces facteurs déterminent différents états de la communauté zooplanctonique. Enfin, le dernier chapitre propose un modèle du zooplancton basé sur sa structuration en taille. Puisque les modèles classiques, en boîte, représentent difficilement la dynamique du zooplancton, l'approche par la taille fut proposée comme alternative. Le modèle présenté est exploratoire, incluant la croissance du zooplancton selon une modélisation de type "budget énergétique dynamique" et la prédation selon des rapports de taille proies/prédateurs. le but étant de comprendre ce qui détermine la structure en taille du zooplancton dans l'environnement. Les simulations effectuées sont ainsi comparées à la dynamique observée dans les phases majeures identifiées au chapitre précédent. C'est un premier pas vers l'intégration de ce type de modèles au sein de modèles plus généraux en vue d'améliorer la qualité de représentation du zooplancton. Le présent travail enrichit la connaissance du concept plus vaste de l'observation et de l'analyse théorique de la structuration en taille du zooplancton, mais il enrichit aussi la compréhension des liens entre le zooplancton et son environnement.

Mots-clés Zooplancton – Mer Ligure – ZooScan – Spectre de taille – Modèles structurés en taille – Séries temporelles

Title Decadal evolution of Ligurian Sea zooplankton linked to environmental fluctuations. From imaging systems to size-based models.

Abstract Imaging methods have recently emerged as tools to measure the zooplankton dynamics. These methods give both a taxonomic and size structure information on the community. The two kinds of information are necessary to understand the zooplankton dynamics and its links to the environment. Yet, the present work will focalize more on the zooplankton size structuration information. The manuscript is organized in three chapters: methodology, ecological analysis and description of an eleven years time series, and modeling. The methodological chapter assesses the validity of imaging methods as tools to measure zooplankton size spectra by investigating the effect of new biases onto the said size spectra (touching objects during the image acquisition process, efficiency of the automatic classification, model use to compute individuals biovolumes/biomasses). It is a discussion about what the scientist want to measure and what he finally analyze giving the methodological constraints. The second chapter relates to the analysis of the temporal evolution (1995-2005) of Ligurian Sea ecosystems, mainly from data recorded at the coastal monitoring station of the bay of Villefranche-sur-Mer. Combining the data (taxonomic and size structure, zooplankton, climatic, meteorological, hydrological and biological), physical, chemical and biological factors determining the ecosystem dynamic are proposed — mostly precipitations and temperatures in winter as well as solar irradiation in spring/summer. The interactions between them lead to different phases of the zooplankton community. In the end, the last chapter proposes a zooplankton size-based model. Since classic box models generally failed in representing correctly the zooplankton, size-based approaches are suggested as alternatives. The presented model is exploratory, so as to understand what determines the zooplankton size structuration. It includes growth of zooplankton through "dynamic energy budget" like modeling and predation through size dependent prey/predator relationships. The size-based model simulations are then compared to the dynamics of the zooplankton size-spectra in the main phases identified in the preceeding chapter. This is a first step toward an integration of such models into global ones in order to improve the quality of the representation of zooplankton. The present work enriches our knowledge of the more global concept of size-spectra observations and theory, and it also helps to better understand the links between zooplankton and environment.

Keywords Zooplankton – Ligurian Sea – Zooscan – Size spectra – Size structured models – Time series

Titre Évolution décennale du zooplancton de la Mer Ligure en relation avec les fluctuations environnementales. De l'imagerie à la modélisation basée en taille.

Résumé L'imagerie a récemment émergée comme outil de mesure de la dynamique du zooplancton en donnant des informations à la fois taxonomiques et de structure en taille de la communauté — nécessaires à la bonne compréhension de la dynamique du zooplancton au sein de l'ecosystème pélagique. Ce travail est cependant davantage centré sur l'étude de la structure en taille du zooplancton dont différents aspects seront examinés au cours de trois chapitres: méthodes, analyse et description écologique d'une série temporelle de 11 ans, modélisation. Le chapitre méthodologique évalue la validité de l'imagerie en examinant l'effet de nouveaux biais, directement issus de l'imagerie, sur ledit spectre de taille (objets en contact au cours de l'acquisition d'image, efficacitée de la classification automatique, modèle utilisé pour le calcul des biovolumes et biomasses). Il s'agit d'une discussion sur ce que le scientifique veut mesurer et sur ce qu'il analyse finalement compte tenu des contraintes méthodologiques. Le second chapitre est consacré à l'évolution temporelle (1995-2005) de l'écosystème pélagique de la mer Ligure — plus spécifiquement de la station d'observation côtière de la rade de Villefranche-sur-Mer. Par l'étude combinée des données disponibles (taxonomie, structure en taille, climat, météorologie locale, hydrologie et biologie), les facteurs physiques, chimiques et biologiques déterminant pour l'écosystème sont extraits. Il s'agit principalement du climat hivernal, précipitations et températures, ainsi que de l'irradiation solaire reçu au printemps et en été. Les interactions entre ces facteurs déterminent différents états de la communauté zooplanctonique. Enfin, le dernier chapitre propose un modèle du zooplancton basé sur sa structuration en taille. Puisque les modèles classiques, en boîte, représentent difficilement la dynamique du zooplancton, l'approche par la taille fut proposée comme alternative. Le modèle présenté est exploratoire, incluant la croissance du zooplancton selon une modélisation de type "budget énergétique dynamique" et la prédation selon des rapports de taille proies/prédateurs. le but étant de comprendre ce qui détermine la structure en taille du zooplancton dans l'environnement. Les simulations effectuées sont ainsi comparées à la dynamique observée dans les phases majeures identifiées au chapitre précédent. C'est un premier pas vers l'intégration de ce type de modèles au sein de modèles plus généraux en vue d'améliorer la qualité de représentation du zooplancton. Le présent travail enrichit la connaissance du concept plus vaste de l'observation et de l'analyse théorique de la structuration en taille du zooplancton, mais il enrichit aussi la compréhension des liens entre le zooplancton et son environnement.

Mots-clés Zooplancton – Mer Ligure – ZooScan – Spectre de taille – Modèles structurés en taille – Séries temporelles

Title Decadal evolution of Ligurian Sea zooplankton linked to environmental fluctuations. From imaging systems to size-based models.

Abstract Imaging methods have recently emerged as tools to measure the zooplankton dynamics. These methods give both a taxonomic and size structure information on the community. The two kinds of information are necessary to understand the zooplankton dynamics and its links to the environment. Yet, the present work will focalize more on the zooplankton size structuration information. The manuscript is organized in three chapters: methodology, ecological analysis and description of an eleven years time series, and modeling. The methodological chapter assesses the validity of imaging methods as tools to measure zooplankton size spectra by investigating the effect of new biases onto the said size spectra (touching objects during the image acquisition process, efficiency of the automatic classification, model use to compute individuals biovolumes/biomasses). It is a discussion about what the scientist want to measure and what he finally analyze giving the methodological constraints. The second chapter relates to the analysis of the temporal evolution (1995-2005) of Ligurian Sea ecosystems, mainly from data recorded at the coastal monitoring station of the bay of Villefranche-sur-Mer. Combining the data (taxonomic and size structure, zooplankton, climatic, meteorological, hydrological and biological), physical, chemical and biological factors determining the ecosystem dynamic are proposed — mostly precipitations and temperatures in winter as well as solar irradiation in spring/summer. The interactions between them lead to different phases of the zooplankton community. In the end, the last chapter proposes a zooplankton size-based model. Since classic box models generally failed in representing correctly the zooplankton, size-based approaches are suggested as alternatives. The presented model is exploratory, so as to understand what determines the zooplankton size structuration. It includes growth of zooplankton through "dynamic energy budget" like modeling and predation through size dependent prey/predator relationships. The size-based model simulations are then compared to the dynamics of the zooplankton size-spectra in the main phases identified in the preceeding chapter. This is a first step toward an integration of such models into global ones in order to improve the quality of the representation of zooplankton. The present work enriches our knowledge of the more global concept of size-spectra observations and theory, and it also helps to better understand the links between zooplankton and environment.

Keywords Zooplankton – Ligurian Sea – Zooscan – Size spectra – Size structured models – Time series